Developing sustainable seaweed aquaculture of the native kelp *Ecklonia radiata* in New Zealand

A thesis

Submitted in partial fulfilment

of the requirements for the degree

of

Doctor of Philosophy in Biological Science

at

The University of Waikato

by

Jacob Nepper-Davidsen

THE UNIVERSITY OF
WAIKATO
Te Whare Wānanga o Waikato

2023

Preface

Writing a PhD can be hard sometimes - remember the good things

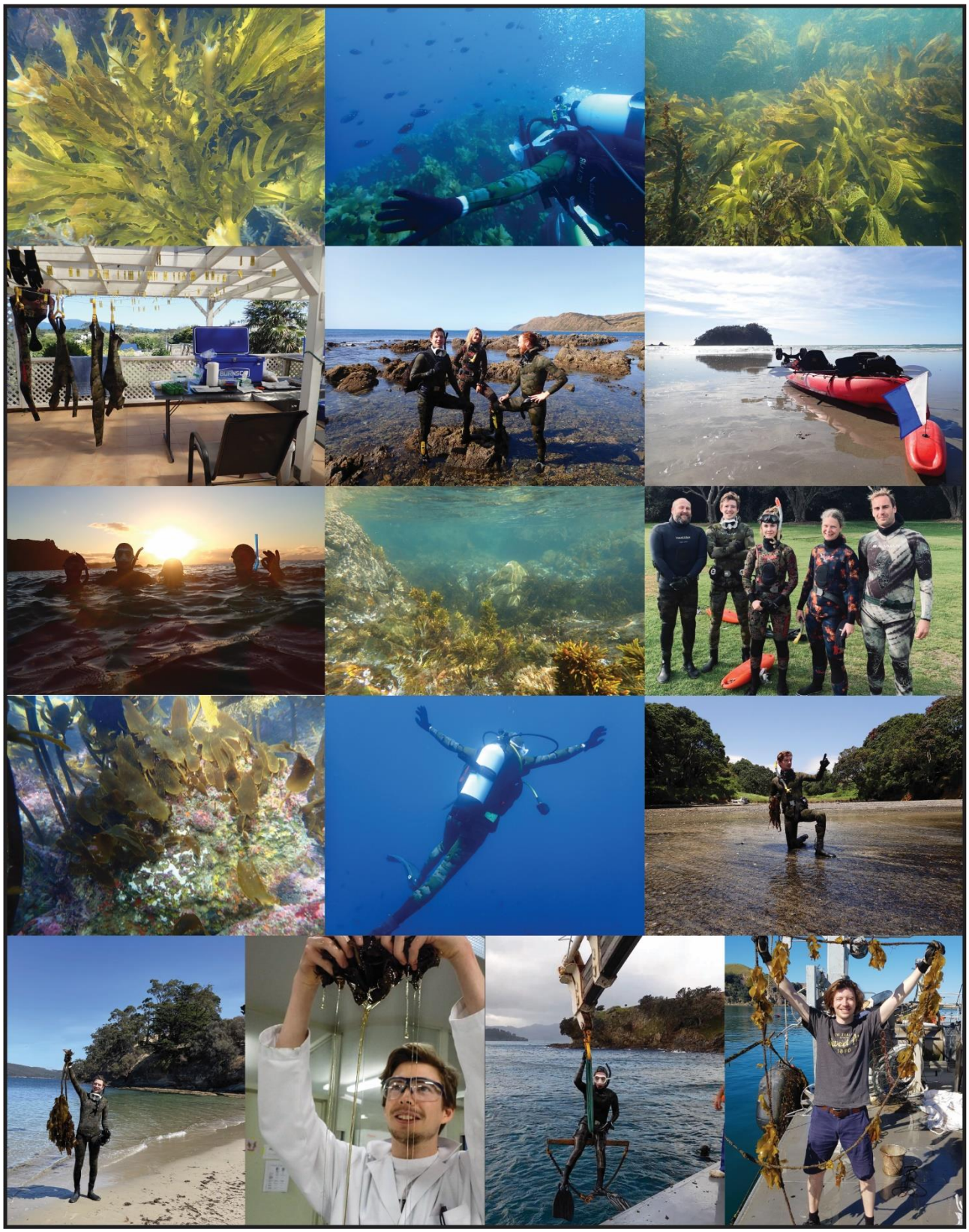

Abstract

The native kelp *Ecklonia radiata* is a target species for seaweed aquaculture in New Zealand because of its broad distribution and desirable biomass profile (e.g., alginate, fucoidan, and phlorotannins). However, commercial farming practices for *E. radiata* are not yet developed. The objective of this thesis was therefore to create foundations for sustainable seaweed aquaculture of *E. radiata* in New Zealand by filling key knowledge gaps regarding patterns of genetic structure (Chapter 2), spatial and temporal variation in biomass composition (Chapter 3), the development of high-throughput methods for biomass grading (Chapter 4), and marine farm design (Chapter 5).

The development of specialised cultivars is central for optimising key commercial traits for seaweed aquaculture; however, the introduction of genotypes from significantly different genetic sub-populations can reduce genetic diversity and genetic structure of wild populations. Analysis of molecular variance in populations of *E. radiata* in the North Island of New Zealand revealed significant differences at all three hierarchical levels of genetic structure that were analysed. The highest regional differentiation occurred between Wellington and other regions and was supported by Bayesian and redundancy models showing a high degree of genetic clustering among regions. Furthermore, pairwise F_{ST} (genetic differentiation) revealed significant differences between most sites showing strong genetic structure and low connectivity also at a local level. These findings indicate that cultivars of *E. radiata* should not be translocated outside their area of origin, to prevent introducing genotypes from significantly different genetic sub-populations to wild sub-populations.

Most analysed biomass components of *E. radiata* showed high spatial variation between sites, including alginate, glucose, and phlorotannins. However, there was no clear pattern in biomass composition among regions, indicating that these differences in biomass content are unlikely to be caused by genetic differences (i.e., Wellington samples did not stand out). Conversely, a strong seasonal pattern was detected with significant temporal variation detected for half of the quantified components. These results indicate that environmental variation is a key driver for the biomass

composition of *E. radiata* and that the high spatial variation was due to do site-specific environmental conditions. In general, the biomass composition of *E. radiata* was comparable to that of commercially grown northern hemisphere species and could be a suitable southern hemisphere alternative for a wide range of commercial applications.

The large spatial and temporal variation in biomass composition creates a need for high-throughput grading of raw biomass. Highly accurate models were built for estimating biomass concentration of glucose, alginate, phlorotannins, and carbon using mid-infrared (MIR) and near-infrared (NIR) spectroscopy. NIR models generally demonstrated higher accuracy and lower sensitivity to outliers than MIR models. Furthermore, samples from the Wellington region could consistently be identified based on the NIR data, demonstrating strong phenotypic differences between regions. These results show that NIR and MIR are valuable tools for high-throughput grading of raw seaweed biomass samples and can be used to establish provenance.

Finally, farming trials quantified the effect of vertical and horizontal line configurations and farming depth on survival and growth of *E. radiata* at a commercial New Zealand green-lipped mussel (*Perna canaliculus*) marine farm. Only seaweed growing on vertical lines survived four months after deployment, and juvenile growth by elongation and maximum average individual weight was markedly higher on vertical lines compared to horizontal lines. Survival rates on vertical lines decreased at shallow depths, likely influenced by a combination of light and temperature stress. Similarly, the overall high mortality observed during the experiment was likely correlated to the prolonged marine heatwave of the summer of 2021/22 at the farm location. Conclusively, these results support vertical lines rather than horizontal line for farming of *E. radiata*.

In summary, this thesis has significant scientific implications for regulatory (i.e., cultivar translocation), commercial (i.e., harvesting timing, biomass grading, and source tracing), and practical farming aspects (i.e., line configuration and a first proof on concept) of aquaculture of *E. radiata* in New Zealand and provides directions for future research and development.

Acknowledgements

First, I would like to thank my chief supervisor Marie Magnusson, who granted me the opportunity to come here, and my two other supervisors Chris Glasson and Rebecca Lawton. You guys have been rock-solid, highly professional, but also ever supportive and friendly all the way through, and I always felt like you had my back.

I also want to give a special thanks to Peter Randrup for extensive field work assistance and fun times on the road and to Ariane Brandenburg for extensive lab work assistance, without which I would surely have capitulated. Thanks to Alisa Mihaila, Holly Fergusson, Dave Culliford, Alice Morrison, Logan Forsythe, and Katherine Rowe for field work assistance and to Dave Blyth from Goldridge Marine Farms Ltd and Lucas Evans from Premium Seas Ltd for much needed practical assistance on the farm.

During my PhD, I have dived into statistical programming and for this, I want to give a big thanks to my friend Jesper Sonne who has assisted me on video chat from Denmark whenever I was stuck with a problem. A big thanks also to Dale Fletcher and Geoffrey Holmes for assistance in the development of multivariate models.

I would like to thank the University of Waikato, EnviroStrat Ltd., the Augustinus Foundation, the Christian and Ottilia Travel Foundation, and the Knud Hoejgaards Foundation who have made this journey possible through financial support. An additional honourable mention to Annette Bruhn whom I did field work with during the cold Danish winter back in 2019 and who rewarded this by recommending me for the PhD position here in New Zealand.

Lastly, I want to thank my family, my mum, dad, and my brother and my friends from back home who has made the other side of the world seem less far away, and a huge thanks to my new New Zealand family Bev and Bruce, and especially to my sweet fiancé Amber who has given me all the support I could ever need.

Statement on the contribution of others

This research is part of the Entrepreneurial Universities Macroalgal Biotechnologies Program, jointly funded by the University of Waikato and the Tertiary Education Commission. Field work and farm access for Chapter 5 was funded and facilitated by EnviroStrat Ltd. through the NZ Ministry for Primary Industries Sustainable Food and Fibre Futures project "GreenWave NZ: Regenerative Ocean Farming Seaweed Pilot", agreement number SFFF20125. Grants and scholarships were provided by the University of Waikato through the Entrepreneurial Universities Macroalgal Biotechnologies Program, jointly funded by the University of Waikato and the Tertiary Education Commission (Research and Enterprise Study Award), the University of Waikato School of Science Student Trust Research Grant, and by the Augustinus Foundation, the Christian and Ottilia Travel Foundation, and the Knud Hoejgaards Foundation.

Principle and editorial guidance were provided by my supervisors from the University of Waikato Marie Magnusson (primary supervisor), Christopher Glasson (secondary supervisor), and Rebecca Lawton (secondary supervisor). Additional editorial and technical guidance was provided by Phill Ross (University of Waikato), Dale Fletcher (University of Waikato), Geoffrey Holmes (University of Waikato), Jesper Sonne (University of Copenhagen), Gold Ridge Marine Farms Ltd, and Premium Seas Ltd. Laboratory assistance was provided by Arianne Brandenburg and Goldy De Bhowmick, and field work assistance by Peter Randrup, Alisa Mihaila, Holly Fergusson, Dave Culliford, Alice Morrison, Logan Forsythe, Katherine Rowe, and Goldridge Marie Farms. Elemental analysis of samples was determined commercially by OEA labs Ltd (Exeter, UK) and at the University of Waikato Laboratory (Hamilton, New Zealand).

Chapter 2

Jacob Nepper-Davidsen: investigation, data curation, data analysis, visualisation, and writing— original draft, review, and editing.

Marie Magnusson: conceptualisation, design, supervision, funding, and writing— review, and editing.

Christopher Glasson: conceptualisation, supervision, writing—review, and editing.

Phil Ross: writing—review and editing.

Rebecca Lawton: conceptualisation, design, supervision, data analysis, and writing—review, and editing.

Chapter 3

Jacob Nepper-Davidsen: investigation, data curation, data analysis, visualisation, and writing—original draft, review, and editing.

Christopher Glasson: conceptualisation, design, supervision, data curation, writing—review, and editing.

Rebecca Lawton: conceptualisation, design, supervision, and writing—review, and editing.

Marie Magnusson: conceptualisation, design, supervision, funding, and writing— review, and editing.

Chapter 4

Jacob Nepper-Davidsen: investigation, data curation, data analysis, modelling, visualisation, and writing—original draft, review, and editing.

Marie Magnusson: conceptualisation, design, supervision, funding, and writing— review, and editing.

Rebecca Lawton: conceptualisation, design, supervision, and writing—review, and editing.

Dale Fletcher: supervision and writing – review and editing.

Geoffrey Holmes: supervision and writing – review and editing.

Christopher Glasson: conceptualisation, design, supervision, data curation, writing—review, and editing.

Chapter 5

Jacob Nepper-Davidsen: investigation, field work, data analysis, visualisation, and writing—original draft, review, and editing.

Marie Magnusson: conceptualisation, design, field work, supervision, funding, and writing— review, and editing.

Christopher Glasson: supervision, writing—review, and editing.

Rebecca Lawton: conceptualisation, design, field work, supervision, and writing—review, and editing.

Table of contents

List of figures

List of tables

List of appendices

Chapter 1

Introduction to seaweed aquaculture

1.1 Introduction

Seaweed aquaculture has increased exponentially since 1990, reaching an annual production volume of 35.1 million tons and a value of 16.5 billion USD in 2022, equivalent to 28.6 % by volume and 6.2 % by value of the total global aquaculture production (FAO 2022). Seaweed aquaculture accounts for 97 % of total global seaweed production (i.e., seaweed biomass produced in aquaculture, from wild harvest and by beach-cast collection), with wild harvest accounting for only 3 % and beach-cast collection being minimal (Buschmann and Camus 2019; FAO and WHO 2022). Written records of seaweed used for human consumption dates back approximately 2,700 years in Asia (Mouritsen et al. 2018), and historically seaweed has also been used as fertiliser, livestock feed, crafting material, and for medicinal purposes (Buschmann et al. 2017; Thurstan et al. 2018; Wheeler et al. 2021). Today, the global seaweed industry is primarily based on direct human consumption and on extraction of hydrocolloids (gel forming polysaccharides), which are used in food and medicinal products, pharmaceuticals, and textile printing, because of their gelling, thickening, and stabilising properties. The largest seaweed producers are China (55.4 %), where the main species is the kelp *Saccharina japonica,* and Indonesia (29.6 %), where the main species/groups of taxa are the red seaweed *Eucheuma* spp*.* and *Kappaphycus alvarezii* (collectively know as eucheumatoids; Xiao et al. 2017; FAO and WHO 2022). In general, Asian countries account for 97 % of global seaweed biomass produced in aquaculture (FAO and WHO 2022). In New Zealand, commercial seaweed aquaculture has not yet been established and businesses therefore rely on beach-cast collection, wild harvest or imported biomass (White and White 2020; Bradly et al. 2021). However, seaweed aquaculture in New Zealand is showing economic and environmental potential, and creating

sustainable seaweed aquaculture has been set as a strategic goal by the government (New Zealand Government 2021).

1.2 Seaweed products

Seaweed biomass has a broad variety of commercial uses, either unprocessed or through extraction of specific compounds. This diversity of applications creates potential for seaweed biorefineries where multiple products can be made from the same raw material by exploiting the different components of the biomass (see Torres et al. 2019). Human food applications account for 80 % of global seaweed production, with 48 % used directly for human consumption (as fresh, dried, fermented, or cooked) and 32 % consumed indirectly through processed foods (FAO and WHO 2022). Uses of the remaining 20 % of seaweed production include: agricultural applications (as animal food or biostimulants for plant growth), medicinal and pharmaceutical products, and textile and paper printing (FAO and WHO 2022).

1.2.1 Seaweed hydrocolloids

Hydrocolloids (i.e., polysaccharides that forms gels in the presence of water) are commercially the most important seaweed biomass components because of their gelling, thickening and stabilising properties, which give them a broad variety of applications in human and animal food products, pharmaceuticals, cosmetics, textile, and paper production (McHugh 2003). The structural properties of hydrocolloids are not only specific for the different groups of hydrocolloids, but also depend on the algal species from which the compound is extracted, the environmental growth conditions, as well as the processing and extraction method used (Qi et al. 2005; Kraan 2012). These factors may affect the monomer composition of the polysaccharides, the molecular weight, the branching of the molecules, and the binding of ions which affect physical properties such as viscosity, gelling capacity, and gel strength (Haug et al. 1967, 1974; Indergaard et al. 1990). For

example, the ratio between mannuronic and guluronic acid (M:G ratio) is an important feature for gel strength and flexibility of the hydrocolloid alginate and may be related to wave exposure of the growth environment and age of the individual (Munda 1987; Indergaard et al. 1990; McHugh 2003).

The market value of hydrocolloids, therefore, depends on the purity and function of the compound. Carrageenan, agar, and alginate are the three main commercial types of hydrocolloids (Table 1.1), where carrageenan and agar are both found in red algae and used almost exclusively for food products (E407 and E406 for carrageenan and agar products respectively) and alginate is found in brown algae and is used in food products (E400-405 for alginate products), pharmaceuticals, and textiles (Bixler and Porse 2011; Szekalska et al. 2016). Additionally, ulvan is a hydrocolloid found in green algae which is used in nutraceuticals and animal foods (e.g., Olmix Group in France; see Kidgell et al. 2019) but remains a comparatively minor market and is not further discussed in this thesis. Pharmaceuticals make up the high-end market for high-grade hydrocolloids (primarily alginates), food products are of intermediate value, and textiles make up the low-end of the market (Kraan 2012). For example, high grade alginate applicable for pharmaceuticals may be worth 13-15.5 USD kg^{-1}, whereas low grade alginate for food products may be worth 6.5-11 USD kg^{-1} (Kraan 2012). Hydrocolloids are also produced from terrestrial plants, such as locust bean and guar (Barak and Mudgil 2014; Mudgil et al. 2014), however, 75-80 % of the marine hydrocolloid industry can compete with such competition on price and existing demands, and the remaining 20-25 % of the industry targets high value products, capturing new markets (Porse and Rudolph 2017).

Table 1.1 Three main hydrocolloids and main seaweed species, main countries of origin, and main applications (Bixler and Porse 2011; Buschmann et al. 2017), and global volume (% of total), global value (% of total), and mean market value (USD kg-1) from 2015 (Porse and Rudolph 2017)

Hydrocolloid	**Main species**	**Main countries of origin**	**Main applications**	**Global volume (%)**	**Global value (%)**	**Mean value ($ kg^{-1})**
Carrageenan (red algae)	Eucheumatoids	Indonesia, Philippines	Human food (90 %) Animal food (10 %	59	47	9
Agar (red algae)	*Gracilaria* spp.	China	Human food	15	22	17
Alginate (brown algae)	*Saccharina Japonica*	China	Food/pharma-ceuticals (50 %), textiles (50 %)	25	31	14

1.2.2 Seaweed for consumption

Seaweeds are an integral part of the diet in the majority of East-Asian cuisines, where the main food products are *Pyropia* spp. (nori), *Undaria pinnatifida* (wakame) and *Saccharina japonica* (kombu; FAO and WHO 2022). In western societies, there is a growing interest in seaweed for consumption, because of their nutritional profile which makes them attractive as nutraceuticals and functional foods (Shannon and Abu-Ghannam 2019; FAO and WHO 2022; Young et al. 2022). Protein content ranges from 5 to 32 % DW, with the highest levels found in red and green seaweeds (Angell et al. 2016). Essential amino acid content usually accounts for 40-50 % of total amino acids (highest in red seaweeds), giving seaweed a healthy amino acid profile (Černá 2011). Lipid content is generally low in most seaweeds (<5 % DW), though some species may contain up to 20 % DW (Gosch et al. 2012), and high concentrations of omega-3 fatty acids to omega-6 fatty acids gives seaweeds a healthy fatty acid profile (Biancarosa et al. 2018). Seaweed also contain a range of unique biomass compounds of commercial interest for nutraceuticals including fucoidan, a group of bioactive sulfated polysaccharides (e.g., Marinova in Tasmania and Enzalg in New Zealand; see also Hsu and Hwang 2019), and phlorotannins, a group of phenolic compounds with strong anti-oxidants, anti-inflammatory, anti-diabetic, and cholesterol lowering properties (Shin et al. 2012; Ganesan et al. 2019; Shrestha et al. 2021).

Seaweeds readily take up minerals and metals from the surrounding waters and generally have high concentrations of vitamins and essential minerals, compared to terrestrial plant and animal food products (Shannon and Abu-Ghannam 2019). However, seaweed may accumulate toxic levels of heavy metals and minerals which can pose a risk to consumers (Monteiro et al. 2019). A risk assessment based on a weekly intake of 5 g dry weight seaweed for Europeans found the mercury, cadmium, and lead content to be of no significant risk whereas iodine could pose a risk depending on the species of seaweed and whether the consumer is a child or a pregnant woman (Monteiro et al. 2019). However, the seaweed iodine content can be reduced by more than 90 % by blanching, which is a common technique used when preparing seaweed for consumption (Stévant et al. 2018; Nielsen et al. 2020).

1.3 Seaweed production and cultivation

Though there are more than 10,000 known species of seaweeds (Torres et al. 2019), 88 % of global seaweed aquaculture production is made up by only five species (Table 1.2; FAO 2022). In aquaculture, the three most cultivated species/groups of taxa are *S. japonica*, eucheumatoids, and *Gracilaria* spp., with China, Indonesia and the Philippines being the three main producers, accounting for 55, 30, and 6 % of the total seaweed aquaculture production, respectively (FAO and WHO 2022). For wild harvest, the three main species/groups of taxa are *Lessonia nigrescens*, *S. japonica*, and *Gracilaria* spp., accounting for 17, 7, and 4 % of total wild harvest, respectively (FAO 2018a), with the main producers being Chile, China, and Norway, accounting for 37, 23, and 15 % of global wild harvest respectively (FAO and WHO 2022). It is worth pointing out that the presented data are sourced from the Food and Agriculture Organisation of the United Nations (FAO) who gather global statics on seaweed production and markets from local governments. These data are subject to uncertainty as production may be largely overestimated in some areas (Porse and Rudolph 2017; Hermans 2023) but remain the only openly available official data.

Table 1.2 The five main species/groups of taxa for seaweed aquaculture (Buschmann et al. 2017; FAO 2021, 2022)

Species	Main products	Volume (% global WW)	Value (USD)
Saccharina japonica	Alginate	36 %	4.6
Eucheumatoids spp.	Carrageenan	23 %	2.4
Gracilaria spp.	Food, agar	15 %	2.0
Undaria pinnatifida (wakame)	Food	8 %	1.9
Pyropia spp. (nori)	Food	6 %	2.7

1.3.1 Wild harvest

Seaweeds have traditionally been harvested from wild stock or collected as beach-cast (Mac Monagail et al. 2017). Beach-cast collection is gathered along the coastline and still provides a significant source of seaweed material in several regions around the world, including New Zealand (e.g., as commercialised by AgriSea Ltd, Quality Seaweeds), Australia (Tasmanian Government 2017) and South Africa (Amosu et al. 2013). However, beach-cast yields are often highly variable and unreliable (Mac Monagail et al. 2017). In many cases, wild harvest can deliver a more stable supply of seaweed biomass for businesses (Sharp 1987; Vea and Ask 2011) but has often led to over-exploitation of natural stocks. Such examples of over-harvesting have been seen for *Gracilaria parvispora* in Hawaii (Glenn et al. 1998), *Gracilaria chilensis* in Chile (Huanel et al. 2022), coralline red algae (maerl) in Europe (Hall-Spencer et al. 2010), *Gelidium* sp. in Morocco (Callaway 2015), and *Saccharina* spp. in Japan (Hwang et al. 2019).

However, sustainable wild harvest of seaweeds can also be achieved (Lauzon-Guay et al. 2021; Johnston et al. 2023). For example, Norwegian wild harvest of brown seaweeds (mostly *Laminaria hyperborea* and *Ascophyllum nodosum*) accounted for 56 % of the total European production of seaweed in 2014 (Mac Monagail et al. 2017), and the industry has been able to operate sustainably through the implementation of management plans (Vea and Ask 2011). Similarly, in Southern New Zealand, giant kelp *Macrocystis pyrifera* is managed under a quota management system, and 34-79 ton is harvested annually without affecting population density (Pirker 2002; Gibbons 2014). In general, the method of harvest, (i.e., harvest according to thallus

morphology, lifecycle stage, patchiness of seaweed beds, and regrow time) is often more important than how much is harvested (Sharp 1987; Vásquez et al. 2012), and as these examples illustrate, regulation and management of wild seaweed harvests are essential to avoid over-exploitation (Mac Monagail et al. 2017).

In contrast to the expansive growth of the seaweed aquaculture sector, global wild harvest of seaweeds has been stagnant during the last decade (FAO and WHO 2022) and in Europe the production has remained stable since 1950 (Camia et al. 2018). However, in Europe and the Americas, wild harvest is the central source of seaweed biomass (accounting for 96.1 % and 95.3 % of total production, respectively; FAO and WHO 2022).

1.3.2 Aquaculture

The dominance of aquaculture production over wild harvest has been driven by the massive increase in demand for seaweed biomass that started during the 1980's (FAO 2018b), which has largely surpassed the capacity that can be supplied by wild harvest in many regions (Mac Monagail et al. 2017). Asian countries account for more than 97 % of global seaweed aquaculture production, with China and Indonesia accounting for 85 % of total production (FAO and WHO 2022). In Indonesia, eucheumatoid farming (*Eucheuma* spp*.* and *K. alvarezii*) dominates, and the industry has been the central contributor to the expansive growth in global seaweed production during recent years (FAO 2018b). Eucheumatoids grow well in shallow waters, and cultivation is usually primitive with seedlings attached manually to a supporting line. In China, there has been some effort in trying to mechanise seaweed farming, but most industries still rely heavily on manual labour (Zhang 2018). *Saccharina japonica* accounts for 68 % of seaweed production in China and is grown from zoospores to sporophytes in greenhouses after which the sporophytes are transplanted manually onto longlines (Zhang 2018). Except for the cultivation of *Pyropia* spp*.* for nori in China, Korea, and Japan (FAO and WHO 2022), which is a highly industrialised process, seaweed farming in Asia is typically

low-technology, labour intensive and often reliant on low wages and family labour (Zhang 2018; Hurtado et al. 2019).

In Western countries, seaweed aquaculture is still in a developing stage and must rely on automated production methods because of the high cost of labour (Campbell et al. 2019). Kelp is one of the main types of seaweed cultivated in Europe and the US (Camia et al. 2018; Kim et al. 2019), and examples include off-shore longline cultivation of *Saccharina latissima* in the Faroe Islands (Grandorf Bak 2019) and the US (Kim et al. 2019). These industries rely on high-end technology to produce seedlings and the use of advanced machinery to attach seedlings onto the longlines and for harvesting (Grandorf Bak 2019; Kim et al. 2019). In Europe, seaweed aquaculture has increased both in terms of production volume and by number of producing countries during the last two decades (Camia et al. 2018). However, the overall amount of biomass produced is still very limited and most seaweed being processed and sold within the European union is imported from Asia, creating potential for large-scale seaweed aquaculture in the region (European Commission 2019, 2022).

1.4 The seaweed aquaculture industry in New Zealand

The seaweed industry in New Zealand is in a developing stage and is currently focused on biostimulants, food, and health products (White and White 2020; Bradly et al. 2021; Clark et al. 2021; Table 1.3). Traditionally, Māori have used seaweed for food and crafting materials (e.g., *Pyropia* sp. and *Durvillaea* sp.) for hundreds of years and are culturally connected to these species though their whakapapa (genealogy) relationship (Wheeler et al. 2021). However, no commercial aquaculture of seaweeds is currently occurring in New Zealand, and all companies therefore still rely on wild harvest, beach cast collection and import. Compared to the large well established seaweed industries in south-east Asia, the competitive advantage of the New Zealand seaweed sector lies in extraction of high valuable products for niche markets, including products such as high-quality

alginate, fucoidan, and phlorotannins (Bradly et al. 2021; Clark et al. 2021). The development of domestic seaweed aquaculture based on native species is therefore a necessary step forward for producing high-quality products.

Table 1.3 Seaweed sector in New Zealand

Company	Product	Seaweed species	Supply
AgriSea	Biostimulants	*E. radiata*	Beach-cast
Waikaitu	Biostimulants	*U. pinnatifida*	Wild/nuisance harvest
Quality Seaweeds	Biostimulants	*E. radiata*	Beach-cast
Pacific Harvest	Food	Multiple species	Import
Enzalg	Food & health products	Multiple species	Import
NZ Kelp	Biostimulants & food products	*M. Pyrifera*	Wild harvest
Premium Seas Ltd	Biostimulants & food products	*U. pinnatifida*	Nuisance harvest

The native kelp *Ecklonia radiata (C. Agardh) J. Agardh* (Figure 1.1) is a target species for aquaculture in New Zealand because of its desirable biomass profile which includes commercial compounds such as alginate, fucoidan and phlorotannins (Stewart et al. 1961; Lorbeer et al. 2017; Magnusson et al. 2017) and because it is already used in New Zealand to produce seaweed biostimulants (AgriSea, Quality Seaweeds) and food products for human consumption (Pacific Harvest). Furthermore, *E. radiata* is the most abundant species of seaweed in New Zealand, accounting for more than 25 % of the total seaweed biomass along the coastlines (Shears and Babcock 2007). Here, *E. radiata* grows on rocky reefs from the low tide mark of the subtidal zone down to 65 m depth and form large mono-specific stands, mostly abundant between 7-17 m (Choat and Schiel 1982; Schiel 1990). The depth distribution and abundance of the species is directly related to water temperature and light availability, whereas other physical factors such as wave exposure and nutrient availability may also have significant effect (Wernberg et al. 2019). The highest density of *E. radiata* is found in Northland and Bay of Plenty (Shears and Babcock 2007) which are areas of high interest for cultivation. Globally, brown seaweeds such as *S. japonica, S. latissima,* and *U. pinnatifida* are widely cultivated (Barbier et al. 2019; FAO 2022) for use as popular food products (e.g., kombu and wakame) and for extraction of commercial products (e.g., alginate; Porse and

Rudolph 2017), and *E. radiata* could potentially be a native alternative to these species for aquaculture in New Zealand.

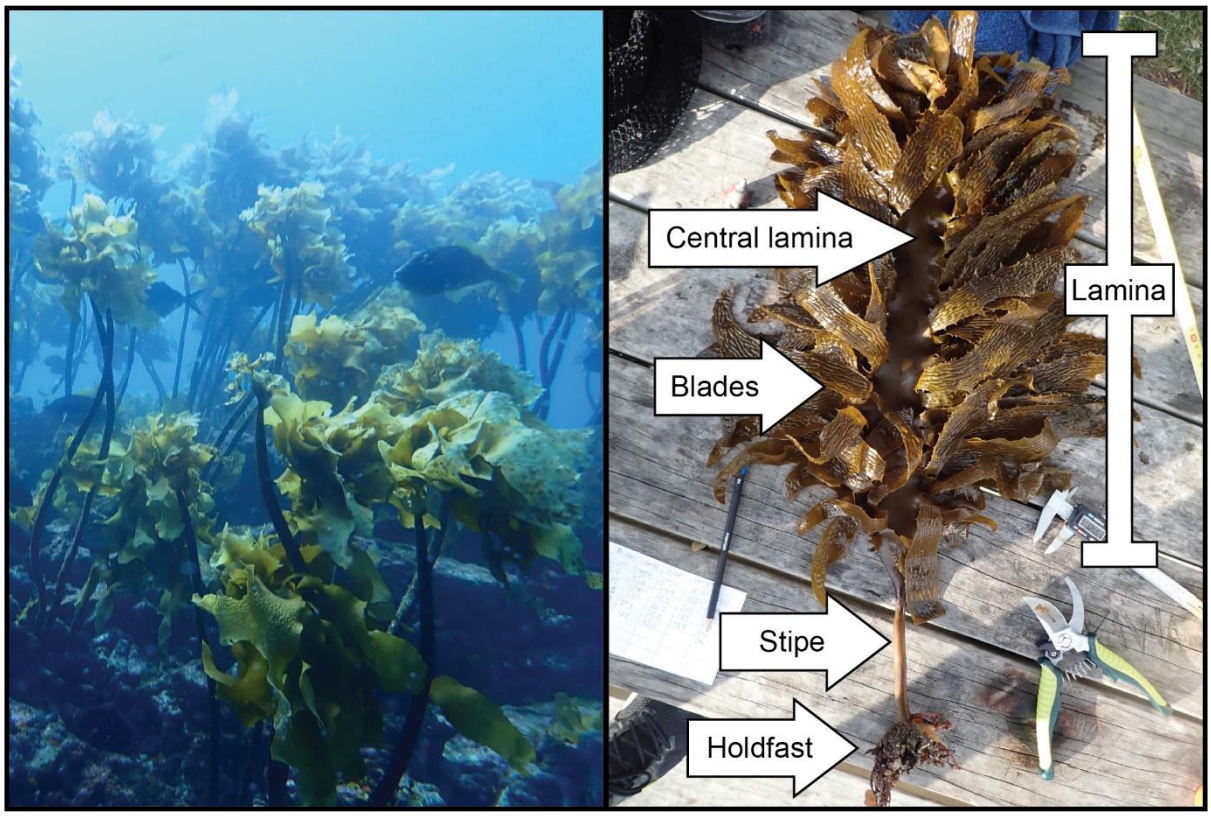

Figure 1.1 *Ecklonia radiata* in natural habitat (left) and a harvested specimen showing morphologically different parts (right)

1.5 Significance of topic and thesis aims

The objective of this thesis was to create foundations for sustainable seaweed aquaculture of *E. radiata* in New Zealand, by filling key knowledge gaps regarding patterns of genetic structure, spatial and temporal variation in biomass composition, the development of high-throughput methods for biomass grading, and marine farm design.

Chapter 2: The expansive growth of seaweed aquaculture in Asia has been enhanced by the development of specialised seaweed cultivars, and through selective breeding and hybridisation it has been possible to improve key traits for cultivation including growth rate, morphology,

reproductive timing, biochemical composition, and stress tolerance (Hwang et al. 2019). However, introduced genotypes from significantly different genetic sub-populations (i.e., genotypes sourced from sub-populations significantly genetically different to the sub-populations they are introduced into) may impact the genetic composition of wild populations, as has been extensively documented for agriculture and animal aquaculture (Haygood et al. 2003; Bolstad et al. 2017) and must be applied with caution (Barbier et al. 2019). The aim of Chapter 2 was therefore to analyse genetic structure and connectivity of *E. radiata* in the North Island of New Zealand to guide decision making around aquaculture translocation activities.

Chapter 3: Intra-specific variation in biomass composition is common within seaweed, due to spatial differences in genotype and environmental conditions between sites and due to temporal differences in environmental conditions between seasons (Gosch et al. 2015; Manns et al. 2017; Mata et al. 2017). Such variation may have significant effect on the biomass quality of the seaweed and its commercial value. The aim of Chapter 3 was therefore to assess spatial and temporal variation in biomass composition of *E. radiata* on the North Island of New Zealand to investigate geographic differences in biomass quality and optimise harvest timing.

Chapter 4: Mid-infrared and near-infrared spectroscopy are widely used methods for high-throughput grading of biological material, e.g., in food industries (Beć et al. 2020). However, predictive chemometric models have only been developed for a few species of seaweed (Robic et al. 2009; Laurens and Wolfrum 2011; Shefer et al. 2017; Peleg et al. 2019), and the use of spectroscopy for biomass profiling of *E. radiata* has not yet been demonstrated. The aim of Chapter 4 was therefore to build high-throughput spectroscopy models for determining composition (grading) and region of origin of raw *E. radiata* biomass for the industry.

Chapter 5: Commercial farming practices for *E. radiata* are not yet developed, although previous studies have successfully demonstrated farming of the kelp in New Zealand at a small research scale (Neill et al. 2009) and of other species of the genus in Korea (Hwang et al. 2009).

Conversely, little work has been done to optimise farm settings, such as line-configuration and farming depth, which must be investigated before large scale trials can be undertaken. The aim of Chapter 5 was therefore to study to effect of line configuration and farming depth on survival and growth of *E. radiata* in a marine farm setting to provide a first proof of concept for further farm development.

Chapter 2

Implications of genetic structure for aquaculture and cultivar translocation of the kelp *Ecklonia radiata* in northern New Zealand

This chapter has been published in Frontiers in Marine Science as:

Nepper-Davidsen J, Magnusson M, Glasson CRK, et al (2021) Implications of genetic structure for aquaculture and cultivar translocation of the kelp *Ecklonia radiata* in northern New Zealand. Front Mar Sci 8:1–11 (Appendix 12).

2.1 Abstract

The fast expansion of the global seaweed aquaculture industry has created an interest in translocating seedlings cultivated from wild type brood stock. However, such translocations must be applied with caution as introduced cultivars can reduce genetic structure and diversity of wild populations. An understanding of the genetic structure and connectivity of target species is required to guide decision making around aquaculture translocation activities. In this study we used 14 microsatellite loci in a three-level hierarchical sampling design to analyse the genetic structure and connectivity of the native kelp *Ecklonia radiata* across 12 sites among four geographic regions (Northland, Bay of Plenty, Gisborne, and Wellington) in the North Island of New Zealand. Our aim was to provide guidance for translocation of cultivars to prevent the introduction of genotypes of *E. radiata* from significantly different genetic sub-populations. Strong genetic structure and low geneflow were observed at all hierarchical levels, indicating the presence of multiple genetically distinct sub-populations. On a regional scale, high genetic differentiation was found between the Wellington region and the other three regions (F_{ST} = 0.407 to 0.545), and within regions most sites were significantly different (measured by pairwise F_{ST}) with high relatedness found between individuals within sites (mean 31.0 % ± 0.6 SE). Bayesian modelling and redundancy analysis showed a high degree of genetic clustering and indicate that ocean currents and other factors that have

resulted in biogeographical breaks along the coast are likely to be the main factors shaping genetic structure and connectivity of *E. radiata* on the North Island, rather than isolation by distance. Based on these findings, we recommend that cultivars of *E. radiata* should not be translocated outside their area of origin to avoid introducing genotypes from significantly different genetic sub-populations to local sub-populations.

2.2 Introduction

Seaweed aquaculture has grown exponentially during the last 50 years and now has a global annual yield of 35.1 million tons and a commercial value of 16.5 billion USD (FAO 2022). The vast expansion of the sector has created an interest in translocating strains (i.e., movement outside region of origin), as intraspecific differentiation in key commercial traits, such as growth rate and biochemical content, is common within seaweeds due to genotypic variation and local adaptation (Oliveira et al. 2013; Gosch et al. 2015b; Mata et al. 2017). However, translocation of seaweed cultivars (i.e., strains selected for cultivation) must be approached with caution. Introduced cultivars can reduce genetic differentiation between wild populations (i.e., reduce genetic structure) by outcompeting unique local genotypes and reduce genetic variation within wild populations (i.e., reduce genetic diversity) by over-dominating the local gene pool (Ellstrand et al. 2013; Bolstad et al. 2017; Valero et al. 2017; Hu et al. 2021). Such genetic changes may have negative ecological and economic consequences, as loss of genetic structure can lead to the extinction of valuable genetic traits adapted to specific ecological niches (Evankow et al. 2019; Shan et al. 2019). Furthermore, the loss of genetic diversity within wild macrophyte populations may decrease productivity and tolerance to environmental stress in these communities (Hughes and Stachowicz 2004; Reusch et al. 2005; Wernberg et al. 2018).

The extent of gene flow from farmed seaweed to wild populations remains poorly quantified (Valero et al. 2017; Campbell et al. 2019) and may vary between species and with cultivation method (Shan et al. 2019). However, evidence to date suggests that gene flow from farmed to wild seaweed

populations is low (Guzinski et al. 2018; Li et al. 2020; Graf et al. 2021). For instance, gene flow from cultivars to wild populations is typically low for *Saccharina japonica* (Liu et al. 2012; Zhang et al. 2017) because selective breeding of cultivars has delayed spore release to late summer when most cultivars have already been harvested and any offspring of remaining cultivars are unlikely to survive high summer temperatures (Shan et al. 2019). However, gene flow from cultivars to wild populations has been documented extensively for animal aquaculture and agriculture (Ellstrand et al. 2013; Glover et al. 2013), with effects varying from possibly advantageous (e.g., increased fitness in wild lettuce; Hooftman et al. 2009; Hartman et al. 2013) to devastating (e.g., wide-spread changes in age and size at maturation in wild stock of Norwegian Atlantic salmon; Bolstad et al. 2017). Consequently, the introduction of cultivated organisms to wild populations is recognised as one of the main risks associated with aquaculture of any species (Naylor et al. 2001) and the cultivation of seaweed genotypes from genetically distinct sub-populations is often restricted (Loureiro et al. 2015). Therefore, mapping genetic structure and connectivity of wild populations is crucial to ensure that seedlings cultivated from wild type broodstock can be translocated without introducing genotypes from significantly different genetic sub-populations (Barbier et al. 2019; Evankow et al. 2019).

The native kelp *Ecklonia radiata* is a target for aquaculture in New Zealand because of its wide distribution (Shears and Babcock 2007) and commercial applications as biostimulants, sea vegetables and food additives (White and White 2020). However, the genetic structure and connectivity of *E. radiata* has not been investigated in New Zealand. Consequently, the geographic extent that seedlings cultivated from wild type brood stock can be translocated without changing local genetic structure remains unknown. In Australia, the genetic structure of *E. radiata* is largely region specific, with high genetic connectivity among populations on the east coast (Coleman et al. 2011a; Coleman 2013) and low genetic connectivity among populations on the south coast (Coleman et al. 2009). These regional differences in genetic structure are largely attributed to variations in oceanography as the gene flow of *E. radiata* is correlated to the strength of ocean currents (Coleman

et al. 2011b). In New Zealand, ocean currents are known to play a key role in long distance connectivity among populations of seagrass (Jones et al. 2008) and several species of seaweeds (Collins et al. 2010; Macaya and Zuccarello 2010; Buchanan and Zuccarello 2012; Fraser et al. 2013). Accordingly, the genetic structure of *E. radiata* in New Zealand may also be influenced by local oceanographic conditions. Within the North Island of New Zealand, distinct genetic sub-populations exist for multiple taxonomic groups including seaweeds (Buchanan and Zuccarello 2012; Muangmai et al. 2015; Huanel et al. 2020), seagrasses (Jones et al. 2008), anemones (Veale and Lavery 2012), molluscs (Ross et al. 2012), and crustaceans (Stevens 1990). Furthermore, five bioregions have been proposed within the North Island, based on the distribution *E. radiata* and 150 other species of seaweed and invertebrates, indicating that there may be distinct sub-populations within each of these bioregions, and potential breaks in connectivity between bioregions (Shears et al. 2008). This general high level of genetic and distributional subdivision within seaweeds and benthic invertebrates on the North Island suggest that *E. radiata* is also likely to be divided into genetically distinct sub-populations.

In this study, we used 14 polymorphic microsatellite loci in a three-level hierarchical sampling design to analyse the genetic structure and connectivity of *E. radiata* among four regions of the North Island of New Zealand. The aims were to (1) assess patterns of genetic structure at a local (< 300 km) and regional (150-1200 km) level; and (2) estimate levels of genetic connectivity between local and regional populations; to (3) provide guidance for translocation of cultivars to prevent the introduction of genotypes of *E. radiata* from significantly different genetic sub-populations within the North Island of New Zealand.

2.3 Materials & methods

2.3.1 Sample collection

Thirty sporophytes of *E. radiata* were sampled from each of 12 sites on the North Island of New Zealand between September 2019 and March 2020 (Figure 2.1a), conducted under Special Permit 724 issued by the Ministry for Primary Industries, Manatū Ahu Matua to the University of Waikato. A hierarchical design was used with three sites sampled within each of four regions (Northland, Bay of Plenty, Gisborne, and Wellington). At each site, samples of tissue from blades were collected haphazardly by hand from adult (stage 3) plants (Mann and Kirkman 1981) while snorkelling on rocky reefs within 2-5 meters depth and with >1 meter between each sampled individual (sample area ≈ 1000 m^2). After collection, samples were stored in separate polyethylene bags and stored on ice for transport back to the laboratory. Within 24 hours of collection, samples were cleaned using a scalpel and lint free tissue paper to remove epiphytes and a 2 cm^2 blade section was cut and dried in silica gel for storage for a maximum of 12 months until further processing (Coleman et al. 2009). Blade tissue was homogenised using a Precellys Evolution Homogenizer (Bertin Instruments, France) and genomic DNA was extracted using a DNeasy® Plant Pro Kit (Qiagen, Germany) following the manufacturer's instructions with the addition of 80-100 µL of PS solution to each sample.

2.3.2 Primer selection

Twenty-five microsatellite loci developed for three other species of *Ecklonia* (Itou et al. 2012; Akita et al. 2018, 2020) were tested to determine their suitability for use in *E. radiata* (Appendix 1). All loci were initially tested on 8 individuals from five different sites within the four sampling regions. DNA was amplified in 25 µL singleplex PCR reactions containing 12.5 µL MyTag HS Red Mix (MilliporeSigma, Germany), 0.4 µM non-labelled forward primer, 0.4 µM fluorescent-labelled reverse primer, and 1 µL of genomic DNA. PCRs were run on an Applied Biosystems

SimplyAmp Thermal Cycler (Thermo Fisher Scientific, USA) and comprised of an initial denaturation phase at 95 °C for 1 min, 35 cycles of denaturation at 95 °C for 30 seconds, annealing at 57 °C for 30 seconds, and extension at 72 °C for 30 seconds, with a final extension at 72 °C for 7 min. Five µL of PCR product was run on a 2 % agarose gel and amplicon size was determined using a size standard marker (Bioline HyperLadder™ 25 bp). Loci showing strong evidence of primer dimer on gels were discarded. Loci that produced an amplicon within 150 bp of the expected size range in at least 6 of the 8 tested individuals were selected for genotyping. Loci showing no or inconsistent amplification on gels were further tested on six new individuals, using the same parameters described above. Again, loci were amplified, visualised, and selected for genotyping as described earlier and loci that did not consistently produce an amplicon within 150 bp of the expected size range were omitted from further testing. Following this process, 20 loci were selected and subsequently genotyped across all 360 samples (30 samples from each of the 12 sites). Loci were amplified in PCR reactions using the same parameters described above. Multiplex genotyping was carried out by Genetic Analysis Service, Department of Anatomy, University of Otago using an ABI 3730xl DNA Analyser (Thermo Fisher Scientific, USA) and allele sizes were scored using GeneMarker® (SOFTGENETICS, USA). Three of the 20 loci that were genotyped produced electropherograms too variable for allele sizes to be scored consistently across the 360 samples and were discarded (Appendix 1).

2.3.3 Data analyses

Data (Appendix 1) was checked for deviations from Hardy-Weinberg equilibrium and presence of linkage disequilibrium using Genepop on the Web v4.7 (Raymond and Rousset 1995; Rousset 2008). Three of the 17 genotyped loci were too monomorphic to enable testing of Hardy-Weinberg equilibrium at any site and were therefore excluded from further statistical analysis (Appendices 1 and 2). None of the remaining 14 loci deviated significantly from Hardy-Weinberg equilibrium when data was analysed collectively across all sites. However, it is likely that some of these loci were not in Hardy-Weinberg equilibrium as 12 of the 14 loci were monomorphic (or

almost monomorphic) at one or more sites. Consequently, it was not possible to test for Hardy-Weinberg equilibrium at these sites and they therefore could not be included in the collective assessment of Hardy-Weinberg equilibrium. To determine the influence of this high level of monomorphism on results, a sensitivity analysis was run where all analyses described below were conducted with all 14 loci, and then were repeated excluding all loci where more than half the sites were too monomorphic to calculate Hardy-Weinberg equilibrium. This sensitivity analysis showed that excluding the 8 loci with the highest monomorphism had no major influence on the main results and all 14 selected loci where therefore retained for analysis (Appendices 3 and 4). Linkage disequilibrium was tested across all sites and loci, and P-values were adjusted using the false discovery rate correction in the R-studio STATS package (Team RStudio 2022). No significant linkage disequilibrium was found between any loci but an average 58 % ± 15 SD of the loci combinations could not be checked for linkage disequilibrium due to monomorphism. However, as this uncertainty was evenly spread across all loci with no consistent patterns, all remaining loci were retained for analysis.

Allele frequencies and total number of alleles were calculated for each locus using GeneAlEx v6.5 (Peakall and Smouse 2006, 2012). Arlequin v.3.5.2.2 (Excoffier and Lischer 2010) was used to perform global analysis of molecular variance (AMOVA) as weighted average over all 14 loci within the three hierarchical sampling levels with 1,000 permutations. The number of genetic clusters (K) was analysed using a Bayesian modelling approach in STRUCTURE v2.3.4 (Pritchard et al. 2000), running 100,000 burn-in and 300,000 Monte Carlo Marco chain repeats after burn-in with 20 iterations for all analysed levels of K (1-14). Clustering was analysed using an admixture model with correlated allele frequencies and no prior information about the data. STRUCTURE HARVESTER (Earl and vonHoldt 2012) was used to find the number of clusters best fitting the data based on highest delta K and to find the iteration with the highest likelihood (Evanno et al. 2005). The clustering analysis was run multiple times to successively identify all hierarchical layers of structuring within the data. All samples were included in the first analysis and for each subsequent analysis, the

samples within each of the previously identified clusters were analysed in separate simulations. F_{ST} is a measure of genetic differentiation ranging from 0 to 1, with 0 showing no genetic difference between samples and 1 showing maximum genetic difference between samples. F_{ST} was calculated in Arlequin. Within region F_{ST} was calculated as the average pairwise F_{ST} between each pair of sites within each region. Between regions F_{ST} was calculated by treating each region as one single population and calculating a single pairwise F_{ST} value for each pair of regions. Pairwise F_{ST} between sites was visualised using R-studio (script sourced from The Banta Lab: https://sites.google.com/site/thebantalab/home?authuser=0).

Relatedness between the individuals collected from each site was quantified using ML-Relate (Kalinowski et al. 2006) which includes a null allele correction for any loci at any site that showed significant heterozygote deficiency ($\alpha = 0.05$). Relatedness was further quantified using maximum likelihood estimates, counting all estimates of half sibling, full sibling, and parent/offspring (i.e., not unrelated) as related. Individuals with missing values at more than 2/3 of the loci showed abnormally high values of relatedness and were therefore deleted and not used in any analysis (13 samples out of 360). High levels of relatedness were found between individuals at all sites (mean 28.2 % ± 0.7 SE) which can bias genetic analysis (Waples and Anderson 2017). To determine the influence of this high level of relatedness on results, another sensitivity analysis was run where all analyses described below were repeated excluding all samples that were related to more than 33.3 % of the other samples within their sites (thereby lowing mean relatedness to 21.1 % ± 0.6 SE). This sensitivity analysis showed that excluding the 97 most related samples had no major effect on the main results and all 347 samples were therefore retained for analysis (Appendices 3 and 4). To determine the influence of geographic distance on genetic structure, a redundancy analysis was performed in R-studio using the vegan package (Oksanen et al. 2020) and visualised using ggplot (Wickham 2016). Site coordinates (longitude and latitude) were set as independent variables and site-specific allele frequencies (72 different alleles in total across the 14 selected loci) as constrained dependent variables (Meirmans 2015).

2.4 Results

Genetic diversity was highest within northern sites (sites within the Northland and Bay of Plenty regions) compared to southern sites (sites within the Gisborne and Wellington regions, Table 2.1). The mean total number of alleles and mean number of unique alleles were 34.83 and 2.8 respectively for northern sites, compared to 26.2 and 0.7 respectively for southern sites. Relatedness between individuals was high at all sites (mean 28.2 % ± 0.7 SE), with individuals within southern sites being slightly more related than samples within the northern sites (32.0 % ± 1.0 SE and 24.3 % ± 0.8 SE, respectively).

Analysis of molecular variance showed high genetic variation among regions (27.41 %) and low genetic variation among sites within regions (7.10 %), with all levels of variation being significant ($p<0.001$, Table 2.2). The same pattern was evident for genetic differentiation (F_{ST}, Appendices 5 and 6). F_{ST} values were low within regions (F_{ST} = 0.070 to 0.160, Figure 2.1c), indicating low genetic differentiation, but were generally higher between regions (F_{ST} = 0.040 to 0.545, Figure 2.1d), indicating comparatively higher genetic differentiation. Between region F_{ST} was high between the Wellington region and the three other regions (F_{ST} = 0.407 to 0.545) and low between the Northland, Bay of Plenty and Gisborne regions (F_{ST} = 0.040 to 0.044). Pairwise F_{ST} between sites showed significant genetic differentiation between all sites except for 2 pairs (Figure 2.2). Highest pairwise F_{ST} was again found between the Wellington sites and sites from the other regions, with Titahi Bay and Mākara Beach showing the highest differentiation from other sites and Wellington Harbour showing only intermediate differentiation.

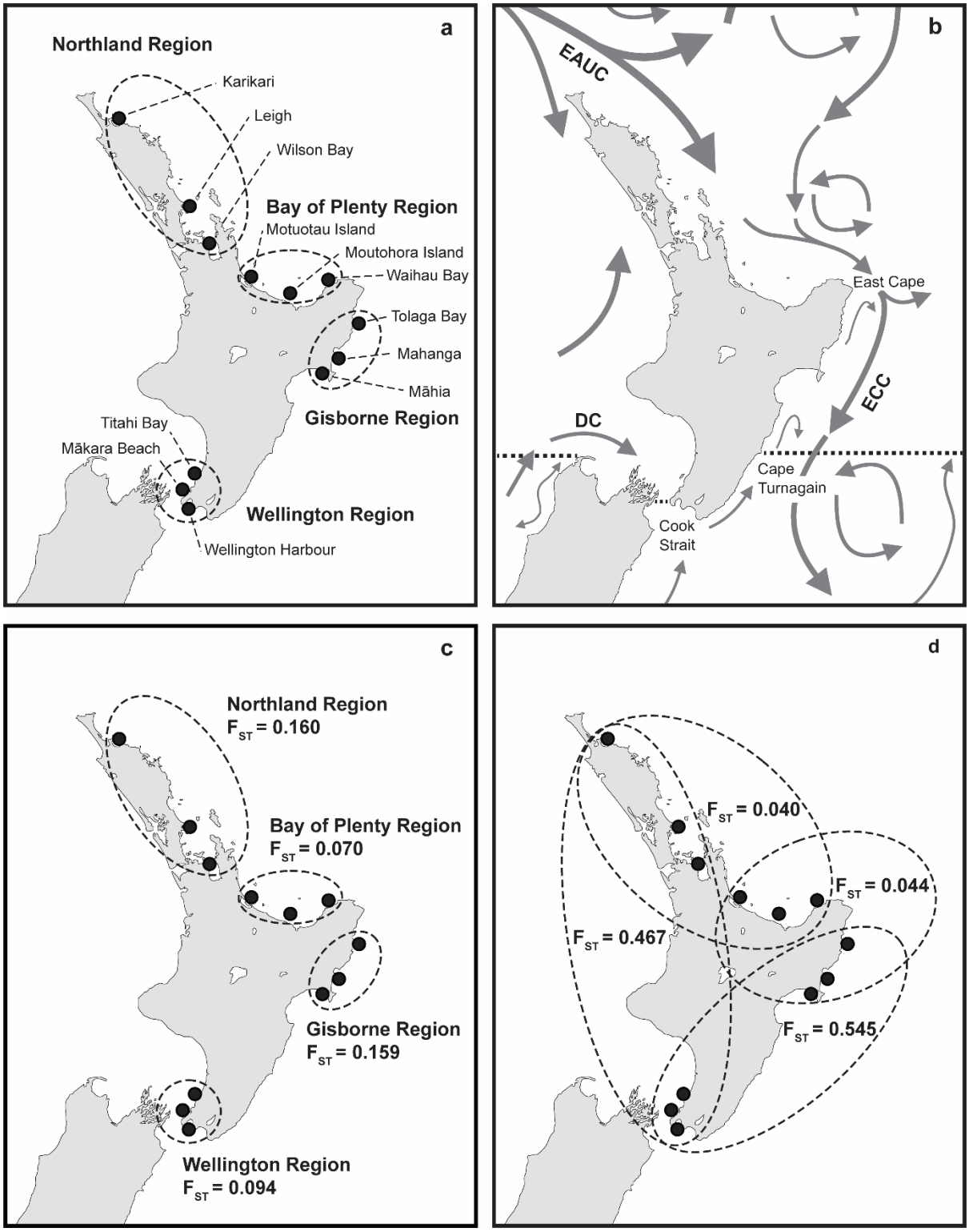

Figure 2.1 Map of New Zealand with a) sampling sites (filled black circles) and sampling regions (dashed circles), b) major ocean currents (Heath 1985), proposed biogeographic breaks (dashed black lines, Shears et al., 2008) and locations referred to in the text, c) genetic differentiation (F_{ST}) of *E. radiata* within each region and d) F_{ST} between each neighbouring region (F_{ST} Northland vs. Gisborne = 0.043, F_{ST} Bay of Plenty vs. Wellington = 0.407). EAUC: East Auckland Current; ECC: East Cape Current; DC: D'Urville Current. Figure 1b modified with permission from Buchanan and Zuccarello (2012)

Table 2.1 Number of individuals genotyped (n), total and mean number of alleles per loci, and number of unique alleles, and % relatedness between individuals ± standard error for each of the 12 sampling sites and across the entire dataset. All measurements of number of alleles, and relatedness are across all 14 loci

Location	Region	*n*	Number of alleles			Relatedness
			Total	Mean	Unique	% ± SE
Karikari	Northland	28	35	2.5	4	26.2 ± 1.7
Leigh	Northland	25	38	2.7	3	24.3 ± 2.3
Wilson Bay	Northland	30	29	2.1	2	25.1 ± 1.4
Motuotau island	Bay of Plenty	27	39	2.8	1	24.2 ± 2.0
Moutohora Island	Bay of Plenty	30	36	2.6	4	26.0 ± 2.2
Waihau Bay	Bay of Plenty	29	32	2.3	3	20.1 ± 1.8
Tolaga Bay	Gisborne	30	28	2.0	2	31.7 ± 2.9
Mahanga	Gisborne	28	25	1.8	0	34.4 ± 2.0
Māhia	Gisborne	30	19	1.4	0	27.4 ± 2.2
Wellington Harbour	Wellington	30	30	2.1	1	32.0 ± 2.1
Mākara Beach	Wellington	30	26	1.9	0	27.4 ± 1.9
Titahi Bay	Wellington	30	29	2.1	1	39.3 ± 2.7
All		347	72	5.1		28.2 ± 0.7

Table 2.2 Global analysis of molecular variance (AMOVA) for *E. radiata* among the four regions, among the three sites within each region, and among the individuals (25-30) within each site. All levels of variation are significant at p<0.001

Source of Variation	df	SS	Variance Component	Percentage variation
Among regions	3	222.87	0.416	27.41
Among sites within regions	8	56.18	0.108	7.10
Within sites (among individuals)	336	651.98	0.994	65.49
Total	347	937.03	1.517	

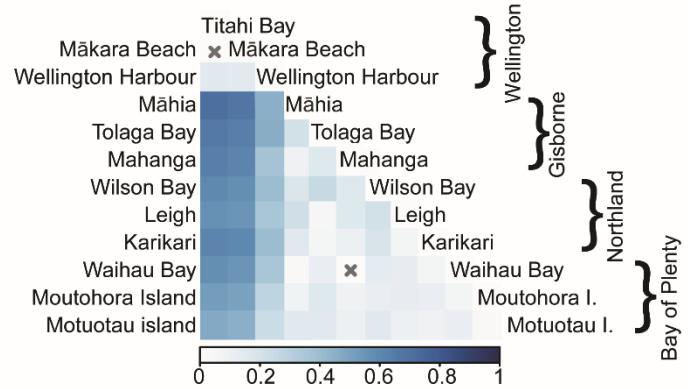

Figure 2.2 Pairwise genetic differentiation (F_{ST}) between each site (F_{ST} values indicated by colour gradient) with X indicating that sites are not significantly different

Bayesian modelling of population structure predicted that the most likely number of genetic clusters (inferred from delta K) for any of the STRUCTURE simulations was two (K = 2, Figure 2.3). When all samples were included in the analysis, the three Wellington sites were all grouped into one distinct cluster and the nine sites from the other three regions were grouped into a second distinct cluster. At the lower hierarchical levels of clustering 1) the Northland region separated from the Bay of Plenty and Gisborne region, 2) the Bay of Plenty region separated slightly from the Gisborne region, and 3) Wellington Harbour separated sharply from the Wellington open coast sites, Mākara Beach and Titahi Bay. There was no evidence of genetic structure among sites within each of the Northland, Bay of Plenty, and Gisborne regions.

Redundancy analysis showing the effect of geographic location (latitude and longitude) on allele frequency was highly significant (P = 0.001, 74 % constrained variance and 26 % unconstrained variance), with latitude and longitude explaining 74 % of the genetic variation in the data (Figure 2.4). The redundancy analysis showed the same pattern of population structure as the clustering analysis, with strong genetic separation between the wellington sites and the other sites along the RDA 1 axis (67 % of the total variation) and a weaker genetic separation between the Northland sites and the other sites along the RDA 2 axis (7 % of total variation). Most of the 72 alleles analysed across the 14 loci were plotted in the centre of the graph and only 8 alleles were plotted outside the centre, indicating that most of the variation in the data was provided by these 8 alleles.

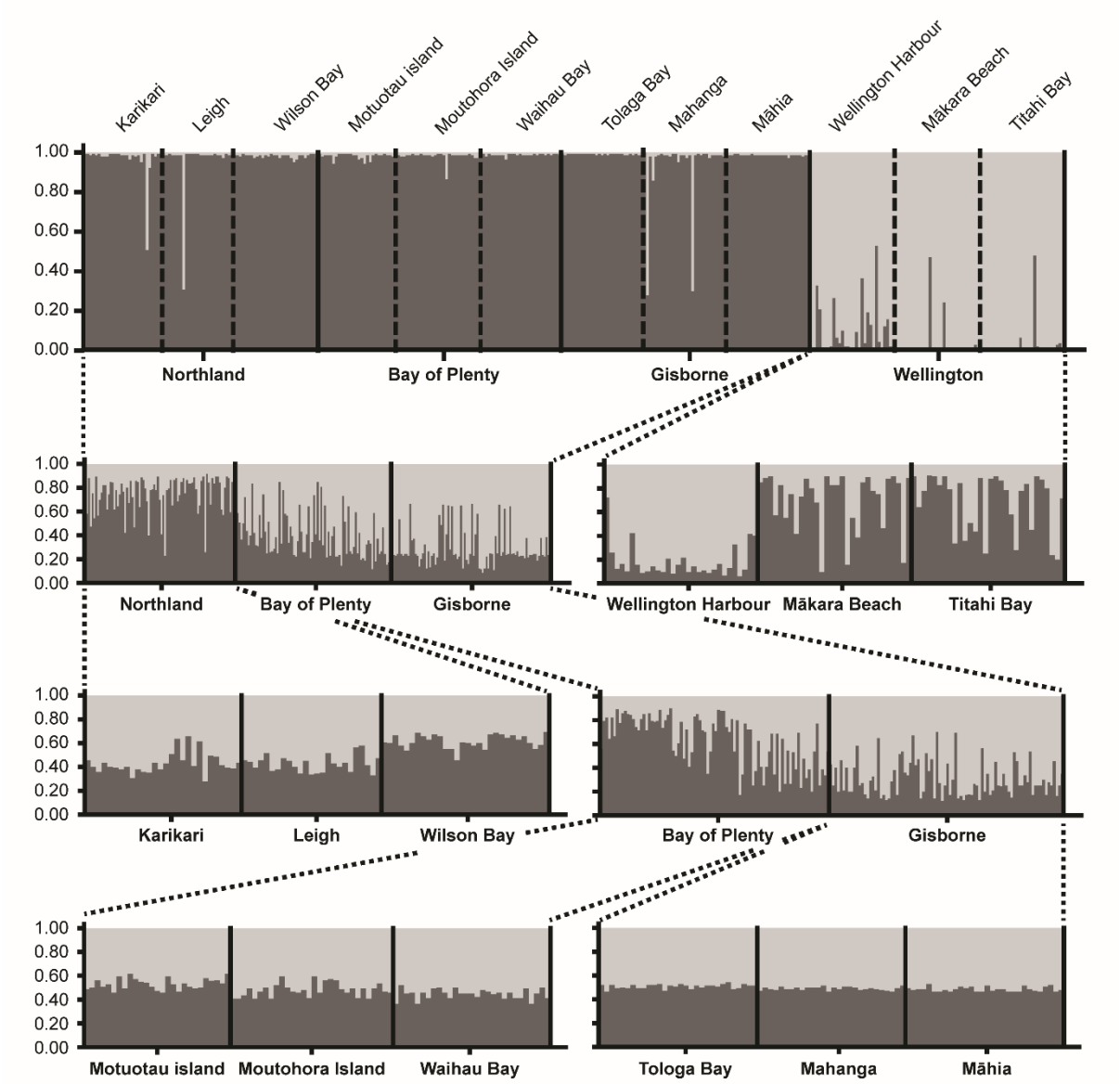

Figure 2.3 Bayesian modelling of population structure for *E. radiata* obtained using STRUCTURE (K = 2 for all plots). Top plot was run with all samples included and each subplot underneath was run with a subset of the samples indicated by the dashed lines. The x-axes show all individuals included in the simulations, with each individual represented by a column and grouped within their sites and regions. The y-axes show the genetic membership of each individual to the two clusters

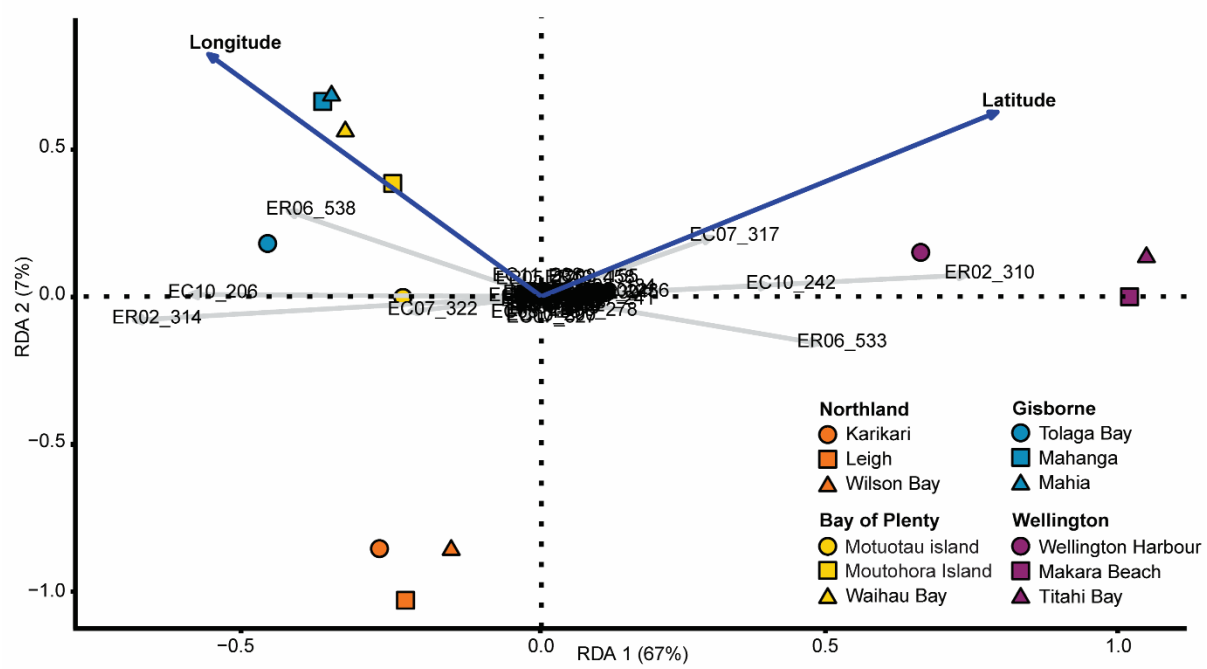

Figure 2.4 Redundancy analysis (RDA) of allele frequencies explained by geographical location (longitude and latitude). Grey vectors with allele names indicate magnitude and direction of the variation associated with each identified allele where the vector length indicates the amount of variation, and the vector direction indicates the correlation of the variation with the two RDA axes (parallel lines being highly correlated). Similarly, the blue vectors indicate the magnitude and direction of the variation associated with the latitude and longitude coordinates of the sites. Sites are plotted according to region (colour) and position within region (shape). The percent variation explained by the two RDA components are shown on the two axes

2.5 Discussion

2.5.1 Genetic structure and connectivity of *Ecklonia radiata*

Genetic analysis of microsatellite loci showed strong population structure and low genetic connectivity of *E. radiata* within the North Island of New Zealand. Clustering analysis showed structural differences on all hierarchical levels, with the Wellington region separating from the other regions at the highest level, the Northland region separating from the Bay of plenty and Gisborne regions at the intermediate level, and Wellington Harbour separating from Mākara Beach and Titahi Bay at the within region level (Figure 2.3). This same pattern of hierarchical genetic structuring was found through analysis of pairwise genetic differentiation (F_{ST}) and redundancy analysis, which showed clear distinction between the Wellington region and the other regions and between

Wellington Harbour and the other sites within the Wellington region (Figures 2.1 and 2.4). These findings demonstrate high levels of genetic structure both across long and short geographic distances. The high level of relatedness between individuals within sites and the large number of sites that were significantly different from one another (all but two site pairs through Pairwise F_{ST}), suggest that geneflow is generally low. However, regional F_{ST} showed that gene flow was higher among the Northland, Bay of Plenty and Gisborne regions (F_{ST} = 0.040 to 0.044) than between these regions and Wellington (F_{ST} = 0.407 to 0.545). Further support for the notion of reduced connectivity in the Wellington region was provided by the higher levels of relatedness recorded for southern sites (32.0 % ± 1.0 SE) compared to those in the north (24.3 % ± 0.8 SE). The redundancy analysis showed high correlation between genetic structure and geographic location (74 % constrained variance), but also showed a high degree of clustering in agreement with the groupings identified using STRUCTURE, indicating that gene flow in *E. radiata* in New Zealand is primarily shaped by dispersal barriers rather than by isolation by distance. In combination, these analyses suggest that multiple sub-populations of *E. radiata* are present within the locations sampled in this study and that genetic connectivity is limited.

Ecklonia radiata has a life cycle of two alternate generations where macroscopic diploid sporophytes produce spores that develop into microscopic haploid gametophytes (males and females) which then produce eggs and sperm that fuse and grow into sporophytes. The pelagic phase of *E. radiata* zoospores is relatively short (i.e., usually 1-2 hours; Wernberg et al. 2019) and based on studies of related species, gametophyte sperm dispersal is expected to occur over the scale of centimetres, whereas spore dispersal has an estimated maximum dispersal range of 1 km (Reed 1990; Gaylord et al. 2006). Because *E. radiata* is negatively buoyant, long-distance dispersal of mature plants is unlikely unless rafting with buoyant species (Fraser et al. 2009). Consequently, the dispersal potential of *E. radiata* is likely to be limited. These expectations were generally met as evidenced by significant levels of genetic differentiation between most sub-populations. Furthermore, this low dispersal life history may also explain the high levels of relatedness recorded

for individuals within sites. High levels of relatedness have previously been reported for the related species *E. cava* (Itou et al. 2019), and these results indicate inbreeding, which may have contributed to the high F_{ST} values.

Strong genetic differentiation between Wellington and the three northern regions matches patterns of genetic structure reported for other seaweed and invertebrate species. For these species, populations in the Wellington region have been shown to be distinct from northern populations, and more closely aligned to a South Island sub-population, indicating a major break in connectivity on the North Island for these species (Ross et al. 2009, 2012; Buchanan and Zuccarello 2012; Veale and Lavery 2012). Shears et al. (2008) found major biogeographic breaks based on distributional data covering *E. radiata* and 150 species of seaweed and invertebrates. In this case, the location of the genetic breaks recorded for *E. radiata* (between Wellington and northern regions and between the sites within the Wellington region), coincide with the biogeographic boundaries reported by Shears et al. (2008). This suggests that the sharp breaks in *E. radiata* connectivity between and within regions are most likely generated by the same processes (oceanography and climate) that influence the distribution of a numerous other marine species in the area.

Our detection of regional differences in genetic connectivity is similar to that reported for *E. radiata* in Australia, where this species displays high genetic connectivity along the west coast, but low connectivity along the south coast (Coleman et al., 2009, 2011a; Coleman, 2013). Ocean currents are a strong driver of differences in genetic connectivity among *E. radiata* populations in Australia (Coleman et al., 2011b) and may also explain the patterns of genetic connectivity observed in this study. Ocean currents in New Zealand are thought to shape long distance connectivity among other species of seaweeds (Collins et al., 2010; Macaya and Zuccarello, 2010; Buchanan and Zuccarello, 2012; Fraser et al., 2013) and seagrass (Jones et al., 2008). The two main ocean currents shaping the oceanography along the north-east coast of the North Island of New Zealand are the East Auckland Current and the East Cape Current, which travel south-eastward through the

Northland, Bay of Plenty and Gisborne region, passing Cape Turnagain where the East Cape Current turns east with the Chatham Rise into the Pacific (Figure 2.1b, Heath, 1985). The higher genetic connectivity of *E. radiata* found along the north-eastern coast of the North Island compared to low connectivity found between Wellington and the other regions may therefore be facilitated by these major ocean currents. In the Wellington region, water movement northwards is prevented by the D'Urville Current, which pushes water south-eastwards through Cook Straight.

2.5.2 Implications for aquaculture

In commercial kelp cultivation, new broodstock is cultivated and seeded onto ropes in on-shore hatcheries, and then, following a nursey period, the ropes are deployed off-shore for the juvenile kelp to mature (Zhang 2018; Kim et al. 2019). This process creates high potential for spread of genotypes from significantly different genetic sub-populations, which may affect the genetic structure of wild populations and leave them more vulnerable to environmental stress (Ellstrand et al. 2013; Bolstad et al. 2017; Wernberg et al. 2018). The spread of such genetically distinct genotypes can be avoided by developing local cultivars for local use only (Barbier et al. 2019). Our analysis showed clear distinction between the Wellington region and the three other regions but also revealed strong genetic structure and significant differentiation within and between individual sites. We therefore recommend that cultivars of *E. radiata* should not be translocated outside their area of origin to avoid introducing genotypes from significantly different genetic sub-populations to local sub-populations. Specific guidelines for the scale of translocation of kelp seed-stock have already been developed in some locations (e.g., Gulf of Alaska, USA, Kim et al., 2019), and based on the results of this study and future genetic research, similar guidelines could be developed for *E. radiata* in New Zealand.

Microsatellite markers have proven to be a powerful tool for the assessment of genetic structure and connectivity of natural populations (Guichoux et al. 2011). However, results provided by microsatellites may be less detailed than what might have been revealed through full genome

sequencing (Graf et al. 2021). Therefore, it is possible that further genetic differentiation among *E. radiata* sub-populations in New Zealand could be revealed through detailed genomic analysis. Still, given the large number of samples genotyped (360) and the high number of loci (14) included in our analyses, we believe that the results presented here are representative of the general genetic structure and connectivity of *E. radiata* in New Zealand. The patterns of low geneflow presented here suggest that the genetic structure of *E. radiata* in the South Island of New Zealand is also likely to be strong. Therefore, we recommend a similarly conservative approach to the translocation of kelp cultivars in this region.

Selective breeding is an integral part of the global seaweed aquaculture industry and has made it possible to improve key cultivar traits such as growth rate, morphology, reproductive timing, biochemical content, stress tolerance, texture, and taste (Hwang et al. 2019). However, selective breeding tends to reduce the genetic diversity of cultivars as it often leads to inbreeding, whether intentional or not (Valero et al. 2017). Reducing the genetic diversity of cultivars is not only a threat to the gene pool of local wild populations (Haygood et al. 2003; Bolstad et al. 2017) but may also leave cultivars more susceptible to pathogens (Hwang et al., 2019). For instance, low genetic diversity caused by inbreeding was the main cause of the heavy ice-ice disease outbreak that led to the sharp decline of the eucheumatoid seaweed farming in the Philippines (Trono and Largo 2019). It is therefore important in aquaculture not only to use local cultivars, but also to maintain a large effective population size and frequently introduce new genotypes from wild type broodstock to ensure high genetic diversity among cultivars (Barbier et al. 2019; Graf et al. 2021; Hu et al. 2021). As has previously been recorded in other New Zealand seaweed species, substantially higher genetic diversity was found among the northern sub-population of *E. radiata* compared to the southern sub-populations (Fraser et al. 2009; Buchanan and Zuccarello 2012; Muangmai et al. 2015). The northern regions seem therefore to be the best suited areas for *E. radiata* cultivation with regards to maintaining high genetic diversity among cultivars.

2.6 Conclusion

The strong genetic structure found at all hierarchical levels for *E. radiata* in the North Island of New Zealand underlines the general need for population genetic analyses to be conducted before initiating translocation of broodstock for seaweed aquaculture. Bayesian analysis of population structure, redundancy analysis and measurements of genetic differentiation (F_{ST}) all showed high levels of genetic variation and indicated that genetically distinct sub-populations are likely to be present both between and within regions. From a genetic perspective, we therefore recommend that cultivars of *E. radiata* should not be translocated outside their area of origin to avoid introducing genotypes from significantly different genetic sub-populations to local sub-populations. The high relatedness between samples found here highlights the importance of increasing the distance between collected individuals of *Ecklonia sp.* for genetic analysis (preferably more than 4 m, Itou et al. 2019) to minimise the impact of non-random mating and increase the importance of migration and drift within the signal. The microsatellite data collected in this study can serve as a reference set for future analysis of the genetic structure of *E. radiata* by comparing the genetic membership of individuals from sites outside the range of this study with the sub-populations sampled here.

Chapter 3

High spatial and temporal variation in biomass composition of the novel aquaculture target *Ecklonia radiata*

This chapter has been published in Journal of Applied Phycology as:

Nepper-Davidsen J, Glasson CRK, Lawton RJ, Magnusson M (2023) High spatial and temporal variation in biomass composition of the novel aquaculture target *Ecklonia radiata*. J Appl Phycol (Appendix 12).

3.1 Abstract

The biomass composition of kelp varies within species both spatially and temporally. However, this variation in biomass quality has not yet been investigated for the native kelp *Ecklonia radiata* within New Zealand, where the kelp is a target for the emerging seaweed aquaculture industry. In this study we quantified spatial and temporal variation in the composition of *E. radiata* biomass, collected from 12 sites around the North Island of New Zealand and from 12 months across a full year at a single site (n = 138). High spatial variation was detected for most components, including alginate (range: 16.6 – 22.7 % DW, n = 12), fucoidan (range: 1.2 – 1.6 % DW, n = 12), phlorotannins (range: 4.8 – 9.3 % DW, n = 72), and glucose (range: 9.3 – 22.6 % DW, n = 12). The biomass composition of *E. radiata* varied significantly among sites but with no clear patterns among regions, indicating that geographic differences were mostly local rather than regional, possibly due to site-specific environmental conditions. Significant temporal variation (measured by positive autocorrelation between months) was detected in the content of lipids, proteins, glucose, guluronic acid, nitrogen, phosphorous, iodine, arsenic, and mercury, and for the mannuronic to guluronic acid (M:G) ratio. Overall, *E. radiata* had comparable biomass composition to that of commercially grown northern hemisphere species but with substantially higher phlorotannin content. These results

demonstrate that *E. radiata* could be a viable southern hemisphere alternative for a broad range of commercial applications.

3.2 Introduction

The native kelp *Ecklonia radiata* is a target species for the emerging seaweed aquaculture industry in both New Zealand and Australia, with broad distribution across New Zealand (Shears and Babcock 2007), and along the temperate and subtropical coasts of Australia (Wernberg et al. 2019). Recent development of hatchery cultivation protocols (Praeger et al. 2022a, b) has facilitated ocean farming trials in New Zealand and fuelled further interest in the aquaculture of this species. The biomass of *E. radiata* contains a range of biomolecules of commercial interest unique to brown seaweed including 1) alginate, a gelling polysaccharide (hydrocolloid) used in food products, pharmaceuticals, textile printing, and cosmetics (Porse and Rudolph 2017), 2) fucoidan, a bioactive sulfated polysaccharide used in nutraceutical and personal health products (Mak et al. 2013; Hsu and Hwang 2019) and, 3) phlorotannins, a group of bioactive phenolic compounds with potential uses in nutraceuticals, cosmetics, and novel biomaterials (Magnusson et al. 2017; Shrestha et al. 2021). Furthermore, *E. radiata* biomass contains laminarin, a storage polysaccharide important for producing fermented commodities such as biostimulants, plant tonics, and food products (Battacharyya et al. 2015), which is currently the biggest market for kelp biomass in New Zealand (Bradly et al. 2021). Other biomass components include proteins, lipids, and minerals which contribute to the nutritional value and suitability of the seaweed biomass for human consumption - a market that accounts for approximately 1/3 of the total value of the global seaweed industry (FAO 2021). Consequently, the commercial value and application of *E. radiata* will depend largely on biomass composition.

The biomass composition of seaweeds varies within species both spatially, due to genotypic variation and differences in environmental conditions between locations, and temporally, due to variation in environmental conditions between seasons (Gosch et al. 2015; Manns et al. 2017; Mata

et al. 2017). For instance, spatial variation in phlorotannin content may be correlated to genotypic differences (Honkanen and Jormalainen 2005) and changes in environmental conditions such as salinity, nutrient availability, and herbivory pressure (Targett and Arnold 1998). Similarly, spatial variation in lipid content was linked to genotypic differences in light and nitrogen availability (Gosch et al. 2015), while spatial variation in alginate content may be corelated to wave exposure (Munda 1987; McHugh 2003). Overall, temporal changes in temperature have been identified as a main driver for temporal variation in carbohydrate and mineral content in kelp (compared to salinity and nutrient availability; Manns et al. 2017).

To date, spatial variation in the biomass composition of *E. radiata* in New Zealand has not been investigated. The large environmental variability within the North Island of New Zealand, such as differences in water temperature between north and south (14 - 21 °C summer temperature; Wijffels et al. 2018) and local differences in nutrient availability from runoff (20-fold differences in nitrate levels between estuarine systems; Plew et al. 2018), may cause morphological and biochemical variation in *E. radiata* (Targett and Arnold 1998; Fowler-Walker et al. 2006; Manns et al. 2017). Furthermore, *E. radiata* shows strong genetic structure and low gene flow within New Zealand (Chapter 2/Nepper-Davidsen et al. 2021), potentially resulting in spatial variation in biomass composition between genetically distinct sub-populations (Honkanen and Jormalainen 2005; Gosch et al. 2015). This environmental and genetic differentiation between sites and regions is therefore likely to result in significant spatial differences in the biomass composition of *E. radiata* within New Zealand.

Temporal variation in biomass composition of *E. radiata* in New Zealand has also never been studied. Temporal studies of the alginate content of *E. radiata* from Australia show inconsistent results, with either the highest content found in austral spring and the lowest in austral autumn in the state of Victoria (Stewart et al. 1961) or the lowest content found in austral spring and the highest in austral winter in the state of South Australia (Lorbeer et al. 2017). Additionally, previous

studies on temporal variation in the biomass composition of *E. radiata* were conducted with low temporal resolution (e.g., Stewart et al. 1961; Lorbeer et al. 2017) but indicated that location may be a key driver for variation in biomass composition and that temporal patterns may vary between locations (Jennings and Steinberg 1994). These inconsistencies in temporal patterns and the low temporal resolution of previous studies makes it difficult to draw any general conclusions about patterns of temporal variation in biomass composition for *E. radiata* and highlight the need for detailed studies in New Zealand to be undertaken to inform the emerging seaweed aquaculture industry.

The aim of this research was therefore to analyse spatial and temporal changes in the biomass composition of *E. radiata* within the North Island of New Zealand. Specifically, we wanted to assess 1) the spatial and temporal changes in proximate composition (carbohydrates, proteins, lipids, and minerals) and specific key components (alginate, fucoidan, laminarin, and phlorotannins), 2) whether spatial changes are local and/or regional, and 3) any relationships between biomass composition and morphology.

3.3 Materials & methods

3.3.1 Sample collection

Two groups of *E. radiata* samples were collected – one spatial and one temporal. For the spatial samples, six whole adult specimens (Stage 3; Mann and Kirkman 1981) were collected on a single occasion at 12 different sites within four regions of the North Island of New Zealand, ranging from sub-tropical (Northland region) to temperate (Wellington region) climate (Figure 3.1). The spatial samples were collected over a 14 week period from October 2019 to January 2020 (except for the Moutohora Island samples which were collected in March 2020) to minimise temporal variability. For the temporal samples, another six whole adult specimens were collected once every month on 12 occasions during a full year cycle from November 2019 to November 2020 at Motuotau

Island in Tauranga (Covid-19 lockdown prevented sampling in April 2020). Samples were collected haphazardly by cutting with a knife just above the holdfast (i.e., samples included lamina and stipe, but no holdfast) while snorkelling on rocky reefs within 2-6 meters depth and with >2 meters between each sampled individual. A total of 138 samples (replicated samples) were collected (spatial samples mean weight: 80.7 ± 42.5 SD g dry weight (DW), n = 72; temporal samples mean weight: 80.4 ± 39.2 SD g DW, n = 72) with the 6 samples collected at Motuotau Island in November 2019 included in both sample groups. Morphology of the stipe, primary lamina, and blades of each specimen were measured in the field after collection (Appendix 7). Samples were stored in separate polyethylene sealable bags and immediately placed on ice for transport back to the laboratory (maximum 48 hours). Samples were rinsed in seawater at the collection sites or in 5µm filtered seawater immediately upon return to the laboratory to remove epiphytes and debris, then weighed (wet weight, WW) and frozen at -20 °C. Samples were freeze-dried to dryness (BUCHI, Lyovapor™, L-200, Switzerland; 2 mbar, -50 °C), then weighed (DW), milled to <0.5 mm fine particles (Pulverisette 15 cutting mill, Fritsch GmbH, Germany), and stored in double polyethylene sealable bags with silica gel until further processing. Twenty-four homogenised samples were made by combining subsamples (2.0 g DW) from each of the six samples collected at each site to give 12 spatial samples (one for each site), and from each of the six samples collected each month to give 12 monthly samples (Figure 3.2). Mean moisture content following freeze drying was 1.0 ± 0.2 SD % DW for all replicated and homogenised samples (n = 162).

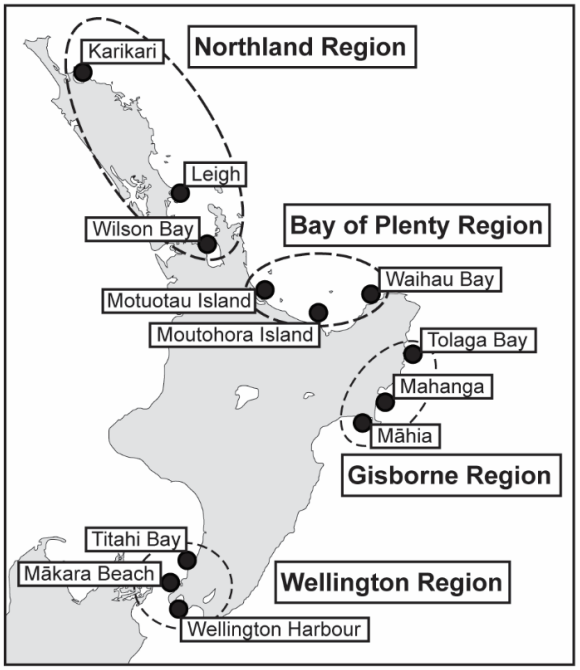

Figure 3.1 Sampling sites and sampling regions within the North Island of New Zealand

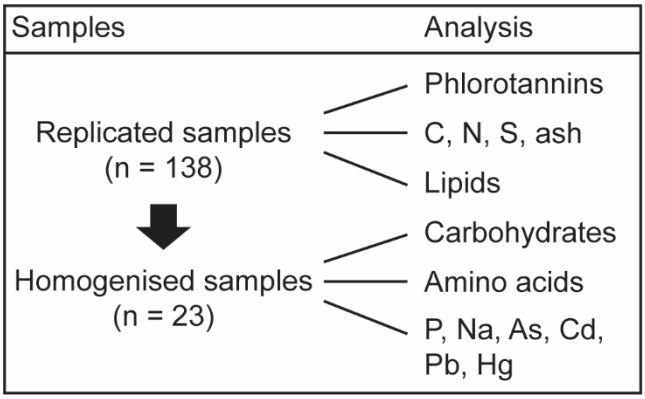

Figure 3.2 Overview of analyses of biomass components for replicated and homogenised samples. Homogenised samples were made from 2 g DW of each replicated sample, combining the six samples collected at each site and each sampling month

3.3.2 Constituent sugar content

Constituent sugars analysis was adapted and improved from Rozaklis et al. (2002) and Lorbeer et al. (2015). Dried milled biomass samples (10-11 mg weighed to 0.1 mg precision) were hydrolysed in 13 M sulfuric acid (300 µL) for 60 min with stirring, and then diluted with H_2O (3.6 mL) to 1 M sulfuric acid and heated at 100 °C for an additional 3 hours. Following neutralisation with 2 M NaOH (100 µL), hydrolysed samples (100 µL), with added 2-deoxy-D-glucose (40 µL of 10 mg/mL) as internal standard, were derivatised by addition of PMP-derivatising regent (400 µL of 250 mM 1-phenyl-3-methyl-5-pyrazolone with 400 mM NH_3) and heating at 70 °C over 90 min with constant

stirring. This solution was then neutralisation with 0.8 M formic acid (400 µL) and extracted with $CHCl_3$ (750 µL) to remove excess PMP. Finally, the supernatant was centrifuged (5 min at 16,200 rcf) and transferred to a 2 mL Shimadzu HPLC vial (Product #: 226-50512-00) for analysis. Derivatised monosaccharides were quantified using a Shimadzu Prominence LC-20AD (Japan) fitted with a Restek Raptor ARC-18 column (5 µm particle size, 5 µm, 150 x 4.6 mm, Catalogue #: 9314565) with an oven temperature of 30 °C and flow rate of 0.8 mL min^{-1}. Derivatised monosaccharides were separated after injection of 5 µL of sample by a isocratic/gradient elution with solvent A (0.1 M phosphate buffer at pH 7 in 10 % acetonitrile) and solvent B (0.1 M phosphate buffer at pH 7 in 17 % acetonitrile); 25 % solvent B for 15 min, linear increase from 25 % to 100 % solvent B over 25 min, 100 % solvent B for 15 min, and finally 25 % solvent B for 5 min. Derivatised monosaccharides were detected at 254 nm using a Photo Diode-Array detector. The sugars (D-glucose, L-guluronic acid, D-mannuronic acid, L-fucose, D-mannose, D-galactose, D-xylose, L-rhamnose, D-glucuronic acid, and L-arabinose) were identified from their relative retention times compared to the internal standard and quantified using response calibration curves generated from sugar standards with concentrations in the range of 0.01 – 1.0 mg mL^{-1}. The % DW and normalised mol % of each anhydro-sugar (as this is the form of sugar present in a polysaccharide) was presented. Total carbohydrates (% DW) were also calculated by deducting the percentages of lipid, protein, phlorotannin, and ash content from 100 %.

3.3.3 Phlorotannin content

Phlorotannin content was estimated as total phenols (Shrestha et al. 2021) which was measured using the Folin-Ciocalteu's phenol reagent method (Zhang et al. 2006) adjusted by diluting the extracts to 50 % concentration prior to the reaction and by incubating the reactants at 40 °C for 30 min at 100 rpm prior to absorbance reading at 750nm (SPECTROstar® Nano, BMG Labtech, Germany). Phloroglucinol was used as a reference standard, and the results were expressed as phloroglucinol equivalents (PGE, % of DW).

3.3.4 Amino acid content

Amino acid content was commercially analysed by the Australian Proteome Analysis Facility (Sydney, Australia; anhydro-amino acids) as described in Angell et al. (2014) and included all essential amino acids except cysteine (usually a minor constituent). Protein content was estimated as the sum of the 16 quantified amino acids (Angell et al. 2016) and a nitrogen to protein conversion factor was calculated from the nitrogen and protein content (Protein:N = Protein % DW / N % DW).

3.3.5 Ash and mineral content

Elemental analysis of carbon, hydrogen, nitrogen, and sulfur (CHNS), iodine, and content of ash were determined commercially by OEA labs Ltd (Exeter, UK). Contents of CHNS were determined by gas chromatography coupled to a thermal conductivity detector (GC-TCD), while contents of iodine were determined using ion chromatography (IC) following hydropyrolysis combustion. Content of ash was determined by micro-ashing (Prometheus Kilns® Pro1-PRG, Turkey). Further element analysis of phosphorous, potassium, arsenic, cadmium, lead, and mercury (and other minerals: Appendices 8 and 9) was analysed commercially at the University of Waikato Laboratory (Hamilton, New Zealand) by inductively coupled plasma (ICP) – mass spectroscopy (MS) on homogenised samples (n = 24).

3.3.6 Lipid content

Lipid content was quantified following Folch et al. (1957), as modified and described in Gosch et al. (2012), using dichloromethane and methanol solution at 60 °C for 1 hour for extraction, followed by microfiltration of the extract, and addition of 20 % (v/v) of a 0.9 % sodium chloride solution to separate the lipid fraction. Finally, the solvent was removed from the lipid fraction by heating at 40 °C in a heating block and the weight of the residue was recorded.

3.3.7 Data analysis

Data analyses were carried out in R-Studio (Team RStudio 2022) and PRIMER 7 (Clarke and Gorley 2015), and legibility of figures was improved in Adobe Illustrator. Significance of temporal patterns (November 2019 to November 2020) was analysed using Durbin-Watson's test (lmtest package in R-Studio) which returns a d-value from 0 to 4 where values of 0 to 2 indicate positive autocorrelation, values of 2 indicate no autocorrelation, and values of 2 to 4 indicate negative autocorrelation. Significance of spatial variation was analysed using permutational multivariate analysis of variance (PERMANOVA; as assumptions for analysis of variance (ANOVA) were not generally met) in PRIMER 7 and was calculated for all biomass components measured with replication (i.e., not components quantified from homogenised samples). A nested PERMANOVA design was chosen, testing for differences among regions (fixed factor) and sites nested within regions (random factor), and analyses were run with individual models for each biomass component, using Euclidian distance as distance measurement, and 9,999 unrestricted permutations of raw data. Some significant differences in dispersion were detected among sites and regions using test of homogeneity of dispersion (PERMDISP), however in many cases such differences will not significantly inflate the error rates of PERMANOVA (Anderson et al. 2016). Relationships between morphology and biomass composition were analysed using Pearson correlation coefficients and linear regression models in R-Studio, and correlations were visualised using the ggcorrplot package. Analysis of equal variance between spatial and temporal samples were calculated with Levene's test (car package in R-studio) using the mean value for each site and each monthly sample. Non-metric MDS was carried out in PRIMER 7 to assess overall patterns in biomass composition among sites within regions and among monthly samples. Data was square root transformed and normalised, and Euclidian distance was used as distance measurement, with 100 restarts and 1 Kruskal fit scheme for each plot.

3.4 Results

3.4.1 Spatial variation

High levels of spatial variation between sites were found for most quantified components of *E. radiata* biomass (Table 3.1). Significant differences between sites were found for all biomass components measured with replication, including total carbohydrates (range: 58.0 – 71.8 % DW, n = 72), phlorotannins (range: 4.8 – 9.3 % DW, n = 72), ash (range: 16.2 – 25.1 % DW, n = 72), nitrogen (range: 0.9 – 1.6 % DW, n = 72), and sulfur (range: 0.6 – 1.1 % DW, n = 72; Table 3.2). Among biomass components not measured with replication (i.e., spatial homogenised samples, n = 12; no statistical analysis), glucose content was highly variable among sites (range: 9.3 – 22.6 % DW, n = 12), whereas guluronic acid (range: 9.0 - 12.2 % DW, n = 12), mannuronic acid (range: 7.6 – 10.8 % DW, n = 12), fucose (range: 1.2 – 1.6 % DW, n = 12), and the mannuronic to guluronic ratio (M:G ratio, range: 0.75 – 0.99, n = 12) were more stable (Figure 3.3a). Concentrations of mannose, galactose and xylose were generally low (combined range: 0.3 - 0.9 % DW, n = 12), while rhamnose, glucuronic acid, and arabinose were also identified but at concentrations too low for consistent quantification. Proteins also varied substantially (range: 4.6 - 8.6 % DW, n = 12), with aspartic acid and glutamic acid being the most variable amino acids, varying two-fold among sites (range: 0.7 -1.2 and 0.8 – 1.7 % DW, respectively, n = 12; Table 3.3). Among minerals, a two-fold difference was detected for phosphorous (range: 0.09 – 0.19 % DW, n = 12) and potassium (range: 2.2 – 4.0 % DW, n = 12). Non-metric MDS showed limited spatial clustering among sites within regions (Figure 3.4a), and similarly, PERMANOVA showed no significant difference between regions (except for lipids; Table 3.2).

Table 3.1 Spatial variation in biomass content of *E. radiata* collected at 12 sites across the North Island of New Zealand with SD shown in brackets (n = 72 for components measured with replication and n = 12 for other components). Total carbohydrates (Carbs), phlorotannins (Phlo), proteins, ash, lipids, glucose (Glc), guluronic acid (GulA), mannuronic acid (ManA), fucose (Fuc), mannose (Man), galactose (Gal), xylose (Xyl), nitrogen (N), phosphorus (P), potassium (K), sulfur (S), and iodine (I) are shown as % DW. Arsenic (As), cadmium (Cd), lead (Pb), and mercury (Hg) are shown as ppm DW. M:G shows the mannuronic to guluronic acid ratio, Protein:N shows the nitrogen to protein conversion factor, and C:N shows the carbon to nitrogen ratio. Site abbreviations are: Karikari (Kari), Leigh (Leig), Wilson Bay (Wils), Motuotau Island (Motu), Moutohora Island (Mout), Waihau Bay (Waih), Tolaga Bay (Tola), Mahanga (Maha), Māhia (Māhi), Wellington Harbour (WH), Mākara Beach (Māka), and Titahi Bay (Tita)

	Kari	Leig	Wils	Motu	Mout	Waih	Tola	Māha	Mahi	WH	Māka	Tita	Mean
Carbs (%)	60.4	58.6	63.2	58 (2.6)	66.5	67.3	71.5	63.2	71.2	61.5	63.6	71.8	64.7 (4.9)
Phlo (%)	9.3 (1.8)	9.1 (1.3)	6.0 (0.7)	8.0 (2.3)	6.3 (0.6)	6.2 (1)	6.0 (1.0)	8.0 (1.4)	5.0 (0.6)	4.8 (0.9)	5.8 (0.8)	5.0 (1.0)	6.6 (1.6)
Protein (%)	6.8	6.6	5.3	8.6	5.6	5.2	4.6	6.1	5.5	7.8	6.4	5.2	6.1 (1.2)
Ash (%)	22.8	25.1	25 (1.9)	24.7	21.5	21 (2.7)	16.2	21.2	16.6	24.4	23.4	17.5	21.6 (3.3)
Lipids (%)	0.7 (0.3)	0.6 (0.3)	0.4 (0.2)	0.7 (0.3)	0.1 (0.1)	0.4 (0.1)	1.7 (0.2)	1.6 (0.1)	1.7 (0.3)	1.4 (0.6)	0.9 (0.4)	0.5 (0.2)	0.9 (0.6)
Glc (%)	11.8	9.5	9.8	9.3	15.3	13.5	22.6	10.1	18.8	12.4	10.9	21.5	13.8 (4.5)
GulA (%)	9.0	9.6	10.5	11.4	11.8	9.6	9.5	11.7	9.4	12.2	12.0	9.8	10.5 (1.1)
ManA (%)	7.6	8.9	10.4	8.9	8.9	9.0	8.5	10.8	9.4	10.0	10.7	9.1	9.4 (0.9)
Fuc (%)	1.4	1.6	1.3	1.4	1.3	1.3	1.2	1.3	1.5	1.5	1.3	1.2	1.4 (0.1)
Man (%)	0.7	0.8	0.8	0.8	0.8	0.8	0.7	0.9	0.8	0.8	0.9	0.7	0.8 (0.1)
Gal (%)	0.6	0.7	0.6	0.6	0.6	0.5	0.6	0.6	0.6	0.7	0.6	0.5	0.6 (0.1)
Xyl (%)	0.3	0.3	0.3	0.3	0.3	0.3	0.3	0.3	0.3	0.3	0.3	0.3	0.3 (0.0)
M:G	0.84	0.93	0.99	0.79	0.75	0.93	0.89	0.93	0.99	0.82	0.89	0.92	0.89 (0.07)
N (%)	1.4 (0.1)	1.3 (0.1)	1 (0.0)	1.6 (0.1)	1.1 (0.1)	1.1 (0.1)	0.9 (0.1)	1.1 (0.1)	1.1 (0.1)	1.5 (0.1)	1.3 (0.0)	1 (0.1)	1.2 (0.2)
P (%)	0.11	0.12	0.17	0.15	0.09	0.11	0.11	0.10	0.11	0.19	0.13	0.13	0.13 (0.03)
K (%)	3.3	3.7	3.9	4.0	3.2	2.8	2.2	3.2	2.4	3.8	3.7	2.5	3.2 (0.6)
S (%)	1.0 (0.1)	1.1 (0.1)	0.7 (0.0)	1.0 (0.1)	0.9 (0.1)	0.8 (0.1)	0.7 (0.1)	0.9 (0.0)	0.7 (0.1)	0.9 (0.1)	0.8 (0.1)	0.6 (0.1)	0.8 (0.1)
Protein:N	4.9	4.9	5.1	5.3	5.1	4.9	5.3	5.5	5.2	5.1	4.9	5.0	5.1 (0.2)
C:N	23.4	23.7	29.5	19.4	29.1	30.4	39.8	29.4	32.3	20.4	24.3	32.8	27.9 (5.9)
I (%)	0.34	0.38	0.40	0.48	0.55	0.44	0.60	0.61	0.46	0.73	0.57	0.66	0.52 (0.12)
As (ppm)	50.8	64.4	43.2	54.8	63.5	40.0	40.1	46.4	48.9	48.1	43.2	44.7	49 (8.2)
Cd (ppm)	1.3	2.2	0.5	1.9	1.5	0.8	0.8	1.5	1.3	1.2	1.4	0.4	1.2 (0.6)
Pb (ppm)	0.3	0.1	0.3	0.2	0.0	0.2	0.7	0.4	0.3	0.5	0.1	0.1	0.3 (0.2)
Hg (ppm)	0.00	0.00	0.04	0.02	0.03	0.01	0.03	0.02	0.03	0.01	0.01	0.01	0.02 (0.01)

Table 3.2 Permutational multivariate analysis of variance (PERMANOVA) between spatial samples of *E. radiata* (n = 72), testing for differences among regions and sites nested within regions for biomass components measured with replication. Significant differences in dispersion among sites and regions are marked with an asterisk and significant p-values are italicised

Source	df	SS	MS	Pseudo-F	P(perm)
Total carbs					
Regions	3	590.4	196.8	1.5	0.282
Sites (nested)	8	1018.4	127.3	18.8	*<0.001*
Res	60	406.8	6.8		
Total	71	2015.5			
Phlorotannins					
Regions	3	75.7	25.2	2.3	0.132
Sites (nested)	8	87.4	10.9	6.1	*<0.001*
Res	60	108.2	1.8		
Total	71	271.3			
Ash					
Regions	3	379.3	126.4	3.1	0.090
Sites (nested)	8	329.2	41.2	5.9	*<0.001*
Res	60	421.2	7.0		
Total	71	1129.7			
Lipids					
Regions	3	16.0	5.3	10.3	*0.007*
Sites (nested)	8	4.2	0.5	5.3	*<0.001*
Res	60	5.8	0.1		
Total	71	26.0			
Nitrogen					
Regions	3	0.9	0.3	1.0	0.465
Sites (nested)	8	2.6	0.3	32.8	*<0.001*
Res	60	0.6	0.0		
Total	71	4.1			
Sulfur					
Regions	3	0.4	0.1	1.7	0.257
Sites (nested)	8	0.7	0.1	10.1	*<0.001*
Res	60	0.5	0.0		
Total	71	1.5			

Table 3.3 Amino acids as % DW among spatial samples (all sites, homogenised samples, n = 12, top panel) and temporal samples (Motuotau Island only, homogenised samples, n = 12, lower panel). Amino acid abbreviations are histidine (His), serine (Ser), arginine (Arg), glycine (Gly), aspartic acid (Asp), glutamic acid (Glu), threonine (Thr), alanine (Ala), proline (Pro), lysine (Lys), tyrosine (Tyr), methionine (Met), valine (Val), isoleucine (Ile), leucine (Leu), and phenylalanine (Phe). Site abbreviations are Karikari (Kari), Leigh (Leig), Wilson Bay (Wils), Motuotau Island (Motu), Moutohora Island (Mout), Waihau Bay (Waih), Tolaga Bay (Tola), Mahanga (Maha), Māhia (Māhi), Wellington Harbour (WH), Mākara Beach (Māka), and Titahi Bay (Tita)

	Kari	Leig	Wils	Motu	Mout	Waih	Tola	Maha	Māhi	WH	Māka	Tita	mean (SD)
His	0.14	0.15	0.13	0.18	0.11	0.12	0.11	0.13	0.12	0.17	0.14	0.12	0.13 (0.02)
Ser	0.32	0.33	0.27	0.39	0.26	0.26	0.22	0.29	0.25	0.38	0.31	0.25	0.29 (0.05)
Arg	0.30	0.31	0.25	0.38	0.22	0.23	0.20	0.26	0.23	0.35	0.27	0.23	0.27 (0.05)
Gly	0.35	0.35	0.28	0.41	0.26	0.27	0.23	0.30	0.26	0.40	0.31	0.26	0.31 (0.06)
Asp	0.98	0.93	0.78	1.17	0.81	0.79	0.67	0.95	0.77	1.15	0.97	0.77	0.89 (0.15)
Glu	1.22	1.16	0.81	1.75	1.23	0.84	0.85	1.06	1.14	1.28	1.10	0.89	1.11 (0.25)
Thr	0.35	0.35	0.29	0.45	0.30	0.30	0.25	0.33	0.28	0.44	0.36	0.28	0.33 (0.06)
Ala	0.65	0.58	0.46	0.81	0.49	0.40	0.37	0.49	0.48	0.65	0.55	0.43	0.53 (0.12)
Pro	0.31	0.31	0.25	0.39	0.25	0.25	0.21	0.28	0.23	0.37	0.30	0.24	0.28 (0.05)
Lys	0.38	0.37	0.30	0.47	0.29	0.30	0.26	0.36	0.29	0.48	0.39	0.30	0.35 (0.07)
Tyr	0.14	0.13	0.12	0.18	0.11	0.12	0.11	0.13	0.12	0.20	0.15	0.12	0.13 (0.03)
Met	0.16	0.17	0.14	0.20	0.12	0.13	0.11	0.14	0.13	0.19	0.15	0.13	0.15 (0.03)
Val	0.39	0.39	0.32	0.48	0.30	0.32	0.27	0.36	0.30	0.47	0.37	0.31	0.36 (0.06)
Ile	0.29	0.29	0.24	0.35	0.22	0.22	0.19	0.25	0.22	0.34	0.27	0.22	0.26 (0.05)
Leu	0.49	0.50	0.41	0.60	0.36	0.38	0.34	0.44	0.38	0.57	0.45	0.38	0.44 (0.08)
Phe	0.33	0.33	0.27	0.39	0.24	0.26	0.23	0.30	0.26	0.39	0.31	0.26	0.30 (0.05)

	Nov	Dec	Jan	Feb	Mar	May	Jun	Jul	Aug	Sep	Oct	Nov	mean (SD)
His	0.14	0.15	0.14	0.12	0.11	0.11	0.12	0.12	0.12	0.13	0.15	0.15	0.13 (0.01)
Ser	0.34	0.34	0.34	0.28	0.25	0.27	0.30	0.29	0.32	0.33	0.36	0.35	0.32 (0.03)
Arg	0.32	0.32	0.31	0.24	0.22	0.22	0.25	0.23	0.26	0.27	0.32	0.32	0.27 (0.04)
Gly	0.36	0.36	0.35	0.28	0.26	0.28	0.31	0.29	0.32	0.33	0.37	0.36	0.32 (0.04)
Asp	1.01	1.00	0.98	0.80	0.75	0.80	0.90	0.91	0.97	1.01	1.04	1.00	0.93 (0.10)
Glu	1.53	1.71	1.65	1.57	1.32	1.13	1.08	1.23	1.10	1.04	1.14	1.10	1.30 (0.24)
Thr	0.40	0.38	0.38	0.32	0.29	0.31	0.35	0.35	0.38	0.39	0.41	0.39	0.36 (0.04)
Ala	0.71	0.74	0.70	0.61	0.51	0.50	0.50	0.52	0.49	0.52	0.61	0.56	0.58 (0.09)
Pro	0.34	0.34	0.34	0.28	0.26	0.27	0.30	0.29	0.32	0.33	0.35	0.34	0.31 (0.03)
Lys	0.41	0.41	0.40	0.32	0.29	0.30	0.34	0.33	0.35	0.36	0.40	0.41	0.36 (0.04)
Tyr	0.16	0.15	0.15	0.12	0.10	0.11	0.13	0.13	0.14	0.14	0.16	0.14	0.14 (0.02)
Met	0.17	0.17	0.17	0.13	0.12	0.12	0.13	0.13	0.14	0.14	0.17	0.17	0.14 (0.02)
Val	0.42	0.41	0.40	0.33	0.29	0.31	0.35	0.33	0.36	0.38	0.41	0.41	0.37 (0.040
Ile	0.30	0.30	0.30	0.24	0.21	0.23	0.25	0.23	0.25	0.27	0.30	0.30	0.27 (0.03)
Leu	0.51	0.52	0.51	0.40	0.36	0.38	0.42	0.40	0.44	0.45	0.52	0.51	0.45 (0.06)
Phe	0.34	0.34	0.34	0.27	0.24	0.26	0.29	0.27	0.30	0.31	0.35	0.34	0.30 (0.04)

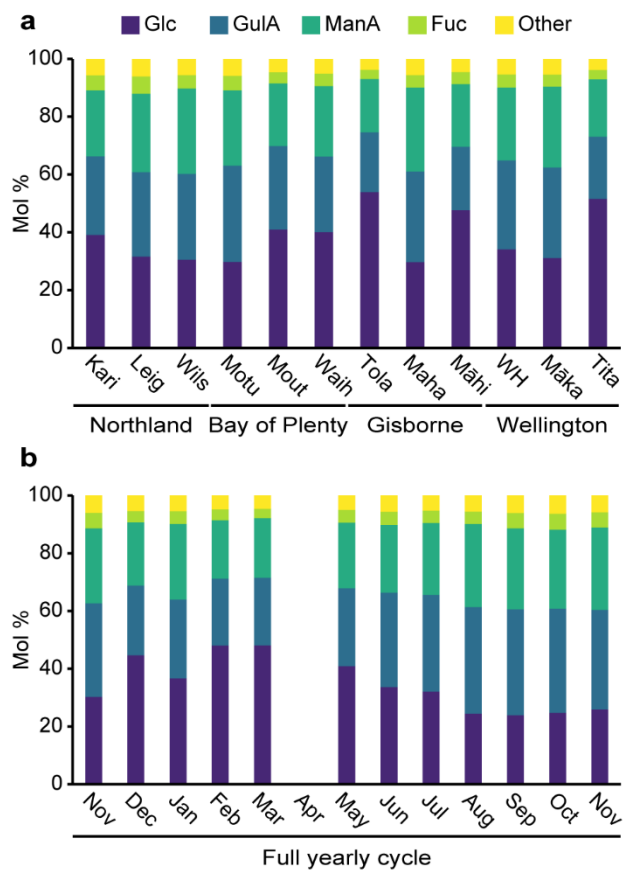

Figure 3.3 Mole percent (mol %) of quantified sugars: glucose (Glu), guluronic acid (GulA), mannuronic acid (ManA), fucose (Fuc), and other sugars (mannose, galactose, and xylose) of (a) spatial homogenised samples among sites (n = 12) and (b) monthly homogenised samples at Motuotau Island (n = 12). Site abbreviations are: Karikari (Kari), Leigh (Leig), Wilson Bay (Wils), Motuotau Island (Motu), Moutohora Island (Mout), Waihau Bay (Waih), Tolaga Bay (Tola), Mahanga (Maha), Māhia (Māhi), Wellington Harbour (WH), Mākara Beach (Māka), and Titahi Bay (Tita)

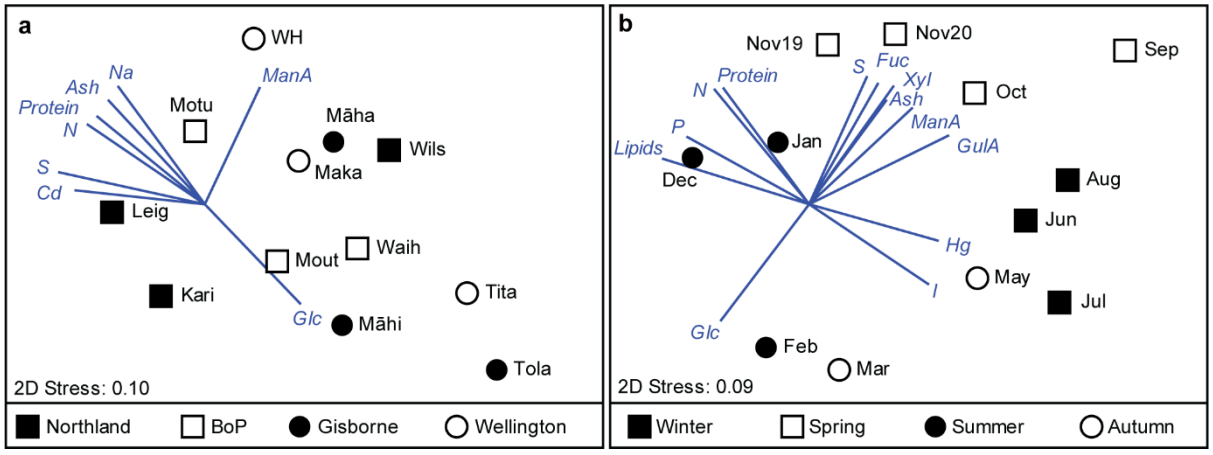

Figure 3.4 Non-metric multi-dimensional scaling (MDS) of biomass composition of *E. radiata* using all 20 measured biomass components (a) among sites within regions (n = 12) and (b) among monthly samples (n = 12). Vectors are shown for biomass components showing > 0.8 correlation (Pearson correlation coefficient). Site and region abbreviations are: Bay of plenty (BoP), Karikari (Kari), Leigh (Leig), Wilson Bay (Wils), Motuotau Island (Motu), Moutohora Island (Mout), Waihau Bay (Waih), Tolaga Bay (Tola), Mahanga (Maha), Māhia (Māhi), Wellington Harbour (WH), Mākara Beach (Māka), and Titahi Bay (Tita). Component abbreviations are: glucose (Glc), guluronic acid (GulA), mannuronic acid (ManA), fucose (Fuc), xylose (Xyl), nitrogen (N), phosphorous (P), potassium (Na), sulfur (S), iodine (I), cadmium (Cd), and mercury (Hg)

3.4.2 Temporal variation

There were significant temporal patterns in the content of glucose, guluronic acid, proteins, nitrogen, lipids, phosphorous, iodine, arsenic, and mercury, and for the M:G ratio (Tables 3.4 and 3.5). The two main sugars, glucose (range: 7.7 – 18.2 % DW, n = 12) and guluronic acid (range: 8.8 – 13.7 % DW, n = 12), showed an inverse relationship where guluronic acid peaked in austral spring but was low during austral summer/autumn and glucose peaked in early austral autumn but was low during austral spring (Figure 3.3b). The M:G ratio (range: 0.72 – 0.96, n = 12) varied with the content of guluronic acid, with the highest in austral summer and lowest in austral winter. Proteins (range: 5.6 – 7.6 % DW, n = 12) and lipids (range: 0.1 - 1.6 % DW, n = 72) showed a unimodal relationship with highest content in late austral spring/early summer and lowest content in austral autumn/winter. Among amino acids, glutamic acid, and aspartic acid (range: 1.0 – 1.7 % DW and 0.7 - 1.0 % DW, respectively, n = 12) were most abundant and accounted for more than 30% of total amino acids on average across a full year (Table 3.3). The content of nitrogen (range: 1.2 – 1.6 % DW, n =72) and phosphorous (range: 0.08 – 0.14 % DW, n = 12) followed a similar pattern, both being higher in late austral spring/early summer and low in austral autumn/winter. Accordingly, the average nitrogen to protein conversion factor (Protein:N) across all sites and months was 4.9 ± 0.4 SD (n = 23), with no significant temporal pattern (Table 3.5). Iodine, arsenic, and mercury (range: 0.46 – 1.06 % DW, 52.5 – 77.4 ppm DW, and 0.01 – 0.03 ppm DW, respectively, n = 12) also followed a unimodal pattern with highest content in late austral autumn/early winter and lowest content in late austral spring/early summer. Non-metric MDS showed a clear circular pattern among monthly samples demonstrating strong temporal correlation in biomass composition (Figure 3.4b). No significant temporal variability was found for total carbohydrates, mannuronic acid, fucose, mannose, galactose, xylose, phlorotannins, ash, potassium, sulfur, cadmium, or lead (Table 3.5).

Table 3.4 Temporal variation in biomass content of *E. radiata* collected monthly at Motuotau Island in New Zealand from November 2019 to November 2020 with SD shown in brackets (n = 72 for components measured with replication and n = 12 for other components). Total carbohydrates (Carbs), phlorotannins (Phlo), proteins, ash, lipids, glucose (Glc), guluronic acid (GulA), mannuronic acid (ManA), fucose (Fuc), mannose (Man), galactose (Gal), xylose (Xyl), nitrogen (N), phosphorus (P), potassium (K), sulfur (S), and iodine (I) are shown as % DW. Arsenic (As), cadmium (Cd), lead (Pb), and mercury (Hg) are shown as ppm DW. M:G shows the mannuronic to guluronic acid ratio, Protein:N shows the nitrogen to protein conversion factor, and C:N shows the carbon to nitrogen ratio

	Nov	Dec	Jan	Feb	Mar	May	Jun	Jul	Aug	Sep	Oct	Nov	Mean
Carbs (%)	59.3 (4.2)	58.2	57.5	63.6	63.7	62.8	58 (1.7)	60 (2.8)	60 (4.1)	59.5	58.6	53.8	59.7 (2.9)
Phlo (%)	7.9 (2.1)	9.3 (1.1)	8.8 (1.2)	8.5 (1.2)	9.3 (1.1)	8.1 (1.1)	9.0 (1.8)	7.8 (1.1)	8.5 (1.7)	7.6 (1.8)	7.6 (0.5)	9.5 (1.4)	8.5 (0.7)
Protein (%)	7.5	7.6	7.5	6.3	5.6	5.6	6.0	6.1	6.3	6.4	7.1	6.9	6.6 (0.7)
Ash (%)	23.7 (4.9)	23.4	25.1	20.8	20.8	23.2	26.7	25.9	24.9	26.4	26.1	29.0	24.7 (2.4)
Lipids (%)	1.6 (0.3)	1.5 (0.2)	1.1 (0.5)	0.8 (0.2)	0.5 (0.4)	0.3 (0.3)	0.3 (0.1)	0.2 (0.2)	0.3 (0.3)	0.1 (0.2)	0.6 (0.3)	0.8 (0.2)	0.7 (0.5)
Glc (%)	9.6	15.0	11.6	16.6	18.2	14.8	11.4	10.1	7.8	8.1	7.7	7.9	11.6 (3.6)
GulA (%)	11.3	8.9	9.4	8.8	9.7	10.7	12.2	11.5	13.0	13.7	12.3	11.6	11.1 (1.5)
ManA (%)	9.0	8.1	9.1	7.7	8.5	9.0	8.8	8.6	10.1	10.5	9.3	9.6	9.0 (0.8)
Fuc (%)	1.5	1.2	1.2	1.1	1.1	1.4	1.3	1.2	1.2	1.6	1.5	1.4	1.3 (0.2)
Man (%)	0.8	0.8	0.7	0.7	0.8	0.8	0.9	0.7	0.8	1.0	0.9	0.8	0.8 (0.1)
Gal (%)	0.6	0.7	0.6	0.6	0.6	0.6	0.6	0.6	0.5	0.6	0.6	0.6	0.6 (0.0)
Xyl (%)	0.3	0.3	0.3	0.3	0.3	0.3	0.3	0.3	0.3	0.4	0.3	0.3	0.3 (0.0)
M:G	0.80	0.91	0.96	0.88	0.88	0.84	0.72	0.74	0.78	0.76	0.76	0.83	0.82 (0.07)
N (%)	1.6 (0.2)	1.6 (0.1)	1.6 (0.1)	1.3 (0.1)	1.2 (0.1)	1.2 (0.1)	1.3 (0.1)	1.3 (0.1)	1.3 (0.1)	1.3 (0.1)	1.5 (0.0)	1.5 (0.1)	1.4 (0.1)
P (%)	0.12	0.14	0.14	0.11	0.09	0.08	0.09	0.10	0.08	0.09	0.12	0.12	0.11 (0.02)
K (%)	3.8	3.4	3.7	3.1	3.1	3.7	4.2	4.1	3.5	3.8	4.0	4.0	3.7 (0.4)
S (%)	1.1 (0.1)	1.0 (0.1)	1.0 (0.1)	0.9 (0.0)	1.0 (0.1)	1.0 (0.0)	1.1 (0.1)	1.0 (0.1)	1.1 (0.1)	1.1 (0.1)	1.0 (0.1)	1.1 (0.1)	1.0 (0.1)
Protein:N	4.4	4.9	4.8	4.5	4.6	4.7	4.3	4.7	4.8	4.8	4.7	4.6	4.7 (0.1)
C:N	19.6	20.6	20.6	25.1	26.4	26.3	24.1	24.3	24.2	22.7	20.6	21.0	23 (2.4)
I (%)	0.51	0.51	0.55	0.64	0.67	1.02	1.04	1.06	0.76	0.83	0.66	0.46	0.73 (0.22)
As (ppm)	52.5	60.9	54.6	53.0	54.1	61.9	67.9	77.4	61.6	56.6	62.1	58.2	60.1 (7.2)
Cd (ppm)	1.9	2.0	1.9	1.7	1.7	1.5	2.0	1.4	1.3	1.2	1.5	1.6	1.7 (0.3)
Pb (ppm)	0.3	0.1	0.1	0.3	0.0	0.1	0.2	0.1	0.1	0.2	0.1	0.2	0.1 (0.1)
Hg (ppm)	0.01	0.01	0.01	0.01	0.02	0.03	0.03	0.02	0.03	0.02	0.02	0.01	0.02 (0.01)

3.4.3 Spatial *vs.* temporal variation

The variation between spatial samples was significantly higher than the variation between temporal samples for sulfur, C:N ratio, lead, and mercury (Appendix 10). No other biomass components showed significant difference between spatial and temporal variation, although the standard deviations between sites were higher than the standard deviations between months for most components (Tables 3.1 and 3.4).

3.4.4 Morphology

Seaweed size was significantly positively correlated with glucose content (linear regression: $F_{(1,21)}$ =18.12, p <0.001, R^2 = 0.46, n = 23; Figure 3.5) but significantly negatively correlated with guluronic acid, mannuronic acid, and fucose content (highest correlation: fucose; linear regression: $F_{(1,21)}$ = 11.01, p = 0.003, R^2 = 0.34, n = 23). Phlorotannin content was significantly negatively correlated with lamina length (linear regression: $F_{(1,21)}$ = 15.13, p <0.001, R^2 = 0.42, n = 23). Furthermore, content of sulfur, iodine, and arsenic were all significantly positively correlated with stipe weight (highest correlation: arsenic; linear regression: $F_{(1,21)}$ = 25.49, p <0.001, R^2 = 0.55, n = 23), whereas phosphorus content was significantly positively correlated with blade length (linear regression: $F_{(1,21)}$ = 8.00, p = 0.010, R^2 = 0.28, n = 23). Overall, solids to moisture ratio was high with low variation across replicated samples: 0.20 ± 0.002 SE DW/WW (n = 138).

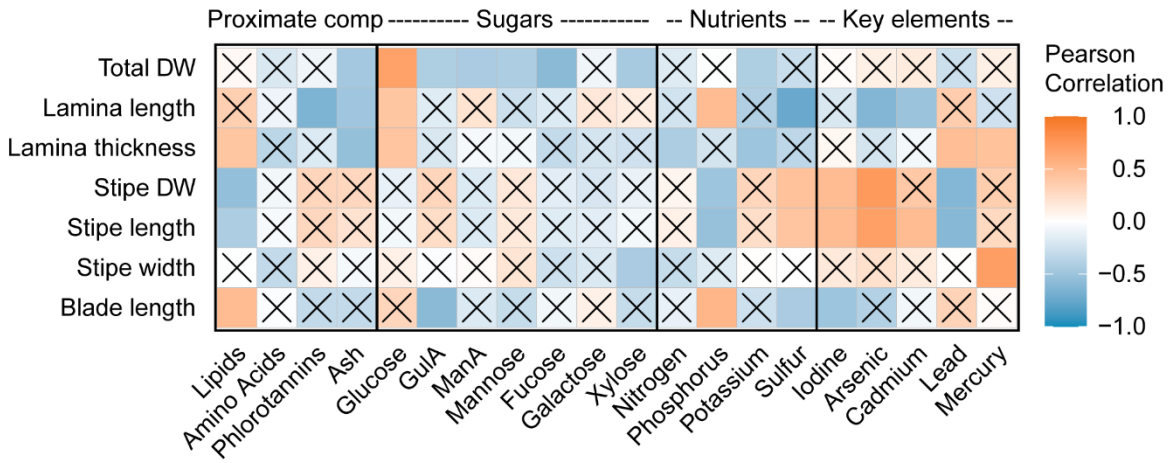

Figure 3.5 Correlation matrix between morphology and biomass composition of *E. radiata* (n = 23) calculated by Pearson correlation coefficient (r). Orange boxes indicate positive correlation and blue boxes indicate negative correlation. Non-significant correlations are marked with an X (α = 0.05)

3.5 Discussion

3.5.1 Biomass composition of *E. radiata*

Ecklonia radiata contains a range of biomass components with commercial potential and may be marketed fresh for human consumption (e.g., Pacific Harvest, New Zealand), processed for extraction of specific components, or fermented for producing biostimulant plant tonics and food products (Battacharyya et al. 2015; Bradly et al. 2021; FAO 2022). In this regard, within the North Island of New Zealand, the major components of *E. radiata* included carbohydrates (mean: 62.4 ± 5.3 SD % DW, n = 23), phlorotannins (7.5 ± 2.0 SD % DW, n = 138), proteins (6.3 ± 0.9 SD % DW, n = 23), and ash (mean: 23.1 ± 4.0 SD % DW, n = 138), with minor contributions from lipids (0.8 ± 0.6 SD % DW, n = 138).

Mannuronic and guluronic acid (syn. alginate; Szekalska et al. 2016) constituted the majority of the quantified sugars (combined mean: 53.6 ± 7.8 SD mol % of total sugars, equivalent to 20.0 ± 2.1 SD % DW, n = 23) and was similar to the commercially cultivated northern hemisphere species *Saccharina latissima* and *Laminaria digitata* (Table 3.6) . The M:G ratio of *E. radiata* was low (range: 0.72 – 1.00, n = 23) compared to *E. radiata* from Australia (range: 1.18 – 1.59; Lorbeer et al. 2017)

and compared to *S. latissima* and *L. digitata* (Table 3.6). Alginate with low M:G ratios (high in guluronic acid) forms stronger and more rigid gels, and our results therefore indicate high quality alginate in New Zealand *E. radiata* (McHugh 2003; Porse and Rudolph 2017). Fucose constituted a smaller fraction of the quantified sugars (mean: 4.4 ± 0.7 SD mol % of total sugars, equivalent to 1.3 ± 0.2 SD % DW, n = 23), half of that in *S. latissima* and *L. digitata* (Table 3.6). Assuming a similar composition of fucoidan as in *Ecklonia maxima* (Sichert et al. 2020) the fucose content in *E. radiata* equates to up to 3.9 % DW of fucoidan. The content of glucose (a component of laminarin; Stewart et al. 1961) in *E. radiata* biomass (range: 23.9 – 53.9 mol % of total sugars, equivalent to 7.7 – 22.6 % DW, n = 23) was similar to that of *S. latissima*, but at the lower end of the range recorded for *L. digitata* (Table 3.6). Overall, the carbohydrate composition *E. radiata* was similar to these commercial northern hemisphere species, although such comparisons may differ between sites (Manns et al. 2017). The inferred levels of alginate, fucoidan, and laminarin (see discussion below) are in accordance with previous findings for *E. radiata* in Australia (Stewart et al. 1961) and contribute significantly to the value of this biomass.

Levels of phlorotannins (range: 3.6 – 12.4 % DW, n = 138) were 10-fold higher than in *S. latissima* and other commercial northern hemisphere species (Schiener et al. 2015; Vilg et al. 2015), but not as high as other sub-tropical browns such as the fucoids *Carpophyllum sp.* and *Cystophora sp.* (mean: 13.4 % DW and 10.4 % DW, respectively; Magnusson et al. 2017). Phlorotannins have substantial commercial potential for cosmetics, functional foods, and biostimulants, given their bioactive activities which includes antioxidant, antimicrobial, antiviral and anti-inflammatory properties (Shrestha et al. 2021).

The content of protein (as total amino acids, range: 4.6 – 7.8 % DW, n = 23) was similar to *S. latissima* and *L. digitata* (Table 3.6), with glutamic acid (mean: 15.5 ± 2.2 SD mol % of total amino acids, n = 23), aspartic acid (mean: 13.3 ± 0.7 SD mol % of total amino acids, n = 23), and alanine (mean: 12.7 ± 0.9 SD mol % of total amino acids, n = 23) also being the dominant amino acids as in *S.*

latissima (Sharma et al. 2018). Conversely, the maximum nitrogen (mean: 1.3 ± 0.2 SD N % DW, n = 138) and phosphorus (mean: 0.11 ± 0.02 P SD % DW, n = 23) contents of *E. radiata* were approximately 2-fold and 5-fold lower, respectively, than that of northern hemisphere kelp species (Table 3.6). However, contents of protein and nitrogen were strongly correlated (linear regression: $F_{(1,21)} = 259.7$, $p < 0.001$, $R^2 = 0.93$; Table 3.5) allowing the calculation of a species specific nitrogen-to-protein conversion factor (Protein:N) for *E. radiata* of 4.9 ± 0.4 SD (n = 23), which was not significantly affected by temporal change (Table 3.5) and very close to the universal seaweed nitrogen-to-protein conversion factor of 4.76 proposed by Angell et al. (2016).

Potentially harmful levels of minerals such as iodine, arsenic, cadmium, lead, and mercury can accumulate in seaweed biomasses, with the risk dependent on the water quality of the growth environment (FAO and WHO 2022; Hahn et al. 2022). Total arsenic contents (mean: 54.5 ± 9.6 SD ppm DW, n = 23) exceeded the threshold set by Food Standards Australia New Zealand (FSANZ) of 1 ppm (FSANZ 2019). However, arsenic is only considered toxic to humans in its inorganic form, and the calculated inorganic arsenic (mean: 0.5 ± 0.1 SD ppm DW, n = 23, estimated as 1 % of total arsenic; Tukai et al. 2002) was 2-fold below the threshold of 1 ppm. The content of iodine and cadmium in *E. radiata* (mean: 6.3 ± 2.0 SD % DW and 1.4 ± 0.5 SD ppm DW, respectively, n = 23) exceeded the recommended threshold values set by the French Agency for Food, Environmental and Occupational Health and Safety (ANSES) for these elements by more than 3-fold (2 % and 0.5 ppm, respectively), while the content of lead and mercury (mean: 0.2 ± 0.2 SD ppm DW and 0.02 ± 0.01 SD ppm DW, respectively, n = 23) were below the threshold (5 and 0.1 ppm, respectively; ANSES 2018, 2020). Cadmium exceeded the recommended threshold level set by ANSES (ANSES 2020), however, to exceed the provisional tolerable intake limit for cadmium (25 µg kg^{-1} bodyweight $month^{-1}$) set by the World Health Organisation (WHO 2011) a 65 kg adult would need to consume 190 g WW *E. radiata* day^{-1}. This level of seaweed consumption is considerably higher than the average intake per capita in Japan of 10.4 g seaweed per day (Murai et al. 2021) and is unlikely to occur. Furthermore, blanching is a common processing technique when preparing seaweed for consumption and may

reduce iodine content by over 90 % (Stévant et al. 2018; Nielsen et al. 2020), which would reduce iodine levels in *E. radiata* below those set by ANSES (ANSES 2018). Overall, our results indicate that *E. radiata* is suitable for human consumption if consumed within intake limits and/or with appropriate processing.

Table 3.5 Biomass composition (% DW) of *E. radiata* and commercial northern hemisphere species *S. latissima* and *L. digitata* with mean values followed by seasonal range in brackets (Manns et al. 2014, 2017; Marinho et al. 2015; Schiener et al. 2015; Sharma et al. 2018). Data estimated from graphs are noted with an asterisk. The seasonal range of laminarin was estimated as the variable seasonal range of glucose minus 2 % DW to account for fluctuation of cellulose and is noted with a double asterisk (Black 1950; Stewart et al. 1961)

Component	*E. radiata*	*S. latissima*	*L. digitata*	Reference
Glucose	12.8 (7.7-18.2)	(3-22)*	(6-54.0)*	Manns et al. 2017
Laminarin	(0-9)**	8.2 (1-14)*	6.7 (1-17)*	Schiener et al. 2015
Alginate	20.0 (16.5-24.2)	28.5 (16-31)*	34.6 (16-31)*	Schiener et al. 2015
M:G ratio	0.86 (0.72-0.96)	(1.33-3.53)	(1.47-3.64)	Manns et al. 2017
Fucose	1.3 (1.1-1.6)	2.9	2.4	Manns et al. 2014
Phlorotannins	7.5 (5.2-12.4)	0.41 (0.23-0.68)	0.15 (0.09-0.18)	Schiener et al. 2015
Protein	6.3 (5.6-7.6)	11.0 (5.1-9.9)	6.9 (4.9-8.2)	Schiener et al. 2015
Glutamic acid	1.2 (1.0-1.7)	(1.68-2.97)		Shama et al. 2018
Aspartic acid	0.9 (0.7-1.0)	(1.40-2.38)		Shama et al. 2018
Alanine	0.5 (0.5-0.7)	(0.92-1.91)		Shama et al. 2018
Ash	23.1 (20.8-29.0)	(20-41)*	(11-30)*	Manns et al. 2017
Nitrogen	1.3 (1.1-1.8)	(0.5-3.1)		Marinho et al. 2015
Phosphorous	0.11 (0.08-0.14)	(0.05-0.82)		Marinho et al. 2015

3.5.2 Spatial and temporal variation in biomass composition

Spatial and temporal variation in biomass composition can affect the quality of the biomass and therefore have significant implications for the aquaculture of *E. radiata* in New Zealand. Significant spatial variation in the biomass composition of *E. radiata* was detected between sites within the North Island of New Zealand (Table 3.2). However, no significant differences were found between regions (except for lipids), no clear spatial trends were detected for biomass composition (Fig 4a), and even sites in close proximity differed substantially in terms of their biomass composition (e.g., Mākara Beach and Titahi Bay: 19 km distance). Consequently, the large variation in biomass composition among sites is likely explained by local rather than regional differences. *Ecklonia radiata* is highly plastic and can express very different morphologies over short distances in

response to changing environmental conditions (Fowler-Walker et al. 2006). Changes in lipids, phlorotannins, polysaccharides, and minerals were significantly correlated to stipe, lamina, and blade morphology. Hence, differences in biomass composition may be related to local morphological differences. However, these correlations between morphology and biomass content were mostly relatively weak. Therefore, the large variation in biomass composition between sites is likely caused by other underlying factors such as differences in environmental conditions (e.g., temperature, water chemistry, wave action) and possibly genetic variations (discussed below). For instance, biosynthetic regulation of the ratio between mannuronic and guluronic acid is an essential mechanism in brown algae for controlling strength and flexibility of tissue structure (Indergaard et al. 1990), indicating that alginate composition and abundance may vary between exposed and sheltered sites (Munda 1987; McHugh 2003). Furthermore, nutrient availability is highly variable within the North Island of New Zealand (Plew et al. 2018) which may cause changes in protein and carbohydrate content (Roleda and Hurd 2019). Site-specific environmental conditions thus likely play an important role in the biomass composition of *E. radiata* on the North Island of New Zealand.

Overall, spatial variation among sites was higher than temporal variation between monthly samples for most biomass components (Appendix 10), indicating that geographic variation is higher than temporal variation. Genetic differences between sub-populations could be contributing to the large geographical variation, as the genetic structure of *E. radiata* is strong within the North Island of New Zealand with sharp differentiation between the Wellington region and the other regions, and with further differentiation between most sites at a local level (Chapter 2/Nepper-Davidsen et al. 2021). Additionally, differences in biomass components such as phlorotannins and lipids have previously been linked to changes in genotype (Honkanen and Jormalainen 2005; Gosch et al. 2015). However, the strong regional patterns evident in the genetic structure (Chapter 2/Nepper-Davidsen et al. 2021) were not reflected in biomass composition here, as the Wellington sites did not stand out from the other sites using clustering analysis (Figure 3.4a). To further investigate the matter common-garden experiments (De Villemereuil et al. 2016) are needed.

Significant temporal variation was also evident for several important biomass components of *E. radiata* within the North Island of New Zealand, similar to previous findings for *E. radiata* in Australia (Stewart et al. 1961) and for *S. latissima* and *L. digitata* in northern Europe (Manns et al. 2017). Alginate and fucoidan both peaked in early austral spring, while proteins, lipids, nitrogen and phosphorous peaked in late austral spring/early summer, and total carbohydrates and glucose peaked in early austral autumn. Water temperature is recognised as a key driver of the temporal variation in the biomass composition of seaweeds (compared to nitrogen, phosphorous, and salinity; Manns et al. 2017), and the observed temporal variation in the current study provides further support for strong environmental effects on the composition of *E. radiata* biomass.

Glucose is the main constituent of laminarin - a primary energy storage polysaccharide - and the glucose content of *E. radiata* followed a similar pattern as laminarin in other kelp species, where it builds up during boreal summer and autumn and depletes during boreal winter (Schiener et al. 2015). Furthermore, the temporal changes in glucose content detected in this study (range: 7.7 - 18.2 % DW, n = 12) correspond to the temporal change in laminarin content previously found for *E. radiata* in Australia (range: 0.0 – 9.8 % DW; Stewart et al. 1961). Glucose is also the main constituent of cellulose - a structural polysaccharide – however, as cellulose content is usually relatively stable throughout the year (1-2 % DW yearly fluctuation; Black 1950) the observed temporal changes in glucose content mainly reflect fluctuations in laminarin content.

3.5.3 Implications for aquaculture

The composition of *E. radiata* biomass was highly site-specific and showed large spatial variation in key commercial components, likely related to local differences in environmental conditions. Chapter 2 (Nepper-Davidsen et al. 2021) recommends not to translocate cultivars of *E. radiata* outside of their area of origin on the North Island of New Zealand to preserve the strong genetic structure of wild populations of this kelp. The biomass composition of local broodstock may therefore be of central importance for optimising the yield of targeted commercial components

when choosing sites for seaweed aquaculture. The biomass content of key commercial components also showed significant temporal variation, underlining the importance of harvest timing for optimising yield depending on the biomass components of interest. We suggest early austral spring harvest for high contents of alginate and fucoidan and late austral spring/early summer harvest for proteins and lipids, with the precaution that seasonal patterns may vary between sites (Jennings and Steinberg 1994; Manns et al. 2017). Total carbohydrates and glucose peaked in early austral autumn, but heavy fouling and high temperatures during austral summer may lower the overall yield and value of the biomass (Handå et al. 2013; Wernberg et al. 2019).

The ratio between carbon and nitrogen content (C:N) in kelp is an indicator of nitrogen availability for primary production, with ratios >20 indicating nitrogen limited growth (Wernberg et al. 2019). The C:N ratio for *E. radiata* biomass (mean: 25.8 ± 5.4 SD, n = 138) was above 20 during most of the year and at most sites, indicating a high degree of nitrogen limitation both spatially and temporally (Tables 3.1 and 3.4). Cultivation in areas of high nutrient loads such as those affected by terrestrial runoff or downstream of animal aquaculture could be used to increase growth and simultaneously reduce the effects of nutrient run-off (Handå et al. 2013; Roleda and Hurd 2019). Indeed, based on the nitrogen and phosphorus contents in the biomass, cultivation of *E. radiata* could remove an estimated 164.6 kg N ha^{-1} and 14.7 kg P ha^{-1} per year (see Appendix 11 for calculations).

In conclusion*, E. radiata* had comparable biomass composition to that of commercial northern hemisphere species such as *S. latissima* and *L. digitata* and could be a viable southern hemisphere alternative for a broad range of commercial applications including extraction of phlorotannins, laminarin, and alginate, markets for human and animal consumption, and production of biostimulants.

Chapter 4

Chemometric models for high-throughput biomass grading of the kelp *Ecklonia radiata*, using mid-infrared (MIR) and near-infrared (NIR) spectroscopy.

This chapter is currently under review for publication in Algal Research as:

Nepper-Davidsen J, Magnusson M, Lawton RJ, Fletcher D, Holmes G, Glasson CRK (2023) Chemometric models for high-throughput biomass grading of the kelp *Ecklonia radiata*, using mid-infrared (MIR) and near-infrared (NIR) spectroscopy.

4.1 Abstract

The kelp *Ecklonia radiata* is a target species for aquaculture in the southern hemisphere, but the biomass quality varies both spatially and temporally, making high-throughput chemometric methods essential for biomass grading. We built partial least squared regression models and partial least squared discriminant analysis models using mid-infrared and near-infrared spectroscopy, based on 162 calibration samples and 24 validation samples. The near-infrared models generally outperformed the mid-infrared models based on both predictions and sensitivity to outliers. Near-infrared partial least squared regression models were highly accurate for predicting glucose, alginate, phlorotannins, and carbon content (relative prediction error < 8 %) and the near-infrared partial least squared discriminant analysis could accurately predict region of origin for Wellington samples (zero false negatives and one false positive). Overall, our results demonstrate that near-infrared and mid-infrared spectroscopy are valuable tools for biomass grading of raw seaweed samples and can be used for establishing provenance.

4.1.1 Graphical abstract

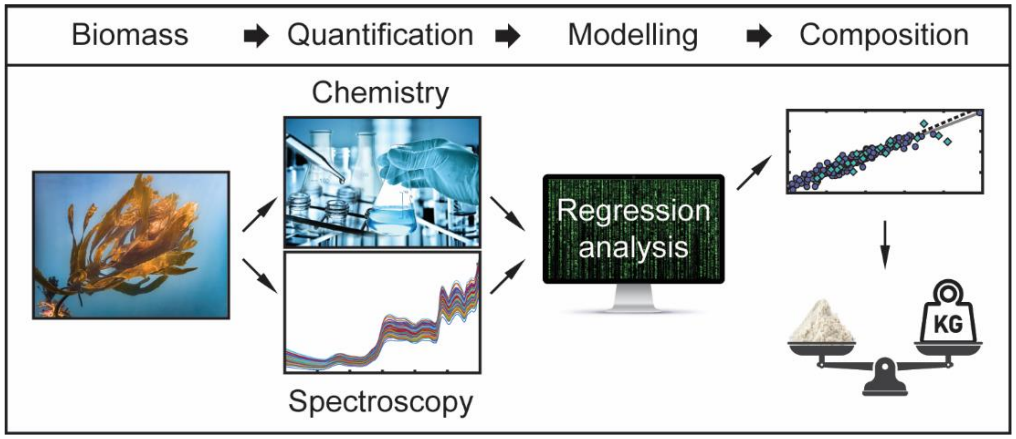

Graphical abstract illustrations are licensed from Totojang1977, TanyaJoy, New Africa, IProPav, StockVector, and Can Yesil – stock.adobe.com

4.2 Introduction

The kelp *Ecklonia radiata* is a southern hemisphere alternative to commercially grown northern hemisphere species for production of biomolecules unique to brown seaweed such as alginate, fucoidan, phlorotannins, and laminarin (Chapter 3/Nepper-Davidsen et al. 2023). Alginate, a heteropolymer of β-D-mannuronic acid and α-L-guluronic acid, is the most abundant polysaccharide in *E. radiata* biomass (range: 29.3-44.0 % DW, Lorbeer et al. 2017; range: 16.5-24.2 % DW, Chapter 3/Nepper-Davidsen et al. 2023) and is used in food products, pharmaceuticals, and textile printing because of its thickening, stabilising, and gelling properties (Porse and Rudolph 2017). The rheological properties of alginate are determined by the mannuronic acid to guluronic acid ratio (M:G ratio), where alginate high in guluronic acid (low M:G ratio) forms stronger and more rigid gels and therefore is more desirable (Indergaard et al. 1990; McHugh 2003). Fucoidan is a bioactive sulfated polysaccharide with a backbone of fucose, and although it is usually a smaller component of *E. radiata* biomass (range: 1.1-1.6 % DW, Chapter 3/Nepper-Davidsen et al. 2023), it is of commercial interest for applications in personal health products and nutraceuticals (Mak et al. 2013; Hsu and Hwang 2019). Phlorotannins represent a large proportion of *E. radiata* biomass (5.5 % DW, Magnusson et al. 2017; seasonal range: 7.6-9.5 % DW, Chapter 3/Nepper-Davidsen et al. 2023) compared to other commercial kelp species such as *Saccharina latissima* (seasonal range: 0.23-

0.68 % DW, Schiener et al. 2015) and are a group of bioactive phenolic compounds with potential application in cosmetics and nutraceuticals (Shrestha et al. 2021). *Ecklonia radiata* biomass is also high in glucose (seasonal range: 7.7-18.2 % DW; Chapter 3/Nepper-Davidsen et al. 2023), partly in the form laminarin (seasonal range: 0.0-9.8 % DW; Stewart et al. 1961), which is important for the production of plant biostimulants (Aziz et al. 2003). Similar to other kelp species, the composition of *E. radiata* biomass varies both spatially and temporally (Schiener et al. 2015; Manns et al. 2017; Chapter 3/Nepper-Davidsen et al. 2023). Therefore, the commercial quality of the crop will vary depending on the location of its cultivation and timing of its harvest, making high-throughput chemometric methods essential for grading and determining the end-use of *E. radiata* biomass.

Mid-infrared (MIR) and near-infrared (NIR) spectroscopy are common approaches for high-throughput grading of biological matrices, using multivariate regression models (e.g., partial least squares regression, PLSR) for calibration of spectral and wet chemistry data (Capuano and van Ruth 2016; Beć et al. 2020). MIR absorption spectra (400-4000 cm^{-1}) give spectral bands associated with specific functional groups that arise from molecular vibrations or rotations. MIR are better resolved and more easily assigned than NIR spectra (4000-14000 cm^{-1}) which typically give broad and overlapping spectral bands that arise from molecular vibrational overtones and combination vibrations of fundamental stretching vibrations (e.g., –CH, –OH, –SH, and –NH bonds). Absorption of radiation is usually lower in the NIR than in the MIR leading to greater sample penetration depths in the NIR compared to the MIR (Skoog et al. 2018). Therefore, to obtain equivalent results on heterogeneous samples, such as raw biomass, MIR spectroscopy usually requires more sample preparation than NIR (Capuano and van Ruth 2016). However, unlike MIR, not all analytical targets have absorptions in the NIR, and the lower absorption theoretically leads to higher detection limits for NIR (usually around 0.1 %). Therefore, the use of MIR and NIR spectroscopy may be complementary depending on the target analyte and its physical from.

Predictive chemometric models for biomass assessment using spectroscopy are still lacking for most seaweeds, despite the wide application of MIR and NIR spectroscopy in quantitative and qualitative characterisation of various other kinds of biological materials (Beć et al. 2020). A few studies have successfully coupled spectral and wet chemistry data through chemometric modelling in seaweed, however mostly on the green algae *Ulva* sp. (Robic et al. 2009; Shefer et al. 2017; Peleg et al. 2019). Previous spectroscopy studies on alginate composition have mostly focused on predicting M:G ratios in purified alginate samples for grading (e.g., Mackie 1971; Sakugawa et al. 2004; Salomonsen et al. 2008), and less attention has been paid to estimating alginate content and quality in raw biomass samples. However, Horn et al., (1999) demonstrated highly accurate models for predicting the concentration of alginate in stipes of the kelp *Laminaria hyperborea* using NIR, but single-species models were not accurate when applied to different species of microalgae (Laurens and Wolfrum 2011). To our knowledge, no studies have yet demonstrated the use of spectroscopy for multicomponent biomass profiling of *E. radiata*, and the development of such models will be critical for grading biomass quality for downstream applications.

The aim of this study was therefore to create chemometric models for high-throughput grading of *E. radiata* biomass using MIR and NIR spectroscopy. Most commonly, seaweed is dried on harvesting for shelf-life and logistics purposes (FAO and WHO 2022) and for this reason the models in this study were based on dried biomass samples. Biomass components of interest were chosen based on commercial application and included: glucose, alginate, fucose, phlorotannins, ash, carbon, nitrogen, and sulfur. To increase variation among samples within the model, calibration samples of *E. radiata* were collected across a wide geographical range (the North Island of New Zealand; Chapter 2/Nepper-Davidsen et al. 2021) and over the course of a full year. To test model robustness (i.e., prediction on non-calibrated samples), a separate set of validation samples were collected, including samples from different sites and/or time of collection. Specifically, we wanted to 1) assess which biomass components could be reliably predicted using MIR and NIR spectroscopy, 2) assess

whether MIR or NIR would provide the most reliable predictions. Furthermore, we wanted to assess the use of discriminatory models to determine the provenance of biomass.

4.3 Materials & methods

4.3.1 Sample collection

Calibration samples formed part of the sample collection described in Chapter 2 and 3, with 162 calibration samples of *E. radiata* (138 individuals plus 24 homogenised samples) collected from 12 different sites and within 12 separate months on the North Island of New Zealand (Figure 4.1). Using the same sampling methods, an additional 24 validation samples were collected opportunistically, where eight individuals were collected simultaneously with the calibration samples and 16 individuals were collected at separate sites (Coromandel Harbour and Jones Bay) and/or at separate times (April to August 2021). The calibration samples were adult individuals (stage 3; Mann and Kirkman 1981; mean: 82.1 g dry weight (DW) ± 40.8, n = 138), whereas the validation samples included three samples of stage 1-2 individuals (juveniles) among the 24 samples (mean: 48.3 g DW ± 19.4, n = 24) to validate the model across different age groups. Validation samples were prepared for processing (i.e., rinsed, frozen, freeze dried, milled, and stored) in the same way as the calibration samples, as described in Chapter 3 of this thesis.

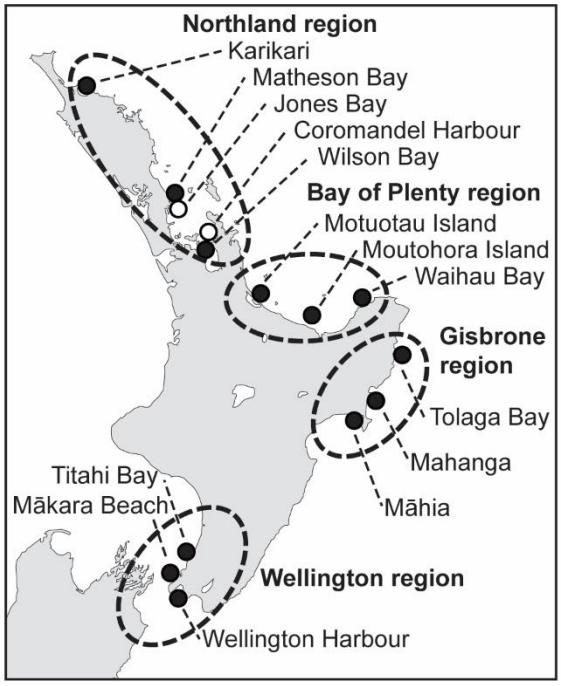

Figure 4.1 Samplings sites and sampling regions across the North Island of New Zealand. Filled circles indicate sites sampled for calibration and/or validation samples and open circles indicate sites only sampled for validation samples

4.3.2 Mid-infrared spectroscopy measurements

MIR spectra were collected on a Fourier-transform MIR (FT-IR) spectrometer (Shimadzu, IRSpirit, QATR-S, Japan), and intensity was measured as absorbance using single reflection attenuated total reflectance (ATR). Data was acquired as the mean of 50 scans (resolution: 4 cm^{-1}, gain: 1) and collected in the range 400-4,000 cm^{-1}. Each sample was homogenised using mortar and pestle, to reduce particle size, and measured as the average of triplicates (with different subsamples for each triplicate) at room temperature (18-22 °C), running a background scan before each measurement.

4.3.3 Near-infrared spectroscopy measurements

NIR spectra were collected on a Fourier-transform NIR (FT-NIR) spectrometer (Antaris II, Thermo fisher scientific, USA), and intensity was measured as absorbance. Data was acquired as the mean of 32 scans (resolution: 4 cm^{-1}, gain: 1), collected in the range 4,000-10,000 cm^{-1}, using an integrating sphere. Samples were measured though a quartz window in a spinning sample cup (internal diameter: 4.9 cm), where the samples were filled to cover the bottom of the cup and

pressed down with a plunger. Measurements were taken at room temperature (18-22 °C) with a background scan every fourth hour.

4.3.4 Wet chemistry measurements

Wet chemistry measurements on calibration samples formed part of the data collected in Chapter 3 and included content of monosaccharides (glucose, mannuronic acid, guluronic acid, and fucose), phenols, ash, carbon, nitrogen, and sulfur. Monosaccharides were only quantified for homogenised samples in Chapter 3 and were therefore quantified for the remaining calibration samples (162 in total) for this chapter. Validation samples were analysed using same methodology as calibration samples (see Chapter 3), where both sets of samples were mixed and analysed together for determination of monosaccharide content but were analysed in separate batches for determination of phenolics, ash, carbon, nitrogen, and sulfur content. Sugar content was estimated in duplicates with a mean relative error (% SD of duplicate mean) of 2.9 % ± 2.3. Alginate content was determined as the total mannuronic and guluronic acid content (Szekalska et al. 2016), and phlorotannin content was determined as total phenols content (Shrestha et al. 2021). All biomass components are expressed as % DW.

4.3.5 Data analysis

Calibration models for biomass profiling of *E. radiata* were built using partial least squares regression (PLSR) in PLS Toolbox (Eigenvector Research Inc. 2022) in MATLAB (MATLAB 2021), based on MIR, NIR, and wet chemistry data. PLSR is a regression tool for dimension reduction of multivariate data, which finds the latent variables (LV's) expressing the highest covariance between the spectral X-data and the wet chemistry Y-data (i.e., finding the spectral variance mostly correlated to the wet chemistry variance). PLSR models were built with a single wet chemistry component (univariate Y-data), using the 162 calibration samples, and validated based on cross-validation of the calibration samples and prediction of the 24 validation samples (external validation). Model

correlation between spectral and wet chemistry data among calibration samples are presented as R^2 (of cross-validation), and error of cross-validation and prediction error of validation samples are presented as root mean squared error of cross-validation (RMSECV) and root mean squared error of prediction (RMSEP), respectively. Furthermore, relative cross-validation error (% RMSECV) and relative prediction error (% RMSEP) was calculated by dividing the error (RMSECV and RMSEP) by the mean % DW of the given component among calibration samples. Cross-validation was estimated using Random subset cross-validation in PLS Toolbox (maximum 10 LV's, 20 data splits, and 1 iteration), and was repeated ten times to calculate the mean and SD of RMSECV. Pre-processing of X- and Y-data and wavelength selection were optimised for lowest RMSECV (see 4.4 Results & Discussion). Increasing the number of LV's may increase the amount of noise modelled and lower the robustness of the model (Nicolaï et al. 2007). The number of LV's was therefore chosen as the number of LV's where the RMSECV no longer decreased markedly with increasing LV's. Outlier removal was kept low to account for high sample variability and outliers were only removed if a sample had high Q-residuals and/or Hotelling T^2 scores (i.e., low conformity to the model and/or high difference in variation within the model) while also deviating markedly from the rest of the samples on the measured *vs.* prediction plot. Local weighted regression (LWR) was tested as an alternative to PLSR but aborted due to the limited amount of data.

Spatial classification of samples based on the region of origin was modelled using partial least squared discriminant analysis (PLS-DA) in PLS-Toolbox. Similar to PLSR, PLS-DA finds LV's expressing the highest covariance between X-data and Y-data, but with categorical Y-data rather than continuous. The PLS-DA models were built using either MIR- or NIR-data as X-data and regional origin as Y-data (class), with the same pre-processing, wavelength selection, and LV selection procedure as applied for the PLSR models. No samples were removed as outliers for the PLS-DA models.

4.4 Results & discussion

4.4.1 Data distribution

Distributions of wet chemistry data (range and mean) were largely similar between the calibration samples (n = 162) and the validation samples (n = 24, Table 4.1). The maximum and minimum range of the validation samples were within the range of the calibration samples for most wet chemistry components, except for fucose, phlorotannins, and ash, where validation samples exceeded the maximum calibrated range (maximum 17 % higher: phlorotannins) and glucose and carbon where validation samples were lower than the minimum calibrated range (maximum 19 % lower: glucose). The variation among calibration data was highest for glucose (40.2 % SD of mean), lowest for carbon (4.7 % SD of mean) and intermediate for the rest of the components (15.0-25.3 % SD of mean). Carbon, alginate, glucose, and ash were the main biomass components among the calibration samples (32.1-23.1 % DW), with phlorotannins, fucose, nitrogen and sulfur being minor components (7.5-0.9 % DW).

Table 4.1 Range % DW, mean % DW ± SD, and % SD of mean for calibration samples (n = 162) and validation samples (n = 24). M:G ratio is the mannuronic to guluronic acid ratio, and C:N ratio is the carbon to nitrogen ratio

Component	Range % DW (cal)	Range % DW (val)	Mean % DW ± SD (cal)	Mean % DW ± SD (val)	% SD of mean (cal)	% SD of mean (val)
Glucose	6.1 - 30.3	4.9 - 20.8	14.2 ± 5.7	9.7 ± 4.2	40.2	43.0
Alginate	18.1 - 39.3	21 - 35.7	24.9 ± 3.7	27 ± 3.9	15.0	14.6
M:G ratio	0.43 - 0.99	0.47 - 0.87	0.65 ± 0.12	0.62 ± 0.10	18.0	16.6
Fucose	1.1 - 2.0	1.1 - 2.1	1.5 ± 0.2	1.6 ± 0.2	15.0	15.8
Phlorotannins	3.6 - 12.4	4.4 - 14.5	7.5 ± 1.9	7.2 ± 2.0	25.3	27.5
Ash	14.5 - 33.3	16.6 - 36.1	23.1 ± 3.9	25.7 ± 4.8	16.9	18.6
Nitrogen	0.8 - 1.8	0.8 - 1.6	1.3 ± 0.2	1.1 ± 0.2	16.7	16.7
Carbon	27.6 - 35.6	24.4 - 34.2	32.1 ± 1.5	30.0 ± 2.2	4.7	7.4
C:N ratio	17.1 - 44.1	20 - 36.1	25.8 ± 5.4	27.2 ± 4.6	20.8	16.7
Sulfur	0.6 - 1.3	0.7 - 1.3	0.9 ± 0.2	1.0 ± 0.1	17.9	14.5

Spectral patterns between samples were similar within MIR and NIR data, and only three spectral outliers were identified by visual inspection among the MIR data (two samples from Wellington Harbour and one from Tolaga Bay) and one among the NIR data (from Motuotau Island in August, Figure 4.2). However, these spectral outliers were kept as they did not consistently appear as outliers within the PLSR models. Baseline shift (i.e., intensity differences) were present in both the MIR and the NIR data, but this is common for these types of data and could be due to inhomogeneity of sample particle size or refractive index and non-uniform scattering among wavelengths (Nicolaï et al. 2007). No spectral tilt (i.e., slope differences) was observed among the MIR and NIR data, but some noisy regions were detected in the MIR data (3900-3600 cm^{-1}, 2400-1700 cm^{-1}, and 650-400 cm^{-1}).

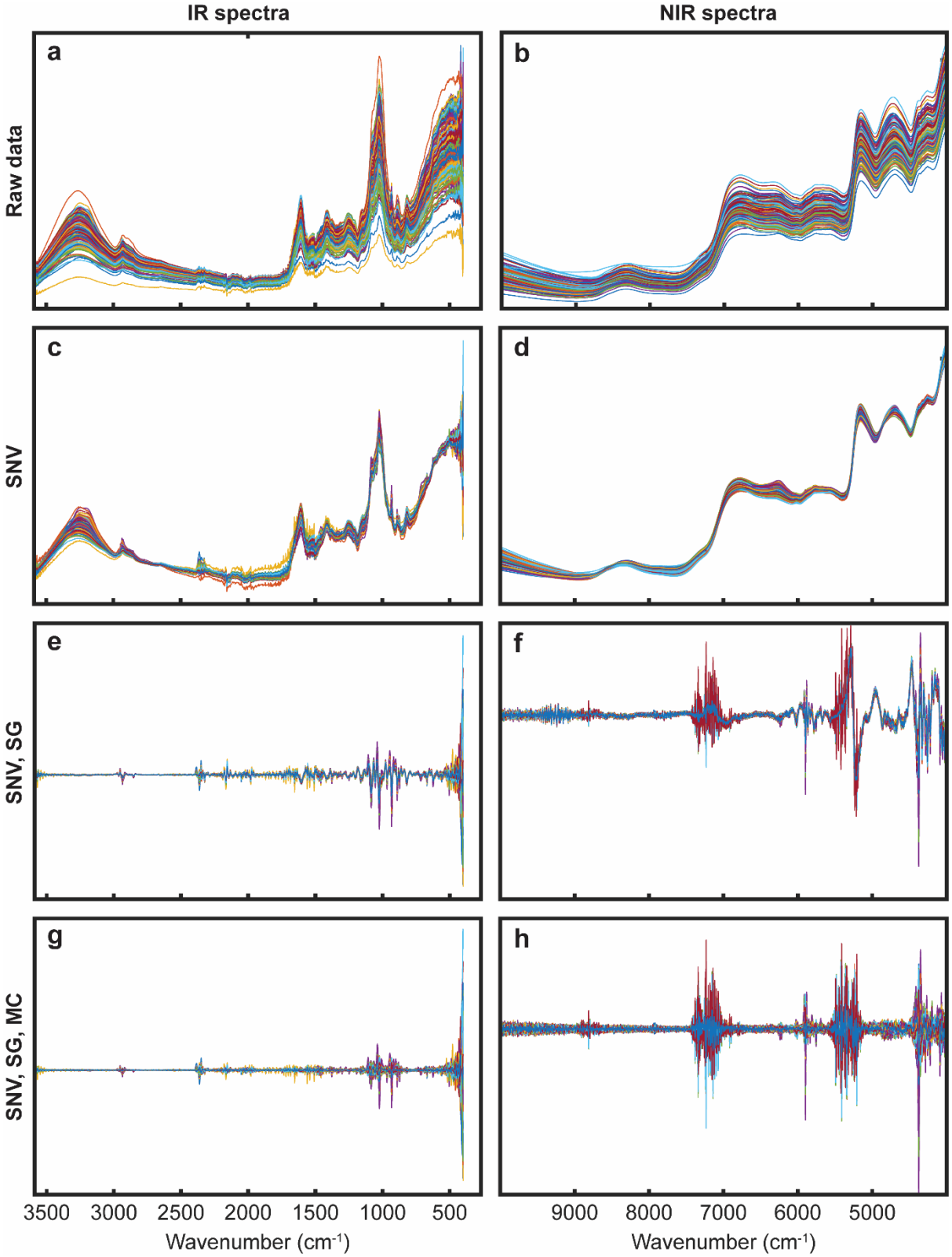

Figure 4.2 Spectral absorption data with various degree of pre-possessing for MIR spectra (left; 4,000-400 cm-1) and NIR spectra (right; 10,000-4,000 cm^{-1}). Pre-processing applied: a, b) none (raw data), c, d) Standard Normal Variate normalisation (SNV), e, f) SNV and Savitzky-Golay (SG) transformation (2nd derivative, 2nd order smoothing, 21 points windows, and weighted tails), and g, h) SNV, SG, and mean centering (MC)

4.4.2 Pre-processing and variable selection

Pre-processing and variable selection (i.e., wavelength selection) were optimised in PLS-Toolbox to reduce the effect of noise and baseline shift in the spectral data and thereby minimise modelling error (RMSECV and RMSEP). A range of pre-processing techniques were tested on the spectroscopy data, including 1) normalisation techniques: Standard Normal Variate (SNV) and Multiplicative Scatter Correction (MSC) for mean and median, 2) transformation techniques: Savitzky-Golay (SG) derivatisation testing 1st, 2nd and 3rd derivative, with 1st, 2nd, 3rd and 4th order smoothing, window range between 7 and 31 points, and with and without weighted tails, and 3) centering and scaling: mean centering, median centering and autoscaling. In the end, SNV normalisation with SG transformation (2nd derivative, 2nd order smoothing, 21 points windows, and weighted tails) and mean centering were chosen for all models (Figure 4.2), as this combination of pre-processing provided the lowest overall RMSECV of MIR and NIR models (mean reduction in RMSECV using the chosen pre-processing compared to just using mean centring: 17.3 % ± 12.8 for MIR models and 30.7 % ± 13.0 for NIR models). The wet chemistry data was mean centred for all models, except for the MIR glucose model, where the glucose data also was square root transformed, due to non-linearity between measurements and predictions (RMSECV decreased by 20 % with square root transformation of glucose data).

Variable selection was initially done manually by choosing the intervals with the highest correlation to the LV's and regression vectors for Y (i.e., correlation to Y-data), however the best results were obtained using the interval PLS (iPLS) variable selection algorithm in PLS Toolbox. The iPLS algorithm cuts the available wavelengths into a number of segments (set by the interval size), running a PLSR model within each of those segments and finds the segment with the best performing model. Selection can be optimised with further repeats of the algorithm, adding the next best performing interval to the variables already selected. In this way, iPLS were run as one interval of 100 variables at a time and repeated, adding more variables (spectral regions), until RMSECV no longer decreased. Venetian Blinds cross-validation (maximum 10 latent variables, 20 splits, and 1

sample per blind) was used for all simulations of iPLS for reproducibility, as this cross-validation uses the same seed every time. iPLS was most effective for improving MIR model predictions (mean reduction in RMSECV using iPLS compared to when all variables were included: 29.7 % ± 14.1 for MIR models and 6.1 % ± 12.0 for NIR models), probably due to the high degree of noise found in specific sections of in the MIR data (Salomonsen et al. 2008). Indeed, the NIR alginate model showed lowest RMSECV when all variables were included, however RMSEP increased 3.3 times more than RMSECV decreased when using all variables, so the iPLS variable selection was retained for this model.

Table 4.2 Results of PLSR models built on spectroscopy data (spectra) and wet chemistry components using 162 calibration samples and 24 validation samples of *E. radiata*. Statistics shown: number of latent variables (LV's), R^2 (of cross-validations), mean root mean square error of cross-validation (RMSECV) with SD in brackets (n = 10), root mean square error of prediction (RMSEP), relative cross-validation error (% RMSECV) with SD in bracket (n = 10), relative prediction error (% RMSEP), and number of outliers removed

Model	LV's	R2	RMSECV	RMSEP	% RMSECV	% RMSEP	Outliers
MIR							
Glucose	6	0.98	0.815 (0.007)	0.925	5.75 (0.05)	6.52	3
Alginate	5	0.80	1.520 (0.013)	1.546	6.11 (0.05)	6.21	
M:G ratio	5	0.30	0.101 (0.001)	0.080	15.42 (0.2)	12.17	2
Fucose	5	0.56	0.130 (0.001)	0.168	8.92 (0.08)	11.52	1
Phlorotannins	4	0.91	0.567 (0.005)	0.834	7.53 (0.06)	11.08	
Ash	6	0.84	1.566 (0.012)	3.743	6.78 (0.05)	16.22	
Nitrogen	9	0.87	0.076 (0.001)	0.154	5.93 (0.06)	11.95	
Carbon	4	0.72	0.776 (0.003)	1.770	2.42 (0.01)	5.51	2
C:N ratio	6	0.89	1.738 (0.029)	3.404	6.74 (0.11)	13.21	
Sulfur	5	0.80	0.075 (0.001)	0.153	8.02 (0.07)	16.35	
NIR							
Glucose	4	0.95	1.216 (0.022)	1.132	8.58 (0.15)	7.99	
Alginate	6	0.88	1.163 (0.011)	1.499	4.67 (0.04)	6.02	
M:G ratio	8	0.77	0.058 (0.001)	0.069	8.82 (0.11)	10.49	
Fucose	7	0.60	0.124 (0.001)	0.162	8.52 (0.07)	11.12	
Phlorotannins	6	0.96	0.366 (0.003)	0.587	4.85 (0.04)	7.80	
Ash	6	0.83	1.630 (0.015)	2.431	7.06 (0.06)	10.53	
Nitrogen	5	0.92	0.061 (0.001)	0.134	4.75 (0.04)	10.42	
Carbon	4	0.76	0.733 (0.002)	1.947	2.28 (0.01)	6.06	
C:N ratio	6	0.92	1.567 (0.013)	3.335	6.08 (0.05)	12.94	
Sulfur	4	0.79	0.076 (0.000)	0.128	8.10 (0.03)	13.68	

4.4.3 Partial least squared regression models

Twenty PLSR models were built for predicting biomass composition of *E. radiata* (i.e., ten using MIR and ten using NIR; Figures 4.3 and 4.4). Model performance was evaluated based on the wet chemistry variance explained by spectral variance (R^2), model accuracy (i.e., cross-validation error of calibration samples: RMSECV), model robustness (i.e., prediction error of validation samples: RMSEP), number of LV's included, and number of outliers removed (Table 4.2). Most models displayed promising performance, except for fucose (syn. fucoidan; Hsu and Hwang 2019, likely due to the low biomass content), ash, and sulfur which will not be discussed any further.

The PLSR glucose models performed well and showed the highest R^2 among the quantified carbohydrates (R^2 = 0.98 and 0.95 for MIR and NIR models, respectively; Figures 4.3a and 4.4a), despite alginate being a larger biomass component. The MIR glucose model outperformed the NIR glucose model both in terms of RMSECV (0.815 ± 0.007 and 1.216 ± 0.022, respectively) and in terms of RMSEP (0.925 and 1.132, respectively). However, the MIR glucose model needed more LV's (6 and 4 LV's for MIR and NIR models, respectively), thus potentially including more noise. Furthermore, the MIR model was also more sensitive to measurement error as three samples had to be excluded as outliers reducing RMSECV from 0.917 to 0.815 (11.2 % reduction) and RMSEP from 1.079 to 0.925 (14.3 % reduction) after removal of outliers. Two spectral intervals were included in the MIR glucose model (2968-2826 cm^{-1} and 1255-828 cm^{-1}), where the low wavenumber interval corresponds to absorptions due to important structural features of polysaccharides (e.g., anomeric and glycosidic bonds; Synytsya and Novak 2014; Rajauria et al. 2021), and the high wavenumber interval likely is related to the abundance of C-H bonds in glucose (2950-2900 cm^{-1}; Silverstein et al. 2014). Spectral intervals included in the NIR glucose model (7469-7278 cm^{-1} and 5540-5350 cm^{-1}) partially overlap NIR regions previously associated with glucose in intact apple fruits (12000-8000 cm^{-1} and 6000-4000 cm^{-1}; Liu et al. 2006).

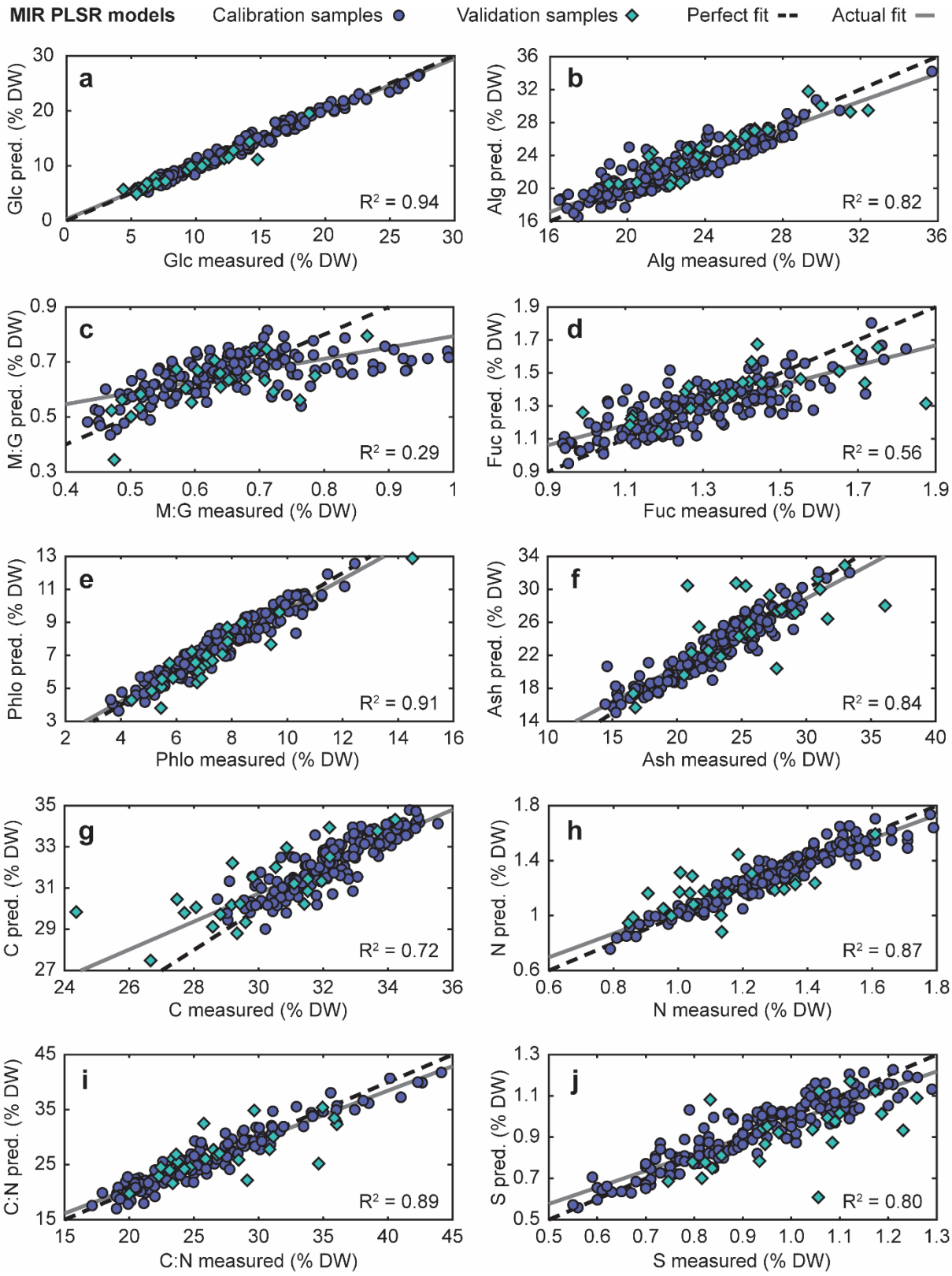

Figure 4.3 Results of PLSR MIR models with predicted (pred.) and measured content of a) glucose (Glc), b) alginate (Alg), c) M:G ratio (M:G), d) fucose (Fuc), e) phlorotannins (Phlo), f) ash, g) carbon (C), h) nitrogen (N), i) C:N ratio (C:N), and j) Sulfur (S) in *E. radiata*. Blue circles: calibration samples, teal diamonds: validation samples, black dotted line: perfect fit, and grey line: actual fit

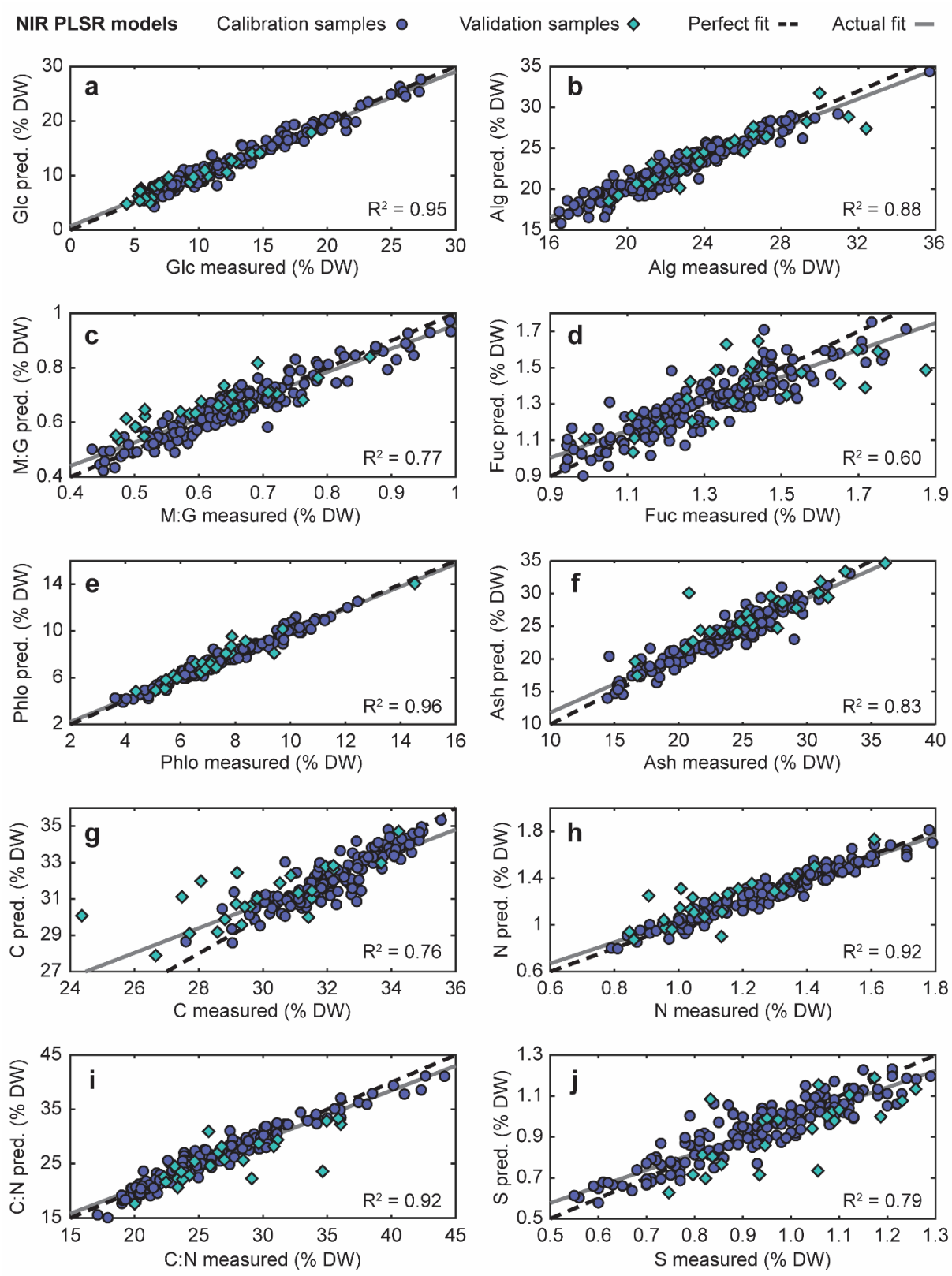

Figure 4.4 Results of PLSR NIR models with predicted (pred.) and measured content of a) glucose (Glc), b) alginate (Alg), c) M:G ratio (M:G), d) fucose (Fuc), e) phlorotannins (Phlo), f) ash, g) carbon (C), h) nitrogen (N), i) C:N ratio (C:N), and j) Sulfur (S) in *E. radiata*. Blue circles: calibration samples, teal diamonds: validation samples, black dotted line: perfect fit, and grey line: actual fit

The PLSR alginate models demonstrated promising performance considering the complexity of the sample matrix (R^2 = 0.80 and 0.88 for MIR and NIR models, respectively; Figures 4.3b and 4.4b). The NIR alginate model strongly outperformed the MIR alginate model based on RMSECV (1.163 ± 0.011 and 1.520 ± 0.013, respectively), while both models displayed similar RMSEP (1.499 and 1.546, respectively). Selected variables for the MIR alginate model (1398-828 cm^{-1}) were within the range of variables selected in previous studies using MIR to predict the M:G ratio of purified alginate samples (1175-905 cm^{-1}, Sakugawa et al. 2004; 1800-650 cm^{-1}, Salomonsen et al. 2008). Inclusion of the higher wavenumbers in the MIR alginate model, as was done by Salomonsen et al. (2008), would include the carboxylic acid peak (C = O_{asym}: 1650-1550 cm^{-1}, Silverstein et al. 2014), however inclusion of this peak (1607 cm^{-1}; Figure 4.2) did not improve model predictions in this study. High error when predicting alginate content in kelp biomass has previously been hypothesised to be linked to a lack of calibration for phenolic content (Horn et al. 1999). However, alginate prediction error did not decrease with the inclusion of phenolics content (i.e., phlorotannins, multivariate Y-data component; PLS2 model), as the MIR and NIR combined alginate and phlorotannin models had higher RMSECV (1.607 ± 0.013 and 1.379 ± 0.007, respectively) and RMSEP (2.189 and 1.739, respectively) than the respective single component MIR and NIR alginate models.

The performance of the PLSR M:G ratio models (i.e., mannuronic acid to guluronic acid ratio) was poor for the MIR model (R^2 = 0.276) but promising for the NIR model (R^2 = 0.767; Figures 4.3c and 4.4c). The relative cross-validation and prediction errors of the NIR M:G ratio model (% RMSECV: 8.9; % RMSEP: 10.6; mean M:G ratio: 0.65 ± 0.12, n = 162) are similar to a previous study predicting M:G ratio in purified alginate samples (% RMSCV of 7.7 and a % RMSEP of 10.0; mean M:G ratio: 1.3; Salomonsen et al. 2008). Although their model used five fewer LV's, the use of purified samples and a larger sample range (0.5-2.1 M:G ratio) is likely to have improved model predictions in the study by Salomonsen et al. (2008), and thus the NIR M:G ratio predicted in this study demonstrates applicability for M:G ratio models for grading of raw biomass. The alginate monosaccharides (mannuronic acid and guluronic acid) are optical isomers (i.e., mirror images), and the lower

performance of the M:G ratio models compared to alginate models indicate that models are able to identify the isomers as a group (i.e., alginate), but cannot properly distinguish between them (i.e., M:G ratio).

The PLSR phlorotannin models performed well both for MIR and NIR spectroscopy (R^2 = 0.91 and 0.96, respectively; Figures 4.3e and 4.4e). The NIR phlorotannin model performed better than the MIR phlorotannin model based on RMSECV (0.366 ± 0.003 and 0.567 ± 0.005, respectively) and RMSEP (0.587 and 0.834, respectively), although the NIR model needed more LV's (6 and 4, respectively). Variable selection for the MIR model (1683-1113 cm^{-1}) was similar to a previous study predicting phenolic compounds in compost (1760-800 cm^{-1}), whereas variable selection for the NIR model (6119-5928 cm^{-1}, 5348-4578 cm^{-1}, and 4383-4192 cm^{-1}) was more specific compared to that same study (9000-4000 cm^{-1}, Cascant et al. 2016).

The PLSR carbon models demonstrated the lowest relative cross-validation error of all models (% RMSECV: 2.42 ± 0.01 and 2.28 ± 0.01 for MIR and NIR models, respectively), due to the high carbon content (mean: 32.1 % DW ± 1.5 SD, n = 162), but also showed low robustness as % RMESP was more than 2-fold that of % RMSECV (% RMSEP: 5.51 and 6.06 for the carbon MIR and NIR models respectively; Figure 4.3g and 4.4g). However, high prediction error was likely due to the low carbon content of the validation samples where 75 % of the samples were in the same range as or lower than the lowest 15 % of the calibration samples, and thus, increasing the lower range of the carbon calibration data is likely to increase predictions of the validation samples. Despite the low robustness and low R^2 (0.72 and 0.76 for MIR and NIR models, respectively), the carbon models demonstrated potential for carbon capturing monitoring (Krause-Jensen and Duarte 2016), because of the low relative prediction error.

The PLSR nitrogen and C:N models demonstrated high performance in terms of R^2 (0.87 or higher; Figures 4.3h, 4.4h, 4.3i, and 4.4i), but similar to the carbon models, the robustness of the models were low, with RMSEP being more than twice as high as RMSECV for some models. Analyses

of carbon, nitrogen, sulfur, and ash were carried out in separate batches for calibration and validation samples with more than a year between analyses, which could potentially have contributed to the discrepancy between these two sets of data. Thus, with additional testing, these models could be useful tools for environmental monitoring of water quality around *E. radiata* farm sites (Wernberg et al. 2019).

4.4.4 Overall partial least squared regression trends

The highest R^2 was detected for the PLSR models of glucose, phlorotannins, nitrogen and C:N ratio ($R^2 \geq 0.87$). However, large differences in biomass contribution between wet chemistry components (i.e., in % of DW) created some discrepancy between correlation and relative prediction error (e.g., the carbon models displayed low R^2, but also low % RMSEP), while other models demonstrated poor prediction on validation samples despite high cross-validation accuracy (e.g., RMSEP was more than twice that of RMSECV for the nitrogen models). Consequently, the PLSR models demonstrating the lowest relative prediction error were the glucose, alginate, phlorotannins, and carbon models showing that these components can be predicted with less than 8 % error (% RMSEP < 8 % for all, except for the MIR phlorotannin model).

The lowest RMSEP were achieved using NIR data for all wet chemistry components except glucose and carbon, demonstrating an overall higher accuracy of the NIR models, although these also generally required more LV's. Four different samples were removed as outliers across all MIR models, where the most problematic sample was removed four times (i.e., out of eight removed outliers in total) and also was a visual outlier on MIR spectra. Comparatively, no outliers were removed from the NIR model, demonstrating a higher degree of measuring error for MIR compared to NIR. Higher MIR error was likely caused by the limited amount of biomass analysed for each spectrum, as MIR only was measured in one fixed spot under the crystal, thereby increasing bias caused by differences in particle size and inhomogeneity of biomass. Comparatively, NIR was measured using a spinning cup module, thus producing spectra averaged over a much larger amount

of biomass. Given the overall higher performance of the NIR models and the easier and more reliable sampling method, NIR spectroscopy seems to be preferable to MIR spectroscopy for this type of analysis.

The three juvenile validation samples were all poorly predicted using the NIR M:G ratio model (along with one other poorly predicted adult validation sample, Figure 4.4c), likely because the tissue content of guluronic acid tends to increase with age in kelp (Indergaard et al. 1990), indicating that this model would need calibration towards juvenile samples in order to accurately predict such samples. However, for all other models, no pattern in outliers among validation samples was found according to age (i.e., the three juvenile validation samples were predicted similarly to the rest), indicating that most models could be applicable across different age groups.

The best predicted wet chemistry components in terms of R^2 (glucose and phlorotannins) also displayed the highest variability among calibration data (40.2 and 25.3 % SD of mean, respectively), suggesting that the prediction of the other components could be improved by adding more calibration data to provide a wider wet chemistry data range.

4.4.5 Partial least squared discriminant analysis models

PLS-discriminant analysis (PLS-DA) models were built using MIR and NIR data to analyse spectral trends based on region of origin, and performance was based on sensitivity (true positives classified as positive) and specificity (true negatives classified as negative) of calibration samples (cross-validation) and validation samples (prediction; Table 4.3, Figure 4.5). Best model performance was achieved by selecting all MIR data except the noisy regions (variables removed: 3900-3600 cm^{-1}, 2400-1700 cm^{-1}, and 650-400 cm^{-1}) and all NIR data, with 9 LV's for both models. The NIR PLS-DA model outperformed the MIR PLS-DA model for all regions and demonstrated highly accurate predictions on region of origin for all regions, based on the calibration samples (cross-validation: sensitivity: 0.91 ± 0.00 SD – 1.00 ± 0.00 SD, n = 3; specificity: 0.95 ± 0.00 SD – 1.00 ± 0.00 SD, n = 3).

However, markedly lower predictive accuracy was demonstrated for validation samples from Northland, Bay of Plenty, and Gisborne, with either low sensitivity (many false negatives) or low specificity (many false positives). Only the Wellington samples displayed high sensitivity and specificity among both calibration and validation samples, where the NIR PLS-DA model classified all true positives as positives and all true negatives as negative, except for once false positive validation sample.

The strong spectral differentiation between samples from the Wellington region and samples from the other regions matches the pattern of the genetic structure of *E. radiata* on the North Island of New Zealand where populations within the Wellington region are highly genetically differentiated from populations within the northern regions of the island (Chapter 2/Nepper-Davidsen et al. 2021). However, the spectral differentiation between Wellington samples and samples from the other regions did not seem to affect the performance of PLSR models, in fact, the models performed worse without the inclusion of the Wellington samples (RMSECV increased by 0.9 % ± 5.5 SD and 3.7 % ± 2.1 SD for the MIR and NIR models respectively without Wellington samples; average of glucose, alginate, M:G ratio, phlorotannins, nitrogen, and carbon models). The validation samples were not evenly distributed among the four regions (17 out of 24 samples were from the Northland region), as the development of PLS-DA models were not the intended design, and a wider selection of samples from the Bay of Plenty, Gisborne, and Wellington region, should therefore be included in further studies to fully validate these findings. However, overall, our results show that MIR and NIR spectroscopy can be effectively used to establish provenance of seaweed using PLS-DA.

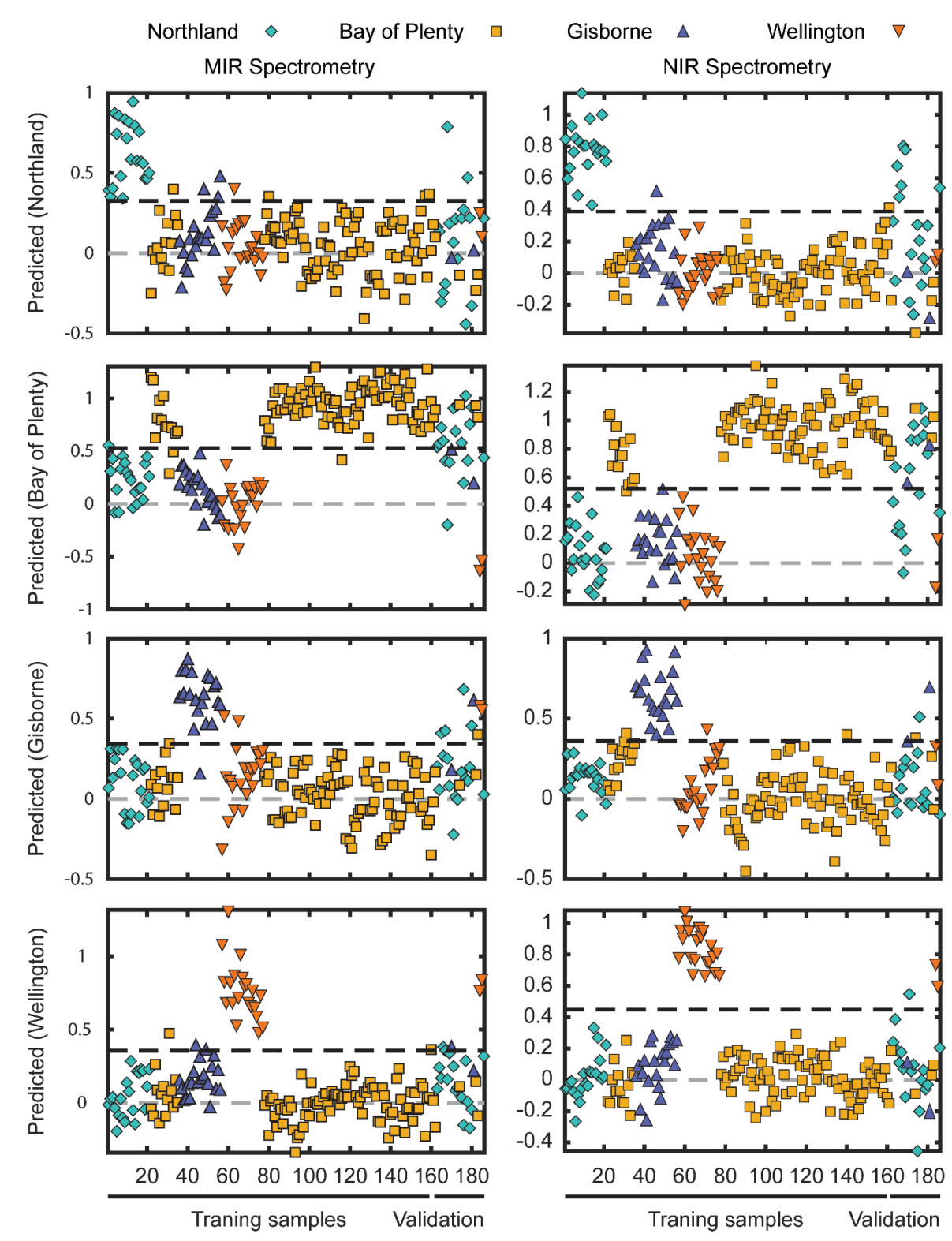

Figure 4.5 PLS-DA models for predicted region of origin for calibration samples (n = 162) and validation samples (n = 24), using MIR (left) and NIR (right) spectroscopy. Sample numbers are shown by the x-axis, with calibration samples to the left (1-162) and validation samples to the right (163-186). Predicted values are shown by the y-axis where 0 means not belonging to the region (not included) and 1 means belonging to the region (included), based on the true region of origin (measured values). The black dotted line shows the cut off value between samples included and not included in the predicted region of origin

Table 4.3 Results of PLS-DA models build on MIR and NIR spectroscopy data with sample region as class, using calibration data (n = 162) and validation data (n = 24). Statistics shown: number of latent variables (#LV), sensitivity (true positive classification) and specificity (true negative classification) of calibration samples with SD in brackets (CV, n = 3) and validation samples (prediction)

Spectra	Region	#LV's	Sensitivity (CV)	Specificity (CV)	Sensitivity (Prediction)	Specificity (Prediction)
MIR	Northland	9	0.78 (0.02)	0.92 (0.00)	0.12	1.00
MIR	Bay of Plenty	9	0.94 (0.01)	0.89 (0.01)	1.00	0.48
MIR	Gisborne	9	0.87 (0.02)	0.95 (0.02)	0.50	0.68
MIR	Wellington	9	1.00 (0.00)	0.97 (0.00)	1.00	0.86
NIR	Northland	9	0.91 (0.00)	0.97 (0.00)	0.35	1.00
NIR	Bay of Plenty	9	0.95 (0.01)	0.95 (0.00)	1.00	0.48
NIR	Gisborne	9	0.91 (0.00)	0.95 (0.00)	0.50	0.91
NIR	Wellington	9	1.00 (0.00)	1.00 (0.00)	1.00	0.96

4.5 Conclusion

High performing PLSR models were built for predicting biomass content of glucose, alginate, M:G ratio, phlorotannins, nitrogen, and carbon in *E. radiata*, where NIR models generally outperformed MIR models. Overall, our results are promising for commercial use of MIR and NIR spectroscopy for high-throughput grading of raw *E. radiata* biomass, given the limited number of samples applied (186 total). Model predictions are likely to improve with additional calibration data, and further research should be undertaken testing the validity of these models on geographically different samples of *E. radiata* and related species of kelp.

Chapter 5

Line configuration and farming depth markedly affect survival and growth in the kelp *Ecklonia radiata*

This chapter is under review for publication in New Zealand Journal of Marine and Freshwater Research as:

Nepper-Davidsen J, Magnusson M, Glasson CRK, Lawton RJ (2023) Line configuration and farming depth markedly affect survival and growth in the kelp *Ecklonia radiata.*

5.1 Abstract

The native kelp *Ecklonia radiata* is a target species for the emerging seaweed aquaculture industry in New Zealand, however, the effect of line configuration on survival and growth of farmed seaweed is unknown. In this study, we outplanted nine seaweed growth lines (with 20 individuals each) in three line configurations (vertical, horizontal 2 m depth, and horizontal 4 m depth) in northern New Zealand for grow-out between August 2021 and April 2022. Initial survival rates were similar between line configurations, but only individuals growing on vertical lines survived after four months (38 % ± 12 SD). Similarly, on vertical lines, average juvenile growth by elongation was 85 % higher (0.11 cm day^{-1} ± 0.03 SD) and maximum average weight of individuals was 77 % higher (106 g WW ± 73 SD), compared to horizontal lines. Unusually warm water temperatures were likely a central driver for the overall high mortality of *E. radiata* observed from January to April, while a combination of temperature and light stress was likely a central driver for higher mortality observed on vertical lines at shallow depths compared to deeper depths. In conclusion, this study supports farming *E. radiata* on vertical dropper lines rather than horizontal lines.

5.2 Introduction

In New Zealand, the emerging seaweed aquaculture sector has the potential to provide significant economic and environmental benefits, however, no commercial seaweed aquaculture has yet been established and production is still based on wild harvest, beach cast collection, and import (Bradly et al. 2021; Clark et al. 2021). The native kelp *Ecklonia radiata* is a target for aquaculture because of its abundant distribution across the country (Shears and Babcock 2007), and because of its desirable biomass profile (Stewart et al. 1961; Magnusson et al. 2017; Chapter 3/Nepper-Davidsen et al. 2023) that is exploited domestically for production of biostimulants and commercial food products (Bradly et al. 2021).

Ecklonia radiata is not currently farmed commercially anywhere in world (Wiltshire et al. 2020), but hatchery farming protocols have recently been developed (Praeger et al. 2022a, b). Furthermore, farming trials have previously been carried out in New Zealand and Australia, identifying seasonality and current flow as critical factors, especially for avoiding heavy fouling of the seaweed during the austral summer (Neill et al. 2009; Wiltshire et al. 2020). In wild populations, the growth of *E. radiata* is usually fastest in the austral spring and early summer and lowest in the austral winter and autumn, primarily due to seasonal changes in temperature and light, and secondarily due to changes in nutrient levels and water motion (Novaczek 1984; Wernberg and Goldberg 2008; Bearham et al. 2013). Specifically, high temperatures during late summer can cause respiration rates to surpass photosynthetic rates and low light levels during winter may be insufficient to saturate photosynthesis beyond respiratory demands, which in both cases results in a negative net carbon balance and can have a significant negative impact on growth (Staehr and Wernberg 2009; Bearham et al. 2013). Thus, understanding how *E. radiata* responds to changes in such environmental factors when farmed on artificial structures (i.e., at sites and environmental conditions where this seaweed may not naturally occur) will be crucial for establishing farm management protocols.

Furthermore, comparative studies on the optimal line configuration for farming of *E. radiata* have not yet been conducted. *Saccharina* spp. (the most farmed seaweed genus worldwide, FAO 2022) and most other kelp species are generally farmed on horizontal longlines submerged just below the surface of the water (Zhang 2018). However, the morphology of *E. radiata* differs markedly from other commonly farmed kelp species, and optimal line configuration may therefore also differ from other species. Specifically, the morphology of *E. radiata* is characterised by a thick elongated stipe, which can be several times the length of the lamina, and growth is mostly lateral, whereas *Saccharina japonica* and *Saccharina latissima* have a much shorter stipe and growth is longitudinal. In addition, farming of *E. radiata* in New Zealand is likely to initially occur by utilising existing mussel farm infrastructure consisting of u-shaped vertical droplines extending 5-20 m down into the water column. It is therefore important to test the effect of farming on horizontal and vertical line configurations to identify any potential effects on the survival and growth of *E. radiata* before large scale farming is undertaken.

In this study we tested aquaculture methods for the farming of *E. radiata*, utilising existing mussel farm infrastructure. The aims of the study were to 1) compare survival and growth of *E. radiata* between horizontal and vertical line configurations, and 2) assess *E. radiata* survival at different depths. Trials were undertaken by transplanting juvenile *E. radiata* individuals from nearby natural populations. Temporal changes in solar irradiation, water temperature, and fouling were quantified to help understand any drivers of survival and growth.

5.3 Materials & methods

5.3.1 Sample collection and experimental design

The experiment took place at the Gold Ridge Marine Farms at Esk Point, Coromandel Harbour, New Zealand (Figure 5.1). This site is located in the Hauraki Gulf (Tīkapa Moana) at the edge of Coromandel Harbour, approximately 120 m from shore with a maximum depth of approximately 7 m. The site is sheltered by the surrounding coastline and islands. Juvenile *E. radiata*

individuals (stage 1 and 2 plants; Mann and Kirkman 1981) were collected under Special Permit 742-3 by scuba diving at Cow Island, Coromandel, New Zealand (approximately 3 km from the farm site) in August 2021. Juveniles (n = 180) with a length of 10-20 cm from the bottom of the stipe to the tip of the central lamina were selected. All individuals were free of fouling and had limited lateral growth (Figure 5.2). Selected juveniles were attached to grow lines (10 mm diameter, polypropylene, twisted rope) by splicing them into the twists of the rope so that the holdfast was sticking out through the twist and would be able to subsequently grow around and attach to the rope. The grow lines were attached to three replicate mussel farm backbone lines held up by mussel floats and were deployed in two configurations (Figure 5.3). Three vertical grow lines were suspended directly from the backbone lines with the seaweed growing at depths of 1 to 5 m. Six additional horizontal grow lines were deployed at 2 and 4 m depth (three lines each), suspended between vertical dropper lines attached to the backbone. On each line, 20 individuals were spaced 20 cm apart over the centre 4 m. For each grow line, an identical control line (without seaweed) was deployed adjacent to the grow line to enable estimation of the amount of fouling on the grow line. A concrete weight was attached to the end of all dropper lines and vertical grow (and control) lines to keep them vertical in the water column. Prior to deployment, all grow and control lines were soaked in seawater for 24 h (renewed twice) to remove manufacturing residues and to enable quantification of the wet weight of the grow lines. A greater number of juveniles were collected than were required for outplanting on experimental grow lines. Therefore, two additional vertical grow lines were deployed for qualitative assessment (i.e., not included in the statistical analysis) using these surplus individuals. Juveniles were attached to these additional grow lines in the same way as the experimental grow lines, but at twice the density, i.e., 40 individuals per 4 m line. The experiment was run for a total of 235 days and was concluded in April 2022.

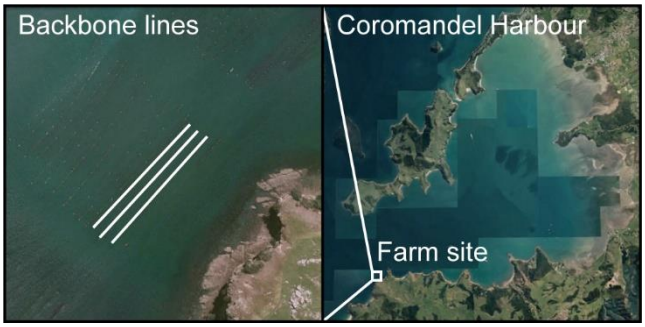

Figure 5.1 Map of study site showing mussel farm backbone lines at Gold Ridge Marine Farms (left; coordinates: -36.809761, 175.436973) in Coromandel Harbour, New Zealand (right). Satellite images sourced from Google Earth Pro

Figure 5.2 *Ecklonia radiata* juveniles collected by scuba diving ready for attachment to grow lines (left), and selected individuals spliced onto a grow line (right)

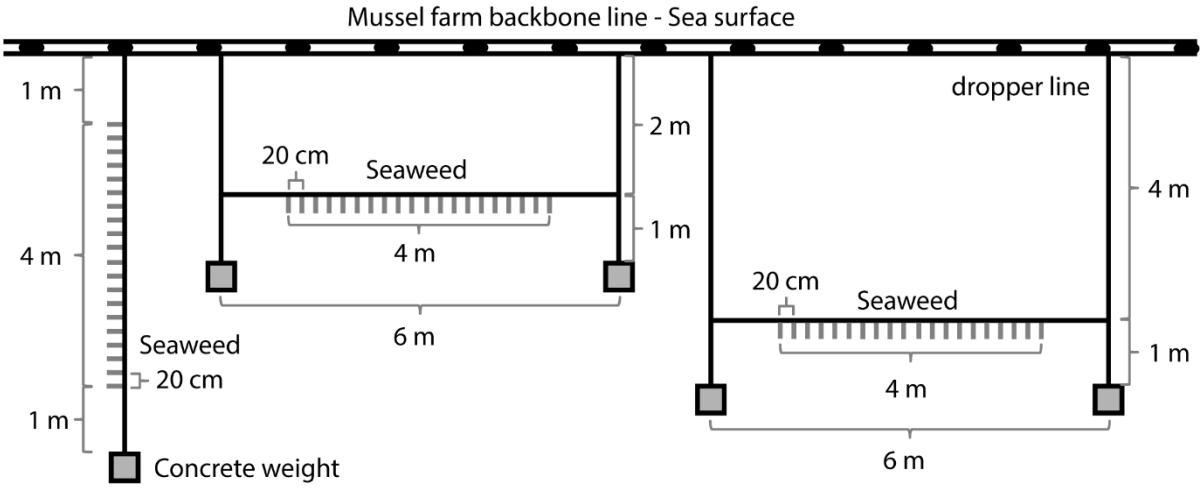

Figure 5.3 Schematic of grow line configurations showing a vertical line to the left, a horizontal line (2 m depth) in the middle, and a horizontal line (4 m depth) to the right. Individuals were spaced 20 cm apart on the lines

5.3.2 Seaweed grow line monitoring

Survival, growth, and the degree of fouling on individuals were monitored on five occasions during the experiment (range: 29-62 days between visits), with frequency dependent on accessibility to the farm due to weather and commercial operations. Detached individuals and individuals without a central lamina (e.g., with only a stipe and holdfast remaining) were considered lost, and survival was measured as % of the initial 20 individuals deployed on each grow line that were remaining on the line at each monitoring occasion. The initial length of all individuals was measured at deployment, and lengthwise growth was measured thereafter on every fifth individual on each line during each monitoring visit. Approximately one month post-deployment (October 2021), most individuals had significant lateral growth. Lengthwise growth is therefore only shown for the first two months as it was no longer representative of the overall growth of individuals for the subsequent months. The average weight of each individual (g wet weight, WW) was estimated for each grow line at each monitoring visit using equation 1. Fouling and the weight of the line was accounted for by subtracting the average weight of control lines from the weight of the grow line. The average weight of all control lines for each month was used in this calculation as the weight of control lines did not significantly differ between configurations for any month (Table 5.1). Grow lines and control lines were weighed on a hanging scale (0.01 kg precision, Burnsco Digital Scale, New Zealand).

$$Average\ individual\ weight = \frac{weight_{grow\ line} - weight_{control\ line}}{number\ of\ individuals\ on\ the\ grow\ line} \qquad (1)$$

Relative growth rate (RGR, day^{-1}) was calculated for each grow line following equation 2, assuming exponential growth.

$$RGR = \frac{\ln(weight_2) - \ln(weight_1)}{t_2 - t_1} \qquad (2)$$

Where weight$_2$ and weight$_1$ are the average individual weight (kg WW) of each line (following eq. 1) at time t_2 and time t_1 (days) respectively.

Fouling on individuals was visually estimated as the average percent of the thallus covered by fouling organisms across all individuals for each grow line. This approach was used rather than quantifying the amount of fouling on each individual due to time constraints on the water. An approximate range of fouling was estimated on grow lines where fouling was highly variable between individuals, but a single number estimate was made on grow lines where fouling was more uniform among individuals. Additionally, the average weight of the control lines was used to provide an overall estimate of the degree of fouling settling on the line itself (as opposed to the seaweed individuals on the line) for each month.

Twelve temperature and light loggers (HOBO MX2202, Onset, US) were deployed on the three vertical seaweed lines at 1, 2, 3, and 4 m depth (i.e., three replicate loggers for each depth) and measurements were taken once every 10 minutes between the 29th of September 2021 and the 15th of April 2022. Backbone 3 sunk 1-2 m below the surface between November and January because a float had detached, and five loggers ran out of battery or were lost with the first one less than halfway through the experiment. These gaps in the data made it impractical to treat the loggers as separate replicates for analysis as the duration of datasets was different between loggers. Therefore, the average temperature (°C) and light (lum m^{-2}) were calculated for every 10 min measurement for each depth across all available data (i.e., average calculated from 1 -3 loggers for each 10 min measurement). An average depth profile for water temperature and light was then calculated from this consolidated data from September to February. Average temperature was calculated between monthly averages (n = 6; all data from September to end of February), and average light intensity was calculated between weekly averages (n = 4) using only data measured during the first week following each visit when loggers were cleaned (due to heavy fouling). Furthermore, all light measurements of 0 (i.e., measurement recorded during night) were excluded from the calculations. A monthly average timeseries between September and April was calculated using the measured temperature at 1 m depth (n = 4032-4464, depending on the number of days in a month), combined with average monthly sea surface temperature (SST) and photoactive radiation

(PAR; µmol m^{-2} s^{-1}) during the past 20 years (July 2002 to June 2022) in the water (0.8 km^{-2} area) around the farm, which were obtained from the online satellite data portal NIWA-SCENZ (Pinkerton et al. 2022).

5.3.3 Data analysis

Differences in juvenile lengthwise growth between August and September were analysed using a one-way ANOVA in R-Studio (Team RStudio 2022), with line configuration as a fixed factor. Normality and homogeneity of variance were checked using the Shapiro-Wilk test of normality (shapiro.test; R-Studio) and Levene's test of equal variance (leveneTest; car package, R-Studio). Differences in control line weight, survival, average individual weight, and RGR were analysed using repeated measures permutational multivariate analysis of variance (repeated measures PERMANOVA) in PRIMER 7 (Clarke and Gorley 2015) as assumptions for ANOVA were not met and because monthly measurements were not independent of each other (lost individuals cannot grow back). Line configuration and month were included as fixed factors, and replicate lines nested within line configuration were included as random factor. Analyses were run as univariate models for control line weight, survival, average individual weight, and RGR, using Euclidian distance resemblance matrices, 9,999 unrestricted permutations of raw data, and Type III sum of squares. Some significant differences in dispersion among line configurations and months were found using tests of homogeneity of dispersion (PERMDISP - an extension of Levene's test), however, such difference typically does not significantly inflate the error rates of PERMANOVA (Anderson et al. 2016). The linear relationship between survival and depth was analysed using the linear model function (lm; stats) in R-Studio. Legibility of figures was improved in Adobe Illustrator.

5.4 Results

5.4.1 Survival

Survival of *E. radiata* was similar between line configurations during the first three months following deployment (August to November), however five months after deployment (January 2022) there were significant differences among configurations, as indicated by a significant configuration x month interaction effect (Table 5.1, Figure 5.4a). By January, all individuals on horizontal lines were lost while on average 38 % ± 12 SD of individuals (n = 3) remained on the vertical lines (Figure 5.4a). By April 2022 (235 days after deployment) only five of the original 60 individuals were left on the vertical lines and all individuals were lost a year after deployment. Individuals generally survived longer in deeper water on vertical lines, however, the relationship between survival and depth was not significant (linear regression: $F_{1,18} = 2.77$, $P = 0.11$, $R^2 = 0.13$; Figure 5.5). The same pattern was observed on the additional vertical lines, where by February 2022 (176 days after deployment), only 1-2 individuals remained on the upper half of the lines (1-3 m depth) but 9-12 individuals still remained on the lower half (3-5 m depth, data not shown).

Table 5.1 Results of repeated measures permutational multivariate analysis of variance (repeated measures PERMANOVA, top panels) testing for differences in weight of control lines (n = 3), survival (% of the initial 20 individuals remaining on each line at each monitoring period, n = 3), individual weight (n = 3), and relative growth rate (RGR, n = 3) between line configurations, months, replicate lines nested within line configuration (Rep (config)), and the line configuration x month interaction. Results of analysis of variance (ANOVA, bottom panel) testing for differences in elongation between line configurations (August to September, n = 3). Significant differences in dispersion among factors are marked with an asterisk and significant P-values are italicised

Repeated measures PERMANOVA						
Source	**df**	**SS**	**MS**	**Pseudo-F**	***P*(perm)**	**Perms.**
Control lines						
Configuration	2	0.005	0.002	0.549	0.612	150
Month*	4	1.402	0.351	71.740	*<0.001*	9968
Rep (config)	6	0.026	0.004	0.891	0.518	9943
Interaction (config x month)	8	0.043	0.005	1.111	0.393	9939
Res	24	0.117	0.005			
Survival						
Configuration*	2	68	34	4.235	0.094	111
Month*	4	2744	686	211.810	*<0.001*	9958
Rep (config)*	6	48	8	2.484	0.055	9922
Interaction (config x month)	8	101	13	3.897	*0.007*	9941
Res	24	78	3			
Individual weight						
Configuration*	2	13336	6668	7.515	*0.004*	280
Month*	4	5419	1355	2.625	*0.022*	9932
Rep (config)*	6	5324	887	1.719	0.087	9923
Interaction (config x month)	8	16016	2002	3.880	*0.001*	9942
Res	24	12385	516			
RGR						
Configuration	2	0.003	0.002	24.246	*0.008*	279
Month*	3	0.029	0.010	21.025	*<0.001*	9952
Rep (config)	6	0.000	0.000	0.156	0.985	9957
Interaction (config x month)	6	0.004	0.001	1.570	0.215	9941
Res	18	0.008	0.000			
ANOVA						
Source	**df**	**SS**	**MS**	**F**	**P**	
Juvenile growth by elongation						
Configuration	2	0.021	0.011	4.644	*0.0605*	
Res	6	0.014	0.002			
Total	8	0.035				

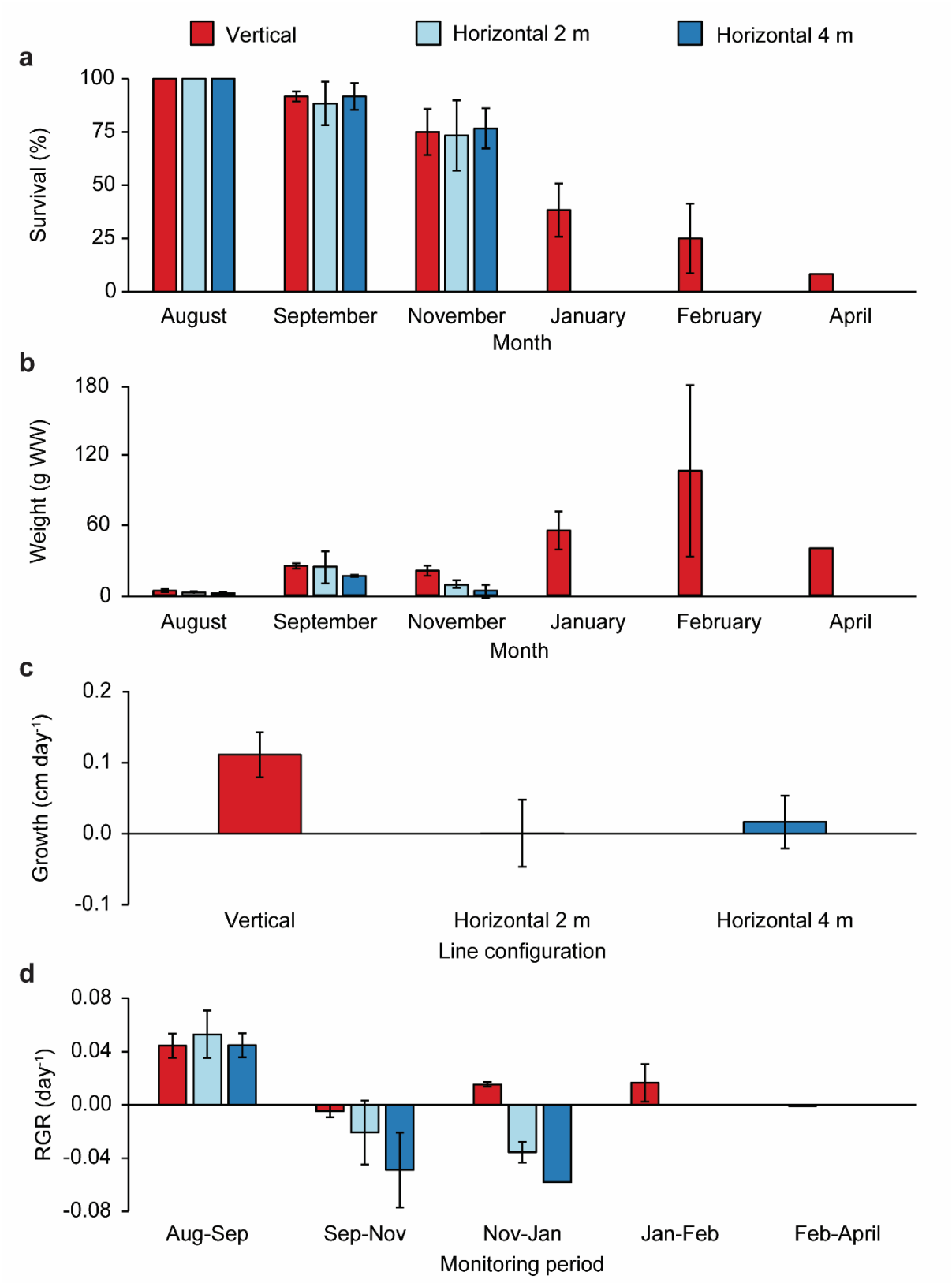

Figure 5.4 Average (± SD, n = 3) survival and growth of *E. radiata* on three line configurations for each month of monitoring following deployment in August 2021, with A) survival (% of the initial 20 individuals remaining on each line at each monitoring period) B) weight (g WW) of individuals, C) growth by elongation (cm day^{-1}); only during the first 44 days (August to September) after deployment, and D) relative growth rate (RGR; day^{-1}). All surviving individuals in April were on the same vertical line

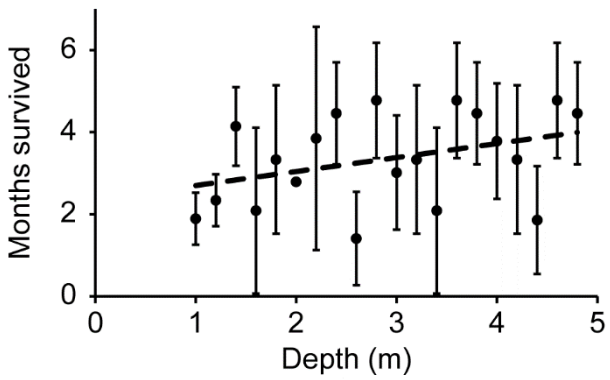

Figure 5.5 Average (± SD) number of months survived (August to February) per individual as a function of depth for vertical lines (n = 3). Linear regression (dotted line): $F_{1,18} = 2.77$, $P = 0.11$, $R^2 = 0.13$

5.4.2 Growth rates

The average weight of *E. radiata* individuals was significantly different among line configurations and between monitoring months, and there was a significant interaction effect between these factors (Table 5.1). The average weight of *E. radiata* on vertical lines increased exponentially from 4 g WW ± 1 SD per individual (n = 3) at deployment in August up to 106 g WW ± 73 SD per individual (n = 3) in February, after which time weight decreased (Figure 5.4b). Meanwhile, weight increase was much lower for individuals growing on horizontal lines, with the average weight of individuals reaching a maximum of only 24 g WW ± 13 SD and 16 g WW ± 1 SD for lines at 2 m and 4 m depth, respectively, in September (one month after deployment), before decreasing again. Similarly, growth of juveniles by elongation during the first 44 days after deployment (August to September) was markedly higher for individuals growing on vertical lines (0.11 cm day^{-1} ± 0.03 SD, n = 3) compared to horizontal lines (2 m depth: 0.00 cm day^{-1} ± 0.05 SD; 4 m depth: 0.02 cm day^{-1} ± 0.04 SD), although differences were not significant (Figure 5.4c, Table 5.1). RGR was significantly different among line configurations and between monitoring months (Table 5.1, Figure 5.4d). RGR was highest in the austral late winter/early spring (from August to September) for all line configurations, but only individuals on vertical lines maintained a positive growth rate after November.

5.4.3 Fouling

All individuals were fouled to some degree throughout the experiment (range: 5–75 % cover of fouling on thallus, n = 9; Table 5.2). Fouling of *E. radiata* was highest in the austral spring (September to November), where seaweed on horizontal lines were generally more fouled than seaweed on vertical lines. However, fouling was highly variable between individuals on replicate lines during this season, with two of the vertical replicate lines showing little fouling among individuals (range: 5-25 % thallus cover) and one replicate line showing high fouling on some individuals (range: 5-75 % thallus cover). During the austral summer (December to February), fouling was lower and less variable among the surviving individuals on the vertical lines (range: 10-33 % thallus cover, n = 3). A similar pattern was detected for fouling on the line itself (as opposed to fouling on the seaweed), where control lines were heaviest and had the highest densities of fouling organisms in spring (September and November, Figure 5.6).

Table 5.2 Fouling of seaweed individuals (% cover of thallus) on three line configurations from September 2021 to February 2022, estimated by eye as the average percent of thallus covered in fouling across all individuals on each replicate line (Rep). An approximate range of fouling was estimated on grow lines where fouling was highly variable between individuals, and a single number estimate was made on grow lines where fouling was more uniform among individuals. Note that all individuals on horizontal lines were lost by January

Fouling % Configuration	**Rep**	**Sep**	**Nov**	**Jan**	**Feb**
Vertical	1	25-75	5-50	10	33
Vertical	2	10	5	10	20
Vertical	3	10-25	5	5	33
Hor. 2m	1	25-50	75	n/a	n/a
Hor. 2m	2	50-75	75	n/a	n/a
Hor. 2m	3	25	75	n/a	n/a
Hor. 4m	1	50	75	n/a	n/a
Hor. 4m	2	50	25	n/a	n/a
Hor. 4m	3	50	25-50	n/a	n/a

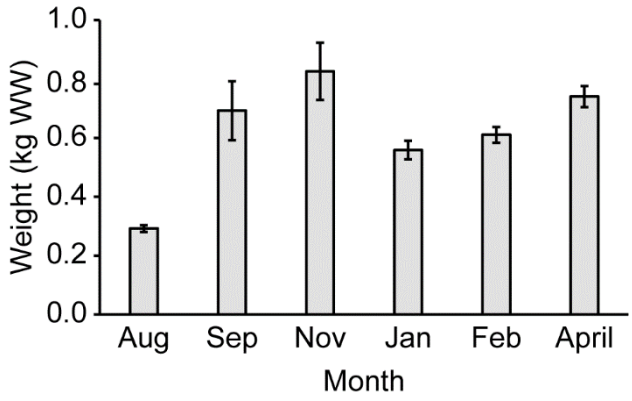

Figure 5.6 Average (± SD) weight (kg WW) of control lines for each monitoring month (n = 9)

5.4.4 Temperature and irradiation

Water temperature (averaged across 1-4 m depth) ranged from 14.7 to 21.7 °C during the austral spring (first measurement; 29th of September), from 18.5 to 24.7 °C during the austral summer (highest temperature: 12th of February), and from 19.5 to 24.0 °C during the austral autumn (last measurement; 15th of April). Both water temperature and irradiance decreased with depth, although this effect was only minor for temperature (Figure 5.7). The average water temperature between September and February (average between months) was 1.2 % lower at 4 m depth (19.1 °C ± 3.2 SD, n = 6) compared to 1 m depth (19.3 °C ± 3.3, n = 6). In contrast, irradiance between September and February was 54.8 % lower at 4 m depth (3,628 lum m^{-2} ± 969 SD, n = 4) compared to 1 m depth (8,026 lum m^{-2} ± 1,140 SD, n = 4). The average measured temperature at 1 m depth during the experiment was 0.6 ^{o}C above the average SST at the farm during the past 20 years from September to April, reaching a maximum of 1.1 ^{o}C above the monthly 20-year average in December (Figure 5.8; Pinkerton et al. 2022). Average monthly photosynthetically active radiation (PAR; µmol m^{-2} s^{-1}) peaked between November and January, with January showing the highest average light radiation.

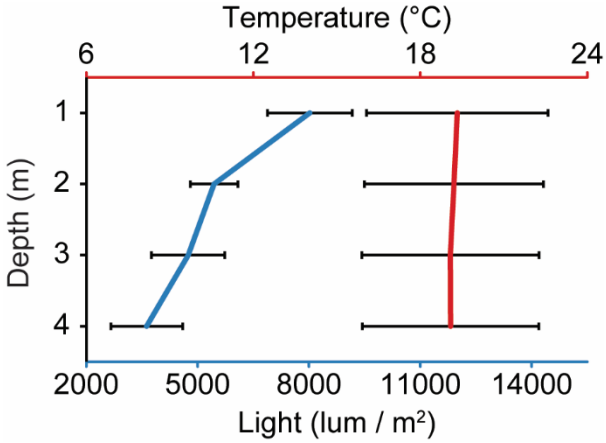

Figure 5.7 Depth profiles of average (± SD) water temperature (°C) and light (lum m^{-2}) from the 29th of September 2021 to 28th of February 2022. Measurements were taken once every 10 min, and water temperature is show as average between months (n = 6) and light is shown as average between weeks (n = 4), including only light data measured during the first week following each visit and omitting values of zero (night measurements)

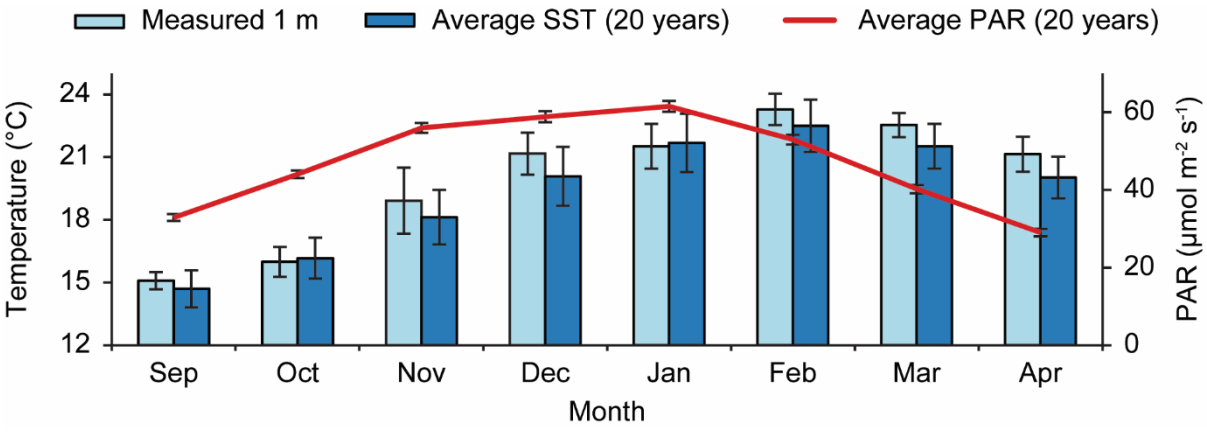

Figure 5.8 Average (± SD) measured monthly temperature (°C) at 1 m depth at the farm during the trial (light blue bars), average (± SD) monthly sea surface temperature (SST) at the farm during the last 20 years (dark blue bars), and average (± SD) monthly photosynthetically active radiation (PAR; µmol m^{-2} s^{-1}) at the farm during the last 20 years (red line). SD's on light blue bars express variation within months during the experiment (n = 4032–4464, depending on the number of days in a month), and SD's on dark blue bars and the red line express variation between months during the last 20 years (n = 20). Average monthly SST and PAR are obtained from the online data portal NIWA-SCENZ (Pinkerton et al. 2022)

5.5 Discussion

5.5.1 Line configuration

This study compared survival and growth of *E. radiata* on horizontal long lines (similar to farming methods for other commercially farmed kelps; lines at 2 and 4 m depth tested) and on vertical dropper lines (similar to farming methods for mussels). Although survival was similar between line configurations during the first three months (August to November), growth of *E.*

radiata during this time (measured by average individual weight) was exponential on vertical lines but was limited on horizontal lines. Similarly, elongation rates for juvenile individuals (during spring) were by far highest on vertical grow lines (average: 0.11 cm day^{-1} ± 0.03 SD, n = 3), but were lower than those reported for natural populations of adult *E. radiata* in Australia during the same period (average: 0.19 ± 0.1 SD and 0.16 ± 0.01 SD, at 3 and 5 m depth respectively; Fairhead and Cheshire 2004). Although, the RGR was comparable for all line configurations in the August to September period, it was higher for vertical lines compared to horizontal lines in all subsequent months. In accordance with the low growth observed on horizontal lines, most individuals on these lines were more severely fouled and eroded compared to individuals on the vertical lines. Furthermore, all individuals were lost on horizontal lines during the austral summer (i.e., by January), while 25 % of individuals on vertical lines still remained by February. This is the first time that survival and growth of *E. radiata* on different line configurations has been investigated, and our results show that survival and growth is higher on vertical lines compared to horizontal lines, when growing at 1-5 m depths in shallow semi-sheltered waters.

5.5.2 Light and temperature

A decrease in kelp abundance during summer is often driven by high water temperatures (Pehlke and Bartsch 2008; Moy and Christie 2012) which may cause respiration rates to exceed photosynthetic rates, resulting in a net carbon loss (Gerard 1988; Bearham et al. 2013). High summer temperatures have previously been identified as a main driver for reduced growth in *E. radiata* (Kirkman 1984), and water temperatures above 20-21 °C are associated with negative growth for *E radiata* in Australia (Hatcher et al. 1987; Bearham et al. 2013). Notably, high water temperature at 1 m depth were observed in this study (compared to the 20-year average SST), where the average monthly temperature exceeded 21 °C from December to April (Figure 5.8). In fact, a 29-week continuous marine heat wave was observed in the Hauraki Gulf (location of the farm) from November 2021 to May 2022, reaching a maximum intensity of 3.8 °C above average

temperature in late November to early December (Bell et al. 2022). Although upper thermal limits for survival may differ for *E. radiata* in Australia and New Zealand as thermal responses in kelp are often related to local growth conditions (Gerard and Du Bois 1988; Staehr and Wernberg 2009), heat stress was likely a central driver for the high mortality of *E. radiata* observed in the current study from January to April.

Average survival of *E. radiata* increased with increasing depth for the three experimental vertical lines, with the same pattern observed on the additional vertical lines that were not included in the formal analyses. Similarly, in a previous farming trial in New Zealand, all surviving individuals of *E. radiata* were found at the lowest measured depth (6 m) by the end of the trial (Neill et al. 2009), and in the North Sea, growth of farmed *Saccharina latissima* increased with depth between 2 and 8 m (Handå et al. 2013). In this study, average monthly water temperature was unusually high in November and December, and during this time the water temperature at 1 and 4 m depth reached a maximum difference of 2.0 °C or more on 17 days (non-consecutive, data not shown). However, from September to February, the average water temperature at 4 m depth was only 0.2 °C (1.2 %) lower than at 1 m depth. Therefore, it is unlikely that thermal stress alone explains the higher survival of individuals with increased depth. In comparison, average light levels (September to February) decreased considerably with depth and were 55 % lower at 4 m depth relative to 1 m depth. Exposure to high light levels may cause photoinhibition, reducing photosynthetic performance, and may also cause oxidative stress, when energy absorption by photosynthetic pigments exceeds what can be utilised for photochemistry (Adams III et al. 2008). Furthermore, seaweed may be more susceptible to photoinhibition and light-related oxidative stress during heat stress, as high temperatures may reduce photosynthetic rates and thereby lower the capacity to utilise absorbed energy (Bruhn and Gerard 1996; Lesser 2006; Heinrich et al. 2012). Daily irradiation peaked during the months of high mortality (November to February, Figure 5.8), and the higher mortality of *E. radiata* in shallower waters may therefore be due to a combination of light and temperature stress. Further indicating that light stress was contributing to mortality during summer,

wild individuals were observed in the upper 1 m of the water column in February growing in the shade attached to the underside of large floats on the farm. In contrast to the unhealthy individuals on the grow lines growing in full light, wild individuals under the floats were healthy in condition. However, although high light stress may be a crucial factor for survival in the upper layers of the water during summer, insufficient light in deeper water may also increase mortality as more light may be needed during elevated temperatures in summer to compensate for low photosynthetic efficiency and increased respiration rates (Staehr and Wernberg 2009). Indeed, in New Zealand, natural populations of *E. radiata* grew faster and were more abundant at 7 m depth compared 15 m depth (Novaczek 1984) and laminarian kelp forests generally decline in density at around 12-14 m depth, although dispersal has been observed down to 65 m depth (Choat and Schiel 1982). Thus, the optimal farming depth for *E. radiata* is likely to be somewhere below the upper portion of the water column where light stress is severe, but above the point where light levels become insufficient for obtaining positive net photosynthesis.

5.5.3 Implications for aquaculture

Juveniles of *E. radiata* on vertical lines grew to maturity (average individual weight: 106 g WW, n = 3 lines) within 6 months of deployment (from August to February), however survival decreased markedly during summer. High mortality and low growth rate during summer has previously been observed in *E. radiata* farming trials, recommending farming from early autumn to late spring to avoid high temperatures and fouling during these months (Neill et al. 2009; Wiltshire et al. 2020). Though growth rate is usually slower during autumn and winter (Wernberg and Goldberg 2008; Bearham et al. 2013), kelp is typically outplanted earlier in the year (e.g., early autumn) to increase growing time before a potential harvest in late spring/early summer, and to possibly lower overall mortality (Broch et al., 2019; Hwang et al., 2020). Previous studies on *E. radiata* in New Zealand and on commercial northern hemisphere kelp species have found fouling to be heaviest during summer (Neill et al. 2009; Handå et al. 2013). In contrast, we found that fouling

was most prevalent in spring. However, we may have missed the peak of fouling during the summer months as monitoring was not conducted in December. The negative physiological effects of temperature are likely to be most prevalent at shallow sheltered sites as water temperature at these sites will often be higher compared to deeper and more exposed sites (Bearham et al. 2013). In the current study, *E. radiata* was farmed within 50 m of the shore in a semi-sheltered area (outer Coromandel Harbour) and higher growth and survival rates may therefore be achieved in a setting further off-shore that has higher flow rates and deeper waters. The unusually high water temperatures (compared to the 20-year average) observed during November and December likely contributed to the high mortality of *E. radiata* observed between November and January (Moy and Christie 2012; Nepper-Davidsen et al. 2019), and thus, results of the current study may not necessarily represent a general scenario. However, marine heat waves are predicted to become more frequent, longer lasting and more extreme as global warming intensifies (Oliver et al. 2018). Therefore, adapting to these environmental changes will be crucial for future-proofing a successful kelp farming industry in New Zealand. Such adaptations could be 1) choosing farm sites and farming depths accordingly (Choat and Schiel 1982; Novaczek 1984), 2) harvesting before summer temperatures reach harmful intensities, and 3) selecting and breeding more heat tolerant cultivars (Hwang et al. 2019).

This study constituted the first practical step in an ongoing development of farming practices for *E. radiata* in New Zealand, aiming to provide an initial proof of concept and fast-tracking results on farming settings and timing of outplanting and harvest. It is important to note that the presented results are based on transplanted wild collected seaweed individuals and therefore are not necessarily transferable to faming trials employing a hatchery phase, which would be included in an actual aquaculture setting. In conclusion, this study supports farming *E. radiata* on vertical dropper lines rather than horizontal lines, but given the limited level of replication, the overall high mortality, and unusually high SST during the experiment, more studies are needed to further test these findings.

Chapter 6

General Discussion

6.1 Main research findings and implications

The objective of this thesis was to create foundations for sustainable seaweed aquaculture of the native kelp *Ecklonia radiata* in New Zealand. The research included field collections of seaweed samples and field trials on the North Island of New Zealand, laboratory analysis of genetic and biochemical properties, multivariate modelling, and statistical and data management programming.

Newly developed breeding protocols for *E. radiata* (Praeger et al. 2022a, b) create an incentive for translocation of cultivars from centralised on-shore hatcheries to farming sites of interest. However, significant genetic differences were detected at all hierarchical levels, with a high degree of genetic clustering among regions and among sites within regions, and a high degree of significant genetic differences between sites. These findings indicate strong genetic structure and low gene flow of *E. radiata* on the North Island of New Zealand and suggest the presence of several genetically distinct sub-populations. Based on these results, and in agreement with European guidelines (Barbier et al. 2019), cultivars should therefore not be translocated outside their area of origin to prevent changes to the genetic structure and diversity of wild populations. This finding means that target strains of *E. radiata* for cultivation will need to be identified from natural populations within the vicinity of a potential farm sites, which may be affected by spatial and temporal variation in biomass quality.

The biochemical composition of *E. radiata* may vary between sub-populations, due to the strong genetic structure, as has been suggested for components such as phlorotannins and lipids in other seaweed (Honkanen and Jormalainen 2005; Gosch et al. 2015). High spatial variation between sites was detected among key commercial components such as alginate, phlorotannins, and glucose,

however there was no clear spatial pattern among regions. The large spatial differences were therefore unlikely to be caused by genetic differences, as the genetic pattern observed in Chapter 2 (Nepper-Davidsen et al. 2021) was not reflected in the measured biomass components (i.e., the Wellington sites were most genetically distinct but did not stand out in terms of biomass composition). Conversely, there was a strong seasonal pattern in biomass composition with significant temporal variation in key commercial components such as alginate, glucose, proteins, and lipids. These data indicate that environmental variation may be a key driver of biomass composition in *E. radiata* and that high spatial variation may be due to site-specific environmental conditions, such as temperature, wave exposure and nutrients (McHugh 2003; Manns et al. 2017; Roleda and Hurd 2019). The biomass quality of local broodstock therefore will be a critical consideration when selecting sites for seaweed aquaculture, and the optimal harvest timing will depend on the components of interest, where alginate content is likely to peak in early austral spring and protein and lipid content is likely to peak in late austral spring/early summer.

Methods for high-throughput grading of raw biomass are needed to account for the large spatial and temporal variation in biomass composition of *E. radiata* in New Zealand. Models were therefore developed to predict biomass content (partial least squared regression models; PLSR) and region of origin (partial least squared discriminant analysis models; PLS-DA) using mid-infrared (MIR) and near-infrared (NIR) spectroscopy, as has been widely applied for other biological materials in commercial in-line systems (Capuano and van Ruth 2016; Beć et al. 2020). The PLSR models demonstrated high predictive accuracy for most components, with glucose, phlorotannins, nitrogen, and the mannuronic to guluronic acid ratio (M:G ratio) showing highest correlation (R^2) among calibration samples and glucose, alginate, phlorotannins and carbon content showing lowest relative prediction error of validation samples (% RMSEP). The NIR models generally outperformed the MIR models with higher accuracy and less sensitivity to measurement error (fewer outliers). The PLS-DA models demonstrated high accuracy for predicting region of origin based on spectral data, where samples from the Wellington region were most accurately predicted, followed by samples from the

Gisborne region. These spectral differences reveal phenotypic variations in *E. radiata* between regions and match the genetic pattern observed in Chapter 2 (Nepper-Davidsen et al. 2021), where Northland and Bay of Plenty samples were most similar, and Gisborne and Wellington samples showed intermediate and highest genetic differentiation from the northern samples, respectively. However, these differences in genotype and phenotype do not seem to be related to the biomass components quantified in Chapter 3 (Nepper-Davidsen et al. 2023), which did not follow the same spatial pattern among regions. The PLSR models further indicated that the phenotypic differences were not related to the measured biomass components as modelled predictions of biomass content did not improve by excluding the Wellington samples (but decreased instead), thus demonstrating uniform correlation between the spectral data and the measured biomass components across all samples, despite the regional spectral differences. Overall, the models show that NIR and MIR can be effective tools for high-throughput biomass grading of *E. radiata* biomass, to establish provenance, and to analyse biogeography of seaweeds. In addition, the PLSR models may be important tools enabling rapid screening of wild types for desirable traits for strain selection and breeding.

Farm trials are necessary to monitor cultivar performance and to test settings before large scale practices can be adopted. The final part of this thesis constituted the first practical step in an ongoing development of farming practices for *E. radiata* in New Zealand and investigated the effects of line configuration and cultivation depth on growth and survival of *E. radiata* in a commercial, green-lipped mussel (*Perna canaliculus*) marine farm setting. The biology of *E. radiata* has been studied extensively (see review by Wernberg et al. 2019), however no largescale commercial cultivation has yet been established (Wiltshire et al. 2020), and little work has been done to optimise farm settings. Among the tested line configurations (vertical, horizontal 2 m depth, and horizontal 4 m depth), *E. radiata* showed highest survival and growth rates when growing on vertical lines. Only *E. radiata* growing on vertical lines had survived four months following deployment, and this pattern was reflected in the maximum average individual weight and juvenile growth by elongation which were higher on vertical lines compared to horizontal lines. An unusually long and severe marine heat

wave was recorded in the area of the farm (Hauraki Gulf; Bell et al. 2022) during most of the experiment, which was likely a main driver for the high mortality (Moy and Christie 2012; Nepper-Davidsen et al. 2019). Furthermore, mortality of *E. radiata* increased at shallow depths on vertical lines which may have been correlated to a combination of temperature and light stress (Bruhn and Gerard 1996; Heinrich et al. 2012). Overall, these results support the use of vertical dropper lines rather than horizontal lines for *E. radiata* farming and provide a first proof of concept for farm settings and further development.

6.2 Future research directions

This thesis has significant implications for seaweed aquaculture in New Zealand and directions for future research.

Chapter 2 concludes not to translocate *E. radiata* cultivars outside their area of origin, however the practical scale of this precaution is still unknown due to the large geographical distance between sampling sites. Further research should therefore be conducted analysing genetic structure at a finer scale and in other regions (e.g., the North Island east coast, the South Island, and Stewart Island) to provide more precise guidelines for translocation policy in New Zealand. However, care is needed to avoid over-restricting the development of the seaweed aquaculture sector. Balanced risk-benefit assessments should therefore be conducted on seaweed cultivar translocation in New Zealand to determine the acceptable risk, from both an ecological, social, and financial perspective. Furthermore, the caution advised around translocation of *E. radiata* cultivars may not apply for other target species of seaweed for aquaculture (e.g., the regional genetic connectivity of *Carpophyllum maschalocarpum* in New Zealand is high; Buchanan and Zuccarello 2012), and translocation guidelines are thus likely to be species specific depending on life history, dispersal of spores, and buoyancy/rafting potential (Gaylord et al. 2006; Fraser et al. 2013; Muangmai et al. 2015).

Chapter 3 finds environmental variation to be a key driver for high spatial and temporal differences in biomass composition, but many of these mechanisms are still poorly understood. For instance, *E. radiata* showed large spatial variation in alginate content, however the effect of wave exposure on alginate content, though widely referred to, is not well documented (see Munda 1987; Indergaard et al. 1990; McHugh 2003). Furthermore, spatial variation in biomass components, such as phlorotannins and lipids, has been linked to genotypic differences in seaweed (Honkanen and Jormalainen 2005; Gosch et al. 2015), but no regional pattern in biomass composition was detected, despite high genetic differentiation between regions. Common garden experiments (De Villemereuil et al. 2016) are therefore needed to determine the relative effects of genotype and environmental conditions on key commercial traits such as biochemical content, growth rate, and heat tolerance of *E. radiata*. Similar biochemical analysis should be conducted for other targeted species to enable determination of aquaculture potential in terms of spatiotemporal variability in biomass quality. It is also worth noting that temporal variation was measured at only one site during a single 1-year period, and such temporal patterns may vary between sites and from year to year (Jennings and Steinberg 1994; Schiener et al. 2015; Manns et al. 2017). Thus, to further investigate these patterns, additional sites should be included and monitored across several growth seasons. However, overall patterns such as the seasonal fluctuation in laminarin are likely to be similar between sites and at different years, being related to overall growth patterns controlled by seasonal changes in temperature and light availability. Finally, the low content of toxic arsenic found in *E. radiata* assumes that arsenic is only toxic to humans in its inorganic form and that the amount of inorganic arsenic in the kelp can be estimated roughly as 1 % of the total arsenic, as was found for Australian *E. radiata* (Tukai et al. 2001). These assumptions should be further investigated to ensure that the arsenic levels in *E. radiata* from New Zealand are safe for human consumption.

Chapter 4 successfully demonstrated the use of NIR and MIR spectroscopy for predicting biomass content and region of origin in raw biomass samples of *E. radiata*. The models included a large number of samples (138 calibration and 24 validation samples), but additional calibration

samples would further increase model accuracy and robustness by including a wider range of concentrations of analytical targets and by including samples from more regions. The models performed well on samples from the Wellington region, despite the observed phenotypic and genotypic differences between regions, however, it would be useful to test how well the models perform across the full geographical range of *E. radiata* (e.g., by testing samples from Australia). A previous study found that single-species models were not applicable to microalgal species of different kingdoms and phyla (Laurens and Wolfrum 2011), but the models developed in this study could be applicable to related species of *Ecklonia* or similar kelp species (e.g., *Lessonia variegata*). It is therefore worth investigating their transferability before similar work is undertaken for related kelp species. It would be interesting to develop PLSR models based on the genetic microsatellite data and the biochemistry data (both analyses measured on the same individuals) to analyse correlations between genetic structure and biochemical composition of *E. radiata*, although additional genetic data may be needed as the microsatellite data only make up 28 data variables per individual (14 loci times 2) and because microsatellites are noncoding DNA regions. Such a study could be further extended by incorporating environmental data for each site (e.g., water temperature, light radiation, nutrients availability, water flow; Manns et al. 2017) testing the correlation between seasonal fluctuations in environmental conditions and biomass content and the relative influence of genetic and environmental factors on biomass composition. Similarly, developing PLS-DA models predicting region of origin based on the microsatellite data could be useful for establishing provenance based on genetic structure in high-throughput genetic applications.

Chapter 5 identified cultivation depth as a central factor for survival of farmed *E. radiata*, in terms of finding the balance between light stress at shallow depths (Bruhn and Gerard 1996; Heinrich et al. 2012) and sub-saturating light levels at deep depths (Staehr and Wernberg 2009). Natural populations of *E. radiata* in New Zealand are typically most abundant around 10 m depth (Choat and Schiel 1982). However, the optimal light profile for farming of the kelp is still largely unknown and may vary between sites, depending on conditions such as turbidity/light penetration

and water temperature (Bruhn and Gerard 1996; Bearham et al. 2013). An understanding of the effect of light profiles on survival and growth of *E. radiata* at different sites (i.e., with different turbidity/light penetration) will therefore be crucial for choosing farming locations and cultivation depth. Furthermore, heat stress was identified as a main driver for the high mortality observed during late austral spring and summer and could be mitigated by selecting sites with lower average water temperature, and by improving cultivar heat tolerance by selecting for heat resistant strains among local broodstock (Hwang et al. 2019). Indeed, environmental stressors such as light, temperature, and nutrient limitation are likely to interact synergistically (Heinrich et al. 2012; Roleda and Hurd 2019), and thus reducing one of these stressors is likely to reduce the effect of the others also. Understanding direct physiological responses to heat and light stress (e.g., on survival, growth, biomass composition) will be central for determining when to outplant seedlings, when to harvest, and ultimately to extend the growth period of *E. radiata*. Chapter 3 (Nepper-Davidsen et al. 2023) indicated a high degree of nitrogen limitation in *E. radiata* and selecting sites high in nitrogen concentration may therefore improve growth and stress tolerance of the farmed seaweed (Roleda and Hurd 2019).

6.3 Conclusion

This thesis addresses key knowledge gaps for establishing sustainable aquaculture of *E. radiata* in New Zealand within four research areas which have gained little previous attention.

1) The genetic analysis indicated that cultivars should not be translocated outside their area of origin.

2) The biochemical analysis demonstrated overall high biomass content of phlorotannins and alginate and emphasises the importance of site selection due to site specific differences in biomass quality.

3) The chemometric models demonstrated that MIR and NIR spectroscopy can be valuable tools for high-throughput biomass grading of *E. radiata* and to establish provenance.

4) The farm trial demonstrated successful farming of *E. radiata*, when grown on vertical lines, and identified farming depth and temperature stress as central factors to investigate for further farm trials.

Together these findings provide a major step forward towards creating sustainable aquaculture practices of *E. radiata* in New Zealand and proof of concept for further development to build upon. Similar studies should be conducted for other target species for seaweed aquaculture in New Zealand. To further develop aquaculture of *E. radiata,* the next steps should be:

1. To upscale farming practises using a hatchery stage, testing different sites and different depths, with site selection targeting lower average water temperature (i.e., than experienced during these trials), high nutrient availability, and high water flow.
2. To conduct detailed analysis of the genetic structure of *E. radiata* (using the same 14 microsatellite loci) within areas of interest for aquaculture (e.g., the Bay of Plenty) to provide more precise guidelines on translocation on a local scale; and to further conduct balanced risk-benefit assessments on seaweed cultivar translocation in New Zealand to determine the acceptable risk, from both an ecological, social, and financial perspective.
3. To extend the calibrated range of the chemometric models and apply them to monitor development in biomass quality of farmed cultivars and for selection of new cultivar strains.

References

Adams III WW, Zarter CR, Mueh KE, et al (2008) Energy dissipation and photoinhibition: a continuum of photoprotection. In: Demming-Adams B, Adams W, Mattoo A (eds) Photoprotection, photoinhibition, gene regulation, and environment. Springer Netherlands, Dordrecht, pp 49–64

Akita S, Hashimoto K, Hanyuda T, Kawai H (2020) Molecular phylogeny and biogeography of *Ecklonia* spp. (Laminariales, Phaeophyceae) in Japan revealed taxonomic revision of *E. kurome* and *E. stolonifera*. Phycologia 59:330–339. https://doi.org/10.1080/00318884.2020.1756123

Akita S, Koiwai K, Hanyuda T, et al (2018) Development of 11 *Ecklonia radicosa* (Phaeophyceae, Laminariales) SSRs markers using next-generation sequencing and intra-genus amplification analysis. J Appl Phycol 30:2111–2115. https://doi.org/10.1007/s10811-018-1406-5

Amosu AO, Robertson-andersson D V, Maneveldt GW, et al (2013) South African seaweed aquaculture: a sustainable development example for other African coastal countries. 8:5268–5279. https://doi.org/10.5897/AJAR2013

Anderson MJ, Gorley RN, Clarke KR (2016) PERMANOVA+ for PRIMER: guide to software and statistical methods. PRIMER-E Ltd., Plymouth

Angell AR, Mata L, de Nys R, Paul NA (2016) The protein content of seaweeds: a universal nitrogen-to-protein conversion factor of five. J Appl Phycol 28:511–524. https://doi.org/10.1007/s10811-015-0650-1

Angell AR, Mata L, de Nys R, Paul NA (2014) Variation in amino acid content and its relationship to nitrogen content and growth rate in *Ulva ohnoi* (Chlorophyta). J Phycol 50:216–226. https://doi.org/10.1111/jpy.12154

ANSES (2018) Opinion on the risk of excess iodine intake from the consumption of seaweed in foodstuffs. French agency for food, environmental and occupational health and safety. Paris

ANSES (2020) Opinion on maximum cadmium levels for seaweed intended for human consumption. French agency for food, environmental and occupational health and safety. Paris

Aziz A, Poinssot B, Daire X, et al (2003) Laminarin elicits defense responses in grapevine and induces protection against *Botrytis cinerea* and *Plasmopara viticola*. Mol Plant-Microbe Interact 16:1118–1128. https://doi.org/10.1094/MPMI.2003.16.12.1118

Barak S, Mudgil D (2014) Locust bean gum: processing, properties and food applications - a review. Int J Biol Macromol 66:74–80. https://doi.org/10.1016/j.ijbiomac.2014.02.017

Barbier M, Charrier B, Araujo R, et al (2019) Pegasus - phycomorph European guidelines for a sustainable aquaculture of seaweeds. COST Action FA1406, Roscoff

Battacharyya D, Babgohari MZ, Rathor P, Prithiviraj B (2015) Seaweed extracts as biostimulants in horticulture. Sci Hortic (Amsterdam) 196:39–48. https://doi.org/10.1016/j.scienta.2015.09.012

Bearham D, Vanderklift MA, Gunson JR (2013) Temperature and light explain spatial variation in growth and productivity of the kelp *Ecklonia radiata*. Mar Ecol Prog Ser 476:59–70. https://doi.org/10.3354/meps10148

Beć KB, Grabska J, Huck CW (2020) Biomolecular and bioanalytical applications of infrared spectroscopy – a review. Anal Chim Acta 1133:150–177. https://doi.org/10.1016/j.aca.2020.04.015

Bell JJ, Smith RO, Micaroni V, et al (2022) Marine heat waves drive bleaching and necrosis of temperate sponges. Curr Biol 33:1–6

Biancarosa I, Belghit I, Bruckner CG, et al (2018) Chemical characterization of 21 species of marine macroalgae common in Norwegian waters: benefits of and limitations to their potential use in food and feed. J Sci Food Agric 98:2035–2042. https://doi.org/10.1002/jsfa.8798

Bixler HJ, Porse H (2011) A decade of change in the seaweed hydrocolloids industry. J Appl Phycol 23:321–335. https://doi.org/10.1007/s10811-010-9529-3

Black WAP (1950) The seasonal variation in the cellulose content of the common Scottish Laminariaceae and Fucaceae. J Mar Biol Assoc United Kingdom 29:379–387. https://doi.org/10.1017/S0025315400055429

Bolstad GH, Robertsen G, Jonsson B, et al (2017) Gene flow from domesticated escapes alters the life history of wild Atlantic salmon. Nat Ecol Evol 1, 1024:1–5. https://doi.org/10.1038/s41559-017-0124

Bradly N, Syddall V, Ingram C, et al (2021) Stocktake and characterisation of Aotearoa New Zealand's seaweed sector: market and regulatory focus. EnviroStrat, Auckland

Broch, OJ, Alver, MO, Bekkby, T, et al. (2019) The kelp cultivation potential in coastal and offshore regions of Norway. Front. Mar. Sci. 5, 1–15. doi:10.3389/fmars.2018.00529.Bruhn J, Gerard VA (1996) Photoinhibition and recovery of the kelp *Laminaria saccharina* at optimal and superoptimal temperatures. Mar Biol 125:639–648. https://doi.org/10.1007/BF00349245

Buchanan J, Zuccarello GC (2012) Decoupling of short- and long-distance dispersal pathways in the endemic New Zealand seaweed *Carpophyllum maschalocarpum* (Phaeophyceae, Fucales). J Phycol 48:518–529. https://doi.org/10.1111/j.1529-8817.2012.01167.x

Buschmann AH, Camus C (2019) An introduction to farming and biomass utilisation of marine macroalgae. Phycologia 58:443–445. https://doi.org/10.1080/00318884.2019.1638149

Buschmann AH, Camus C, Infante J, et al (2017) Seaweed production: overview of the global state of exploitation, farming and emerging research activity. Eur J Phycol 52:391–406. https://doi.org/10.1080/09670262.2017.1365175

Callaway E (2015) Lab staple agar hit by seaweed shortage. Nature 528:171–172. https://doi.org/10.1038/528171a

Camia A, Robert N, Jonsson R, et al (2018) Biomass production, supply, uses and flows in the European Union. first results from an integrated assessment. EUR 28993 EN, Publications Office of the European Union, Luxembourg

Campbell I, Macleod A, Sahlmann C, et al (2019) The environmental risks associated with the development of seaweed farming in Europe - prioritizing key knowledge gaps. Front Mar Sci 6:1–22. https://doi.org/10.3389/fmars.2019.00107

Capuano E, van Ruth SM (2016) Infrared spectroscopy: applications, 1st edn. Elsevier Ltd

Cascant MM, Sisouane M, Tahiri S, et al (2016) Determination of total phenolic compounds in compost by infrared spectroscopy. Talanta 153:360–365. https://doi.org/10.1016/j.talanta.2016.03.020

Černá M (2011) Seaweed proteins and amino acids as nutraceuticals. In: Kim SK (ed) Advances in Food and Nutrition Research, 1st edn. Elsevier Inc., pp 297–312

Choat JH, Schiel DR (1982) Patterns of distribution and abundance of large brown algae and

invertebrate herbivores in subtidal regions of northern New Zealand. J Exp Mar Bio Ecol 60:129–162. https://doi.org/10.1016/0022-0981(82)90155-1

Clark D, Newcombe E, Clement D, et al (2021) Stocktake and characterisation of Aotearoa New Zealand's seaweed sector: environmental effects of seaweed wild-harvest and aquaculture. Cawthron, Nelson

Clarke KR, Gorley RN (2015) PRIMER v7: user manual/tutorial. PRIMER-E Ltd., Plymouth

Coleman MA (2013) Connectivity of the habitat-forming kelp, *Ecklonia radiata* within and among estuaries and open coast. PLoS One 8:1–8. https://doi.org/10.1371/journal.pone.0064667

Coleman MA, Chambers J, Knott NA, et al (2011a) Connectivity within and among a network of temperate marine reserves. PLoS One 6:1–10. https://doi.org/10.1371/journal.pone.0020168

Coleman MA, Gillanders BM, Connell SD (2009) Dispersal and gene flow in the habitat-forming kelp, *Ecklonia radiata*: relative degrees of isolation across an eastwest coastline. Mar Freshw Res 60:802–809. https://doi.org/10.1071/MF08268

Coleman MA, Roughan M, Macdonald HS, et al (2011b) Variation in the strength of continental boundary currents determines continent-wide connectivity in kelp. J Ecol 99:1026–1032. https://doi.org/10.1111/j.1365-2745.2011.01822.x

Collins CJ, Fraser CI, Ashcroft A, Waters JM (2010) Asymmetric dispersal of southern bull-kelp (*Durvillaea antarctica*) adults in coastal New Zealand: testing an oceanographic hypothesis. Mol Ecol 19:4572–4580. https://doi.org/10.1111/j.1365-294X.2010.04842.x

De Villemereuil P, Gaggiotti OE, Mouterde M, Till-Bottraud I (2016) Common garden experiments in the genomic era: new perspectives and opportunities. Heredity (Edinb) 116:249–254. https://doi.org/10.1038/hdy.2015.93

Earl DA, vonHoldt BM (2012) STRUCTURE HARVESTER: a website and program for visualizing STRUCTURE output and implementing the Evanno method. Conserv Genet Resour 4:359–361. https://doi.org/10.1007/s12686-011-9548-7

Eigenvector Research Inc. (2022) PLS Toolbox (R9.1), Manson, WA USA; software available at http://www.eigenvector.com

Ellstrand NC, Meirmans P, Rong J, et al (2013) Introgression of crop alleles into wild or weedy populations. Annu Rev Ecol Evol Syst 44:325–345. https://doi.org/10.1146/annurev-ecolsys-110512-135840

European Commission (2019) The EU blue economy report 2019. Publications Office of the European Union, Directorate-General for Maritime Affairs and Fisheries, Joint Research Centre. Luxembourg. https://doi/10.2771/21854

European Commission (2022) ALGEADEMO demonstrates the full potential of seaweed. In: Oceans-and-fisheries.ec.europa.eu. https://oceans-and-fisheries.ec.europa.eu/news/algaedemo-demonstrates-full-potential-seaweed-2022-10-25_en

Evankow A, Christie H, Hancke K, et al (2019) Genetic heterogeneity of two bioeconomically important kelp species along the Norwegian coast. Conserv Genet 20:615–628. https://doi.org/10.1007/s10592-019-01162-8

Evanno G, Regnaut S, Goudet J (2005) Detecting the number of clusters of individuals using the software STRUCTURE: a simulation study. Mol Ecol 14:2611–2620. https://doi.org/10.1111/j.1365-294X.2005.02553.x

Excoffier L, Lischer HEL (2010) Arlequin suite ver 3.5: a new series of programs to perform population genetics analyses under Linux and Windows. Mol Ecol Resour 10:564–567. https://doi.org/10.1111/j.1755-0998.2010.02847.x

Fairhead VA, Cheshire AC (2004) Rates of primary productivity and growth in *Ecklonia radiata* measured at different depths, over an annual cycle, at West Island, South Australia. Mar Biol 145:41–50. https://doi.org/10.1007/s00227-004-1308-8

FAO (2022) The state of world fisheries and aquaculture 2022. towards blue transformation. Food and agriculture organization of the United Nations, Rome. https://doi.org/10.4060/cc0461en

FAO (2018a) The global status of seaweed production, trade and utilization. Globefish Research Programme Volume 124, Rome, 20 pp. Licence: CC BY-NC-SA 3.0 IGO

FAO (2021) Global status of seaweed production, trade and utilization. Food and agriculture organization of the United Nations. Rome *28–29 0ctober 2021*. Food Safety and Quality Series No. 13. Rome. https://doi.org/10.4060/cc0846en

FAO (2018b) The State of World Fisheries and Aquaculture 2018 - Meeting the sustainable development goals. Food and agriculture organization of the United Nations, Rome, Licence: CC BY-NC-SA 3.0 IGO

FAO, WHO (2022) Report of the expert meeting on food safety for seaweed – current status and future perspectives. Food and agriculture organization of the United Nations, Rome, 8–29 0ctober 2021. Food Safety and Quality Series No. 13. https://doi.org/10.4060/cc0846en

Folch J, Lees M, Sloane Stanley G. (1957) A simple method for the isolation and purification of total lipides from animal tissues. J Biol Chem 226:497–509

Fowler-Walker MJ, Wernberg T, Connell SD (2006) Differences in kelp morphology between wave sheltered and exposed localities: morphologically plastic or fixed traits? Mar Biol 148:755–767. https://doi.org/10.1007/s00227-005-0125-z

Fraser CI, Nikula R, Spencer HG, Waters JM (2009) Kelp genes reveal effects of subantarctic sea ice during the Last Glacial Maximum. Proc Natl Acad Sci U S A 106:3249–3253. https://doi.org/10.1073/pnas.0810635106

Fraser CI, Zuccarello GC, Spencer HG, et al (2013) Genetic affinities between trans-oceanic populations of non-buoyant macroalgae in the high latitudes of the southern hemisphere. PLoS One 8:1–13. https://doi.org/10.1371/journal.pone.0069138

FSANZ (2019) 25th australian total diet study. Food Standards Australia and New Zealand, Canberra

Ganesan AR, Tiwari U, Rajauria G (2019) Seaweed nutraceuticals and their therapeutic role in disease prevention. Food Sci Hum Wellness 8:252–263. https://doi.org/10.1016/j.fshw.2019.08.001

Gaylord B, Reed CD, Raimondi TP, Washburn L (2006) Macroalgal spore dispersal in coastal environments: mechanistic insights revealed by theory and experiment. Ecol Monogr 76:481–502. https://doi.org/https://doi.org/10.1890/0012-9615(2006)076[0481:MSDICE]2.0.CO;2

Gerard VA (1988) Ecotypic differentiation in light-related traits of the kelp *Laminaria saccharina*. Mar Biol 97:25–36. https://doi.org/10.1007/BF00391242

Gerard VA, Du Bois KR (1988) Temperature ecotypes near the southern boundary of the kelp *Laminaria saccharina*. Mar Biol 97:575–580. https://doi.org/10.1007/BF00391054

Gibbons C (2014) Huge potential for the seaweed industry. Seafood New Zealand Magazine 8:24-25

Glenn EP, Moore D, Brown JJ, et al (1998) A sustainable culture system for *Gracilaria parvispora* (Rhodophyta) using sporelings, reef growout and floating cages in Hawaii. Aquaculture 165:221–232. https://doi.org/10.1016/S0044-8486(98)00263-4

Glover KA, Pertoldi C, Besnier F, et al (2013) Atlantic salmon populations invaded by farmed escapees: quantifying genetic introgression with a Bayesian approach and SNPs. BMC Genet 14:1–19. https://doi.org/10.1186/1471-2156-14-74

Gosch BJ, Lawton RJ, Paul NA, et al (2015) Environmental effects on growth and fatty acids in three isolates of *Derbesia tenuissima* (Bryopsidales, Chlorophyta). Algal Res 9:82–93. https://doi.org/10.1016/j.algal.2015.02.022

Gosch BJ, Magnusson M, Paul NA, de Nys R (2012) Total lipid and fatty acid composition of seaweeds for the selection of species for oil-based biofuel and bioproducts. GCB Bioenergy 4:919–930. https://doi.org/10.1111/j.1757-1707.2012.01175.x

Graf L, Shin Y, Yang JH, et al (2021) A genome-wide investigation of the effect of farming and human-mediated introduction on the ubiquitous seaweed *Undaria pinnatifida*. Nat Ecol Evol 5:360–368. https://doi.org/10.1038/s41559-020-01378-9

Grandorf Bak U (2019) Seaweed cultivation in the Faroe Islands: an investigation of the biochemical composition of selected macroalgal species, optimised seeding technics, and open-ocean cultivation methods from a commercial perspective. Technical University of Denmark, Lyngby

Guichoux E, Lagache L, Wagner S, et al (2011) Current trends in microsatellite genotyping. Mol Ecol Resour 11:591–611. https://doi.org/10.1111/j.1755-0998.2011.03014.x

Guzinski J, Ballenghien M, Daguin-Thiébaut C, et al (2018) Population genomics of the introduced and cultivated Pacific kelp *Undaria pinnatifida*: marinas—not farms—drive regional connectivity and establishment in natural rocky reefs. Evol Appl 11:1582–1597. https://doi.org/10.1111/eva.12647

Hahn JL, Van Alstyne KL, Gaydos JK, et al (2022) Chemical contaminant levels in edible seaweeds of the Salish Sea and implications for their consumption. PLoS One 17:e0269269. https://doi.org/10.1371/journal.pone.0269269

Hall-Spencer J, Kelly J, Maggs C (2010) Background document for Maërl beds. OSPAR Commission, London

Handå A, Forbord S, Wang X, et al (2013) Seasonal- and depth-dependent growth of cultivated kelp (*Saccharina latissima*) in close proximity to salmon (*Salmo salar*) aquaculture in Norway. Aquaculture 414–415:191–201. https://doi.org/10.1016/j.aquaculture.2013.08.006

Hartman Y, Uwimana B, Hooftman DAP, et al (2013) Genomic and environmental selection patterns in two distinct lettuce crop-wild hybrid crosses. Evol Appl 6:569–584. https://doi.org/10.1111/eva.12043

Hatcher B., Kirkman H, Wood WF (1987) Growth of the kelp *Ecklonia radiata* near the northern limit of its range in Western Australia. Mar Biol 95:63–73. https://doi.org/10.1038/093124a0

Haug A, Larsen B, Smidsrød O (1967) Studies on the sequence of uronic acid residues in alginic acid. Acta Chem Scand 21:691–704. https://doi.org/10.3891/ACTA.CHEM.SCAND.21-0691

Haug A, Larsen B, Smidsrød O (1974) Uronic acid sequence in alginate from different sources. Carbohydr Res 32:217–225. https://doi.org/10.1016/S0008-6215(00)82100-X

Haygood R, Ives AR, Andow DA (2003) Consequences of recurrent gene flow from crops to wild relatives. R Soc 270:1879–1886. https://doi.org/10.1098/rspb.2003.2426

Heath RA (1985) A review of the physical oceanography of the seas around New Zealand — 1982. New Zeal J Mar Freshw Res 19:79–124. https://doi.org/10.1080/00288330.1985.9516077

Heinrich S, Valentin K, Frickenhaus S, et al (2012) Transcriptomic analysis of acclimation to temperature and light stress in *Saccharina latissima* (Phaeophyceae). PLoS One 7:1–13. https://doi.org/10.1371/journal.pone.0044342

Hermans S (2023) 2023 seaweed state of the industry. In: Phycology.net. https://phyconomy.net/articles/2022-seaweed-review/#more-1935

Honkanen T, Jormalainen V (2005) Genotypic variation in tolerance and resistance to fouling in the brown alga *Fucus vesiculosus*. Oecologia 144:196–205. https://doi.org/10.1007/s00442-005-0053-0

Hooftman DAP, Hartman Y, Oostermeijer JGB, Den Nijs HCM (2009) Existence of vigorous lineages of crop-wild hybrids in lettuce under field conditions. Environ Biosafety Res 8:203–217. https://doi.org/10.1051/ebr/2010001

Horn SJ, Moen E, Østgaard K (1999) Direct determination of alginate content in brown algae by near infra-red (NIR) spectroscopy. J Appl Phycol 11:9–13. https://doi.org/10.1023/A:1008024009954

Hsu H, Hwang P (2019) Clinical applications of fucoidan in translational medicine for adjuvant cancer therapy. Clin Transl Med 8:1–18. https://doi.org/10.1186/s40169-019-0234-9

Hu ZM, Shan TF, Zhang J, et al (2021) Kelp aquaculture in China: a retrospective and future prospects. Rev Aquac 13:1324–1351. https://doi.org/10.1111/raq.12524

Huanel OR, Nelson WA, Robitzch V, et al (2020) Comparative phylogeography of two *Agarophyton* species in the New Zealand archipelago. J Phycol 56:1575–1590. https://doi.org/10.1111/jpy.13046

Huanel, OR, Quesada-Calderón, S, Molina, CR, et al (2022) Pre-domestication bottlenecks of the cultivated seaweed *Gracilaria chilensis*. Mol. Ecol. 31. https://doi.org/https://doi.org/10.1111/mec.16672

Hughes AR, Stachowicz JJ (2004) Genetic diversity enhances the resistance of a seagrass ecosystem to disturbance. Proc Natl Acad Sci U S A 101:8998–9002. https://doi.org/10.1073/pnas.0402642101

Hurtado AQ, Neish IC, Critchley AT (2019) Phyconomy: the extensive cultivation of seaweeds, their sustainability and economic value, with particular reference to important lessons to be learned and transferred from the practice of eucheumatoid farming. Phycologia 58:472–483. https://doi.org/10.1080/00318884.2019.1625632

Hwang EK, Baek JM, Park CS (2009) The mass cultivation of *Ecklonia stolonifera* Okamura as a summer feed for the abalone industry in Korea. J Appl Phycol 21:585–590. https://doi.org/10.1007/s10811-009-9402-4

Hwang, EK., Choi, HG, and Kim, JK (2020) Seaweed resources of Korea. Bot. Mar. 63, 395–405. doi:10.1515/bot-2020-0007.Hwang EK, Yotsukura N, Pang SJ, et al (2019) Seaweed breeding programs and progress in eastern Asian countries. Phycologia 58:484–495. https://doi.org/10.1080/00318884.2019.1639436

Indergaard M, Skjak-Brsk G, Jensen A (1990) Studies on the influence of nutrients on the composition and structure of alginate in *Laminaria saccharina* (L.) Lamour. (Laminariales,

Phaeophyeeae). Bot Mar 33:277–288. https://doi.org/doi.org/10.1515/botm.1990.33.3.277

Itou T, Kanno M, Suyama Y, et al (2012) Development of 12 polymorphic microsatellite DNA markers for the kelp *Ecklonia cava* (Phaeophyceae, Laminariales). Conserv Genet Resour 4:459–461. https://doi.org/10.1007/s12686-011-9574-5

Itou T, Kanno M, Suyama Y, et al (2019) Opening the black box: microspatial patterns of zoospore dispersal, parentage, and selfing in the kelp *Ecklonia cava* as revealed by microsatellite markers. J Appl Phycol 31:3283–3294. https://doi.org/https://doi.org/10.1007/s12686-011-9574-5

Jennings JG, Steinberg PD (1994) In situ exudation of phlorotannins by the sublittoral kelp *Ecklonia radiata*. Mar Biol 121:349–354. https://doi.org/10.1007/BF00346744

Johnston EM, Mittelstaedt HN, Braun LA, et al (2023) Bed-scale impact and recovery of a commercially important intertidal seaweed. J Exp Mar Bio Ecol 561. https://doi.org/10.1016/j.jembe.2023.151869

Jones TC, Gemmill CEC, Pilditch CA (2008) Genetic variability of New Zealand seagrass (*Zostera muelleri*) assessed at multiple spatial scales. Aquat Bot 88:39–46. https://doi.org/10.1016/j.aquabot.2007.08.017

Kalinowski ST, Wagner AP, Taper ML (2006) ML-RELATE: a computer program for maximum likelihood estimation of relatedness and relationship. Mol Ecol Notes 6:576–579. https://doi.org/10.1111/j.1471-8286.2006.01256.x

Kidgell JT, Magnusson M, de Nys R, Glasson CRK (2019) Ulvan: a systematic review of extraction, composition and function. Algal Res 39. https://doi.org/10.1016/j.algal.2019.101422

Kim J, Stekoll M, Yarish C (2019) Opportunities, challenges and future directions of open-water seaweed aquaculture in the United States. Phycologia 58:446–461. https://doi.org/10.1080/00318884.2019.1625611

Kirkman H (1984) Standing stock and production of *Ecklonia radiata* (C.Ag.) J. Agardh. J Exp Mar Bio Ecol 16:119–130

Kraan S (2012) Algal polysaccharides, novel application, and outlook. In: Chang C-F (ed) Carbohydrates – comprehensive studies on glycobiology and glycotechnology. InTech, Rijeka, pp 489–532

Krause-Jensen D, Duarte CM (2016) Substantial role of macroalgae in marine carbon sequestration. Nat Geosci 9:737–742. https://doi.org/10.1038/ngeo2790

Laurens LML, Wolfrum EJ (2011) Feasibility of spectroscopic characterization of algal lipids: chemometric correlation of NIR and FTIR spectra with exogenous lipids in algal biomass. Bioenergy Res 4:22–35. https://doi.org/10.1007/s12155-010-9098-y

Lauzon-Guay JS, Ugarte RA, Morse BL, Robertson CA (2021) Biomass and height of *Ascophyllum nodosum* after two decades of continuous commercial harvesting in eastern Canada. J Appl Phycol 33:1695–1708. https://doi.org/10.1007/s10811-021-02427-x

Lesser MP (2006) Oxidative stress in marine environments: biochemistry and physiological ecology. Annu Rev Physiol 68:253–278. https://doi.org/10.1146/annurev.physiol.68.040104.110001

Li Q, Shan T, Wang X, et al (2020) Evaluation of the genetic relationship between the farmed populations on a typical kelp farm and the adjacent subtidal spontaneous population of *Undaria pinnatifida* (Phaeophyceae, Laminariales) in China. J Appl Phycol 32:653–659. https://doi.org/10.1007/s10811-019-01917-3

Liu F, Yao J, Wang X, et al (2012) Genetic diversity and structure within and between wild and cultivated *Saccharina japonica* (Laminariales, Phaeophyta) revealed by SSR markers. Aquaculture 358–359:139–145. https://doi.org/10.1016/j.aquaculture.2012.06.022

Liu Y, Ying Y, Yu H, Fu X (2006) Comparison of the HPLC method and FT-NIR analysis for quantification of glucose, fructose, and sucrose in intact apple fruits. J Agric Food Chem 54:2810–2815. https://doi.org/10.1021/jf052889e

Lorbeer AJ, Charoensiddhi S, Lahnstein J, et al (2017) Sequential extraction and characterization of fucoidans and alginates from *Ecklonia radiata, Macrocystis pyrifera, Durvillaea potatorum*, and *Seirococcus axillaris*. J Appl Phycol 29:1515–1526. https://doi.org/10.1007/s10811-016-0990-5

Lorbeer AJ, Lahnstein J, Bulone V, et al (2015) Multiple-response optimization of the acidic treatment of the brown alga *Ecklonia radiata* for the sequential extraction of fucoidan and alginate. Bioresour Technol 197:302–309. https://doi.org/10.1016/j.biortech.2015.08.103

Loureiro R, Gachon CMM, Rebours C (2015) Seaweed cultivation: potential and challenges of crop domestication at an unprecedented pace. New Phytol 206:489–492. https://doi.org/10.1111/nph.13278

Mac Monagail M, Cornish L, Morrison L, et al (2017) Sustainable harvesting of wild seaweed resources. Eur J Phycol 52:371–390. https://doi.org/10.1080/09670262.2017.1365273

Macaya EC, Zuccarello GC (2010) DNA barcoding and genetic divergence in the giant kelp *Macrocystis* (laminariales). J Phycol 46:736–742. https://doi.org/10.1111/j.1529-8817.2010.00845.x

Mackie W (1971) Semi-quantitative estimation of composition of alginates by infra-red spectroscopy. Carbohydr Res 20:413–415

Magnusson M, Yuen AKL, Zhang R, et al (2017) A comparative assessment of microwave assisted (MAE) and conventional solid-liquid (SLE) techniques for the extraction of phloroglucinol from brown seaweed. Algal Res 23:28–36. https://doi.org/10.1016/j.algal.2017.01.002

Mak W, Hamid N, Liu T, et al (2013) Fucoidan from New Zealand *Undaria pinnatifida*: monthly variations and determination of antioxidant activities. Carbohydr Polym 95:606–614. https://doi.org/10.1016/j.carbpol.2013.02.047

Mann EH, Kirkman H (1981) Biomass method for measuring productivity of *Ecklonia radiata*, with the potential for adaptation to other large brown algae. Aust J Mar Freshw Res 32:297–304

Manns D, Deutschle AL, Saake B, Meyer AS (2014) Methodology for quantitative determination of the carbohydrate composition of brown seaweeds (Laminariaceae). RSC Adv 4:25736–25746. https://doi.org/10.1039/c4ra03537b

Manns D, Nielsen MM, Bruhn A, et al (2017) Compositional variations of brown seaweeds *Laminaria digitata* and *Saccharina latissima* in Danish waters. J Appl Phycol 29:1493–1506. https://doi.org/10.1007/s10811-017-1056-z

Marinho GS, Holdt SL, Birkeland MJ, Angelidaki I (2015) Commercial cultivation and bioremediation potential of sugar kelp, *Saccharina latissima*, in Danish waters. J Appl Phycol 27:1963–1973. https://doi.org/10.1007/s10811-014-0519-8

Mata L, Lawton RJ, Magnusson M, et al (2017) Within-species and temperature-related variation in the growth and natural products of the red alga *Asparagopsis taxiformis*. J Appl Phycol 29:1437–1447. https://doi.org/10.1007/s10811-016-1017-y

MATLAB (2021) Version 9.11.0 (R2021b). The MathWorks Inc., Natick

McHugh DJ (2003) A guide to the seaweed industry. FAO fisheries technical paper 441. Food and Agriculture Organisation of the United Nations, Rome

Meirmans PG (2015) Seven common mistakes in population genetics and how to avoid them. Mol Ecol 24:3223–3231. https://doi.org/10.1111/mec.13243

Monteiro MS, Sloth J, Holdt S, Hansen M (2019) Analysis and risk assessment of seaweed. EFSA Journal 17 (S2). https://doi.org/10.2903/j.efsa.2019.e170915

Mouritsen OG, Rhatigan P, Pérez-Lloréns JL (2018) World cuisine of seaweeds: science meets gastronomy. Int J Gastron Food Sci 14:55–65. https://doi.org/10.1016/j.ijgfs.2018.09.002

Moy FE, Christie H (2012) Large-scale shift from sugar kelp (*Saccharina latissima*) to ephemeral algae along the south and west coast of Norway. Mar Biol Res 8:309–321. https://doi.org/10.1080/17451000.2011.637561

Muangmai N, Fraser CI, Zuccarello GC (2015) Contrasting patterns of population structure and demographic history in cryptic species of *Bostrychia intricata* (Rhodomelaceae, Rhodophyta) from New Zealand. J Phycol 51:574–585. https://doi.org/10.1111/jpy.12305

Mudgil D, Barak S, Khatkar BS (2014) Guar gum: processing, properties and food applications - A Review. J Food Sci Technol 51:409–418. https://doi.org/10.1007/s13197-011-0522-x

Munda IM (1987) Distribution and use of some economically important seaweeds in Iceland. Hydrobiologia 151–152:257–260. https://doi.org/10.1007/BF00046138

Murai U, Yamagishi K, Kishida R, Iso H (2021) Impact of seaweed intake on health. Eur J Clin Nutr 75:877–889. https://doi.org/10.1038/s41430-020-00739-8

Naylor RL, Williams SL, Strong DR (2001) Aquaculture: a gateway for exotic species. Sci New Ser 294:1655–1656. https://doi.org/10.1126/science.1064875

Neill K, Miller S, Allen S, Heath P (2009) Experimental culture of the kelp *Ecklonia radiata*. NIWA internal report, Auckland

Nepper-Davidsen J, Andersen DT, Pedersen MF (2019) Exposure to simulated heatwave scenarios causes long-term reductions in performance in *Saccharina latissima*. Mar Ecol Prog Ser 630:25–39. https://doi.org/10.3354/meps13133

Nepper-Davidsen J, Glasson CRK, Lawton RJ, Magnusson M (2023) High spatial and temporal variation in biomass composition of the novel aquaculture target *Ecklonia radiata*. J Appl Phycol. https://doi.org/10.1007/s10811-023-02969-2

Nepper-Davidsen J, Magnusson M, Glasson CRK, et al (2021) Implications of genetic structure for aquaculture and cultivar translocation of the kelp *Ecklonia radiata* in northern New Zealand. Front Mar Sci 8:1–11. https://doi.org/10.3389/fmars.2021.749154

New Zealand Government (2021) Accelerate the aquaculture strategy: investment roadmap. New Zealand Government, Wellington

Nicolaï BM, Beullens K, Bobelyn E, et al (2007) Nondestructive measurement of fruit and vegetable quality by means of NIR spectroscopy: a review. Postharvest Biol Technol 46:99–118. https://doi.org/10.1016/j.postharvbio.2007.06.024

Nielsen CW, Holdt SL, Sloth JJ, et al (2020) Reducing the high iodine content of *Saccharina latissima* and improving the profile of other valuable compounds by water blanching. Foods 9:1–15. https://doi.org/10.3390/foods9050569

Novaczek I (1984) Development and phenology of *Ecklonia radiata* at two depths in Goat Island Bay, New Zealand. Mar Biol 81:189–197

Oksanen J, Guillaume Blanchet F, Friendly M, et al (2020) Vegan: community ecology package. R package version 2.5-7

Oliveira AS, Sudatti DB, Fujii MT, et al (2013) Inter- and intrapopulation variation in the defensive chemistry of the red seaweed *Laurencia dendroidea* (Ceramiales, Rhodophyta). Phycologia 52:130–136. https://doi.org/10.2216/12-058.1

Oliver ECJ, Donat MG, Burrows MT, et al (2018) Longer and more frequent marine heatwaves over the past century. Nat Commun 9:1–12. https://doi.org/10.1038/s41467-018-03732-9

Peakall R, Smouse PE (2006) GENALEX 6: genetic analysis in Excel. population genetic software for teaching and research. Mol Ecol Notes 6:288–295. https://doi.org/10.1111/j.1471-8286.2005.01155.x

Peakall R, Smouse PE (2012) GenALEx 6.5: genetic analysis in Excel. population genetic software for teaching and research - an update. Bioinformatics 28:2537–2539. https://doi.org/10.1093/bioinformatics/bts460

Pehlke C, Bartsch I (2008) Changes in depth distribution and biomass of sublittoral seaweeds at Helgoland (North Sea) between 1970 and 2005. Clim Res 37:135–147. https://doi.org/10.3354/cr00767

Peleg Y, Shefer S, Anavy L, et al (2019) Sparse NIR optimization method (SNIRO) to quantify analyte composition with visible (VIS)/near infrared (NIR) spectroscopy (350 nm-2500 nm). Anal Chim Acta 1051:32–40. https://doi.org/10.1016/j.aca.2018.11.038

Pinkerton M, Gall M, Steinmetz T, Wood S (2022) NIWA seas, coasts and estuaries New Zealand (NIWA-SCENZ): image services of satellite (MODIS-Aqua) water quality products for coastal New Zealand. data product version 1.0. NIWA, Wellington. https://data-niwa.opendata.arcgis.com/documents/niwa-scenz-ocean-colour-application/explore. Accessed 10 Jan 2023

Pirker JG (2002) Demography, biomass production and effects of harvesting giant kelp *Macrocystis pyrifera* (Linnaeus) in Southern New Zealand [PhD thesis]. University of Canterbury

Plew DR, Zeldis JR, Shankar U, Elliott AH (2018) Using simple dilution models to predict New Zealand estuarine water quality. Estuaries and Coasts 41:1643–1659. https://doi.org/10.1007/s12237-018-0387-6

Porse H, Rudolph B (2017) The seaweed hydrocolloid industry: 2016 updates, requirements, and outlook. J Appl Phycol 29:2187–2200. https://doi.org/10.1007/s10811-017-1144-0

Praeger C, Magnusson ME, Lawton RJ (2022a) Successful initiation of sorus formation and viable zoospores in *Ecklonia radiata* on isolated lateral fronds under hatchery conditions. J Appl Phycol. https://doi.org/https://doi.org/10.1007/s10811-022-02894-w

Praeger C, Magnusson ME, Lawton RJ (2022b) Optimising the zoospore release, germination, development of gametophytes and formation of sporophytes of *Ecklonia radiata*. J Appl Phycol 34:2535–2549. https://doi.org/https://doi.org/10.1007/s10811-022-02806-y

Pritchard JK, Stephens M, Donelly P (2000) Inference of population structure using multilocus genotype data. Genetics 155:945–959. https://doi.org/10.1111/j.1471-8286.2007.01758.x

Qi H, Zhao T, Zhang Q, et al (2005) Antioxidant activity of different molecular weight sulfated polysaccharides from *Ulva pertusa* Kjellm (Chlorophyta). J Appl Phycol 17:527–534.

https://doi.org/10.1007/s10811-005-9003-9

Rajauria G, Ravindran R, Garcia-Vaquero M, et al (2021) Molecular characteristics and antioxidant activity of laminarin extracted from the seaweed species *Laminaria hyperborea*, using hydrothermal-assisted extraction and a multi-step purification procedure. Food Hydrocoll 112:106332. https://doi.org/10.1016/j.foodhyd.2020.106332

Raymond M, Rousset F (1995) Genpop 1.2 Population genetics software for exact test and ecumenicism. J Hered 86:248–249. https://doi.org/doi.org/10.1093/oxfordjournals.jhered.a111573

Reed DC (1990) The effects of variable settlement and early competition on patterns of kelp recruitment. Ecology 71:776–787

Reusch TBH, Ehlers A, Hämmerli A, Worm B (2005) Ecosystem recovery after climatic extremes enhanced by genotypic diversity. Proc Natl Acad Sci U S A 102:2826–2831. https://doi.org/10.1073/pnas.0500008102

Robic A, Bertrand D, Sassi JF, et al (2009) Determination of the chemical composition of ulvan, a cell wall polysaccharide from *Ulva* spp. (Ulvales, Chlorophyta) by FT-IR and chemometrics. J Appl Phycol 21:451–456. https://doi.org/10.1007/s10811-008-9390-9

Roleda MY, Hurd CL (2019) Seaweed nutrient physiology: application of concepts to aquaculture and bioremediation. Phycologia 58:552–562. https://doi.org/10.1080/00318884.2019.1622920

Ross PM, Hogg ID, Pilditch CA, et al (2012) Population genetic structure of the New Zealand estuarine clam *Austrovenus stutchburyi* (Bivalvia: Veneridae) reveals population subdivision and partial congruence with biogeographic boundaries. Estuaries and Coasts 35:143–154. https://doi.org/10.1007/s12237-011-9429-z

Ross PM, Hogg ID, Pilditch CA, Lundquist CJ (2009) Phylogeography of New Zealand's coastal benthos. New Zeal J Mar Freshw Res 43:1009–1027. https://doi.org/10.1080/00288330.2009.9626525

Rousset F (2008) GENEPOP'007: a complete re-implementation of the Genepop software for Windows and Linux. Mol Ecol Resour 8:103–106. https://doi.org/10.1111/j.1471-8286.2007.01931.x

Rozaklis T, Ramsay SL, Whitfield PD, et al (2002) Determination of oligosaccharides in Pompe disease by electrospray ionization tandem mass spectrometry. Clin Chem 48:131–139. https://doi.org/10.1093/clinchem/48.1.131

Sakugawa K, Ikeda A, Takemura A, Ono H (2004) Simplified method for estimation of composition of alginates by FTIR. J Appl Polym Sci 93:1372–1377. https://doi.org/10.1002/app.20589

Salomonsen T, Jensen HM, Stenbæk D, Engelsen SB (2008) Chemometric prediction of alginate monomer composition: a comparative spectroscopic study using IR, Raman, NIR and NMR. Carbohydr Polym 72:730–739. https://doi.org/10.1016/j.carbpol.2007.10.022

Schiel DR (1990) Macroalgal assemblages in New Zealand: structure, interactions and demography. Hydrobiologia 192:59-76. https://doi.org/10.1007/BF00006227

Schiener P, Black KD, Stanley MS, Green DH (2015) The seasonal variation in the chemical composition of the kelp species *Laminaria digitata*, *Laminaria hyperborea*, *Saccharina latissima* and *Alaria esculenta*. J Appl Phycol 27:363–373. https://doi.org/10.1007/s10811-014-0327-1

Shan T, Li Q, Wang X, et al (2019) Assessment of the genetic connectivity between farmed populations on a typical kelp farm and adjacent spontaneous populations of *Saccharina*

japonica (Phaeophyceae, Laminariales) in China. Front Mar Sci 6:1–7. https://doi.org/10.3389/fmars.2019.00494

Shannon E, Abu-Ghannam N (2019) Seaweeds as nutraceuticals for health and nutrition. Phycologia 58:563–577. https://doi.org/10.1080/00318884.2019.1640533

Sharma S, Neves L, Funderud J, et al (2018) Seasonal and depth variations in the chemical composition of cultivated *Saccharina latissima*. Algal Res 32:107–112. https://doi.org/10.1016/j.algal.2018.03.012

Sharp G (1987) *Ascophyllum nodosum* and its harvesting in Eastern Canada. In: Doty MS, Caddy JS, Santelices B (eds) *Case studies of seven commercial seaweed resources*. Food and agriculture organization of the United Nations, Rome

Shears NT, Babcock RC (2007) Quantitative description of mainland New Zealand's shallow subtidal reef communities. Department of Conservation, Wellington

Shears NT, Smith F, Babcock RC, et al (2008) Evaluation of biogeographic classification schemes for conservation planning: application to New Zealand's coastal marine environment. Conserv Biol 22:467–481. https://doi.org/10.1111/j.1523-1739.2008.00882.x

Shefer S, Israel A, Golberg A, Chudnovsky A (2017) Carbohydrate-based phenotyping of the green macroalga *Ulva fasciata* using near-infrared spectrometry: potential implications for marine biorefinery. Bot Mar 60:219–228. https://doi.org/10.1515/bot-2016-0039

Shin HC, Kim SH, Park Y, et al (2012) Effects of 12-week oral supplementation of *Ecklonia cava* polyphenols on anthropometric and blood lipid parameters in overweight Korean individuals: a double-blind randomized clinical trial. Phyther Res 26:363–368. https://doi.org/10.1002/ptr.3559

Shrestha S, Zhang W, Smid SD (2021) Phlorotannins: a review on biosynthesis, chemistry and bioactivity. Food Biosci 39:1–11. https://doi.org/10.1016/j.fbio.2020.100832

Sichert A, Corzett CH, Schechter MS, et al (2020) Verrucomicrobia use hundreds of enzymes to digest the algal polysaccharide fucoidan. Nat Microbiol 5:1026–1039. https://doi.org/10.1038/s41564-020-0720-2

Silverstein RM, Webster FX, Kiemle DJ, Bryce DL (2014) Spectrometric identification of organic compounds. John Wiley & Sons Inc, New York

Skoog DA, Holler FJ, Crouch SR (2018) Applications of infrared spectrometry. In: Princeples of instrumental analysis, 7th edn. Cengage learning, Boston, pp 412–433

Staehr PA, Wernberg T (2009) Physiological responses of *Ecklonia radiata* (laminariales) to a latitudinal gradient in ocean temperature. J Phycol 45:91–99. https://doi.org/10.1111/j.1529-8817.2008.00635.x

Stévant P, Marfaing H, Duinker A, et al (2018) Biomass soaking treatments to reduce potentially undesirable compounds in the edible seaweeds sugar kelp (*Saccharina latissima*) and winged kelp (*Alaria esculenta*) and health risk estimation for human consumption. J Appl Phycol 30:2047–2060. https://doi.org/10.1007/s10811-017-1343-8

Stevens PM (1990) A genetic analysis of the pea crabs (Decapoda: Pinnotheridae) of New Zealand. I. Patterns of spatial and host-associated genetic structuring in *Pinnotheres novaezelandiae* Filhol. J Exp Mar Bio Ecol 141:195–212. https://doi.org/10.1016/0022-0981(90)90224-Z

Stewart CH, Higgins HG, Austin S (1961) Seasonal variation in alginic acid, mannitol, laminarin and fucoidin in the brown alga, *Ecklonia radiata*. Nature 192:1208

Synytsya A, Novak M (2014) Structural analysis of glucans. Ann Transl Med 2:1–14. https://doi.org/10.3978/j.issn.2305-5839.2014.02.07

Szekalska M, Puciłowska A, Szymańska E, et al (2016) Alginate: current use and future perspectives in pharmaceutical and biomedical applications. Int J Polym Sci 2016:1–17. https://doi.org/10.1155/2016/7697031

Targett NM, Arnold TM (1998) Predicting the effects of brown algal phlorotannins on marine herbivores in tropical and temperate oceans. J Phycol 34:195–205. https://doi.org/10.1046/j.1529-8817.1998.340195.x

Tasmanian Government (2017) Tasmanian marine plants fishery. Department Of Primary Industries, Parks, Water And Environment, Hobart

Team RStudio (2022) RStudio: integrated development environment for R. RStudio. PBC, Boston

Thurstan RH, Brittain Z, Jones DS, et al (2018) Aboriginal uses of seaweeds in temperate Australia: an archival assessment. J Appl Phycol 30:1821–1832. https://doi.org/10.1007/s10811-017-1384-z

Torres MD, Kraan S, Domínguez H (2019) Seaweed biorefinery. Rev Environ Sci Biotechnol 18:335–388. https://doi.org/10.1007/s11157-019-09496-y

Trono GC, Largo DB (2019) The seaweed resources of the Philippines. Bot Mar 62:483–498. https://doi.org/10.1515/bot-2018-0069

Tukai R, Maher WA, McNaught IJ, et al (2002) Occurrence and chemical form of arsenic in marine macroalgae from the east coast of Australia. Mar Freshw Res 53:971–980. https://doi.org/10.1071/MF01230

Valero M, Guillemin M-L, Destombe C, et al (2017) Perspectives on domestication research for sustainable seaweed aquaculture. Perspect Phycol 4:33–46. https://doi.org/10.1127/pip/2017/0066

Vásquez JA, Piaget N, Vega JMA (2012) The Lessonia nigrescens fishery in northern Chile: “how you harvest is more important than how much you harvest.” J Appl Phycol 417–426. https://doi.org/10.1007/s10811-012-9794-4

Vea J, Ask E (2011) Creating a sustainable commercial harvest of *Laminaria hyperborea*, in Norway. J Appl Phycol 23:489–494. https://doi.org/10.1007/s10811-010-9610-y

Veale AJ, Lavery SD (2012) The population genetic structure of the waratah anemone (*Actinia tenebrosa*) around New Zealand. New Zeal J Mar Freshw Res 46:523–536. https://doi.org/10.1080/00288330.2012.730053

Vilg JV, Nylund GM, Werner T, et al (2015) Seasonal and spatial variation in biochemical composition of *Saccharina latissima* during a potential harvesting season for Western Sweden. Bot Mar 58:435–447. https://doi.org/10.1515/bot-2015-0034

Waples RS, Anderson EC (2017) Purging putative siblings from population genetic data sets: a cautionary view. Mol Ecol 26:1211–1224. https://doi.org/10.1111/mec.14022

Wernberg T, Coleman MA, Babcock RC, et al (2019) Biology and ecology of the globally significant kelp *Ecklonia Radiata*. Oceanogr Mar Biol 57:265–324. https://doi.org/10.1201/9780429026379-6

Wernberg T, Coleman MA, Bennett S, et al (2018) Genetic diversity and kelp forest vulnerability to climatic stress. Sci Rep 8:1–9. https://doi.org/10.1038/s41598-018-20009-9

Wernberg T, Goldberg N (2008) Short-term temporal dynamics of algal species in a subtidal kelp bed in relation to changes in environmental conditions and canopy biomass. Estuar Coast Shelf Sci 76:265–272. https://doi.org/10.1016/j.ecss.2007.07.008

Wheeler T, Major R, Ogilvie S, et al (2021) Stocktake and characterisation of New Zealand's seaweed sector: species characteristics and Te Tiriti o Waitangi considerations. Cawthron, Nelson

White LN, White WL (2020) Seaweed utilisation in New Zealand. Bot Mar 63:303–313. https://doi.org/10.1515/bot-2019-0089

WHO (2011) Safety evaluation of certain food additives and contaminants. World Health Organization, Geneva

Wickham H (2016) ggplot2: elegant graphics for data analysis. Springer-Verlag, New York

Wijffels SE, Beggs H, Griffin C, et al (2018) A fine spatial-scale sea surface temperature atlas of the Australian regional seas (SSTAARS): seasonal variability and trends around Australasia and New Zealand revisited. J Mar Syst 187:156–196. https://doi.org/10.1016/j.jmarsys.2018.07.005

Wiltshire KH, Gurgel CFD, Marty D, Jason T (2020) Application of seaweeds to integrated multi-trophic aquaculture in southern Australia: identifying and investigating suitable native species [PhD thesis]. The University of Adelaide, Adelaide

Xiao X, Agusti S, Lin F, et al (2017) Nutrient removal from Chinese coastal waters by large-scale seaweed aquaculture. Sci Rep 7:1–6. https://doi.org/10.1038/srep46613

Young M, Paul N, Birch D, Swanepoel L (2022) Factors influencing the consumption of seaweed amongst young adults. Foods 11. https://doi.org/10.4324/9781315735948-10

Zhang J (2018) Seaweed industry in China. Innovation Norway, Beijing

Zhang J, Wang X, Yao J, et al (2017) Effect of domestication on the genetic diversity and structure of *Saccharina japonica* populations in China. Sci Rep 7:1–11. https://doi.org/10.1038/srep42158

Zhang Q, Zhang J, Shen J, et al (2006) A simple 96-well microplate method for estimation of total polyphenol content in seaweeds. J Appl Phycol 18:445–450. https://doi.org/10.1007/s10811-006-9048-4

Appendices

Appendix 1 Microsatellite loci tested for inclusion in this study. Expected forward and reverse repeat motifs based on original publications, observed size rage (bp) of alleles from the current study, Amplification (Amp): loci that consistently amplified with *E. radiata* during initial screening, Allele scoring (Score): loci with consistent allele scoring across all samples following genotyping, Polymorphic (Poly): loci polymorphic at least at two of the 12 sites. All loci of EC, Eradic and EK originally designed for E. cava (Itou et al. 2012), E. radicosa (Akita et al. 2018), and E. kurome (Akita et al. 2020) respectively

Primer	Expected repeat motif		F sequence 5' - 3'	Size range	Amp	Score	Poly
EC03	(CAA)10	F:	CCCATCAACAGGACAACGAAG	178-187	✓	✓	✓
		R:	GTTTCTTGCCGGCGTGAGTAGGAGTTC				
EC06	(GGT)7	F:	GCGGGAAGGAAAAATAAGCAC	159-162	✓	✓	✓
		R:	GTTTCTTGCGACCACGGACTACATCAT				
EC07	$(GTGCT)_{10}$	F:	CGTTCCAGACATCAGACACA	287-327	✓	✓	✓
		R:	GTTTCTTTGGTAGTCAATGGCATAGG				
EC08	$(GCA)_{14}$	F:	AGTAGCAGCAGTAACCCGTGAA	129-158	✓	✓	✓
		R:	GTTTCTTCAAATCGCCACCGCTAT				
EC09	$(CCA)_7$---$(GCA)_{12}$	F:	CGGCCATAAGAGACGTAGATTT	290-297	✓	✓	✓
		R:	GTTTCTTCGCCTCAACCGCTGATGACTT				
EC10	$(CAA)_{12}CAT(CAA)_6$	F:	GTCCCCACATCCGAAAGGTAAC	200-270	✓	✓	✓
	$CAT(CAA)_2CAT(CAA)_9$	R:	GTTTCTTCAAGCGGTAAGGGTGTCAAG				
EC11	$(GCT)_{13}$	F:	GTTATAGCTGGTCGGCGATAG	235-282	✓	✓	✓
		R:	GTTTCTTCTGCTGCAAATCCTTGGTA				
Eradic01	$(GAGCC)_{16}$	F:	ATTCGAATTGTGCGAGATCC	372-405	✓	✓	✓
		R:	CTTGGTCGGCAAAAGTCATT				
Eradic02	$(CCGT)_{14}$	F:	TCCTCGAACCCCTACCTACAC	307-330	✓	✓	✓
		R:	GTTTCTTAGCATGGCAGCGGAGAT				
Eradic05	(TGC)17	F:	GAAGATGCCCCTTGAGAACA	272-281	✓	✓	✓
		R:	AAGGAGTCCCACTGAGCAGA				
Eradic06	$(GCACA)_{30}$	F:	ATCCGCACTCAACACCTACC	508-548	✓	✓	✓
		R:	CAACTGTTGACTTCGCTTGC				
Eradic07	$(GCT)_{16}$	F:	TATGTCACGTCTCTGGCTCG	166-169	✓	✓	✓
		R:	TCGGACAAGTCTCCTCAACC				
Eradic10	$(AGC)_{13}$	F:	TCCTGGTGATGAGAAGGGTC	452-482	✓	✓	✓
		R:	CGCCGCGATCTTAGTTAGAC				
EK03	$(AGC)_{15}$	F:	CCCATCAACAGGACAACGAAG	110-119	✓	✓	✓
		R:	GTTTCTTGCCGGCGTGAGTAGGAGTTC				
EC01	$(CCACA)_7$	F:	CCTTAACTGTCTTCTGCTGAC	136-151	✓	✓	X
		R:	GTTTCTTCGTGGTTTGATCTGGTG				
EC02	$(CCT)_6$	F:	TCCTCGAACCCCTACCTACAC	217	✓	✓	X
		R:	GTTTCTTAGCATGGCAGCGGAGAT				
Eradic03	$(TTGGTA)_{22}$	F:	TGCGCTCGTACTGATACTCG	226-245	✓	✓	X
		R:	AGAGGTGCAGAGGTCCTCAA				
Eradic09	$(ACGC)_9$	F:	GGTAAGGCGATGGACGATAA	194-202	✓	X	X
		R:	TCTTACGGTAGCCCGAGAAA				
EC12	$(GGT)_{16}$	F:	TCCTGGAACTCCGCGATCTTC	161-201	✓	X	X

		R:	GTTTCTTGCAATTATAGAGGGCGGTGAA				
Eradic04	(GCT)16	F:	ACGTCTTCTGGTGTGCTGTG	196-203	✓	X	X
		R:	AAATGTCGTCAAATGTGGCA				
EC04	(TA)5	F:	GTATTGCAGCAGCAGTAAAC		X	X	X
		R:	GTTTCTTGGACGAGTACGTACGAGCAC				
EC05	(AC)5	F:	CACACAAGAAAAATGGATAAC		X	X	X
		R:	GTTTCTTAAACGGCTACGGACAC				
ER08	(ACT)14	F:	CAGCCAGCTTTCTTCAGGAC		X	X	X
		R:	CGCTATAATACGAGCTGGGC				
ER11	(TGT)14	F:	GCCCCGTCTATAATTCACGA		X	X	X
		R:	AATGGGTTTCTGCACCACTC				
EK09	$(GGA)_{14}$	F:	TCGTATGCCGTATCATCGTC		X	X	X
		R:	CGCCCCTTTTTCCTAAAGA				

Appendix 2 P-values for tests of Hardy-Weinberg equilibrium (H_0 = data is in Hardy-Weinberg equilibrium) for all 17 genotyped loci at each site. Sites with a too high degree of monomorphism to calculate test of Hardy-Weinberg equilibrium for a given loci are marked with an X. Loci excluded from data analysis due to monomorphism are marked with a double asterisk. Of the 14 Loci selected for data analysis, loci with a too high degree of monomorphism to calculate test of Hardy-Weinberg equilibrium at more than half of the sites are marked with a single asterisk and were excluded in the sensitivity analysis. Site abbreviation; KA: Karikari, LE: Leigh, WB: Wilson Bay, MO: Motuotau island, MT: Moutohora Island, WA: Waihau Bay, TO: Tolaga Bay, MG: Mahanga, MH: Māhia, WH: Wellington Harbour, MA: Mākara Beach, TI: Titahi Bay

Site	EC01**	EC02**	EC03	EC06*	EC07	EC08*	EC09*	EC10	EC11	ER01*	ER02*	ER03**	ER05*	ER06	ER07*	ER10	EK03*
KA	X	X	1.00	X	0.62	X	X	0.36	1.00	X	X	X	X	0.89	X	1.00	X
LE	X	X	1.00	1.00	0.49	X	1.00	0.72	1.00	X	1.00	X	X	0.90	1.00	0.18	X
WB	X	X	0.23	X	0.08	0.48	X	0.26	1.00	1.00	X	X	X	0.56	X	1.00	X
MO	X	X	0.08	X	0.06	1.00	X	0.27	0.33	1.00	1.00	X	1.00	1.00	X	1.00	1.00
MT	X	X	1.00	1.00	0.01	1.00	X	1.00	1.00	X	X	X	X	0.34	1.00	1.00	1.00
WA	X	X	1.00	X	0.41	X	1.00	1.00	X	X	1.00	X	1.00	1.00	X	X	X
TO	X	X	1.00	X	1.00	X	X	1.00	1.00	X	X	X	1.00	X	X	1.00	X
MG	X	X	1.00	X	1.00	X	X	X	1.00	X	X	X	1.00	1.00	X	X	X
MH	X	X	0.10	X	0.62	X	X	1.00	X	X	X	X	X	1.00	X	X	X
WH	X	X	0.33	X	1.00	X	X	0.32	1.00	X	0.20	X	X	0.05	X	1.00	X
MA	X	X	1.00	X	1.00	X	X	0.05	1.00	X	X	X	X	0.55	X	X	X
TI	X	X	0.02	X	1.00	X	X	0.69	1.00	X	X	X	X	0.33	X	X	X
All	X	X	0.55	1.00	0.40	0.96	1.00	0.77	1.00	1.00	0.92	X	1.00	0.93	1.00	1.00	1.00

Appendix 3 Genetic differentiation (F_{ST}) of *E. radiata* within each region and between each region. Manuscript data (14 loci): F_{ST} as presented in the paper with all 14 selected loci, Monomorphism cut (6 loci): F_{ST} calculated with only the 6 loci showing the least amount of monomorphism, Relatedness cut (14 loci) F_{ST} calculated with all 14 selected loci, but without samples showing more than 33 % relatedness (250 used, 97 samples removed). Region abbreviations; North: Northland, BoP: Bay of Plenty, Gis: Gisborne, Well: Wellington

Region	Manuscript data (14 loci)	Monomorphism cut (6 loci)	Relatedness cut (14 loci)
Within region			
North	0.160	0.122	0.164
BoP	0.070	0.088	0.053
Gis	0.159	0.144	0.146
Well	0.094	0.074	0.083
Between region			
North - BoP	0.040	0.048	0.032
North - Gis	0.043	0.021	0.033
North - Well	0.467	0.312	0.427
BoP - Gis	0.044	0.052	0.027
BoP - Well	0.407	0.230	0.371
Gis - Well	0.545	0.388	0.495

Appendix 4 Global analysis of molecular variance (AMOVA) for *E. radiata* among the four regions, among the three sites within each region, and among the individuals. Manuscript data (14 loci): AMOVA as presented in the paper with all 14 selected loci, Monomorphism cut (6 loci): AMOVA calculated with only the 6 loci showing the least amount of monomorphism, Relatedness cut (14 loci): AMOVA calculated with all 14 selected loci, but without samples showing more than 33 % relatedness (250 used, 97 samples removed). All levels of variation are significant at $p<0.001$

Source of Variation	df	SS	Variance Component	Percent variation
Manuscript data (14 loci)				
Among regions	3	222.87	0.416	27.41
Among sites within regions	8	56.18	0.108	7.1
Within sites (among individuals)	336	651.98	0.994	65.49
Total	347	937.03	1.517	
Monomorphism cut (6 loci)				
Among regions	3	124.62	0.218	19.39
Among sites within regions	8	41.80	0.079	7.01
Within sites (among individuals)	336	542.25	0.829	73.60
Total	347	708.66	1.127	
Relatedness cut (14 loci)				
Among regions	3	139.60	0.34	21.39
Among sites within regions	8	46.45	0.117	7.35
Within sites (among individuals)	239	534.65	1.133	71.26
Total	250	1303.48	2.132	

Appendix 5 Pairwise F_{ST} between all pair of sites. Site abbreviation; KA: Karikari, LE: Leigh, WB: Wilson Bay, MO: Motuotau island, MT: Moutohora Island, WA: Waihau Bay, TO: Tolaga Bay, MG: Mahanga, MH: Māhia, WH: Wellington Harbour, MA: Mākara Beach, TI: Titahi Bay

	KA	LE	WB	MO	MT	WA	TO	MG	MH	WH	MA	TI
KA	0.000											
LE	0.074	0.000										
WB	0.190	0.217	0.000									
MO	0.099	0.102	0.155	0.000								
MT	0.114	0.127	0.119	0.021	0.000							
WA	0.072	0.123	0.136	0.112	0.077	0.000						
TO	0.066	0.059	0.256	0.159	0.165	0.116	0.000					
MG	0.110	0.162	0.169	0.108	0.090	-0.015	0.165	0.000				
MH	0.151	0.222	0.182	0.157	0.081	0.030	0.216	0.097	0.000			
WH	0.618	0.567	0.598	0.473	0.522	0.579	0.662	0.647	0.714	0.000		
MA	0.601	0.550	0.580	0.458	0.504	0.558	0.646	0.616	0.690	-0.010	0.000	
TI	0.400	0.365	0.402	0.245	0.283	0.368	0.461	0.380	0.456	0.152	0.141	0.000

Appendix 6 Pairwise F_{ST} between all pairs of regions, calculated by treating each region as one single population

	Northland	Bay of Plenty	Gisborne	Wellington
Northland	0.000			
Bay of Plenty	0.040	0.000		
Gisborne	0.043	0.044	0.000	
Wellington	0.467	0.407	0.545	0.000

Appendix 7 Morphological data among spatial samples (all sites, top panel, n = 72) and temporal samples (only Motuotau Island, lower panel, n = 72). Stipe width (Stipe wid.), stipe length (Stipe len.), lamina thickness (Lam thick.), lamina length (Lam len.), lamina width (Lam wid.), and blade length (Blade len.) are in cm; DW total and DW stipe are in g. Site abbreviations are: Karikari (Kari), Leigh (Leig), Wilson Bay (Wils), Motuotau Island (Motu), Moutohora Island (Mout), Waihau Bay (Waih), Tolaga Bay (Tola), Mahanga (Maha), Māhia (Māhi), Wellington Harbour (WH), Mākara Beach (Māka), and Titahi Bay (Tita)

	Kari	Leig	Wils	Motu	Mout	Waih	Tola	Maha	Māhi	WH	Māka	Tita	Mean
Stipe wid.	0.9	1.4	2.1	1.2	1.8	1.1	1.6	1.8	1.9	1.1	1.3	1.1	1.4
SD	(0.1)	(0.4)	(1.1)	(0.1)	(0.2)	(0.4)	(0.1)	(0.2)	(0.1)	(0.2)	(0.2)	(0.1)	(0.4)
Stipe len.	10.7	29.9	13.3	26.1	61.7	27.3	18.1	23.4	35.5	15.1	36.3	15.4	26.1
SD	(4.0)	(15.4)	(4.9)	(20.8)	(12.0)	(11.4)	(7.0)	(6.4)	(10.5)	(3.7)	(13.2)	(2.7)	(13.5)
Lam thick.	0.3	0.3	0.4	0.3	0.5	0.4	0.8	0.9	0.9	0.4	0.4	0.4	0.5
SD	(0.0)	(0.1)	(0.1)	(0.0)	(0.1)	(0.1)	(0.0)	(0.0)	(0.1)	(0.1)	(0.1)	(0.0)	(0.2)
Lam len.	29.1	19.3	24.0	17.4	18.3	19.5	28.5	25.6	25.0	41.7	38.3	41.1	27.3
SD	(5.9)	(5.9)	(6.3)	(5.6)	(4.6)	(6.7)	(6.7)	(6.9)	(4.2)	(4.3)	(14.2)	(9.8)	(8.4)
Lam wid.	6.6	7.9	8.2	5.2									7.0
SD	(1.1)	(2.2)	(2.4)	(1.2)									(1.2)
Blade len.	28.6	33.1	40.1	33.9	32.1	34.7	36.3	30.0	37.3	29.9	31.6	30.4	33.2
SD	(6.0)	(5.4)	(8.6)	(9.8)	(4.3)	(9.3)	(4.1)	(4.5)	(2.3)	(4.4)	(3.7)	(3.2)	(3.3)
DW total	54.0	78.9	55.9	46.6	155.4	50.3	88.6	66.0	95.8	77.9	79.4	120.1	80.7
SD	(27.0)	(31.8)	(20.5)	(26.7)	(68.8)	(25.0)	(23.9)	(28.7)	(27.3)	(16.0)	(16.2)	(42.8)	(30.4)
DW stipe	1.7	9.3	6.4	8.1	28.9	8.9	4.0	6.2	8.8	3.1	8.2	3.3	8.1
SD	(1.0)	(5.1)	(4.5)	(8.2)	(12.3)	(5.4)	(1.8)	(2.7)	(3.7)	(1.0)	(3.8)	(1.0)	(6.7)

	Nov	Dec	Jan	Feb	Mar	May	Jun	Jul	Aug	Sep	Oct	Nov	Mean
Stipe wid.	1.2	1.7	1.4	2.0	1.7	1.5	1.8	1.6	1.5	1.5	1.5	1.5	1.6
SD	(0.1)	(0.2)	(0.2)	(0.2)	(0.1)	(0.1)	(0.2)	(0.1)	(0.2)	(0.1)	(0.3)	(0.2)	(0.2)
Stipe len.	26.1	37.8	34.6	41.0	47.9	43.0	49.6	52.6	34.6	38.2	40.0	31.4	39.7
SD	(20.8)	(10.8)	(16)	(13.6)	(8.1)	(9.3)	(11.8)	(11.7)	(12.4)	(14.5)	(15)	(15.3)	(7.4)
Lam thick.	0.3	0.4	0.4	1.0	0.5	0.4	0.5	0.5	0.4	0.4	0.4	0.4	0.5
SD	(0.0)	(0.0)	(0.1)	(0.1)	(0.1)	(0.1)	(0.1)	(0.1)	(0.1)	(0.1)	(0.1)	(0.1)	(0.2)
Lam len.	17.4	19.8	18.7	19.6	19.8	18.7	13.2	16.2	18.5	13.6	14.7	12.7	16.9
SD	(5.6)	(4.8)	(5.8)	(8.4)	(2.2)	(5.5)	(4.7)	(4.1)	(5.8)	(3.1)	(5.3)	(2.1)	(2.6)
Lam wid.	5.2							11.4	6.9	6.7	7.7	8.7	7.7
SD	(1.2)							(1.6)	(2.9)	(1.6)	(2.8)	(2.7)	(1.9)
Blade len.	33.9	37.9	38.0	38.3	19.8	28.6	27.8	26.9	18.7	24.0	27.3	28.3	29.1
SD	(9.8)	(3.6)	(9.7)	(5.4)	(2.2)	(5.8)	(5.6)	(4.2)	(3.2)	(3.4)	(6.8)	(3.9)	(6.4)
DW total	46.6	128.9	92.6	117.4	134.6	81.5	76.2	80.5	46.8	42.5	62.7	54.9	80.4
SD	(26.7)	(31.3)	(41.9)	(25.1)	(30.0)	(17.8)	(19.2)	(10.8)	(25.0)	(15.5)	(30.1)	(27.9)	(30.9)
DW stipe	8.1	13.1	11.8	14.2	18.5	16.4	19.7	21.6	13.5	14.9	15.7	10.6	14.8
SD	(8.2)	(6.0)	(8.1)	(6.1)	(1.6)	(3.9)	(4.7)	(6.3)	(10.0)	(8.3)	(9.4)	(6.9)	(3.7)

Appendix 8 Elemental analysis across spatial homogenised samples (n = 12) in % DW and ppm. Site abbreviations are: Karikari (Kari), Leigh (Leig), Wilson Bay (Wils), Motuotau Island (Motu), Moutohora Island (Mout), Waihau Bay (Waih), Tolaga Bay (Tola), Mahanga (Maha), Māhia (Māhi), Wellington Harbour (WH), Mākara Beach (Māka), and Titahi Bay (Tita)

	Kari	Leig	Wils	Motu	Mout	Waih	Tola	Māha	Mahi	WH	Māka	Tita	Mean
% DW													
H	4.90	4.75	4.87	4.76	5.04	5.11	5.46	5.15	5.65	4.98	5.07	5.56	5.11
C	32.63	31.82	31.04	31.58	32.23	32.56	34.55	32.53	34.13	31.24	31.64	34.03	32.50
Na	1.73	1.89	1.68	1.80	1.46	1.63	1.37	1.51	1.51	1.43	1.43	1.43	1.57
Mg	0.34	0.40	0.35	0.36	0.32	0.33	0.30	0.34	0.32	0.31	0.31	0.31	0.33
Ca	1.08	1.06	1.03	1.01	1.08	1.01	0.90	1.09	0.96	1.14	1.14	1.01	1.04
Ppm													
Al	26.55	5.36	15.22	5.20	3.08	8.96	10.13	5.25	5.86	2.96	3.67	13.90	8.85
V	0.77	0.67	0.33	0.61	0.82	0.69	0.35	1.03	0.67	0.65	1.23	0.78	0.72
Cr	0.30	0.19	0.17	0.15	0.23	0.43	0.17	0.17	0.16	0.19	0.12	0.17	0.21
Mn	3.11	2.88	3.04	2.93	2.05	2.17	2.22	2.20	2.49	2.88	2.23	3.03	2.60
Fe	89.94	24.01	36.16	19.82	25.41	44.14	45.65	25.82	30.82	56.40	26.21	48.28	39.39
Co	0.09	0.18	0.10	0.06	0.20	0.11	0.23	0.20	0.17	0.07	0.09	0.14	0.14
Ni	0.31	0.35	0.19	0.25	0.33	0.21	0.28	0.18	0.25	0.43	0.25	0.24	0.27
Cu	0.42	0.78	0.79	0.81	0.68	1.01	1.75	0.61	1.14	7.27	0.65	1.08	1.42
Zn	3.73	5.32	6.53	8.26	4.05	4.78	6.93	5.55	6.50	10.28	3.21	7.56	6.06
Se	0.06	0.03	0.04	0.04	0.03	0.02	0.03	0.03	0.06	0.04	0.04	0.03	0.04
Sr	640.2	701.4	770.8	729.6	786.4	746.1	622.0	780.9	645.4	882.2	866.5	728.4	741.66
Se	0.09	0.05	0.05	0.07	0.06	0.04	0.05	0.04	0.05	0.08	0.05	0.06	0.06
Ag	0.19	0.86	2.23	0.62	0.81	0.85	0.14	0.90	0.73	1.34	0.48	0.14	0.77
Ba	7.74	8.16	10.44	7.90	7.40	8.98	10.60	9.18	8.29	10.35	9.23	9.10	8.95
U	0.20	0.26	0.30	0.33	0.18	0.29	0.15	0.32	0.13	0.26	0.23	0.20	0.24

Appendix 9 Elemental analysis across temporal homogenised samples collected monthly at Motuotau Island (n = 12) in % DW and ppm

	Nov	Dec	Jan	Feb	Mar	May	Jun	Jul	Aug	Sep	Oct	Nov
% DW												
H	4.89	5.08	4.99	5.22	5.13	4.97	4.78	4.96	4.97	4.75	4.85	4.74
C	31.46	32.99	32.16	33.22	32.97	31.79	30.86	31.25	31.67	30.44	30.96	30.96
Na	1.45	1.41	1.40	1.41	1.38	1.34	1.33	1.64	1.25	1.36	1.37	1.35
Mg	0.30	0.30	0.30	0.30	0.30	0.29	0.28	0.32	0.27	0.29	0.29	0.28
Ca	1.02	0.88	0.95	0.85	0.96	1.11	1.18	1.05	1.20	1.28	1.17	1.07
Ppm												
Al	6.09	9.01	4.04	6.31	7.84	11.12	18.98	14.70	4.54	13.35	13.25	13.92
V	0.63	0.75	0.74	0.61	0.99	0.77	0.71	0.65	0.55	0.55	0.61	0.68
Cr	0.16	0.14	0.15	0.33	0.17	0.23	0.27	0.22	0.16	0.23	0.25	0.18
Mn	2.89	3.22	2.88	2.63	2.54	2.23	2.48	2.04	1.93	1.87	2.50	2.98
Fe	21.53	22.24	22.52	35.23	21.08	32.18	38.51	34.65	16.48	20.33	29.62	30.84
Co	0.06	0.08	0.07	0.09	0.09	0.10	0.12	0.13	0.08	0.07	0.07	0.07
Ni	0.26	0.34	0.24	0.33	0.29	0.33	0.41	0.40	0.24	0.24	0.27	0.21
Cu	0.81	0.84	0.92	1.16	0.82	1.09	1.12	1.46	0.64	0.81	0.80	0.68
Zn	8.57	7.05	6.02	6.06	5.64	8.00	8.94	10.26	6.49	7.64	6.94	6.63
Se	0.02	0.03	0.03	0.03	0.03	0.04	0.04	0.06	0.02	0.02	0.03	0.06
Sr	774.5	569.4	650.7	540.0	611.9	779.9	872.5	988.8	931.1	1038.0	921.1	785.07
Se	0.06	0.07	0.07	0.07	0.08	0.06	0.05	0.06	0.05	0.05	0.07	0.10
Ag	0.69	0.72	0.60	0.67	0.74	0.93	0.92	1.06	0.61	0.50	0.77	0.61
Ba	7.91	4.73	7.38	4.45	5.34	7.74	8.35	10.21	8.96	9.04	8.35	8.16
U	0.31	0.21	0.25	0.20	0.26	0.21	0.23	0.25	0.33	0.39	0.29	0.38

Appendix 10 Spatial and temporal variation between samples (n = 12). Differences between spatial and temporal variation was analysed using Levene's test of equal variance (n = 24). Significant p-value are italicised ($\alpha = 0.05$)

	Spatial % SD of mean	Temporal % SD of mean	df	F-value	p-value
Lipids (%)	61.7	75.1	1,22	0.12	0.733
Protein (%)	19.1	11.0	1,22	1.58	0.222
Phlo (%)	23.7	8.2	1,22	3.07	0.094
Ash (%)	15.1	9.8	1,22	1.20	0.286
Carbs (%)	7.6	4.8	1,22	3.04	0.095
Glc (%)	34.4	32.1	1,22	0.11	0.740
GulA (%)	11.2	14.5	1,22	0.56	0.462
ManA (%)	10.4	8.8	1,22	0.36	0.557
Fuc (%)	8.7	12.8	1,22	2.70	0.115
Man (%)	9.7	10.3	1,22	0.11	0.746
Gal (%)	10.3	6.0	1,22	1.81	0.192
Xyl (%)	5.8	6.5	1,22	0.08	0.780
M:G	8.6	8.9	1,22	0.00	0.955
N (%)	18.7	10.3	1,22	1.00	0.329
P (%)	24.3	21.0	1,22	0.18	0.674
K (%)	19.3	9.7	1,22	3.54	0.073
S (%)	15.2	5.3	1,22	7.15	*0.014*
Protein:N	4.0	2.0	1,22	2.59	0.122
C:N	21.0	10.5	1,22	4.44	*0.047*
I (%)	23.2	29.9	1,22	2.54	0.125
As (ppm)	16.7	11.9	1,22	0.16	0.695
Cd (ppm)	44.7	16.4	1,22	2.82	0.107
Pb (ppm)	68.7	54.8	1,22	5.70	*0.026*
Hg (ppm)	72.4	33.9	1,22	10.40	*<0.001*

Appendix 11 Cultivation of *E. radiata* (mean nitrogen: 1.3 ± 0.2 SD % DW, n = 138, and mean phosphorous: 0.11 ± 0.03 SD % DW, n = 23) could remove an estimated 164.6 kg N ha^{-1} and 14.7 kg P ha^{-1} per year. This is assuming a farm layout with 10 rows of 100 m backbone lines ha^{-1} with 10 m deep loops droppers every 1 meter of backbone (20 m seaweed line per loop) and with 8 seaweed specimens on average per meter seaweed line (80 g DW (sample mean) * 10 * 100 * 20 * 8 = 12.8 t DW ha^{-1})

Appendix 12 Chapters published as papers

Nepper-Davidsen J, Magnusson M, Glasson CRK, et al (2021) Implications of genetic structure for aquaculture and cultivar translocation of the kelp *Ecklonia radiata* in northern New Zealand. Front Mar Sci 8:1–11. https://doi.org/10.3389/fmars.2021.749154

Nepper-Davidsen J, Glasson CRK, Lawton RJ, Magnusson M (2023) High spatial and temporal variation in biomass composition of the novel aquaculture target *Ecklonia radiata*. J Appl Phycol. https://doi.org/10.1007/s10811-023-02969-2

frontiers in Marine Science

ORIGINAL RESEARCH
published: 22 November 2021
doi: 10.3389/fmars.2021.749154

Implications of Genetic Structure for Aquaculture and Cultivar Translocation of the Kelp *Ecklonia radiata* in Northern New Zealand

Jacob Nepper-Davidsen[1,2], Marie Magnusson[1,2], Christopher R. K. Glasson[1,2], Philip M. Ross[1,2] and Rebecca J. Lawton[1,2]*

[1] Coastal Marine Field Station, School of Science, University of Waikato, Tauranga, New Zealand, [2] Environmental Research Institute, University of Waikato, Tauranga, New Zealand

The fast expansion of the global seaweed aquaculture industry has created an interest in translocating seedlings cultivated from wild type brood stock. However, such translocations must be applied with caution as introduced cultivars can reduce genetic structure and diversity of wild populations. An understanding of the genetic structure and connectivity of target species is required to guide decision making around aquaculture translocation activities. In this study we used 14 microsatellite loci in a three-level hierarchical sampling design to analyze the genetic structure and connectivity of the native kelp *Ecklonia radiata* across 12 sites among four geographic regions (Northland, Bay of Plenty, Gisborne, and Wellington) in the North Island of New Zealand. Our aim was to provide guidance for translocation of cultivars to prevent the introduction of locally absent genotypes of *E. radiata*. Strong genetic structure and low geneflow were observed at all hierarchical levels, indicating the presence of multiple genetically distinct sub-populations. On a regional scale, high genetic differentiation was found between the Wellington region and the other three regions (F_{ST} = 0.407–0.545), and within regions most sites were significantly different (measured by pairwise F_{ST}) with high relatedness found between individuals within sites (mean 28.2% ± 0.7 SE). Bayesian modeling and redundancy analysis showed a high degree of genetic clustering and indicate that ocean currents and other factors that have resulted in biogeographical breaks along the coast are likely to be the main factors shaping genetic structure and connectivity of *E. radiata* on the North Island, rather than isolation by distance. Based on these findings, we recommend that that cultivars of *E. radiata* should not be translocated outside their area of origin to avoid introducing locally absent genotypes to local sub-populations.

Keywords: seaweed, marine, farming, genetic differentiation, sub-populations, microsatellites, translocation

OPEN ACCESS

Edited by:
Matthias Schmid,
Trinity College Dublin, Ireland

Reviewed by:
Trevor Bringloe,
The University of Melbourne, Australia
David Seth Portnoy,
Texas College, United States

****Correspondence:***
Jacob Nepper-Davidsen
Jn100@students.waikato.ac.nz

Specialty section:
This article was submitted to Marine Fisheries, Aquaculture and Living Resources, a section of the journal Frontiers in Marine Science

Received: *29 July 2021*
Accepted: *01 November 2021*
Published: *22 November 2021*

Citation:
Nepper-Davidsen J, Magnusson M, Glasson CRK, Ross PM and Lawton RJ (2021) Implications of Genetic Structure for Aquaculture and Cultivar Translocation of the Kelp Ecklonia radiata in Northern New Zealand. Front. Mar. Sci. 8:749154. doi: 10.3389/fmars.2021.749154

INTRODUCTION

Seaweed aquaculture has grown exponentially during the last 50 years and now has a global annual yield of 32 million tons and a commercial value of US$13.3 billion (FAO, 2020). The vast expansion of the sector has created an interest in translocating strains (i.e., movement outside area of origin), as intraspecific differentiation in key commercial traits, such as growth rate and biochemical

content, is common within seaweeds due to genotypic variation and local adaptation (Oliveira et al., 2013; Gosch et al., 2015; Mata et al., 2017). However, translocation of seaweed cultivars (i.e., strains selected for cultivation) must be approached with caution. Introduced cultivars can reduce genetic differentiation between wild populations (i.e., reduce genetic structure) by outcompeting unique local genotypes and reduce genetic variation within wild populations (i.e., reduce genetic diversity) by over-dominating the local gene pool (Ellstrand et al., 2013; Bolstad et al., 2017; Valero et al., 2017; Hu et al., 2021). Such genetic changes may have negative ecological and economic consequences, as loss of genetic structure can lead to the extinction of valuable genetic traits adapted to specific ecological niches (Evankow et al., 2019; Shan et al., 2019). Furthermore, the loss of genetic diversity within wild macrophyte populations may decrease productivity and tolerance to environmental stress in these communities (Hughes and Stachowicz, 2004; Reusch et al., 2005; Wernberg et al., 2018).

The extent of gene flow from farmed seaweed to wild populations remains poorly quantified (Valero et al., 2017; Campbell et al., 2019) and may vary between species and with cultivation method (Shan et al., 2019). However, evidence to date suggests that gene flow from farmed to wild seaweed populations is low (Guzinski et al., 2018; Li et al., 2020; Graf et al., 2021). For instance, gene flow from cultivars to wild populations is typically low for *Saccharina japonica* (Liu et al., 2012; Zhang et al., 2017) because selective breeding of cultivars has delayed spore release to late summer when most cultivars have already been harvested and any offspring of remaining cultivars are unlikely to survive high summer temperatures (Shan et al., 2019). However, gene flow from cultivars to wild populations has been documented extensively for animal aquaculture and agriculture (Ellstrand et al., 2013; Glover et al., 2013), with effects varying from possibly advantageous (e.g., increased fitness in wild lettuce; Hooftman et al., 2009; Hartman et al., 2013) to devastating (e.g., wide-spread changes in age and size at maturation in wild stock of Norwegian Atlantic salmon; Bolstad et al., 2017). Consequently, the introduction of cultivated organisms to wild populations is recognized as one of the main risks associated with aquaculture of any species (Naylor et al., 2001) and the cultivation of locally absent seaweed genotypes is often restricted (Loureiro et al., 2015). Therefore, mapping genetic structure and connectivity of wild populations is crucial to ensure that seedlings cultivated from wild type broodstock can be translocated without introducing locally absent genotypes (Barbier et al., 2019; Evankow et al., 2019).

The native kelp *Ecklonia radiata* (C.Agardh.) J.Agardh is a target for aquaculture in New Zealand because of its wide distribution (Shears and Babcock, 2007) and commercial applications as biostimulants, sea vegetables and food additives (White and White, 2020). However, the genetic structure and connectivity of *E. radiata* has not been investigated in New Zealand. Consequently, the geographic extent that seedlings cultivated from wild type brood stock can be translocated without changing local genetic structure remains unknown. In Australia, the genetic structure of *E. radiata* is largely region specific, with high genetic connectivity among populations on the west coast (Coleman et al., 2011a; Coleman, 2013) and low genetic connectivity among populations on the south coast (Coleman et al., 2009). These regional differences in genetic structure are largely attributed to variations in oceanography as the gene flow of *E. radiata* is correlated to the strength of ocean currents (Coleman et al., 2011b). In New Zealand, ocean currents are known to play a key role in long distance connectivity among populations of seagrass (Jones et al., 2008) and several species of seaweeds (Collins et al., 2010; Macaya and Zuccarello, 2010; Buchanan and Zuccarello, 2012; Fraser et al., 2013). Accordingly, the genetic structure of *E. radiata* in New Zealand may also be influenced by local oceanographic conditions. Within the North Island of New Zealand, distinct genetic sub-populations exist for multiple taxonomic groups including seaweeds (Buchanan and Zuccarello, 2012; Muangmai et al., 2015; Huanel et al., 2020), seagrasses (Jones et al., 2008), anemones (Veale and Lavery, 2012), mollusks (Ross et al., 2012), and crustaceans (Stevens, 1990). Furthermore, five bioregions have been proposed within the North Island, based on the distribution *E. radiata* and 150 other species of seaweed and invertebrates, indicating that there may be distinct sub-populations within each of these bioregions, and potential breaks in connectivity between bioregions (Shears et al., 2008). This general high level of genetic and distributional subdivision within seaweeds and benthic invertebrates on the North Island suggest that *E. radiata* is also likely to be divided into genetically distinct sub-populations.

In this study, we used 14 polymorphic microsatellite loci in a three-level hierarchical sampling design to analyze the genetic structure and connectivity of *E. radiata* among four regions of the North Island of New Zealand. The aims were to (1) assess patterns of genetic structure at a local (<300 km) and regional (150–1,200 km) level; and (2) estimate levels of genetic connectivity between local and regional populations; in order to (3) provide guidance for translocation of cultivars to prevent the introduction of locally absent genotypes of *E. radiata* within the North Island of New Zealand.

MATERIALS AND METHODS

Sample Collection

Thirty sporophytes of *E. radiata* were sampled from each of 12 sites on the North Island of New Zealand between September 2019 and March 2020 (**Figure 1A**), conducted under Special Permit 724 issued by the Ministry for Primary Industries, Manatū Ahu Matua to the University of Waikato. A hierarchical design was used with three sites sampled within each of four regions (Northland, Bay of Plenty, Gisborne, and Wellington). At each site, samples of tissue from secondary blades were collected haphazardly by hand from adult (stage 3) plants (Mann and Kirkman, 1981) while snorkeling on rocky reefs within 2–5 m depth and with>1 m between each sampled individual (sample area $\approx$ 1,000 m^2). After collection, samples were stored in separate polyethylene bags and stored on ice for transport back to the laboratory. Within 24 h of collection, samples were cleaned using a scalpel and lint free tissue paper to remove epiphytes and a 2 cm^2 blade section was cut and dried in silica gel for storage for a

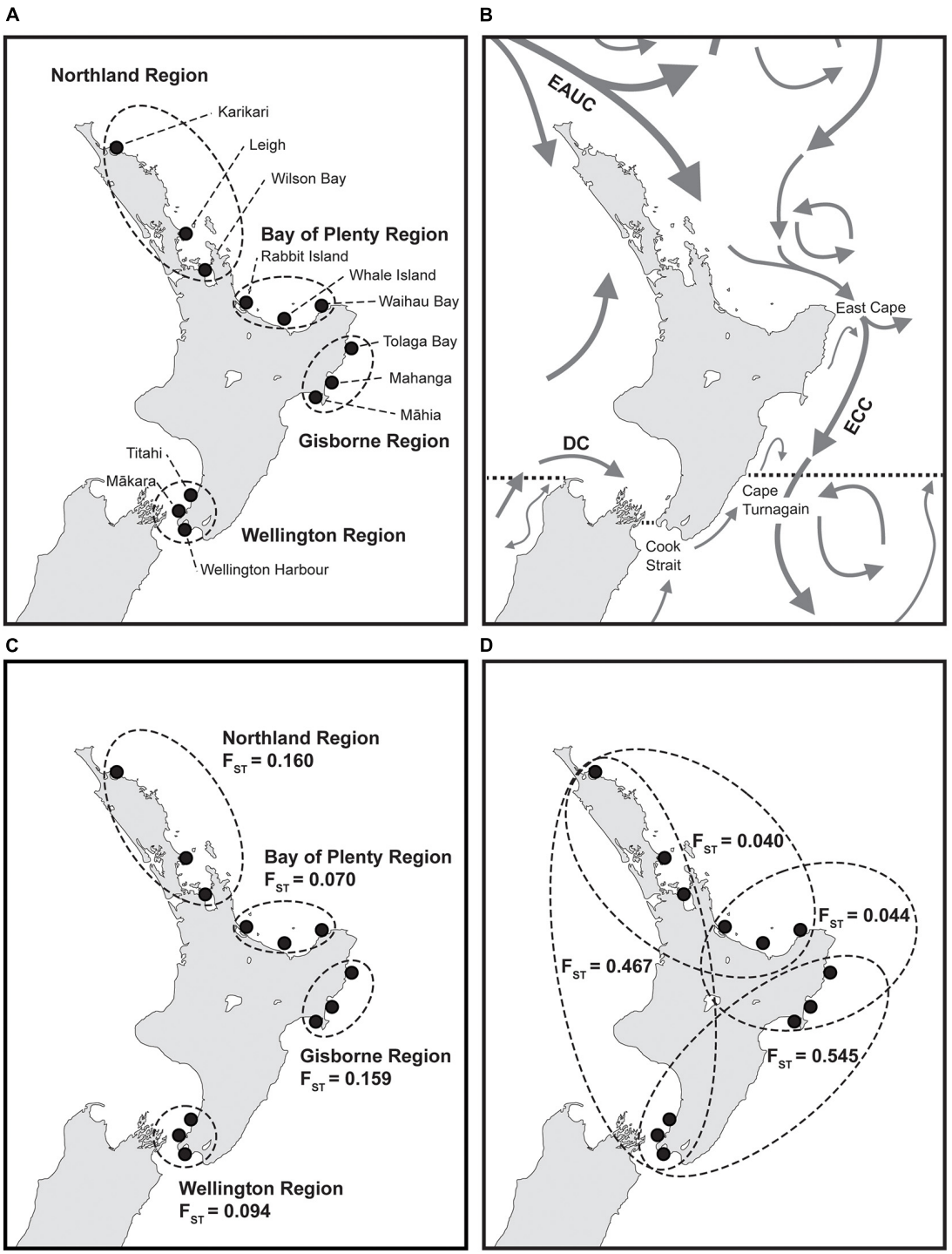

FIGURE 1 | Map of New Zealand with **(A)** sampling sites (filled black circles) and sampling regions (dashed circles), **(B)** major ocean currents (Heath, 1985), proposed biogeographic breaks (dashed black lines, Shears et al., 2008) and locations referred to in the text, **(C)** genetic differentiation (F_{ST}) of *E. radiata* within each region and **(D)** F_{ST} between each neighboring region (F_{ST} Northland vs. Gisborne = 0.043, F_{ST} Bay of Plenty vs. Wellington = 0.407). EAUC: East Auckland Current; ECC: East Cape Current; DC: D'Urville Current. **(B)** Modified with permission from Buchanan and Zuccarello (2012).

maximum of 12 months until further processing (Coleman et al., 2009). Blade tissue was homogenized using a Precellys Evolution Homogenizer (Bertin Instruments, France) and genomic DNA was extracted using a DNeasy® Plant Pro Kit (Qiagen, Germany) following the manufacturer's instructions with the addition of 80–100 μL of PS solution to each sample.

Primer Selection

Twenty five microsatellite loci developed for three other species of *Ecklonia* (Itou et al., 2012; Akita et al., 2018, 2020) were tested to determine their suitability for use in *E. radiata* (**Supplementary Table 1**). All loci were initially tested on 8 individuals from five different sites within the four sampling regions. DNA was amplified in 25 μL singleplex PCR reactions containing 12.5 μL MyTag HS Red Mix (MilliporeSigma, Germany), 0.4 μM non-labeled forward primer, 0.4 μM fluorescent-labeled reverse primer, and 1 μL of genomic DNA. PCRs were run on an Applied Biosystems SimplyAmp Thermal Cycler (Thermo Fisher Scientific, United States) and comprised of an initial denaturation phase at 95°C for 1 min, 35 cycles of denaturation at 95°C for 30 s, annealing at 57°C for 30 s, and extension at 72°C for 30 s, with a final extension at 72°C for 7 min. Five microliter of PCR product was run on a 2% agarose gel and amplicon size was determined using a size standard marker (Bioline HyperLadder^{TM} 25 bp). Loci showing strong evidence of primer dimer on gels were discarded. Loci that produced an amplicon within 150 bp of the expected size range in at least 6 of the 8 tested individuals were selected for genotyping. Loci showing no or inconsistent amplification on gels were further tested on six new individuals, using the same parameters described above. Again, loci were amplified, visualized and selected for genotyping as described earlier and loci that did not consistently produce an amplicon within 150 bp of the expected size range were omitted from further testing. Following this process, 20 loci were selected and subsequently genotyped across all 360 samples (30 samples from each of the 12 sites). Loci were amplified in PCR reactions using the same parameters described above. Multiplex genotyping was carried out by Genetic Analysis Service, Department of Anatomy, University of Otago using an ABI 3730xl DNA Analyzer (Thermo Fisher Scientific, United States) and allele sizes were scored using GeneMarker® (SOFTGENETICS, United States). Three of the 20 loci that were genotyped produced electropherograms too variable for allele sizes to be scored consistently across the 360 samples and were discarded (**Supplementary Table 1**).

Data Analyses

Data (**Supplementary Data 1**) was checked for deviations from Hardy-Weinberg equilibrium and presence of linkage disequilibrium using Genepop on the Web v4.7 (Raymond and Rousset, 1995; Rousset, 2008). Three of the 17 genotyped loci were too monomorphic to enable testing of Hardy-Weinberg equilibrium at any site and were therefore excluded from further statistical analysis (**Supplementary Tables 1, 2**). None of the remaining 14 loci deviated significantly from Hardy-Weinberg equilibrium when data was analyzed collectively across all sites. However, it is likely that some of these loci were not in Hardy-Weinberg equilibrium as 12 of the 14 loci were monomorphic (or almost monomorphic) at one or more sites. Consequently, it was not possible to test for Hardy-Weinberg equilibrium at these sites and they therefore could not be included in the collective assessment of Hardy-Weinberg equilibrium. To determine the influence of this high level of monomorphism on results, a sensitivity analysis was run where all analyses described below were conducted with all 14 loci, and then were repeated excluding all loci where more than half the sites were too monomorphic to calculate test Hardy-Weinberg equilibrium. This sensitivity analysis showed that excluding the 8 loci with the highest monomorphism had no major influence on the main results and all 14 selected loci where therefore retained for analysis (**Supplementary Tables 3, 4**). Linkage disequilibrium was tested across all sites and loci, and *P*-values were adjusted using the false discovery rate (fdr) correction in the R-studio STATS package (Team RStudio, 2021). No significant linkage disequilibrium was found between any loci but an average 58% ± 15 SD of the loci combinations could not be checked for linkage disequilibrium due to monomorphism. However, as this uncertainty was evenly spread across all loci with no consistent patterns, all remaining loci were retained for analysis.

Allele frequencies and total number of alleles were calculated for each locus using GeneAlEx v6.5 (Peakall and Smouse, 2006, 2012). Arlequin v.3.5.2.2 (Excoffier and Lischer, 2010) was used to perform global analysis of molecular variance (AMOVA) as weighted average over all 14 loci within the three hierarchical sampling levels with 1,000 permutations. The number of genetic clusters (K) was analyzed using a Bayesian modeling approach in STRUCTURE v2.3.4 (Pritchard et al., 2000), running 100,000 burn-in and 300,000 Monte Carlo Marco chain repeats after burn-in with 20 iterations for all analyzed levels of K (1–14). Clustering was analyzed using an admixture model with correlated allele frequencies and no prior information about the data. STRUCTURE HARVESTER (Earl and vonHoldt, 2012) was used to find the number of clusters best fitting the data based on highest delta K and to find the iteration with the highest likelihood (Evanno et al., 2005). The clustering analysis was run multiple times to successively identify all hierarchical layers of structuring within the data. All samples were included in the first analysis and for each subsequent analysis, the samples within each of the previously identified clusters were analyzed in separate simulations. F_{ST} is a measure of genetic differentiation ranging from 0 to 1, with 0 showing no genetic difference between samples and 1 showing maximum genetic difference between samples. F_{ST} was calculated in Arlequin. Within region F_{ST} was calculated as the average pairwise F_{ST} between each pair of sites within each region. Between regions F_{ST} was calculated by treating each region as one single population and calculating a single pairwise F_{ST} value for each pair of regions. Pairwise F_{ST} between sites was visualized using R-studio (script sourced from The Banta Lab).[1]

Relatedness between the individuals collected from each site was quantified using ML-Relate (Kalinowski et al., 2006) which includes a null allele correction for any loci at any site that showed significant heterozygote deficiency ($\alpha = 0.05$). Relatedness was further quantified using maximum likelihood estimates, counting all estimates of half sibling, full sibling, and parent/offspring (i.e., not unrelated) as related. Individuals with missing values at more than 2/3 of the loci showed abnormally high values of relatedness and were therefore deleted and not used in any

[1] https://sites.google.com/site/thebantalab/home?authuser=0

analysis (13 samples out of 360). High levels of relatedness were found between individuals at all sites (mean 28.2% ± 0.7 SE) which can bias genetic analysis (Waples and Anderson, 2017). To determine the influence of this high level of relatedness on results, another sensitivity analysis was run where all analyses described below were repeated excluding all samples that were related to more than 33.3% of the other samples within their sites (thereby lowing mean relatedness to 21.1% ± 0.6 SE). This sensitivity analysis showed that excluding the 97 most related samples had no major effect on the main results and all 347 samples were therefore retained for analysis (**Supplementary Tables 3, 4**). To determine the influence of geographic distance on genetic structure, a redundancy analysis was performed in R-studio using the vegan package (Oksanen et al., 2020) and visualized using ggplot (Wickham, 2016). Site coordinates (longitude and latitude) were set as independent variables and site-specific allele frequencies (72 different alleles in total across the 14 selected loci) as constrained dependent variables (Meirmans, 2015).

RESULTS

Genetic diversity was highest within northern sites (sites within the Northland and Bay of Plenty regions) compared to southern sites (sites within the Gisborne and Wellington regions, **Table 1**). The mean total number of alleles and mean number of unique alleles were 34.83 and 2.8, respectively, for northern sites, compared to 26.2 and 0.7, respectively, for southern sites. Relatedness between individuals was high at all sites (mean 28.2% ± 0.7 SE), with individuals within southern sites being slightly more related than samples within the northern sites (32.0% ± 1.0 SE and 24.3% ± 0.8 SE, respectively).

Analysis of molecular variance showed high genetic variation among regions (27.41%) and low genetic variation among sites within regions (7.10%), with all levels of variation being significant ($p < 0.001$, **Table 2**). The same pattern was evident for genetic differentiation (F_{ST}, **Supplementary Tables 5, 6**). F_{ST} values were low within regions (F_{ST} = 0.070–0.160, **Figure 1C**), indicating low genetic differentiation, but were generally higher between regions (F_{ST} = 0.040–0.545, **Figure 1D**), indicating comparatively higher genetic differentiation. Between region F_{ST} was high between the Wellington region and the three other regions (F_{ST} = 0.407–0.545) and low between the Northland, Bay of Plenty and Gisborne regions (F_{ST} = 0.040–0.044). Pairwise F_{ST} between sites showed significant genetic differentiation between all sites except for 2 pairs (**Figure 2**). Highest pairwise F_{ST} was again found between the Wellington sites and sites from the other regions, with Titahi Bay and Mākara Beach showing the highest differentiation from other sites and Wellington Harbor showing only intermediate differentiation.

Bayesian modeling of population structure predicted that the most likely number of genetic clusters (inferred from delta K) for any of the STRUCTURE simulations was two (K = 2, **Figure 3**). When all samples were included in the analysis, the three Wellington sites were all grouped into one distinct cluster and the nine sites from the other three regions were grouped into a second distinct cluster. At the lower hierarchical levels of clustering (1) the Northland region separated from the Bay of Plenty and Gisborne region, (2) the Bay of Plenty region

TABLE 1 | Number of individuals genotyped (*n*); total and mean number of alleles, and number of unique alleles; and% relatedness between individuals ± standard error.

Location	Region	*n*	Number of alleles			Relatedness
			Total	Mean	Unique	% ± SE
Karikari	Northland	28	35	2.5	4	26.2 ± 1.7
Leigh	Northland	25	38	2.7	3	24.3 ± 2.3
Wilson bay	Northland	30	29	2.1	2	25.1 ± 1.4
Rabbit island	Bay of Plenty	27	39	2.8	1	24.2 ± 2.0
Whale island	Bay of Plenty	30	36	2.6	4	26.0 ± 2.2
Waihau bay	Bay of Plenty	29	32	2.3	3	20.1 ± 1.8
Tolaga bay	Gisborne	30	28	2.0	2	31.7 ± 2.9
Mahanga	Gisborne	28	25	1.8	0	34.4 ± 2.0
Māhia	Gisborne	30	19	1.4	0	27.4 ± 2.2
Wellington harbor	Wellington	30	30	2.1	1	32.0 ± 2.1
Mākara beach	Wellington	30	26	1.9	0	27.4 ± 1.9
Titahi	Wellington	30	29	2.1	1	39.3 ± 2.7
All		347	72	5.1		28.2 ± 0.7

All measurements of number of alleles, heterozygosity, and relatedness are across all 14 loci.

TABLE 2 | Global analysis of molecular variance (AMOVA) for *E. radiata* among the four regions, among the three sites within each region, and among the individuals (25–30) within each site.

Source of variation	df	Sum of squares	Variance component	Percentage variation
Among regions	3	222.87	0.416	27.41
Among sites within regions	8	56.18	0.108	7.10
Within sites (among individuals)	336	651.98	0.994	65.49
Total	347	937.03	1.517	

All levels of variation are significant at $p < 0.001$.

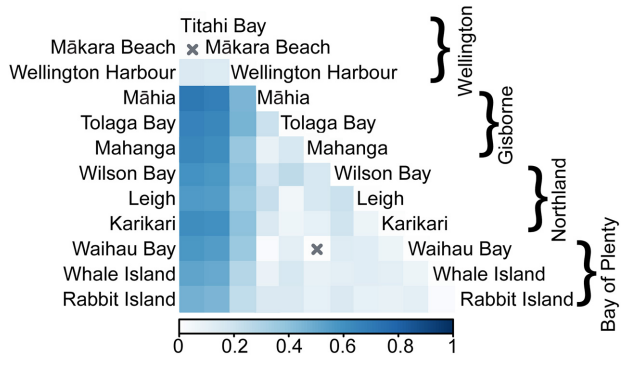

FIGURE 2 | Pairwise genetic differentiation (F_{ST}) between each site (F_{ST} values indicated by color gradient) with X indicating that sites are not significantly different.

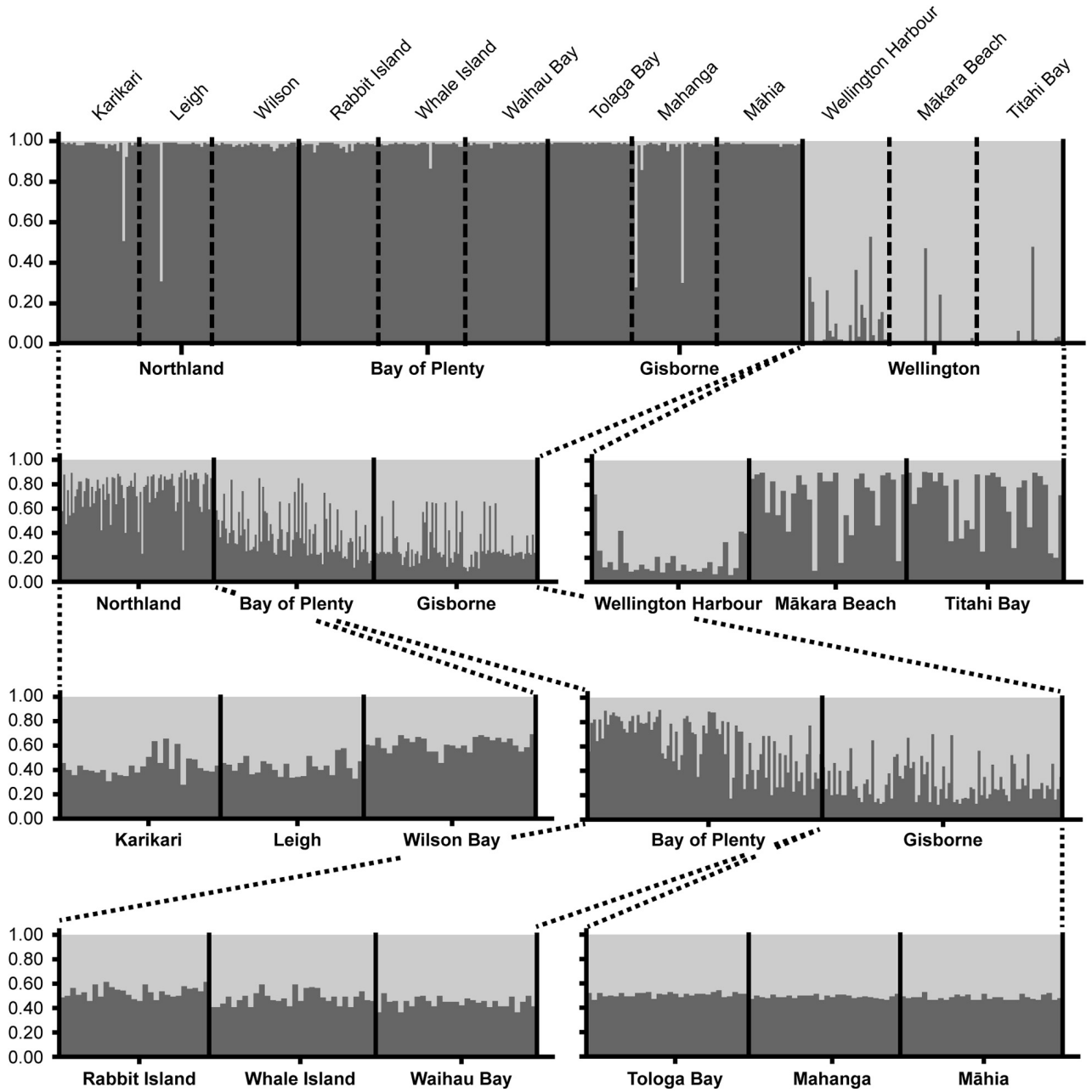

FIGURE 3 | Bayesian modeling of population structure for *E. radiata* obtained using STRUCTURE (K = 2 for all plots). Top plot was run with all samples included and each subplot underneath was run with a subset of the samples indicated by the dashed lines. The x-axes show all individuals included in the simulations, with each individual represented by a column and grouped within their sites and regions. The y-axes show the genetic membership of each individual to the two clusters.

separated slightly from the Gisborne region, and (3) Wellington Harbor separated sharply from the Wellington open coast sites, Mākara Beach and Titahi Bay. There was no evidence of genetic structure among sites within each of the Northland, Bay of Plenty, and Gisborne regions.

Redundancy analysis showing the effect of geographic location (latitude and longitude) on allele frequency was highly significant (P = 0.001, 74% constrained variance and 26% unconstrained variance), with latitude and longitude explaining 74% of the genetic variation in the data (**Figure 4**). The redundancy analysis showed the same pattern of population structure as the clustering analysis, with strong genetic separation between the wellington sites and the other sites along the RDA 1 axis (67% of the total variation) and a weaker genetic separation between the Northland sites and the other sites along the RDA 2 axis (7% of total variation). Most of the 72 alleles analyzed across the 14 loci were plotted in the center of the graph and only 8 alleles were plotted outside the center,

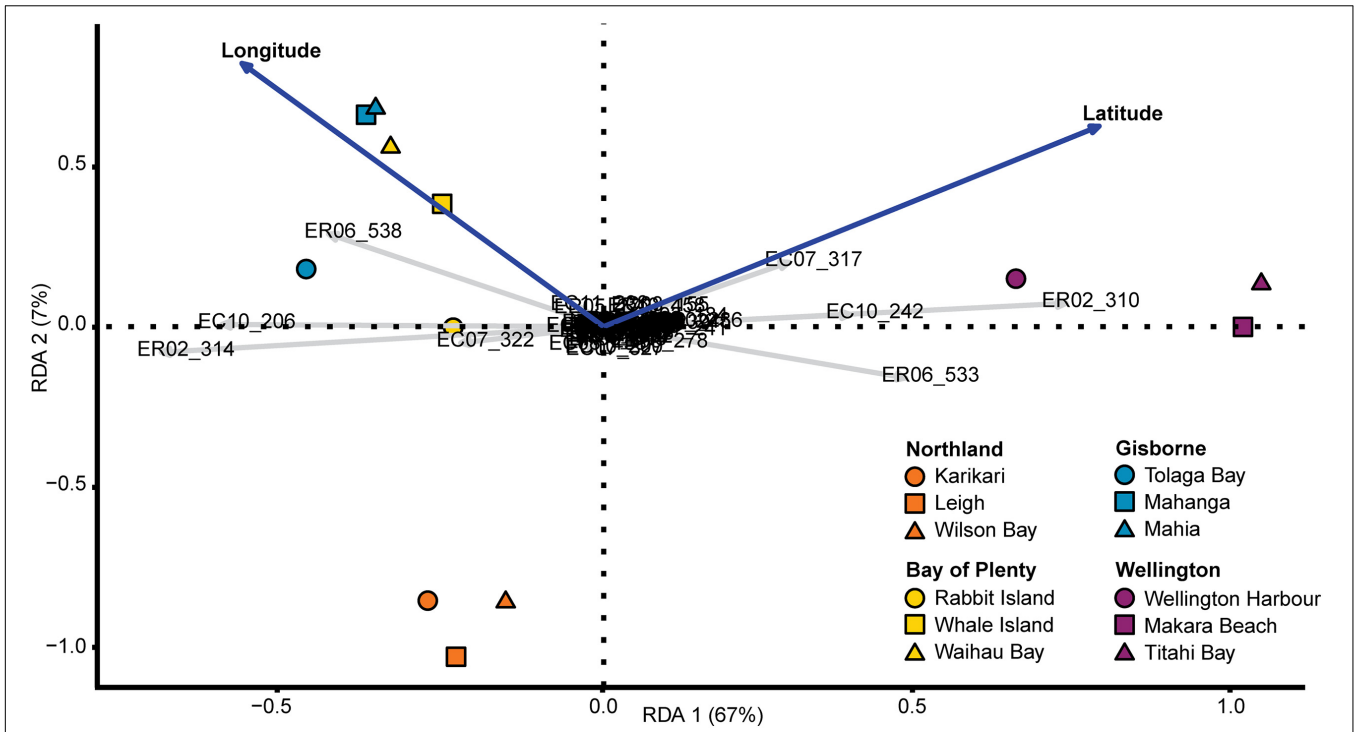

FIGURE 4 | Redundancy analysis (RDA) of allele frequencies explained by geographical location (longitude and latitude). Gray vectors with allele names indicate magnitude and direction of the variation associated with each identified allele where the vector length indicates the amount of variation and the vector direction indicates the correlation of the variation with the two RDA axes (parallel lines being highly correlated). Similarly, the blue vectors indicate the magnitude and direction of the variation associated with the latitude and longitude coordinates of the sites. Sites are plotted according to region (color) and position within region (shape). The percent variation explained by the two RDA components are shown on the two axes.

indicating that most of the variation in the data was provided by these 8 alleles.

DISCUSSION

Genetic Structure and Connectivity of *Ecklonia radiata*

Genetic analysis of microsatellite loci showed strong population structure and low genetic connectivity of *E. radiata* within the North Island of New Zealand. Clustering analysis showed structural differences on all hierarchical levels, with the Wellington region separating from the other regions at the highest level, the Northland region separating from the Bay of plenty and Gisborne regions at the intermediate level, and Wellington Harbor separating from Mākara Beach and Titahi Bay at the within region level (**Figure 3**). This same pattern of hierarchical genetic structuring was found through analysis of pairwise genetic differentiation (F_{ST}) and redundancy analysis, which showed clear distinction between the Wellington region and the other regions and between Wellington Harbor and the other sites within the Wellington region (**Figures 1**, **4**). These findings demonstrate high levels of genetic structure both across long and short geographic distances. The high level of relatedness between individuals within sites and the large number of sites that were significantly different from one another (all but two site pairs through Pairwise F_{ST}), suggest that geneflow is generally low. However, regional F_{ST} showed that gene flow was higher among the Northland, Bay of Plenty and Gisborne regions (F_{ST} = 0.040–0.044) than between these regions and Wellington (F_{ST} = 0.407–0.545). Further support for the notion of reduced connectivity in the Wellington region was provided by the higher levels of relatedness recorded for southern sites (32.0% ± 1.0 SE) compared to those in the north (24.3% ± 0.8 SE). The redundancy analysis showed high correlation between genetic structure and geographic location (74% constrained variance), but also showed a high degree of clustering in agreement with the groupings identified using STRUCTURE, indicating that gene flow in *E. radiata* in New Zealand is primarily shaped by dispersal barriers rather than by isolation by distance. In combination, these analyses suggest that multiple sub-populations of *E. radiata* are present within the locations sampled in this study and that genetic connectivity is limited.

E. radiata has a life cycle of two alternate generations where macroscopic diploid sporophytes produce spores that develop into microscopic haploid gametophytes (males and females) which then produce eggs and sperm that fuse and grow into sporophytes. The pelagic phase of *E. radiata* zoospores is relatively short (usually 1–2 h, Wernberg et al., 2019) and based on studies of related species, gametophyte sperm dispersal is expected to occur over the scale of centimeters,

whereas spore dispersal has an approximate maximum dispersal range of 1 km (Reed, 1990; Gaylord et al., 2006). Because *E. radiata* is negatively buoyant, long-distance dispersal of mature plants is unlikely unless rafting with buoyant species (Fraser et al., 2013). Consequently, the dispersal potential of *E. radiata* is likely to be limited. These expectations were generally met as evidenced by significant levels of genetic differentiation between most sub-populations. Furthermore, this low dispersal life history may also explain the high levels of relatedness recorded for individuals within sites. High levels of relatedness have previously been reported for the related species *E. cava* (Itou et al., 2019), and these results indicate inbreeding, which may have contributed to the high F_{ST} values.

Strong genetic differentiation between Wellington and the three northern regions matches patterns of genetic structure reported for other seaweed and invertebrate species. For these species, populations in the Wellington region have been shown to be distinct from northern populations, and more closely aligned to a South Island sub-population, indicating a major break in connectivity on the North Island for these species (Ross et al., 2009, 2012; Buchanan and Zuccarello, 2012; Veale and Lavery, 2012). Shears et al. (2008) found major biogeographic breaks based on distributional data covering *E. radiata* and 150 species of seaweed and invertebrates. In this case, the location of the genetic breaks recorded for *E. radiata* (between Wellington and northern regions and between the sites within the Wellington region), coincide with the biogeographic boundaries reported by Shears et al. (2008). This suggests that the sharp breaks in *E. radiata* connectivity between and within regions are most likely generated by the same processes (oceanography and climate) that influence the distribution of a numerous other marine species in the area.

Our detection of regional differences in genetic connectivity is similar to that reported for *E. radiata* in Australia, where this species displays high genetic connectivity along the west coast, but low connectivity along the south coast (Coleman et al., 2009, 2011a; Coleman, 2013). Ocean currents are a strong driver of differences in genetic connectivity among *E. radiata* populations in Australia (Coleman et al., 2011b) and may also explain the patterns of genetic connectivity observed in this study. Ocean currents in New Zealand are thought to shape long distance connectivity among other species of seaweeds (Collins et al., 2010; Macaya and Zuccarello, 2010; Buchanan and Zuccarello, 2012; Fraser et al., 2013) and seagrass (Jones et al., 2008). The two main ocean currents shaping the oceanography along the north-east coast of the North Island of New Zealand are the East Auckland Current and the East Cape Current, which travel south-eastward through the Northland, Bay of Plenty and Gisborne region, passing Cape Turnagain where the East Cape Current turns east with the Chatham Rise into the Pacific (**Figure 1B**; Heath, 1985). The higher genetic connectivity of *E. radiata* found along the north-eastern coast of the North Island compared to low connectivity found between Wellington and the other regions may therefore be facilitated by these major ocean currents. In the Wellington region, water movement northwards is prevented by the D'Urville Current, which pushes water south-eastwards through Cook Straight.

Implications for Aquaculture

In commercial kelp cultivation, new broodstock is cultivated and seeded onto ropes in on-shore hatcheries, and then, following a nursery period, the ropes are deployed off-shore for the juvenile kelp to mature (Zhang, 2018; Kim et al., 2019). This process creates high potential for spread of locally absent cultivar alleles, which may affect the genetic structure of wild populations and leave them more vulnerable to environmental stress (Ellstrand et al., 2013; Bolstad et al., 2017; Wernberg et al., 2018). The spread of locally absent cultivar alleles can be avoided by developing local cultivars for local use only (Barbier et al., 2019). Our analysis showed clear distinction between the Wellington region and the three other regions but also revealed strong genetic structure and significant differentiation within and between individual sites. We therefore recommend that cultivars of *E. radiata* should not be translocated outside their area of origin to avoid introducing locally absent genotypes to local sub-populations. Specific guidelines for the scale of translocation of kelp seed-stock have already been developed in some locations (e.g., Gulf of Alaska, United States, Kim et al., 2019), and based on the results of this study and future genetic research, similar guidelines could be developed for *E. radiata* in New Zealand.

Microsatellite markers have proven to be a powerful tool for the assessment of genetic structure and connectivity of natural populations (Guichoux et al., 2011). However, results provided by microsatellites may be less detailed than what might have been revealed through full genome sequencing (e.g., Graf et al., 2021). Therefore, it is possible that further genetic differentiation among *E. radiata* sub-populations in New Zealand could be revealed through detailed genomic analysis. Still, given the large number of samples genotyped (360) and the high number of loci (14) included in our analyses, we believe that the results presented here are representative of the general genetic structure and connectivity of *E. radiata* in New Zealand. The patterns of low geneflow presented here suggest that the genetic structure of *E. radiata* in the South Island of New Zealand is also likely to be strong. Therefore, we recommend a similarly conservative approach to the translocation of kelp cultivars in this region.

Selective breeding is an integral part of the global seaweed aquaculture industry and has made it possible to improve key cultivar traits such as growth rate, morphology, reproductive timing, biochemical content, stress tolerance, texture, and taste (Hwang et al., 2019). However, selective breeding tends to reduce the genetic diversity of cultivars as it often leads to inbreeding, whether intentional or not (Valero et al., 2017). Reducing the genetic diversity of cultivars is not only a threat to the genepool of local wild populations (Haygood et al., 2003; Bolstad et al., 2017), but may also leave cultivars more susceptible to pathogens (Hwang et al., 2019). For instance, low genetic diversity caused by inbreeding was the main cause of the heavy ice-ice disease outbreak that lead to the sharp decline of the eucheumatoid

seaweed farming in the Philippines (Trono and Largo, 2019). It is therefore important in aquaculture not only to use local cultivars, but also to maintain a large effective population size and frequently introduce new genotypes from wild type broodstock to ensure high genetic diversity among cultivars (**Table 1**; Barbier et al., 2019; Graf et al., 2021; Hu et al., 2021). As has previously been recorded in other New Zealand seaweed species, substantially higher genetic diversity was found among the northern sub-population of *E. radiata* compared to the southern sub-populations (Fraser et al., 2009; Buchanan and Zuccarello, 2012; Muangmai et al., 2015). The northern regions seem therefore to be the best suited areas for *E. radiata* cultivation with regards to maintaining high genetic diversity among cultivars.

CONCLUSION

The strong genetic structure found at all hierarchical levels for *E. radiata* in the North Island of New Zealand underlines the general need for population genetic analyses to be conducted before initiating translocation of broodstock for seaweed aquaculture. Bayesian analysis of population structure, redundancy analysis and measurements of genetic differentiation (F_{ST}) all showed high levels of genetic variation and indicated that genetically distinct sub-populations are likely to be present both between and within regions. From a genetic perspective, we therefore recommend that cultivars of *E. radiata* should not be translocated outside their area of origin to avoid introducing locally absent genotypes to local sub-populations. The high relatedness between samples found here highlights the importance of increasing the distance between collected individuals of *Ecklonia sp.* for genetic analysis (preferably to more than 4 m, Itou et al., 2019) to minimize the impact of non-random mating and increase the importance of migration and drift within the signal. The microsatellite data collected in this study can serve as a reference set for future analysis of the genetic structure of *E. radiata* by comparing the genetic membership of individuals from sites outside the range of this study with the sub-populations sampled here.

DATA AVAILABILITY STATEMENT

The original contributions presented in the study are included in the article/**Supplementary Material**, further inquiries can be directed to the corresponding author/s.

AUTHOR CONTRIBUTIONS

JN-D: investigation, data curation, data analysis, visualization, and writing—original draft, review, and editing. MM: conceptualization, design, supervision, funding, and writing—review, and editing. CG: conceptualization, supervision, writing—review, and editing. PR: writing—review, and editing. RL: conceptualization, design, supervision, data analysis, and writing—review, and editing. All authors contributed to the article and approved the submitted version.

FUNDING

This research is part of the Entrepreneurial Universities Macroalgal Biotechnologies Program, jointly funded by the University of Waikato and the Tertiary Education Commission.

ACKNOWLEDGMENTS

We thank Peter Randrup and Alisa Mihaila for sample collection and sample processing assistance. We also thank the two reviewers for very constructive feedback and suggestions for data analysis and literature.

SUPPLEMENTARY MATERIAL

The Supplementary Material for this article can be found online at: https://www.frontiersin.org/articles/10.3389/fmars.2021.749154/full#supplementary-material

REFERENCES

Akita, S., Hashimoto, K., Hanyuda, T., and Kawai, H. (2020). Molecular phylogeny and biogeography of *Ecklonia* spp. (Laminariales, Phaeophyceae) in Japan revealed taxonomic revision of *E. kurome* and *E. stolonifera*. *Phycologia* 59, 330–339. doi: 10.1080/00318884.2020.1756123

Akita, S., Koiwai, K., Hanyuda, T., Kato, S., Nozaki, R., Uchino, T., et al. (2018). Development of 11 *Ecklonia radicosa* (Phaeophyceae, Laminariales) SSRs markers using next-generation sequencing and intra-genus amplification analysis. *J. Appl. Phycol.* 30, 2111–2115. doi: 10.1007/s10811-018-1406-5

Barbier, M., Charrier, B., Araujo, R., Holdt, S. L., Jacquemin, B., and Rebours, C. (2019). in *Pegasus - Phycomorph European Guidelines for a Sustainable Aquaculture of Seaweeds COST Action FA1406*, eds M. Barbier and B. Charrier (Roscoff: European Commission), doi: 10.21411/2c3w-yc73

Bolstad, G. H., Robertsen, G., Jonsson, B., Sægrov, H., Diserud, O. H., Fiske, P., et al. (2017). Gene flow from domesticated escapes alters the life history of wild Atlantic salmon. *Nat. Ecol. Evol.* 1:0124 . doi: 10.1038/s41559-017-0124

Buchanan, J., and Zuccarello, G. C. (2012). Decoupling of short- and long-distance dispersal pathways in the endemic New Zealand seaweed *Carpophyllum maschalocarpum* (Phaeophyceae, Fucales). *J. Phycol.* 48, 518–529. doi: 10.1111/j.1529-8817.2012.01167.x

Campbell, I., Macleod, A., Sahlmann, C., Neves, L., Funderud, J., Øverland, M., et al. (2019). The environmental risks associated with the development of seaweed farming in Europe – prioritizing key knowledge gaps. *Front. Mar. Sci.* 6:107. doi: 10.3389/fmars.2019.00107

Coleman, M. A. (2013). Connectivity of the habitat-forming kelp, Ecklonia radiata within and among estuaries and open coast. *PLoS One* 8:e64667. doi: 10.1371/journal.pone.0064667

Coleman, M. A., Chambers, J., Knott, N. A., Malcolm, H. A., Harasti, D., Jordan, A., et al. (2011a). Connectivity within and among a network of temperate marine reserves. *PLoS One* 6:e20168. doi: 10.1371/journal.pone.0020168

Coleman, M. A., Roughan, M., Macdonald, H. S., Connell, S. D., Gillanders, B. M., Kelaher, B. P., et al. (2011b). Variation in the strength of continental boundary

currents determines continent-wide connectivity in kelp. *J. Ecol.* 99, 1026–1032. doi: 10.1111/j.1365-2745.2011.01822.x

Coleman, M. A., Gillanders, B. M., and Connell, S. D. (2009). Dispersal and gene flow in the habitat-forming kelp, *Ecklonia radiata*: relative degrees of isolation across an eastwest coastline. *Mar. Freshw. Res.* 60, 802–809. doi: 10.1071/MF08268

Collins, C. J., Fraser, C. I., Ashcroft, A., and Waters, J. M. (2010). Asymmetric dispersal of southern bull-kelp (*Durvillaea antarctica*) adults in coastal New Zealand: testing an oceanographic hypothesis. *Mol. Ecol.* 19, 4572–4580. doi: 10.1111/j.1365-294X.2010.04842.x

Earl, D. A., and vonHoldt, B. M. (2012). Structure harvester: a website and program for visualizing structure output and implementing the Evanno method. *Conserv. Genet. Resour.* 4, 359–361. doi: 10.1007/s12686-011-9548-7

Ellstrand, N. C., Meirmans, P., Rong, J., Bartsch, D., Ghosh, A., de Jong, T. J., et al. (2013). Introgression of crop alleles into wild or weedy populations. *Annu. Rev. Ecol. Evol. Syst.* 44, 325–345. doi: 10.1146/annurev-ecolsys-110512-135840

Evankow, A., Christie, H., Hancke, K., Brysting, A. K., Junge, C., Fredriksen, S., et al. (2019). Genetic heterogeneity of two bioeconomically important kelp species along the Norwegian coast. *Conserv. Genet.* 20, 615–628. doi: 10.1007/s10592-019-01162-8

Evanno, G., Regnaut, S., and Goudet, J. (2005). Detecting the number of clusters of individuals using the software structure: a simulation study. *Mol. Ecol.* 14, 2611–2620. doi: 10.1111/j.1365-294X.2005.02553.x

Excoffier, L., and Lischer, H. E. L. (2010). Arlequin suite ver 3.5: a new series of programs to perform population genetics analyses under Linux and Windows. *Mol. Ecol. Resour.* 10, 564–567. doi: 10.1111/j.1755-0998.2010.02847.x

FAO (2020). *The State of World Fisheries and Aquaculture 2020. Sustainability in Action*. Rome: FAO, doi: 10.4060/ca9229en

Fraser, C. I., Nikula, R., Spencer, H. G., and Waters, J. M. (2009). Kelp genes reveal effects of subantarctic sea ice during the Last Glacial Maximum. *Proc. Natl. Acad. Sci. U.S.A.* 106, 3249–3253. doi: 10.1073/pnas.0810635106

Fraser, C. I., Zuccarello, G. C., Spencer, H. G., Salvatore, L. C., Garcia, G. R., and Waters, J. M. (2013). Genetic affinities between trans-oceanic populations of non-buoyant macroalgae in the high latitudes of the southern hemisphere. *PLoS One* 8:e69138. doi: 10.1371/journal.pone.0069138

Gaylord, B., Reed, C. D., Raimondi, T. P., and Washburn, L. (2006). Macroalgal spore dispersal in coastal environments: mechanistic insights revealed by theory and experiment. *Ecol. Monogr.* 76, 481–502. doi: 10.1890/0012-96152006076[0481:MSDICE]2.0.CO;2

Glover, K. A., Pertoldi, C., Besnier, F., Wennevik, V., Kent, M., and Skaala, Ø (2013). Atlantic salmon populations invaded by farmed escapees: quantifying genetic introgression with a Bayesian approach and SNPs. *BMC Genet.* 14:74. doi: 10.1186/1471-2156-14-74

Gosch, B. J., Paul, N. A., de Nys, R., and Magnusson, M. (2015). Spatial, seasonal, and within-plant variation in total fatty acid content and composition in the brown seaweeds *Dictyota bartayresii* and *Dictyopteris australis* (Dictyotales, Phaeophyceae). *J. Appl. Phycol.* 27, 1607–1622. doi: 10.1007/s10811-014-0474-4

Graf, L., Shin, Y., Yang, J. H., Choi, J. W., Hwang, I. K., Nelson, W., et al. (2021). A genome-wide investigation of the effect of farming and human-mediated introduction on the ubiquitous seaweed *Undaria pinnatifida*. *Nat. Ecol. Evol.* 5, 360–368. doi: 10.1038/s41559-020-01378-9

Guichoux, E., Lagache, L., Wagner, S., Chaumeil, P., Léger, P., Lepais, O., et al. (2011). Current trends in microsatellite genotyping. *Mol. Ecol. Resour.* 11, 591–611. doi: 10.1111/j.1755-0998.2011.03014.x

Guzinski, J., Ballenghien, M., Daguin-Thiébaut, C., Lévêque, L., and Viard, F. (2018). Population genomics of the introduced and cultivated Pacific kelp *Undaria pinnatifida*: marinas—not farms—drive regional connectivity and establishment in natural rocky reefs. *Evol. Appl.* 11, 1582–1597. doi: 10.1111/eva.12647

Hartman, Y., Uwimana, B., Hooftman, D. A. P., Schranz, M. E., van de Wiel, C. C. M., Smulders, M. J. M., et al. (2013). Genomic and environmental selection patterns in two distinct lettuce crop-wild hybrid crosses. *Evol. Appl.* 6, 569–584. doi: 10.1111/eva.12043

Haygood, R., Ives, A. R., and Andow, D. A. (2003). Consequences of recurrent gene flow from crops to wild relatives. *R. Soc.* 270, 1879–1886. doi: 10.1098/rspb.2003.2426

Heath, R. A. (1985). A review of the physical oceanography of the seas around New Zealand — 1982. *New Zeal. J. Mar. Freshw. Res.* 19, 79–124. doi: 10.1080/00288330.1985.9516077

Hooftman, D. A. P., Hartman, Y., Oostermeijer, J. G. B., and Den Nijs, H. C. M. (2009). Existence of vigorous lineages of crop-wild hybrids in lettuce under field conditions. *Environ. Biosafety Res.* 8, 203–217. doi: 10.1051/ebr/2010001

Hu, Z. M., Shan, T. F., Zhang, J., Zhang, Q. S., Critchley, A. T., Choi, H. G., et al. (2021). Kelp aquaculture in China: a retrospective and future prospects. *Rev. Aquac.* 13, 1324–1351. doi: 10.1111/raq.12524

Huanel, O. R., Nelson, W. A., Robitzch, V., Mauger, S., Faugeron, S., Preuss, M., et al. (2020). Comparative phylogeography of two Agarophyton species in the New Zealand archipelago. *J. Phycol.* 56, 1575–1590. doi: 10.1111/jpy.13046

Hughes, A. R., and Stachowicz, J. J. (2004). Genetic diversity enhances the resistance of a seagrass ecosystem to disturbance. *Proc. Natl. Acad. Sci. U.S.A.* 101, 8998–9002. doi: 10.1073/pnas.0402642101

Hwang, E. K., Yotsukura, N., Pang, S. J., Su, L., and Shan, T. F. (2019). Seaweed breeding programs and progress in eastern Asian countries. *Phycologia* 58, 484–495. doi: 10.1080/00318884.2019.1639436

Itou, T., Kanno, M., Suyama, Y., Inaba, K., and Aoki, M. N. (2019). Opening the black box: microspatial patterns of zoospore dispersal, parentage, and selfing in the kelp *Ecklonia cava* as revealed by microsatellite markers. *J. Appl. Phycol.* 31, 3283–3294. doi: 10.1007/s12686-011-9574-5

Itou, T., Kanno, M., Suyama, Y., Kamiyama, A., Sakamoto, S. X., Kijima, A., et al. (2012). Development of 12 polymorphic microsatellite DNA markers for the kelp *Ecklonia cava* (Phaeophyceae, Laminariales). *Conserv. Genet. Resour.* 4, 459–461.

Jones, T. C., Gemmill, C. E. C., and Pilditch, C. A. (2008). Genetic variability of New Zealand seagrass (*Zostera muelleri*) assessed at multiple spatial scales. *Aquat. Bot.* 88, 39–46. doi: 10.1016/j.aquabot.2007.08.017

Kalinowski, S. T., Wagner, A. P., and Taper, M. L. (2006). ML-RELATE: a computer program for maximum likelihood estimation of relatedness and relationship. *Mol. Ecol. Notes* 6, 576–579. doi: 10.1111/j.1471-8286.2006.01256.x

Kim, J., Stekoll, M., and Yarish, C. (2019). Opportunities, challenges and future directions of open-water seaweed aquaculture in the United States. *Phycologia* 58, 446–461. doi: 10.1080/00318884.2019.1625611

Li, Q., Shan, T., Wang, X., Su, L., and Pang, S. (2020). Evaluation of the genetic relationship between the farmed populations on a typical kelp farm and the adjacent subtidal spontaneous population of *Undaria pinnatifida* (Phaeophyceae, Laminariales) in China. *J. Appl. Phycol.* 32, 653–659. doi: 10.1007/s10811-019-01917-3

Liu, F., Yao, J., Wang, X., Repnikova, A., Galanin, D. A., and Duan, D. (2012). Genetic diversity and structure within and between wild and cultivated *Saccharina japonica* (Laminariales, Phaeophyta) revealed by SSR markers. *Aquaculture* 35, 139–145. doi: 10.1016/j.aquaculture.2012.06.022

Loureiro, R., Gachon, C. M. M., and Rebours, C. (2015). Seaweed cultivation: potential and challenges of crop domestication at an unprecedented pace. *New Phytol.* 206, 489–492. doi: 10.1111/nph.13278

Macaya, E. C., and Zuccarello, G. C. (2010). DNA barcoding and genetic divergence in the giant kelp *Macrocystis* (laminariales). *J. Phycol.* 46, 736–742. doi: 10.1111/j.1529-8817.2010.00845.x

Mann, E. H., and Kirkman, H. (1981). Biomass method for measuring productivity of Ecklonia radiata, with the potential for adaptation to other large brown algae. *Aust. J. Mar. Freshw. Res.* 32, 297–304.

Mata, L., Lawton, R. J., Magnusson, M., Andreakis, N., De Nys, R., Paul, N. A., et al. (2017). Within-species and temperature-related variation in the growth and natural products of the red alga Asparagopsis taxiformis. *J. Appl. Phycol.* 29, 1437–1447. doi: 10.1007/s10811-016-1017-y

Meirmans, P. G. (2015). Seven common mistakes in population genetics and how to avoid them. *Mol. Ecol.* 24, 3223–3231. doi: 10.1111/mec.13243

Muangmai, N., Fraser, C. I., and Zuccarello, G. C. (2015). Contrasting patterns of population structure and demographic history in cryptic species of *Bostrychia intricata* (Rhodomelaceae, Rhodophyta) from New Zealand. *J. Phycol.* 51, 574–585. doi: 10.1111/jpy.12305

Naylor, R. L., Williams, S. L., and Strong, D. R. (2001). Aquaculture: a gateway for exotic species. *Sci. New Ser.* 294, 1655–1656. doi: 10.1126/science.1064875

Oksanen, J., Guillaume Blanchet, F., Friendly, M., Kindt, R., Legendre, P., McGlinn, D., et al. (2020). *Vegan: Community Ecology Package. R Package Version 2.5-7*. Available online at: https://cran.r-project.org/package=vegan (accessed November 28, 2020).

Oliveira, A. S., Sudatti, D. B., Fujii, M. T., Rodrigues, V., and Pereira, R. C. (2013). Inter- and intrapopulation variation in the defensive chemistry of the red seaweed *Laurencia dendroidea* (Ceramiales, Rhodophyta). *Phycologia* 52, 130–136. doi: 10.2216/12-058.1

Peakall, R., and Smouse, P. E. (2006). GENALEX 6: genetic analysis in Excel. Population genetic software for teaching and research. *Mol. Ecol. Notes* 6, 288–295. doi: 10.1111/j.1471-8286.2005.01155.x

Peakall, R., and Smouse, P. E. (2012). GenALEx 6.5: genetic analysis in Excel. Population genetic software for teaching and research-an update. *Bioinformatics* 28, 2537–2539. doi: 10.1093/bioinformatics/bts460

Pritchard, J. K., Stephens, M., and Donelly, P. (2000). Inference of population structure using multilocus genotype data. *Genetics* 155, 945–959. doi: 10.1111/j.1471-8286.2007.01758.x

Raymond, M., and Rousset, F. (1995). Genpop 1.2 Population genetics software for exact test and ecumenicism. *J. Hered.* 86, 248–249. doi: 10.1093/oxfordjournals.jhered.a111573

Reed, D. C. (1990). The effects of variable settlement and early competition on patterns of kelp recruitment. *Ecology* 71, 776–787.

Reusch, T. B. H., Ehlers, A., Hämmerli, A., and Worm, B. (2005). Ecosystem recovery after climatic extremes enhanced by genotypic diversity. *Proc. Natl. Acad. Sci. U.S.A.* 102, 2826–2831. doi: 10.1073/pnas.0500008102

Ross, P. M., Hogg, I. D., Pilditch, C. A., and Lundquist, C. J. (2009). Phylogeography of New Zealand's coastal benthos. *New Zeal. J. Mar. Freshw. Res.* 43, 1009–1027. doi: 10.1080/00288330.2009.9626525

Ross, P. M., Hogg, I. D., Pilditch, C. A., Lundquist, C. J., and Wilkins, R. J. (2012). Population genetic structure of the New Zealand estuarine clam *Austrovenus stutchburyi* (Bivalvia: Veneridae) reveals population subdivision and partial congruence with biogeographic boundaries. *Estuar. Coast.* 35, 143–154. doi: 10.1007/s12237-011-9429-z

Rousset, F. (2008). GENEPOP'007: a complete re-implementation of the genepop software for Windows and Linux. *Mol. Ecol. Resour.* 8, 103–106. doi: 10.1111/j.1471-8286.2007.01931.x

Shan, T., Li, Q., Wang, X., Su, L., and Pang, S. (2019). Assessment of the genetic connectivity between farmed populations on a typical kelp farm and adjacent spontaneous populations of *Saccharina japonica* (Phaeophyceae, Laminariales) in China. *Front. Mar. Sci.* 6:494. doi: 10.3389/fmars.2019.00494

Shears, N. T., and Babcock, R. C. (2007). *Quantitative Description Mainland New Zealand's Shallow Subtidal Reef Communities*. Wellington: Department of Conservation.

Shears, N. T., Smith, F., Babcock, R. C., Duffy, C. A. J., and Villouta, E. (2008). Evaluation of biogeographic classification schemes for conservation planning: application to New Zealand's coastal marine environment. *Conserv. Biol.* 22, 467–481. doi: 10.1111/j.1523-1739.2008.00882.x

Stevens, P. M. (1990). A genetic analysis of the pea crabs (Decapoda: Pinnotheridae) of New Zealand. I. Patterns of spatial and host-associated genetic structuring in Pinnotheres novaezelandiae Filhol. *J. Exp. Mar. Biol. Ecol.* 141, 195–212. doi: 10.1016/0022-0981(90)90224-Z

Team RStudio (2021). *RStudio: Integrated Development Environment for R*. Boston, MA: RStudio.

Trono, G. C., and Largo, D. B. (2019). The seaweed resources of the Philippines. *Bot. Mar.* 62, 483–498. doi: 10.1515/bot-2018-0069

Valero, M., Guillemin, M.-L., Destombe, C., Jacquemin, B., Gachon, C. M. M., Badis, Y., et al. (2017). Perspectives on domestication research for sustainable seaweed aquaculture. *Perspect. Phycol.* 4, 33–46. doi: 10.1127/pip/2017/0066

Veale, A. J., and Lavery, S. D. (2012). The population genetic structure of the waratah anemone (*Actinia tenebrosa*) around New Zealand. *New Zeal. J. Mar. Freshw. Res.* 46, 523–536. doi: 10.1080/00288330.2012.730053

Waples, R. S., and Anderson, E. C. (2017). Purging putative siblings from population genetic data sets: a cautionary view. *Mol. Ecol.* 26, 1211–1224. doi: 10.1111/mec.14022

Wernberg, T., Coleman, M. A., Babcock, R. C., Bell, S. Y., Bolton, J. J., Connell, S. D., et al. (2019). Biology and ecology of the globally significant kelp *Ecklonia radiata*. *Oceanogr. Mar. Biol.* 57, 265–324. doi: 10.1201/9780429026379-6

Wernberg, T., Coleman, M. A., Bennett, S., Thomsen, M. S., Tuya, F., and Kelaher, B. P. (2018). Genetic diversity and kelp forest vulnerability to climatic stress. *Sci. Rep.* 8:1851 . doi: 10.1038/s41598-018-20009-9

White, L. N., and White, W. L. (2020). Seaweed utilisation in New Zealand. *Bot. Mar.* 63, 303–313. doi: 10.1515/bot-2019-0089

Wickham, H. (2016). *ggplot2: Elegant Graphics for Data Analysis*. New York, NY: Springer-Verlag.

Zhang, J. (2018). *Seaweed Industry in China*. Beijing: Innovation Norway.

Zhang, J., Wang, X., Yao, J., Li, Q., Liu, F., Yotsukura, N., et al. (2017). Effect of domestication on the genetic diversity and structure of Saccharina japonica populations in China. *Sci. Rep.* 7:42158. doi: 10.1038/srep42158

Conflict of Interest: The authors declare that the research was conducted in the absence of any commercial or financial relationships that could be construed as a potential conflict of interest.

Publisher's Note: All claims expressed in this article are solely those of the authors and do not necessarily represent those of their affiliated organizations, or those of the publisher, the editors and the reviewers. Any product that may be evaluated in this article, or claim that may be made by its manufacturer, is not guaranteed or endorsed by the publisher.

Journal of Applied Phycology
https://doi.org/10.1007/s10811-023-02969-2

RESEARCH

High spatial and temporal variation in biomass composition of the novel aquaculture target *Ecklonia radiata*

Jacob Nepper-Davidsen[1,2] · Christopher R. K. Glasson[1,2] · Rebecca J. Lawton[1,2] · Marie Magnusson[1,2]

Received: 6 December 2022 / Revised: 28 March 2023 / Accepted: 1 April 2023

Abstract

The biomass composition of kelp varies within species both spatially and temporally. However, this variation in biomass quality has not yet been investigated for the native kelp *Ecklonia radiata* within New Zealand, where the kelp is a target for the emerging seaweed aquaculture industry. In this study we quantified spatial and temporal variation in the composition of *E. radiata* biomass, collected from 12 sites around the North Island of New Zealand and from 12 months across a full year at a single site ($n = 138$). High spatial variation was detected for most components, including alginate (range: 16.6 – 22.7% DW, $n = 12$), fucoidan (range: 1.2 – 1.6% DW, $n = 12$), phlorotannins (range: 4.8 – 9.3% DW, $n = 72$), and glucose (range: 9.3 – 22.6% DW, $n = 12$). The biomass composition of *E. radiata* varied significantly among sites but with no clear patterns among regions, indicating that geographic differences were mostly local rather than regional, possibly due to site-specific environmental conditions. Significant temporal variation (measured by positive autocorrelation between months) was detected in the content of lipids, proteins, glucose, guluronic acid, nitrogen, phosphorous, iodine, arsenic, and mercury, and for the mannuronic to guluronic acid (M:G) ratio. Overall, *E. radiata* had comparable biomass composition to that of commercially grown northern hemisphere species but with substantially higher phlorotannin content. These results demonstrate that *E. radiata* could be a viable southern hemisphere alternative for a broad range of commercial applications.

Keywords Kelp · Seaweed · Phaeophyceae · Biochemistry · Polysaccharides · Phlorotannins · New Zealand

Introduction

The native kelp *Ecklonia radiata* (C.Ag.) J. Agardh is a target species for the emerging seaweed aquaculture industry in both New Zealand and Australia, with broad distribution across New Zealand (Shears and Babcock 2007) and along the temperate and subtropical coasts of Australia (Wernberg et al. 2019). Recent development of hatchery cultivation protocols (Praeger et al. 2022) has facilitated ocean farming trials in New Zealand and fuelled further interest in the aquaculture of this species. The biomass of *E. radiata* contains a range of biomolecules of commercial interest unique to brown seaweed including 1) alginate, a gelling polysaccharide (hydrocolloid) used in food products, pharmaceuticals, textile printing, and cosmetics (Porse and Rudolph 2017), 2) fucoidan, a bioactive sulfated polysaccharide used in nutraceutical and personal health products (Mak et al. 2013; Hsu and Hwang 2019) and, 3) phlorotannins, a group of bioactive phenolic compounds with potential uses in nutraceuticals, cosmetics, and novel biomaterials (Magnusson et al. 2017; Shrestha et al. 2021). Furthermore, *E. radiata* biomass contains laminarin, a storage polysaccharide important for producing fermented commodities such as biostimulants, plant tonics, and food products (Battacharyya et al. 2015), which is currently the biggest market for kelp biomass in New Zealand (Bradly et al. 2021). Other biomass components include proteins, lipids, and minerals which contribute to the nutritional value and suitability of the seaweed biomass for human consumption—a market that accounts for approximately 1/3 of the total value of the global seaweed industry (FAO 2021). Consequently, the commercial value and application of *E. radiata* will depend largely on biomass composition.

The biomass composition of seaweeds varies within species both spatially, due to genotypic variation and differences

✉ Jacob Nepper-Davidsen
Jn100@students.waikato.ac.nz

[1] Coastal Marine Field Station, School of Science, University of Waikato, Tauranga, New Zealand

[2] Environmental Research Institute, The University of Waikato, Tauranga, New Zealand

Published online: 28 April 2023

in environmental conditions between locations, and temporally, due to variation in environmental conditions between seasons (Gosch et al. 2015; Manns et al. 2017; Mata et al. 2017). For instance, spatial variation in phlorotannin content may be correlated to genotypic differences (Honkanen and Jormalainen 2005) and changes in environmental conditions such as salinity, nutrient availability, and herbivory pressure (Targett and Arnold 1998). Similarly, spatial variation in lipid content was linked to genotypic differences in light and nitrogen availability (Gosch et al. 2015), while spatial variation in alginate content may be corelated to wave exposure (Munda 1987; McHugh 2003). Overall, temporal changes in temperature have been identified as a main driver for temporal variation in carbohydrate and mineral content in kelp (compared to salinity and nutrient availability; Manns et al. 2017).

To date, spatial variation in the biomass composition of *E. radiata* in New Zealand has not been investigated. The large environmental variability within the North Island of New Zealand, such as differences in water temperature between north and south (14—21 °C summer temperature; Wijffels et al. 2018) and local differences in nutrient availability from runoff (20-fold differences in nitrate levels between estuarine systems; Plew et al. 2018), may cause morphological and biochemical variation in *E. radiata* (Targett and Arnold 1998; Fowler-Walker et al. 2006; Manns et al. 2017). Furthermore, *E. radiata* shows strong genetic structure and low gene flow within New Zealand (Nepper-Davidsen et al. 2021), potentially resulting in spatial variation in biomass composition between genetically distinct sub-populations (Honkanen and Jormalainen 2005; Gosch et al. 2015). This environmental and genetic differentiation between sites and regions is therefore likely to result in significant spatial differences in the biomass composition of *E. radiata* within New Zealand.

Temporal variation in biomass composition of *E. radiata* in New Zealand has also never been studied. Temporal studies of the alginate content of *E. radiata* from Australia show inconsistent results, with either the highest content found in austral spring and the lowest in austral autumn in the state of Victoria (Stewart et al. 1961) or the lowest content found in austral spring and the highest in austral winter in the state of South Australia (Lorbeer et al. 2017). Additionally, previous studies on temporal variation in the biomass composition of *E. radiata* were conducted with low temporal resolution (e.g. Stewart et al. 1961; Lorbeer et al. 2017) but indicated that location may be a key driver for variation in biomass composition and that temporal patterns may vary between locations (Jennings and Steinberg 1994). These inconsistencies in temporal patterns and the low temporal resolution of previous studies makes it difficult to draw any general conclusions about patterns of temporal variation in biomass composition for *E. radiata* and highlight the need for detailed studies in New Zealand to be undertaken to inform the emerging seaweed aquaculture industry.

The aim of this research was therefore to analyse spatial and temporal changes in the biomass composition of *E. radiata* within the North Island of New Zealand. Specifically, we wanted to assess 1) the spatial and temporal changes in proximate composition (carbohydrates, proteins, lipids and minerals) and specific key components (alginate, fucoidan, laminarin, and phlorotannins), 2) whether spatial changes are local and/or regional, and 3) any relationships between biomass composition and morphology.

Materials & methods

Sample collections

Two groups of *Ecklonia radiata* samples were collected – one spatial and one temporal. For the spatial samples, six whole adult specimens (Stage 3, Kirkman 1984) were collected on a single occasion at 12 different sites within four regions of the North Island of New Zealand, ranging from sub-tropical (Northland region) to temperate (Wellington region) climate (Fig. 1). The spatial samples were collected over a 14 week period from October 2019 to January 2020 (except for the Moutohora Island samples which were collected in March 2020) to minimise temporal variability. For

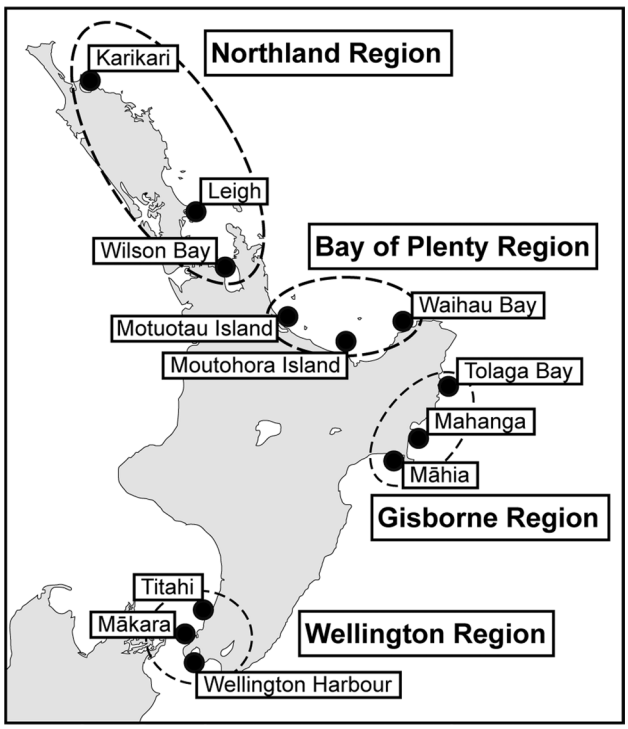

Fig. 1 Sampling sites and sampling regions within the North Island of New Zealand

the temporal samples, another six whole adult specimens were collected once every month on 12 occasions during a full year cycle from November 2019 to November 2020 at Motuotau Island in Tauranga (Covid-19 lockdown prevented sampling in April 2020). Samples were collected haphazardly by cutting with a knife just above the holdfast (i.e., samples included thallus and stipe, but no holdfast) while snorkelling on rocky reefs within 2–6 m depth and with > 2 m between each sampled individual. A total of 138 samples (replicated samples) were collected (spatial samples mean weight: 80.7 ± 42.5 SD g dry weight (DW), $n = 72$; temporal samples mean weight: 80.4 ± 39.2 SD g DW, $n = 72$) with the 6 samples collected at Motuotau Island in November 2019 included in both sample groups. Morphology of the stipe, primary lamina, and blades of each specimen were measured in the field after collection (Online resource 1). Samples were stored in separate polyethylene sealable bags and immediately placed on ice for transport back to the laboratory (maximum 48 h). Samples were rinsed in seawater at the collection sites or in 5 µm filtered seawater immediately upon return to the laboratory to remove epiphytes and debris, then weighed (wet weight, WW) and frozen at -20 °C. Samples were freeze-dried to dryness (Buchi, Lyovapor, L-200, Switzerland; 2 mbar, -50 °C), then weighed (DW), milled to < 0.5 mm fine particles (Pulverisette 15 cutting mill, Fritsch GmbH, Germany), and stored in double polyethylene sealable bags with silica gel until further processing. Twenty-four homogenised samples were made by combining subsamples (2.0 g DW) from each of the six samples collected at each site to give 12 spatial samples (one for each site), and from each of the six samples collected each month to give 12 monthly samples (Fig. 2). Mean moisture content following freeze drying was 1.0 ± 0.2 SD % DW for all replicated and homogenised samples ($n = 162$).

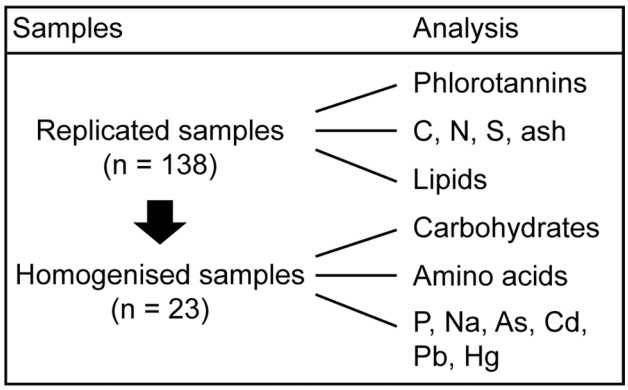

Fig. 2 Overview of analyses of biomass components for replicated and homogenised samples. Homogenised samples were made from 2 g DW of each replicated sample, combining the six samples collected at each site and each sampling month

Constituent sugar content

Constituent sugars analysis was adapted and improved from Rozaklis et al. (2002) and Lorbeer et al. (2015). Dried milled biomass samples (10–11 mg weighed to 0.1 mg precision) were hydrolysed in 13 M sulfuric acid (300 µL) for 60 min with stirring, and then diluted with H_2O (3.6 mL) to 1 M sulfuric acid and heated at 100 °C for an additional 3 h. Following neutralisation with 2 M NaOH (100 µL), hydrolysed samples (100 µL), with added 2-deoxy-D-glucose (40 µL of 10 mg mL^{-1}) as internal standard, were derivatised by addition of PMP-derivatising regent (400 µL of 250 mM 1-phenyl-3-methyl-5-pyrazolone with 400 mM NH_3) and heating at 70 °C over 90 min with constant stirring. This solution was then neutralisation with 0.8 M formic acid (400 µL) and extracted with $CHCl_3$ (750 µL) to remove excess PMP. Finally, the supernatant was centrifuged (5 min at 13,000 rpm) and transferred to a 2 mL Shimadzu HPLC vial (Product #: 226–50,512-00) for analysis. Derivatised monosaccharides were quantified using a Shimadzu Prominence LC-20AD (Japan) fitted with a Restek Raptor ARC-18 column (5 µm particle size, 5 µm, 150 × 4.6 mm, Catalogue #: 9,314,565) with an oven temperature of 30 °C and flow rate of 0.8 mL min^{-1}. Derivatised monosaccharides were separated after injection of 5 µL of sample by a isocratic/gradient elution with solvent A (0.1 M phosphate buffer at pH 7 in 10% acetonitrile) and solvent B (0.1 M phosphate buffer at pH 7 in 17% acetonitrile); 25% solvent B for 15 min, linear increase from 25 to 100% solvent B over 25 min, 100% solvent B for 15 min, and finally 25% solvent B for 5 min. Derivatised monosaccharides were detected at 254 nm using a photo diode-array detector. The sugars (D-glucose, L-guluronic acid, D-mannuronic acid, L-fucose, D-mannose, D-galactose, D-xylose, L-rhamnose, D-glucuronic acid, and L-arabinose) were identified from their relative retention times compared to the internal standard and quantified using response calibration curves generated from sugar standards with concentrations in the range of 0.01 – 1.0 mg mL^{-1}. The % DW and normalised mol % of each anhydro-sugar (as this is the form of sugar present in a polysaccharide) was presented. Total carbohydrates (% DW) were also calculated by deducting the percentages of lipid, protein, phlorotannin, and ash content from 100%.

Phlorotannin content

Phlorotannin content was estimated as total phenols (Shrestha et al. 2021) which was measured using the Folin-Ciocalteu phenol reagent method (Zhang et al. 2006) adjusted by diluting the extracts to 50% concentration prior to the reaction and by incubating the reactants at 40 °C for 30 min at 100 rpm prior to absorbance reading at 750 nm

(SPECTROstar Nano, BMG Labtech, Germany). Phloroglucinol was used as a reference standard, and the results were expressed as phloroglucinol equivalents (PGE, % of DW).

Amino acid content

Amino acid content was commercially analysed by the Australian Proteome Analysis Facility (Sydney, Australia; anhydro-amino acids) as described in Angell et al. (2014) and included all essential amino acids except cysteine (usually a minor constituent). Protein content was estimated as the sum of the 16 quantified amino acids (Angell et al. 2016) and a nitrogen to protein conversion factor was calculated from the nitrogen and protein content (Protein:N = Protein % DW / N % DW).

Ash and mineral content

Elemental analysis of carbon, hydrogen, nitrogen, and sulfur (CHNS), iodine, and content of ash were determined commercially by OEA labs Ltd (Exeter, UK). Contents of CHNS were determined by gas chromatography coupled to a thermal conductivity detector (GC-TCD), while contents of iodine were determined using ion chromatography (IC) following hydropyrolysis combustion. Content of ash was determined by micro-ashing (Prometheus Kilns Pro1-PRG, Turkey). Further element analysis of phosphorous, potassium, arsenic, cadmium, lead, and mercury (and other minerals: see Online resources 2 and 3) was analysed commercially at the University of Waikato Laboratory (Hamilton, New Zealand) by inductively coupled plasma (ICP) – mass spectroscopy (MS) on homogenised samples (n = 24).

Lipid content

Lipid content was quantified following Folch et al. (1957), as modified and described in Gosch et al. (2012), using dichloromethane and methanol solution at 60 °C for 1 h for extraction, followed by microfiltration of the extract, and addition of 20% (v/v) of a 0.9% sodium chloride solution to separate the lipid fraction. Finally, the solvent was removed from the lipid fraction by heating at 40 °C in a heating block and the weight of the residue was recorded.

Statistical analysis

Statistical analyses were carried out in R-Studio (Team RStudio 2022) and PRIMER 7 (Clarke and Gorley 2015), and legibility of figures was improved in Adobe Illustrator. Significance of temporal patterns (November 2019 to November 2020) was analysed using Durbin-Watson's test (lmtest package in R-Studio) which returns a d-value from 0 to 4 where values of 0 to 2 indicate positive autocorrelation, values of 2 indicate no autocorrelation, and values of 2 to 4 indicate negative autocorrelation. Significance of spatial variation was analysed using permutational multivariate analysis of variance (PERMANOVA; as assumptions for analysis of variance (ANOVA) were not generally met) in PRIMER 7 and was calculated for all biomass components measured with replication (i.e. not components quantified from homogenised samples). A nested PERMANOVA design was chosen, testing for differences among regions (fixed factor) and sites nested within regions (random factor), and analyses were run with individual models for each biomass component, using Euclidian distance as distance measurement, and 9,999 unrestricted permutations of raw data. Some significant differences in dispersion were detected among sites and regions using test of homogeneity of dispersion (PERMDISP), however in many cases such differences will not significantly inflate the error rates of PERMANOVA (Anderson et al. 2016). Relationships between morphology and biomass composition were analysed using Pearson correlation coefficients and linear regression models in R-Studio, and correlations were visualised using the ggcorrplot package. Analysis of equal variance between spatial and temporal samples were calculated with Levene's test (car package in R-studio) using the mean value for each site and each monthly sample. Non-metric MDS was carried out in PRIMER 7 to assess overall patterns in biomass composition among sites within regions and among monthly samples. Data was square root transformed and normalised, and Euclidian distance was used as distance measurement, with 100 restarts and 1 Kruskal fit scheme for each plot.

Results

Spatial variation

High levels of spatial variation between sites were found for most quantified components of *E. radiata* biomass (Table 1). Significant differences between sites were found for all biomass components measured with replication, including total carbohydrates (range: 58.0 – 71.8% DW, n = 72), phlorotannins (range: 4.8 – 9.3% DW, n = 72), ash (range: 16.2 – 25.1% DW, n = 72), nitrogen (range: 0.9 – 1.6% DW, n = 72), and sulfur (range: 0.6 – 1.1% DW, n = 72; Table 2). Among biomass components not measured with replication (i.e. spatial homogenised samples, n = 12; no statistical analysis), glucose content was highly variable among sites (range: 9.3 – 22.6% DW, n = 12), whereas guluronic acid (range: 9.0—12.2% DW, n = 12), mannuronic acid (range: 7.6 – 10.8% DW, n = 12), fucose (range: 1.2 – 1.6% DW, n = 12), and the mannuronic to guluronic ratio (M:G ratio, range: 0.75 – 0.99, n = 12) were more stable (Fig. 3a). Concentrations of mannose,

Table 1 Spatial variation in biomass content of *E. radiata* collected at 12 sites across the North Island of New Zealand with SD shown in brackets ($n=72$ for components measured with replication and $n=12$ for other components). Total carbohydrates (Carbs), phlorotannins (Phlo), proteins, ash, lipids, glucose (Glc), guluronic acid (GulA), mannuronic acid (ManA), fucose (Fuc), mannose (Man), galactose (Gal), xylose (Xyl), nitrogen (N), phosphorus (P), potassium (K), sulfur (S), and iodine (I) are shown as % DW. Arsenic (As), cadmium (Cd), lead (Pb), and mercury (Hg) are shown as ppm DW. M:G shows the mannuronic to guluronic acid ratio, Protein:N shows the nitrogen to protein conversion factor, and C:N shows the carbon to nitrogen ratio. Site abbreviations are: Karikari (Kari), Leigh (Leig), Wilson Bay (Wils), Motuotau Island (Motu), Moutohora Island (Mout), Waihau Bay (Waih), Tolaga Bay (Tola), Mahanga (Maha), Māhia (Māhi), Wellington Harbour (WH), Mākara Beach (Māka), and Titahi Bay (Tita)

	Kari	Leig	Wils	Motu	Mout	Waih	Tola	Māha	Mahi	WH	Māka	Tita	Mean
Carbs $_{(\%)}$	60.4 (3.4)	58.6 (2.7)	63.2 (1.5)	58 (2.6)	66.5 (4.0)	67.3 (3.1)	71.5 (2.6)	63.2 (1.5)	71.2 (2.2)	61.5 (3.1)	63.6 (1.5)	71.8 (1.6)	64.7 (4.9)
Phlo $_{(\%)}$	9.3 (1.8)	9.1 (1.3)	6.0 (0.7)	8.0 (2.3)	6.3 (0.6)	6.2 (1)	6.0 (1.0)	8.0 (1.4)	5.0 (0.6)	4.8 (0.9)	5.8 (0.8)	5.0 (1.0)	6.6 (1.6)
Protein $_{(\%)}$	6.8	6.6	5.3	8.6	5.6	5.2	4.6	6.1	5.5	7.8	6.4	5.2	6.1 (1.2)
Ash $_{(\%)}$	22.8 (2.9)	25.1 (1.9)	25 (1.9)	24.7 (2.6)	21.5 (3.7)	21 (2.7)	16.2 (1.3)	21.2 (2.7)	16.6 (1.7)	24.4 (3.2)	23.4 (1.6)	17.5 (1.6)	21.6 (3.3)
Lipids $_{(\%)}$	0.7 (0.3)	0.6 (0.3)	0.4 (0.2)	0.7 (0.3)	0.1 (0.1)	0.4 (0.1)	1.7 (0.2)	1.6 (0.1)	1.7 (0.3)	1.4 (0.6)	0.9 (0.4)	0.5 (0.2)	0.9 (0.6)
Glc $_{(\%)}$	11.8	9.5	9.8	9.3	15.3	13.5	22.6	10.1	18.8	12.4	10.9	21.5	13.8 (4.5)
GulA $_{(\%)}$	9.0	9.6	10.5	11.4	11.8	9.6	9.5	11.7	9.4	12.2	12.0	9.8	10.5 (1.1)
ManA $_{(\%)}$	7.6	8.9	10.4	8.9	8.9	9.0	8.5	10.8	9.4	10.0	10.7	9.1	9.4 (0.9)
Fuc $_{(\%)}$	1.4	1.6	1.3	1.4	1.3	1.3	1.2	1.3	1.5	1.5	1.3	1.2	1.4 (0.1)
Man $_{(\%)}$	0.7	0.8	0.8	0.8	0.8	0.8	0.7	0.9	0.8	0.8	0.9	0.7	0.8 (0.1)
Gal $_{(\%)}$	0.6	0.7	0.6	0.6	0.6	0.5	0.6	0.6	0.6	0.7	0.6	0.5	0.6 (0.1)
Xyl $_{(\%)}$	0.3	0.3	0.3	0.3	0.3	0.3	0.3	0.3	0.3	0.3	0.3	0.3	0.3 (0.0)
M:G	0.84	0.93	0.99	0.79	0.75	0.93	0.89	0.93	0.99	0.82	0.89	0.92	0.89 (0.07)
N $_{(\%)}$	1.4 (0.1)	1.3 (0.1)	1 (0.0)	1.6 (0.1)	1.1 (0.1)	1.1 (0.1)	0.9 (0.1)	1.1 (0.1)	1.1 (0.1)	1.5 (0.1)	1.3 (0.0)	1 (0.1)	1.2 (0.2)
P $_{(\%)}$	0.11	0.12	0.17	0.15	0.09	0.11	0.11	0.10	0.11	0.19	0.13	0.13	0.13 (0.03)
K $_{(\%)}$	3.3	3.7	3.9	4.0	3.2	2.8	2.2	3.2	2.4	3.8	3.7	2.5	3.2 (0.6)
S $_{(\%)}$	1.0 (0.1)	1.1 (0.1)	0.7 (0.0)	1.0 (0.1)	0.9 (0.1)	0.8 (0.1)	0.7 (0.1)	0.9 (0.0)	0.7 (0.1)	0.9 (0.1)	0.8 (0.1)	0.6 (0.1)	0.8 (0.1)
Protein:N	4.9	4.9	5.1	5.3	5.1	4.9	5.3	5.5	5.2	5.1	4.9	5.0	5.1 (0.2)
C:N	23.4	23.7	29.5	19.4	29.1	30.4	39.8	29.4	32.3	20.4	24.3	32.8	27.9 (5.9)
I $_{(\%)}$	0.34	0.38	0.40	0.48	0.55	0.44	0.60	0.61	0.46	0.73	0.57	0.66	0.52 (0.12)
As $_{(ppm)}$	50.8	64.4	43.2	54.8	63.5	40.0	40.1	46.4	48.9	48.1	43.2	44.7	49 (8.2)
Cd $_{(ppm)}$	1.3	2.2	0.5	1.9	1.5	0.8	0.8	1.5	1.3	1.2	1.4	0.4	1.2 (0.6)
Pb $_{(ppm)}$	0.3	0.1	0.3	0.2	0.0	0.2	0.7	0.4	0.3	0.5	0.1	0.1	0.3 (0.2)
Hg $_{(ppm)}$	0.00	0.00	0.04	0.02	0.03	0.01	0.03	0.02	0.03	0.01	0.01	0.01	0.02 (0.01)

Table 2 Permutational multivariate analysis of variance (PERMANOVA) between spatial samples of *E. radiata* ($n = 72$), testing for differences among regions and sites nested within regions for biomass components measured with replication. Significant differences in dispersion among sites and regions are marked with an asterisk and significant *p*-values are italicised

Source	df	SS	MS	Pseudo-F	P(perm)
Total carbs					
Regions	3	590.4	196.8	1.5	0.282
Sites (nested)	8	1018.4	127.3	18.8	*< 0.001*
Res	60	406.8	6.8		
Total	71	2015.5			
Phlorotannins					
Regions	3	75.7	25.2	2.3	0.132
Sites (nested)	8	87.4	10.9	6.1	*< 0.001*
Res	60	108.2	1.8		
Total	71	271.3			
Ash					
Regions	3	379.3	126.4	3.1	0.090
Sites (nested)	8	329.2	41.2	5.9	*< 0.001*
Res	60	421.2	7.0		
Total	71	1129.7			
Lipids					
Regions	3	16.0	5.3	10.3	*0.007*
Sites (nested)	8	4.2	0.5	5.3	*< 0.001*
Res	60	5.8	0.1		
Total	71	26.0			
Nitrogen					
Regions	3	0.9	0.3	1.0	0.465
Sites (nested)	8	2.6	0.3	32.8	*< 0.001*
Res	60	0.6	0.0		
Total	71	4.1			
Sulfur					
Regions	3	0.4	0.1	1.7	0.257
Sites (nested)	8	0.7	0.1	10.1	*< 0.001*
Res	60	0.5	0.0		
Total	71	1.5			

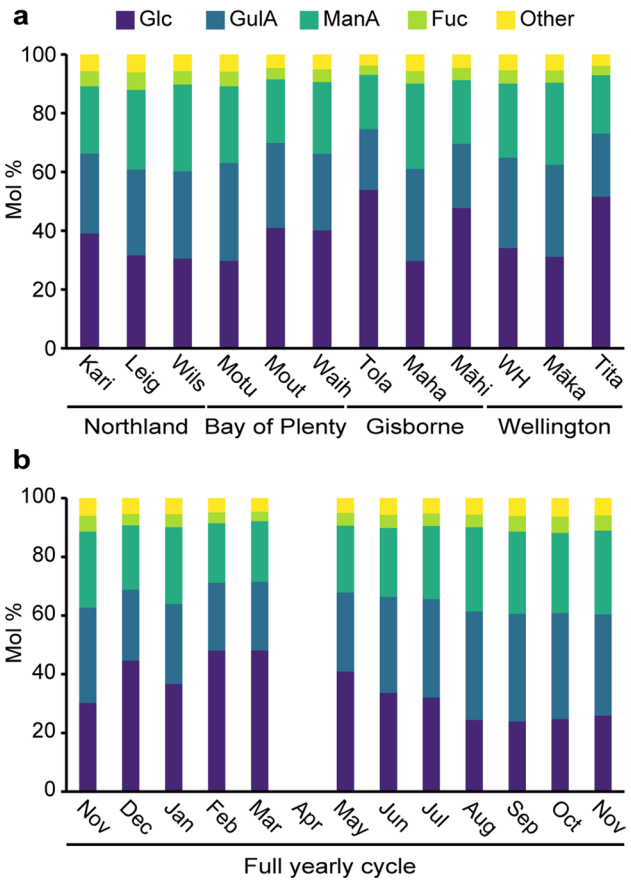

Fig. 3 Mole percent (mol %) of quantified sugars: glucose (Glu), guluronic acid (GulA), mannuronic acid (ManA), fucose (Fuc), and other sugars (mannose, galactose, and xylose) of (a) spatial homogenised samples among sites ($n = 12$) and (b) monthly homogenised samples at Motuotau Island ($n = 12$). Site abbreviations are: Karikari (Kari), Leigh (Leig), Wilson Bay (Wils), Motuotau Island (Motu), Moutohora Island (Mout), Waihau Bay (Waih), Tolaga Bay (Tola), Mahanga (Maha), Māhia (Māhi), Wellington Harbour (WH), Mākara Beach (Māka), and Titahi Bay (Tita)

galactose and xylose were generally low (combined range: 0.3—0.9% DW, $n = 36$), while rhamnose, glucuronic acid, and arabinose were also identified but at concentrations too low for consistent quantification. Proteins also varied substantially (range: 4.6—8.6% DW, $n = 12$), with aspartic acid and glutamic acid being the most variable amino acids, varying two-fold among sites (range: 0.7 -1.2 and 0.8 – 1.7% DW, respectively, $n = 12$; Table 3). Among minerals, a two-fold difference was detected for phosphorous (range: 0.09 – 0.19% DW, $n = 12$) and potassium (range: 2.2 – 4.0% DW, $n = 12$). Non-metric MDS showed limited spatial clustering among sites within regions (Fig. 4a), and similarly, PERMANOVA showed no significant difference between regions (except for lipids; Table 2).

Temporal variation

There were significant temporal patterns in the content of glucose, guluronic acid, proteins, nitrogen, lipids, phosphorous, iodine, arsenic, and mercury, and for the M:G ratio (Tables 4 and 5). The two main sugars, glucose (range: 7.7 – 18.2% DW, $n = 12$) and guluronic acid (range: 8.8 – 13.7% DW, $n = 12$), showed an inverse relationship where guluronic acid peaked in austral spring but was low during austral summer/autumn and glucose peaked in early austral autumn but was low during austral spring (Fig. 3b). The M:G ratio (range: 0.72 – 0.96, $n = 12$) varied with the content of guluronic acid, with the highest in austral summer and lowest in austral winter. Proteins (range: 5.6 – 7.6% DW, $n = 12$) and lipids (range: 0.1—1.6% DW, $n = 72$) showed a unimodal relationship with highest content in late austral spring/early summer and lowest content in austral autumn/winter.

Table 3 Amino acids as % DW among spatial samples (all sites, homogenised samples, $n = 12$, top panel) and temporal samples (Motuotau Island only, homogenised samples, $n = 12$, lower panel). Amino acid abbreviations are: histidine (His), serine (Ser), arginine (Arg), glycine (Gly), aspartic acid (Asp), glutamic acid (Glu), threonine (Thr), alanine (Ala), proline (Pro), lysine (Lys), tyrosine (Tyr), methionine (Met), valine (Val), isoleucine (Ile), leucine (Leu), and phenylalanine (Phe). Site abbreviations are: Karikari (Kari), Leigh (Leig), Wilson Bay (Wils), Motuotau Island (Motu), Moutohora Island (Mout), Waihau Bay (Waih), Tolaga Bay (Tola), Mahanga (Maha), Māhia (Māhi), Wellington Harbour (WH), Mākara Beach (Māka), and Titahi Bay (Tita)

	Kari	Leig	Wils	Motu	Mout	Waih	Tola	Maha	Māhi	WH	Māka	Tita	mean (SD)
His	0.14	0.15	0.13	0.18	0.11	0.12	0.11	0.13	0.12	0.17	0.14	0.12	0.13 (0.02)
Ser	0.32	0.33	0.27	0.39	0.26	0.26	0.22	0.29	0.25	0.38	0.31	0.25	0.29 (0.05)
Arg	0.30	0.31	0.25	0.38	0.22	0.23	0.20	0.26	0.23	0.35	0.27	0.23	0.27 (0.05)
Gly	0.35	0.35	0.28	0.41	0.26	0.27	0.23	0.30	0.26	0.40	0.31	0.26	0.31 (0.06)
Asp	0.98	0.93	0.78	1.17	0.81	0.79	0.67	0.95	0.77	1.15	0.97	0.77	0.89 (0.15)
Glu	1.22	1.16	0.81	1.75	1.23	0.84	0.85	1.06	1.14	1.28	1.10	0.89	1.11 (0.25)
Thr	0.35	0.35	0.29	0.45	0.30	0.30	0.25	0.33	0.28	0.44	0.36	0.28	0.33 (0.06)
Ala	0.65	0.58	0.46	0.81	0.49	0.40	0.37	0.49	0.48	0.65	0.55	0.43	0.53 (0.12)
Pro	0.31	0.31	0.25	0.39	0.25	0.25	0.21	0.28	0.23	0.37	0.30	0.24	0.28 (0.05)
Lys	0.38	0.37	0.30	0.47	0.29	0.30	0.26	0.36	0.29	0.48	0.39	0.30	0.35 (0.07)
Tyr	0.14	0.13	0.12	0.18	0.11	0.12	0.11	0.13	0.12	0.20	0.15	0.12	0.13 (0.03)
Met	0.16	0.17	0.14	0.20	0.12	0.13	0.11	0.14	0.13	0.19	0.15	0.13	0.15 (0.03)
Val	0.39	0.39	0.32	0.48	0.30	0.32	0.27	0.36	0.30	0.47	0.37	0.31	0.36 (0.06)
Ile	0.29	0.29	0.24	0.35	0.22	0.22	0.19	0.25	0.22	0.34	0.27	0.22	0.26 (0.05)
Leu	0.49	0.50	0.41	0.60	0.36	0.38	0.34	0.44	0.38	0.57	0.45	0.38	0.44 (0.08)
Phe	0.33	0.33	0.27	0.39	0.24	0.26	0.23	0.30	0.26	0.39	0.31	0.26	0.30 (0.05)
	Nov	Dec	Jan	Feb	Mar	May	Jun	Jul	Aug	Sep	Oct	Nov	mean (SD)
His	0.14	0.15	0.14	0.12	0.11	0.11	0.12	0.12	0.12	0.13	0.15	0.15	0.13 (0.01)
Ser	0.34	0.34	0.34	0.28	0.25	0.27	0.30	0.29	0.32	0.33	0.36	0.35	0.32 (0.03)
Arg	0.32	0.32	0.31	0.24	0.22	0.22	0.25	0.23	0.26	0.27	0.32	0.32	0.27 (0.04)
Gly	0.36	0.36	0.35	0.28	0.26	0.28	0.31	0.29	0.32	0.33	0.37	0.36	0.32 (0.04)
Asp	1.01	1.00	0.98	0.80	0.75	0.80	0.90	0.91	0.97	1.01	1.04	1.00	0.93 (0.10)
Glu	1.53	1.71	1.65	1.57	1.32	1.13	1.08	1.23	1.10	1.04	1.14	1.10	1.30 (0.24)
Thr	0.40	0.38	0.38	0.32	0.29	0.31	0.35	0.35	0.38	0.39	0.41	0.39	0.36 (0.04)
Ala	0.71	0.74	0.70	0.61	0.51	0.50	0.50	0.52	0.49	0.52	0.61	0.56	0.58 (0.09)
Pro	0.34	0.34	0.34	0.28	0.26	0.27	0.30	0.29	0.32	0.33	0.35	0.34	0.31 (0.03)
Lys	0.41	0.41	0.40	0.32	0.29	0.30	0.34	0.33	0.35	0.36	0.40	0.41	0.36 (0.04)
Tyr	0.16	0.15	0.15	0.12	0.10	0.11	0.13	0.13	0.14	0.14	0.16	0.14	0.14 (0.02)
Met	0.17	0.17	0.17	0.13	0.12	0.12	0.13	0.13	0.14	0.14	0.17	0.17	0.14 (0.02)
Val	0.42	0.41	0.40	0.33	0.29	0.31	0.35	0.33	0.36	0.38	0.41	0.41	0.37 (0.04)
Ile	0.30	0.30	0.30	0.24	0.21	0.23	0.25	0.23	0.25	0.27	0.30	0.30	0.27 (0.03)
Leu	0.51	0.52	0.51	0.40	0.36	0.38	0.42	0.40	0.44	0.45	0.52	0.51	0.45 (0.06)
Phe	0.34	0.34	0.34	0.27	0.24	0.26	0.29	0.27	0.30	0.31	0.35	0.34	0.30 (0.04)

Among amino acids, glutamic acid and aspartic acid (range: 1.0 – 1.7% DW and 0.7—1.0% DW, respectively, $n = 12$) were most abundant and accounted for more than 30% of total amino acids on average across a full year (Table 3). The content of nitrogen (range: 1.2 – 1.6% DW, $n = 72$) and phosphorous (range: 0.08 – 0.14% DW, $n = 12$) followed a similar pattern, both being higher in late austral spring/early summer and low in austral autumn/winter. Accordingly, the average nitrogen to protein conversion factor (Protein:N) across all sites and months was 4.9 ± 0.4 SD ($n = 23$), with no significant temporal pattern (Table 5). Iodine, arsenic, and mercury (range: 0.46 – 1.06% DW, 52.5 – 77.4 ppm DW, and 0.01 – 0.03 ppm DW, respectively, $n = 12$) also followed a unimodal pattern with highest content in late austral autumn/early winter and lowest content in late austral spring/early summer. Non-metric MDS showed a clear circular pattern among monthly samples demonstrating strong temporal correlation in biomass composition (Fig. 4b). No significant temporal variability was found for total carbohydrates, mannuronic acid, fucose, mannose, galactose, xylose, phlorotannins, ash, potassium, sulfur, cadmium, or lead (Table 5).

Spatial vs. temporal variation

The variation between spatial samples was significantly higher than the variation between temporal samples for sulfur, C:N ratio, lead, and mercury (Online resource 4). No other biomass components showed significant difference between spatial and temporal variation, although the standard deviations between sites were higher than the standard deviations between months for most components (Tables 1 and 4).

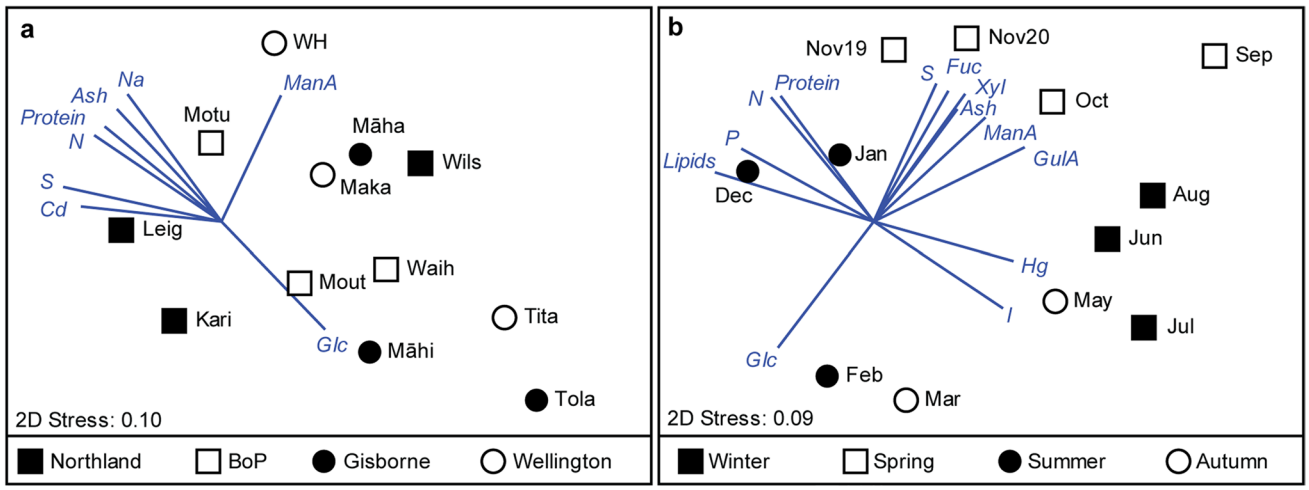

Fig. 4 Non-metric multi-dimensional scaling (MDS) of biomass composition of *E. radiata* using all 20 measured biomass components (**a**) among sites within regions ($n=12$) and (**b**) among monthly samples ($n=12$). Vectors are shown for biomass components showing > 0.8 correlation (Pearson correlation coefficient). Site and region abbreviations are: Bay of plenty (BoP), Karikari (Kari), Leigh (Leig), Wilson Bay (Wils), Motuotau Island (Motu), Moutohora Island (Mout), Waihau Bay (Waih), Tolaga Bay (Tola), Mahanga (Maha), Māhia (Māhi), Wellington Harbour (WH), Mākara Beach (Māka), and Titahi Bay (Tita). Component abbreviations are: glucose (Glc), guluronic acid (GulA), mannuronic acid (ManA), fucose (Fuc), xylose (Xyl), nitrogen (N), phosphorous (P), potassium (Na), sulfur (S), iodine (I), cadmium (Cd), and mercury (Hg)

Morphology

Seaweed size was significantly positively correlated with glucose content (linear regression: $F(1,21)=18.12$, $p<0.001$, $R^2=0.46$, $n=23$; Fig. 5) but significantly negatively correlated with guluronic acid, mannuronic acid, and fucose content (highest correlation: fucose; linear regression: $F(1,21)=11.01$, $p=0.003$, $R^2=0.34$, $n=23$). Phlorotannin content was significantly negatively correlated with lamina length (linear regression: $F(1,21)=15.13$, $p<0.001$, $R^2=0.42$, $n=23$). Furthermore, content of sulfur, iodine, and arsenic were all significantly positively correlated with stipe weight (highest correlation: arsenic; linear regression: $F(1,21)=25.49$, $p<0.001$, $R^2=0.55$, $n=23$), whereas phosphorus content was significantly positively correlated with blade length (linear regression: $F(1,21)=8.00$, $p=0.010$, $R^2=0.28$, $n=23$). Overall, solids to moisture ratio was high with low variation across replicated samples: 0.20 ± 0.002 SE DW/WW ($n=138$).

Discussion

Biomass composition of E. radiata

Ecklonia radiata contains a range of biomass components with commercial potential and may be marketed fresh for human consumption (e.g., Pacific Harvest, New Zealand), processed for extraction of specific components, or fermented for producing biostimulant plant tonics and food products (Battacharyya et al. 2015; Bradly et al. 2021; FAO 2022). In this regard, within the North Island of New Zealand, the major components of *E. radiata* included carbohydrates (mean: 62.4 ± 5.3 SD % DW, $n=23$), phlorotannins (7.5 ± 2.0 SD % DW, $n=138$), proteins (6.3 ± 0.9 SD % DW, $n=23$), and ash (mean: 23.1 ± 4.0 SD % DW, $n=138$), with minor contributions from lipids (0.8 ± 0.6 SD % DW, $n=138$).

Mannuronic and guluronic acid (syn. alginate; Szekalska et al. 2016) constituted the majority of the quantified sugars (combined mean: 53.6 ± 7.8 SD mol % of total sugars, equivalent to 20.0 ± 2.1 SD % DW, $n=23$) and was similar to the commercially cultivated northern hemisphere species *Saccharina latissima* and *Laminaria digitata* (Table 6). The M:G ratio of *E. radiata* was low (range: 0.72 – 1.00, $n=23$) compared to *E. radiata* from Australia (range: 1.18 – 1.59; Lorbeer et al. 2017) and compared to *S. latissima* and *L. digitata* (Table 6). Alginate with low M:G ratios (high in guluronic acid) forms stronger and more rigid gels, and our results therefore indicate high quality alginate in New Zealand *E. radiata* (McHugh 2003; Porse and Rudolph 2017). Fucose constituted a smaller fraction of the quantified sugars (mean: 4.4 ± 0.7 SD mol % of total sugars, equivalent to 1.3 ± 0.2 SD % DW, $n=23$), half of that in *S. latissima* and *L. digitata* (Table 6). Assuming a similar composition of fucoidan as in *Ecklonia maxima* (Sichert et al. 2020) the fucose content in *E. radiata* equates to up to 3.9% DW of fucoidan. The content of glucose (a component of laminarin; Stewart et al. 1961) in *E. radiata* biomass (range: 23.9 – 53.9 mol % of total sugars, equivalent to 7.7 – 22.6% DW,

Table 4 Temporal variation in biomass content of *E. radiata* collected monthly at Motuotau Island in New Zealand from November 2019 to November 2020 with SD shown in brackets ($n=72$ for components measured with replication and $n=12$ for other components). Total carbohydrates (Carbs), phlorotannins (Phlo), proteins, ash, lipids, glucose (Glc), guluronic acid (GulA), mannuronic acid (ManA), fucose (Fuc), mannose (Man), galactose (Gal), xylose (Xyl), nitrogen (N), phosphorus (P), potassium (K), sulfur (S), and iodine (I) are shown as % DW. Arsenic (As), cadmium (Cd), lead (Pb), and mercury (Hg) are shown as ppm DW. M:G shows the mannuronic to guluronic acid ratio, Protein:N shows the nitrogen to protein conversion factor, and C:N shows the carbon to nitrogen ratio

	Nov	Dec	Jan	Feb	Mar	May	Jun	Jul	Aug	Sep	Oct	Nov	Mean
Carbs $_{(\%)}$	59.3 (4.2)	58.2 (2.5)	57.5 (4.1)	63.6 (1.5)	63.7 (2.0)	62.8 (1.7)	58 (1.7)	60 (2.8)	60 (4.1)	59.5 (1.5)	58.6 (1.6)	53.8 (4.3)	59.7 (2.9)
Phlo $_{(\%)}$	7.9 (2.1)	9.3 (1.1)	8.8 (1.2)	8.5 (1.2)	9.3 (1.1)	8.1 (1.1)	9.0 (1.8)	7.8 (1.1)	8.5 (1.7)	7.6 (1.8)	7.6 (0.5)	9.5 (1.4)	8.5 (0.7)
Protein $_{(\%)}$	7.5	7.6	7.5	6.3	5.6	5.6	6.0	6.1	6.3	6.4	7.1	6.9	6.6 (0.7)
Ash $_{(\%)}$	23.7 (4.9)	23.4 (1.7)	25.1 (3.2)	20.8 (1.8)	20.8 (1.4)	23.2 (1.3)	26.7 (2.3)	25.9 (1.7)	24.9 (2.8)	26.4 (1.4)	26.1 (1.3)	29.0 (2.9)	24.7 (2.4)
Lipids $_{(\%)}$	1.6 (0.3)	1.5 (0.2)	1.1 (0.5)	0.8 (0.2)	0.5 (0.4)	0.3 (0.3)	0.3 (0.1)	0.2 (0.2)	0.3 (0.3)	0.1 (0.2)	0.6 (0.3)	0.8 (0.2)	0.7 (0.5)
Glc $_{(\%)}$	9.6	15.0	11.6	16.6	18.2	14.8	11.4	10.1	7.8	8.1	7.7	7.9	11.6 (3.6)
GulA $_{(\%)}$	11.3	8.9	9.4	8.8	9.7	10.7	12.2	11.5	13.0	13.7	12.3	11.6	11.1 (1.5)
ManA $_{(\%)}$	9.0	8.1	9.1	7.7	8.5	9.0	8.8	8.6	10.1	10.5	9.3	9.6	9.0 (0.8)
Fuc $_{(\%)}$	1.5	1.2	1.2	1.1	1.1	1.4	1.3	1.2	1.2	1.6	1.5	1.4	1.3 (0.2)
Man $_{(\%)}$	0.8	0.8	0.7	0.7	0.8	0.8	0.9	0.7	0.8	1.0	0.9	0.8	0.8 (0.1)
Gal $_{(\%)}$	0.6	0.7	0.6	0.6	0.6	0.6	0.6	0.6	0.5	0.6	0.6	0.6	0.6 (0.0)
Xyl $_{(\%)}$	0.3	0.3	0.3	0.3	0.3	0.3	0.3	0.3	0.3	0.4	0.3	0.3	0.3 (0.0)
M:G	0.80	0.91	0.96	0.88	0.88	0.84	0.72	0.74	0.78	0.76	0.76	0.83	0.82 (0.07)
N $_{(\%)}$	1.6 (0.2)	1.6 (0.1)	1.6 (0.1)	1.3 (0.1)	1.2 (0.1)	1.2 (0.1)	1.3 (0.1)	1.3 (0.1)	1.3 (0.1)	1.3 (0.1)	1.5 (0.0)	1.5 (0.1)	1.4 (0.1)
P $_{(\%)}$	0.12	0.14	0.14	0.11	0.09	0.08	0.09	0.10	0.08	0.09	0.12	0.12	0.11 (0.02)
K $_{(\%)}$	3.8	3.4	3.7	3.1	3.1	3.7	4.2	4.1	3.5	3.8	4.0	4.0	3.7 (0.4)
S $_{(\%)}$	1.1 (0.1)	1.0 (0.1)	1.0 (0.1)	0.9 (0.0)	1.0 (0.1)	1.0 (0.0)	1.1 (0.1)	1.0 (0.1)	1.1 (0.1)	1.1 (0.1)	1.0 (0.1)	1.1 (0.1)	1.0 (0.1)
Protein:N	4.4	4.9	4.8	4.5	4.6	4.7	4.3	4.7	4.8	4.8	4.7	4.6	4.7 (0.1)
C:N	19.6	20.6	20.6	25.1	26.4	26.3	24.1	24.3	24.2	22.7	20.6	21.0	23 (2.4)
I $_{(\%)}$	0.51	0.51	0.55	0.64	0.67	1.02	1.04	1.06	0.76	0.83	0.66	0.46	0.73 (0.22)
As $_{(ppm)}$	52.5	60.9	54.6	53.0	54.1	61.9	67.9	77.4	61.6	56.6	62.1	58.2	60.1 (7.2)
Cd $_{(ppm)}$	1.9	2.0	1.9	1.7	1.7	1.5	2.0	1.4	1.3	1.2	1.5	1.6	1.7 (0.3)
Pb $_{(ppm)}$	0.3	0.1	0.1	0.3	0.0	0.1	0.2	0.1	0.1	0.2	0.1	0.2	0.1 (0.1)
Hg $_{(ppm)}$	0.01	0.01	0.01	0.01	0.02	0.03	0.03	0.02	0.03	0.02	0.02	0.01	0.02 (0.01)

Table 5 Durbin-Watson test of autocorrelation testing for significance of temporal patterns ($n = 12$—72). Degree of autocorrelation is expressed by the d-value. Components marked with an asterisk were not normally distributed for their linear model residuals and thus do not meet the requirements of the test. Significant p-values are italicised ($\alpha = 0.05$). M:G shows the mannuronic to guluronic acid ratio, and Protein:N is the nitrogen to protein conversion factor

Component	n	d-value	p-value
Carbohydrates*	12	1.77	0.216
Phlorotannins	72	1.57	0.123
Proteins	12	0.51	*< 0.001*
Ash	72	1.44	0.076
Lipids	72	0.45	*< 0.001*
Glucose	12	1.05	*0.012*
Guluronic Acid	12	1.30	*0.044*
Mannuronic Acid	12	2.11	0.435
Fucose	12	1.56	0.116
Mannose	12	1.95	0.321
Galactose	12	1.95	0.321
Xylose*	12	1.64	0.152
M:G	12	1.27	*0.038*
Nitrogen	72	0.47	*< 0.001*
Phosphorus	12	0.83	*0.002*
Potassium	12	1.46	0.082
Sulphur	72	2.66	0.806
Protein:N	12	2.10	0.424
Iodine	12	0.62	*< 0.001*
Arsenic*	12	1.30	*0.043*
Cadmium	12	1.92	0.307
Lead	12	2.52	0.728
Mercury	12	1.06	*0.012*

$n = 23$) was similar to that of *S. latissima*, but at the lower end of the range recorded for *L. digitata* (Table 6). Overall, the carbohydrate composition *E. radiata* was similar to these commercial northern hemisphere species, although such comparisons may differ between sites (Manns et al. 2017). The inferred levels of alginate, fucoidan, and laminarin (see discussion below) are in accordance with previous findings for *E. radiata* in Australia (Stewart et al. 1961) and contribute significantly to the value of this biomass.

Levels of phlorotannins (range: 3.6 – 12.4% DW, $n = 138$) were tenfold higher than in *S. latissima* and other commercial northern hemisphere species (Schiener et al. 2015; Vilg et al. 2015), but not as high as other sub-tropical browns such as the fucoids *Carpophyllum sp.* and *Cystophora* sp. (mean: 13.4% DW and 10.4% DW, respectively; Magnusson et al. 2017). Phlorotannins have substantial commercial potential for cosmetics, functional foods, and biostimulants, given their bioactive activities which includes antioxidant, antimicrobial, antiviral and anti-inflammatory properties (Shrestha et al. 2021).

The content of protein (as total amino acids, range: 4.6 – 7.8% DW, $n = 23$) was similar to *S. latissima* and *L. digitata* (Table 6), with glutamic acid (mean: 15.5 ± 2.2 SD mol % of total amino acids, $n = 23$), aspartic acid (mean: 13.3 ± 0.7 SD mol % of total amino acids, $n = 23$), and alanine (mean: 12.7 ± 0.9 SD mol % of total amino acids, $n = 23$) also being the dominant amino acids as in *S. latissima* (Sharma et al. 2018). Conversely, the maximum nitrogen (mean: 1.3 ± 0.2 SD N % DW, $n = 138$) and phosphorus (mean: 0.11 ± 0.02 P SD % DW, $n = 23$) content of *E. radiata* were approximately twofold and fivefold lower, respectively, than that of northern hemisphere kelp species (Table 6). However, contents of protein and nitrogen were strongly correlated (linear regression: $F(1,21) = 259.7$, $p < 0.001$, $R^2 = 0.93$; Table 5) allowing the calculation of a species specific nitrogen-to-protein conversion factor (Protein:N) for *E. radiata* of 4.9 ± 0.4 SD ($n = 23$), which was not significantly affected by temporal change (Table 5) and very close to the universal seaweed nitrogen-to-protein conversion factor of 4.76 proposed by Angell et al. (2016).

Potentially harmful levels of minerals such as iodine, arsenic, cadmium, lead, and mercury can accumulate in seaweed biomasses, with the risk dependent on the water quality of the growth environment (FAO and WHO 2022; Hahn et al. 2022). Total arsenic contents (mean: 54.5 ± 9.6 SD ppm DW, $n = 23$) exceeded the threshold set by Food Standards Australia New Zealand (FSANZ) of 1 ppm

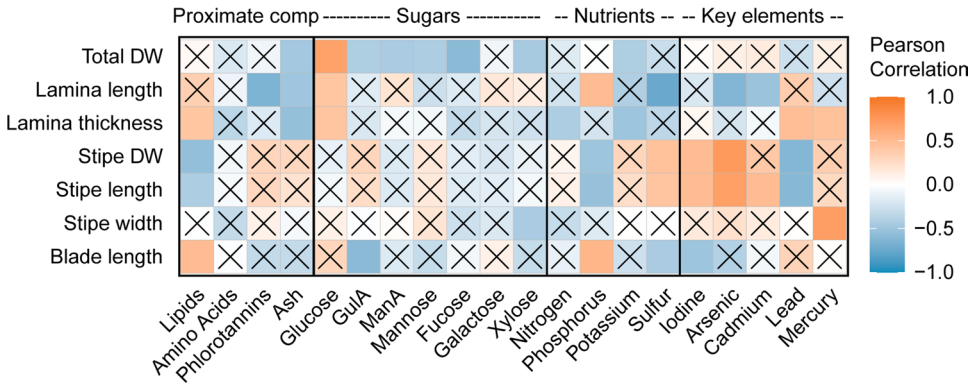

Fig. 5 Correlation matrix between morphology and biomass composition of E. radiata ($n = 23$) calculated by Pearson correlation coefficient (r). Orange boxes indicate positive correlation and blue boxes indicate negative correlation. Non-significant correlations are marked with an X ($\alpha = 0.05$)

Table 6 Biomass composition (% DW) of *E. radiata* and commercial northern hemisphere species *S. latissima* and *L. digitata* with mean values followed by seasonal range in brackets (Manns et al. 2014, 2017; Marinho et al. 2015; Schiener et al. 2015; Sharma et al. 2018). Data estimated from graphs are noted with an asterisk. The seasonal range of laminarin was estimated as the variable seasonal range of glucose minus 2% DW to account for fluctuation of cellulose and is noted with a double asterisk (Black 1950; Stewart et al. 1961)

Component	*E. radiata*	*S. latissima*	*L. digitata*	Reference
Glucose	12.8 (7.7–18.2)	(3–22)*	(6–54.0)*	Manns et al. 2017
Laminarin	(0–9)**	8.2 (1–14)*	6.7 (1–17)*	Schiener et al. 2015
Alginate	20.0 (16.5–24.2)	28.5 (16–31)*	34.6 (16–31)*	Schiener et al. 2015
M:G ratio	0.86 (0.72–0.96)	(1.33–3.53)	(1.47–3.64)	Manns et al. 2017
Fucose	1.3 (1.1–1.6)	2.9	2.4	Manns et al. 2014
Phlorotannins	7.5 (5.2–12.4)	0.41 (0.23–0.68)	0.15 (0.09–0.18)	Schiener et al. 2015
Protein	6.3 (5.6–7.6)	11.0 (5.1–9.9)	6.9 (4.9–8.2)	Schiener et al. 2015
Glutamic acid	1.2 (1.0–1.7)	(1.68–2.97)		Sharma et al. 2018
Aspartic acid	0.9 (0.7–1.0)	(1.40–2.38)		Sharma et al. 2018
Alanine	0.5 (0.5–0.7)	(0.92–1.91)		Sharma et al. 2018
Ash	23.1 (20.8–29.0)	(20–41)*	(11–30)*	Manns et al. 2017
Nitrogen	1.3 (1.1–1.8)	(0.5–3.1)		Marinho et al. 2015
Phosphorous	0.11 (0.08–0.14)	(0.05–0.82)		Marinho et al. 2015

(FSANZ 2019). However, arsenic is only considered toxic to humans in its inorganic form, and the calculated inorganic arsenic (mean: 0.5 ± 0.1 SD ppm DW, $n = 23$, estimated as 1% of total arsenic; Tukai et al. 2002) was twofold below the threshold of 1 ppm. The content of iodine and cadmium in *E. radiata* (mean: 6.3 ± 2.0 SD % DW and 1.4 ± 0.5 SD ppm DW, respectively, $n = 23$) exceeded the recommended threshold values set by the French Agency for Food, Environmental and Occupational Health and Safety (ANSES) for these elements by more than threefold (2000 and 0.5 ppm, respectively), while the content of lead and mercury (mean: 0.2 ± 0.2 SD ppm DW and 0.02 ± 0.01 SD ppm DW, respectively, $n = 23$) were below the threshold (5 and 0.1 ppm, respectively; ANSES 2018, 2020). Cadmium exceeded the recommended threshold level set by ANSES (ANSES 2020), however, to exceed the provisional tolerable intake limit for cadmium (25 µg kg^{-1} bodyweight $month^{-1}$) set by the World Health Organisation (WHO 2011) a 65 kg adult would need to consume 190 g WW *E. radiata* day^{-1}. This level of seaweed consumption is considerably higher than the average intake per capita in Japan of 10.4 g seaweed per day (Murai et al. 2021) and is unlikely to occur. Furthermore, blanching is a common processing technique when preparing seaweed for consumption and may reduce iodine content by over 90% (Stévant et al. 2018; Nielsen et al. 2020), which would reduce iodine levels in *E. radiata* below those set by ANSES (2018). Overall, our results indicate that *E. radiata* is suitable for human consumption if consumed within intake limits and/or with appropriate processing.

Spatial and temporal variation in biomass composition

Spatial and temporal variation in biomass composition can affect the quality of the biomass and therefore have significant implications for the aquaculture of *E. radiata* in New Zealand. Significant spatial variation in the biomass composition of *E. radiata* was detected between sites within the North Island of New Zealand (Table 2). However, no significant differences were found between regions (except for lipids), no clear spatial trends were detected for biomass composition (Fig. 4a), and even sites in close proximity differed substantially in terms of their biomass composition (e.g. Mākara Beach and Titahi Bay: 19 km distance). Consequently, the large variation in biomass composition among sites is likely explained by local rather than regional differences. *Ecklonia radiata* is highly plastic and can express very different morphologies over short distances in response to changing environmental conditions (Fowler-Walker et al. 2006). Changes in lipids, phlorotannins, polysaccharides, and minerals were significantly correlated to stipe, lamina, and blade morphology. Hence, differences in biomass composition may be related to local morphological differences. However, these correlations between morphology and biomass content were mostly relatively weak. Therefore, the large variation in biomass composition between sites is likely caused by other underlying factors such as differences in environmental conditions (e.g. temperature, water chemistry, wave action) and possibly genetic variations (discussed below). For instance, biosynthetic regulation of the ratio between mannuronic and guluronic acid is an essential mechanism in brown algae for controlling strength and flexibility of tissue structure (Indergaard et al. 1990), indicating that alginate composition and abundance may vary between exposed and sheltered sites (Munda 1987; McHugh 2003). Furthermore, nutrient availability is highly variable within the North Island of New Zealand (Plew et al. 2018) which may cause changes in protein and carbohydrate content (Roleda and Hurd 2019). Site-specific environmental

conditions thus likely play an important role in the biomass composition of *E. radiata* on the North Island of New Zealand.

Overall, spatial variation among sites was higher than temporal variation between monthly samples for most biomass components (Online resource 4), indicating that geographic variation is higher than temporal variation. Genetic differences between sub-populations could be contributing to the large geographical variation, as the genetic structure of *E. radiata* is strong within the North Island of New Zealand with sharp differentiation between the Wellington region and the other regions, and with further differentiation between most sites at a local level (Nepper-Davidsen et al. 2021). Additionally, differences in biomass components such as phlorotannins and lipids have previously been linked to changes in genotype (Honkanen and Jormalainen 2005; Gosch et al. 2015). However, the strong regional patterns evident in the genetic structure (Nepper-Davidsen et al. 2021) were not reflected in biomass composition here, as the Wellington sites did not stand out from the other sites using clustering analysis (Fig. 4a). To further investigate the matter common-garden experiments (De Villemereuil et al. 2016) are needed.

Significant temporal variation was also evident for several important biomass components of *E. radiata* within the North Island of New Zealand, similar to previous findings for *E. radiata* in Australia (Stewart et al. 1961) and for *S. latissima* and *L. digitata* in northern Europe (Manns et al. 2017). Alginate and fucoidan both peaked in early austral spring, while proteins, lipids, nitrogen and phosphorous peaked in late austral spring/early summer, and total carbohydrates and glucose peaked in early austral autumn. Water temperature is recognised as a key driver of the temporal variation in the biomass composition of seaweeds (compared to nitrogen, phosphorous, and salinity; Manns et al. 2017), and the observed temporal variation in the current study provides further support for strong environmental effects on the composition of *E. radiata* biomass.

Glucose is the main constituent of laminarin—a primary energy storage polysaccharide—and the glucose content of *E. radiata* followed a similar pattern as laminarin in other kelp species, where it builds up during boreal summer and autumn and depletes during boreal winter (Schiener et al. 2015). Furthermore, the temporal changes in glucose content detected in this study (range: 7.7—18.2% DW, $n = 12$) correspond to the temporal change in laminarin content previously found for *E. radiata* in Australia (range: 0.0 – 9.8% DW; Stewart et al. 1961). Glucose is also the main constituent of cellulose—a structural polysaccharide – however, as cellulose content is usually relatively stable throughout the year (1–2% DW yearly fluctuation; Black 1950) the observed temporal changes in glucose content mainly reflect fluctuations in laminarin content.

Implications for aquaculture

The composition of *E. radiata* biomass was highly site specific and showed large spatial variation in key commercial components, likely related to local differences in environmental conditions. Nepper-Davidsen et al. (2021) recommended not to translocate cultivars of *E. radiata* outside of their area of origin on the North Island of New Zealand to preserve the strong genetic structure of wild populations of this kelp. The biomass composition of local broodstock may therefore be of central importance for optimising the yield of targeted commercial components when choosing sites for seaweed aquaculture. The biomass content of key commercial components also showed significant temporal variation, underlining the importance of harvest timing for optimising yield depending on the biomass components of interest. We suggest early austral spring harvest for high contents of alginate and fucoidan and late austral spring/early summer harvest for proteins and lipids, with the precaution that seasonal patterns may vary between sites (Manns et al. 2017). Total carbohydrates and glucose peaked in early austral autumn, but heavy fouling and high temperatures during austral summer may lower the overall yield and value of the biomass (Handå et al. 2013; Wernberg et al. 2019).

The ratio between carbon and nitrogen content (C:N) in kelp is an indicator of nitrogen availability for primary production, with ratios > 20 indicating nitrogen limited growth (Wernberg et al. 2019). The C:N ratio for E. radiata biomass (mean: 25.8 ± 5.4 SD, $n = 138$) was above 20 during most of the year and at most sites, indicating a high degree of nitrogen limitation both spatially and temporally (Table 1 and 4). Cultivation in areas of high nutrient loads such as those affected by terrestrial runoff or downstream of animal aquaculture could be used to increase growth and simultaneously reduce the effects of nutrient run-off (Handå et al. 2013; Roleda and Hurd 2019). Indeed, based on the nitrogen and phosphorus contents in the biomass, cultivation of *E. radiata* could remove an estimated 164.6 kg N ha^{-1} and 14.7 kg P ha^{-1} per year (see Online resource 5 for calculations).

In conclusion, *E. radiata* had comparable biomass composition to that of commercial northern hemisphere species such as *S. latissima* and *L. digitata* and could be a viable southern hemisphere alternative for a broad range of commercial applications including extraction of phlorotannins, laminarin, and alginate, markets for human and animal consumption, and production of biostimulants.

Supplementary Information The online version contains supplementary material available at https://doi.org/10.1007/s10811-023-02969-2.

Acknowledgements The authors thank Peter Randrup, Alisa Mihaila and Holly Ferguson for field work assistance, Ariane Brandenburg for laboratory assistance, and Jesper Sonne for programming assistance. This research is part of the Entrepreneurial Universities Macroalgal

Biotechnologies Programme, jointly funded by the University of Waikato and the New Zealand Tertiary Education Commission. This study used NCRIS-enabled Australian Proteome Analysis Facility (APAF) infrastructure.

Authors' contribution JN-D: investigation, data curation, data analysis, visualisation, and writing—original draft, review, and editing. CG: conceptualization, design, supervision, data curation, writing—review, and editing. RL: conceptualisation, design, supervision, and writing—review, and editing. MM: conceptualisation, design, supervision, funding, and writing— review, and editing. All authors contributed to the article and approved the submitted version.

Funding Open Access funding enabled and organized by CAUL and its Member Institutions This research is part of the Entrepreneurial Universities Macroalgal Biotechnologies Program, jointly funded by the University of Waikato and the New Zealand Tertiary Education Commission.

Data availability The datasets generated and analysed during the current study are available from the corresponding author on reasonable request.

Declarations

Competing interests The authors declare that the research was conducted in the absence of any commercial or financial relationships that could be construed as a potential conflict of interest.

References

Anderson MJ, Gorley RN, Clarke KR (2016) PERMANOVA+ for PRIMER: Guide to software and statistical methods. PRIMER-E Ltd., Plymouth

Angell AR, Mata L, de Nys R, Paul NA (2014) Variation in amino acid content and its relationship to nitrogen content and growth rate in *Ulva ohnoi* (Chlorophyta). J Phycol 50:216–226

Angell AR, Mata L, de Nys R, Paul NA (2016) The protein content of seaweeds: a universal nitrogen-to-protein conversion factor of five. J Appl Phycol 28:511–524

ANSES (2018) Opinion on the risk of excess iodine intake from the consumption of seaweed in foodstuffs. French Agency for Food, Environmental and Occupational Health and Safety, Paris

ANSES (2020) Opinion on maximum cadmium levels for seaweed intended for human consumption. French Agency for Food, Environmental and Occupational Health and Safety, Paris

Battacharyya D, Babgohari MZ, Rathor P, Prithiviraj B (2015) Seaweed extracts as biostimulants in horticulture. Sci Hort 196:39–48

Black WAP (1950) The seasonal variation in the cellulose content of the common Scottish Laminariaceae and Fucaceae. J Mar Biol Assoc U K 29:379–387

Bradly N, Syddall V, Ingram C, Clarkson R, Elliot A, Major R, Adams S (2021) Stocktake and characterisation of Aotearoa New Zealand 's seaweed sector: market and regulatory focus. Sustainable Seas, New Zealand.

Clarke KR, Gorley RN (2015) PRIMER v7: User manual/tutorial. Plymouth. PRIMER-E Ltd., Plymouth

De Villemereuil P, Gaggiotti OE, Mouterde M, Till-Bottraud I (2016) Common garden experiments in the genomic era: New perspectives and opportunities. Heredity 116:249–254

FAO (2021) Global status of seaweed production, trade and utilization. Food and Agriculture Organization of the United Nations, Rome

FAO (2022) The state of world fisheries and aquaculture 2022. Towards blue transformation. Food and Agriculture Organization of the United Nations, Rome

FAO, WHO (2022) Report of the expert meeting on food safety for seaweed – Current status and future perspectives. Rome, 28–29 October 2021. Food Safety and Quality Series No. 13. Food and Agriculture Organization of the United Nations and World Health Organization, Rome. https://doi.org/10.4060/cc0846en

Folch J, Lees M, Sloane SG (1957) A simple method for the isolation and purification of total lipides from animal tissues. J Biol Chem 226:497–509

Fowler-Walker MJ, Wernberg T, Connell SD (2006) Differences in kelp morphology between wave sheltered and exposed localities: Morphologically plastic or fixed traits? Mar Biol 148:755–767

FSANZ (2019) 25th Australian total diet study. Food Standard Australia New Zealand, Canberra

Gosch BJ, Lawton RJ, Paul NA et al (2015) Environmental effects on growth and fatty acids in three isolates of *Derbesia tenuissima* (Bryopsidales, Chlorophyta). Algal Res 9:82–93

Gosch BJ, Magnusson M, Paul NA, de Nys R (2012) Total lipid and fatty acid composition of seaweeds for the selection of species for oil-based biofuel and bioproducts. GCB Bioenergy 4:919–930

Hahn JL, Van Alstyne KL, Gaydos JK, Wallis LK, West JE, Hollenhorst SJ, Ylitalo GM, Poppenga RH, Bolton JL, McBride DE, Sofield RM (2022) Chemical contaminant levels in edible seaweeds of the Salish Sea and implications for their consumption. PLoS One 17:e0269269

Handå A, Forbord S, Wang X, Broch OJ, Dahle SW, Støseth TR, Reitan KI, Olsen Y, Skjermo J (2013) Seasonal- and depth-dependent growth of cultivated kelp (*Saccharina latissima*) in close proximity to salmon (*Salmo salar*) aquaculture in Norway. Aquaculture 414–415:191–201

Honkanen T, Jormalainen V (2005) Genotypic variation in tolerance and resistance to fouling in the brown alga *Fucus vesiculosus*. Oecologia 144:196–205

Hsu H, Hwang P (2019) Clinical applications of fucoidan in translational medicine for adjuvant cancer therapy. Clin Transl Med 8:15

Indergaard M, Skjak-Brsk G, Jensen A (1990) Studies on the influence of nutrients on the composition and structure of alginate in *Laminaria saccharina* (L.) Lamour. (Laminariales, Phaeophyceae). Bot Mar 33:277–288

Jennings JG, Steinberg PD (1994) In situ exudation of phlorotannins by the sublittoral kelp *Ecklonia radiata*. Mar Biol 121:349–354

Kirkman H (1984) Standing stock and production of *Ecklonia radiata* (C.Ag.). J Agardh J Exp Mar Biol Ecol 16:119–130

Lorbeer AJ, Charoensiddhi S, Lahnstein J, Lars C, Franco CMM, Bulone V, Zhang W (2017) Sequential extraction and characterization of fucoidans and alginates from *Ecklonia radiata, Macrocystis pyrifera, Durvillaea potatorum*, and *Seirococcus axillaris*. J Appl Phycol 29:1515–1526

Lorbeer AJ, Lahnstein J, Bulone V, Nguyen T, Zhang W (2015) Multiple-response optimization of the acidic treatment of the brown

alga *Ecklonia radiata* for the sequential extraction of fucoidan and alginate. Bioresour Technol 197:302–309
Magnusson M, Yuen AKL, Zhang R, Wright JT, Taylor RB, Maschmeyer T, de Nys R (2017) A comparative assessment of microwave assisted (MAE) and conventional solid-liquid (SLE) techniques for the extraction of phloroglucinol from brown seaweed. Algal Res 23:28–36
Mak W, Hamid N, Liu T, Lu J, White WL (2013) Fucoidan from New Zealand *Undaria pinnatifida*: Monthly variations and determination of antioxidant activities. Carbohydr Polym 95:606–614
Manns D, Deutschle AL, Saake B, Meyer AS (2014) Methodology for quantitative determination of the carbohydrate composition of brown seaweeds (Laminariaceae). RSC Adv 4:25736–25746
Manns D, Nielsen MM, Bruhn A, Saake B, Meyer AS (2017) Compositional variations of brown seaweeds *Laminaria digitata* and *Saccharina latissima* in Danish waters. J Appl Phycol 29:1493–1506
Marinho GS, Holdt SL, Birkeland MJ, Angelidaki I (2015) Commercial cultivation and bioremediation potential of sugar kelp, *Saccharina latissima*, in Danish waters. J Appl Phycol 27:1963–1973
Mata L, Lawton RJ, Magnusson M, Andreakis N, de Nys R, Paul NA (2017) Within-species and temperature-related variation in the growth and natural products of the red alga *Asparagopsis taxiformis*. J Appl Phycol 29:1437–1447
McHugh DJ (2003) A guide to the seaweed industry. FAO Fisheries Technical Paper 441. Food and Agriculture Organisation of the United Nations, Rome
Munda IM (1987) Distribution and use of some economically important seaweeds in Iceland. Hydrobiologia 151–152:257–260
Murai U, Yamagishi K, Kishida R, Iso H (2021) Impact of seaweed intake on health. Eur J Clin Nutr 75:877–889
Nepper-Davidsen J, Magnusson M, Glasson CRK, Ross PM, Lawton RJ (2021) Implications of genetic structure for aquaculture and cultivar translocation of the kelp *Ecklonia radiata* in northern New Zealand. Front Mar Sci 8:749154
Nielsen CW, Holdt SL, Sloth JJ, Marinho GS, Sæther M, Funderud J, Rustad T (2020) Reducing the high iodine content of *Saccharina latissima* and improving the profile of other valuable compounds by water blanching. Foods 9:569
Plew DR, Zeldis JR, Shankar U, Elliott AH (2018) Using simple dilution models to predict New Zealand estuarine water quality. Estuar Coasts 41:1643–1659
Porse H, Rudolph B (2017) The seaweed hydrocolloid industry: 2016 updates, requirements, and outlook. J Appl Phycol 29:2187–2200
Praeger C, Magnusson M, Lawton R (2022) Optimising the zoospore release, germination, development of gametophytes and formation of sporophytes of *Ecklonia radiata*. J Appl Phycol 34:2535–2549
Roleda MY, Hurd CL (2019) Seaweed nutrient physiology: Application of concepts to aquaculture and bioremediation. Phycologia 58:552–562
Rozaklis T, Ramsay SL, Whitfield PD, Ranieri E, Hopwood JJ, Meikle PJ (2002) Determination of oligosaccharides in Pompe disease by electrospray ionization tandem mass spectrometry. Clin Chem 48:131–139
Schiener P, Black KD, Stanley MS, Green DH (2015) The seasonal variation in the chemical composition of the kelp species *Laminaria digitata*, *Laminaria hyperborea*, *Saccharina latissima* and *Alaria esculenta*. J Appl Phycol 27:363–373
Sharma S, Neves L, Funderud J, Mydland LT, Øverland M, Horn SJ (2018) Seasonal and depth variations in the chemical composition of cultivated *Saccharina latissima*. Algal Res 32:107–112
Shears NT, Babcock RC (2007) Quantitative description of mainland New Zealand's shallow subtidal reef communities. Department of Conservation, Wellington
Shrestha S, Zhang W, Smid SD (2021) Phlorotannins: A review on biosynthesis, chemistry and bioactivity. Food Biosci 39:100832
Sichert A, Corzett CH, Schechter MS, Unfried F, Becher D, Fernadez-Guerra A, Liebke M, Schweder T, Polz MF, Hehemann J-H (2020) Verrucomicrobia use hundreds of enzymes to digest the algal polysaccharide fucoidan. Nat Microbiol 5:1026–1039
Stévant P, Marfaing H, Duinker A, Fleurence J, Rustad T, Sandbakken I, Chapman A (2018) Biomass soaking treatments to reduce potentially undesirable compounds in the edible seaweeds sugar kelp (*Saccharina latissima*) and winged kelp (*Alaria esculenta*) and health risk estimation for human consumption. J Appl Phycol 30:2047–2060
Stewart CH, Higgins HG, Austin S (1961) Seasonal variation in alginic acid, mannitol, laminarin and fucoidin in the brown alga, *Ecklonia radiata*. Nature 192:1208
Szekalska M, Puciłowska A, Szymańska E, Ciosek P, Winnicka K (2016) Alginate: Current use and future perspectives in pharmaceutical and biomedical applications. Int J Polym Sci 2016:7697031
Targett NM, Arnold TM (1998) Predicting the effects of brown algal phlorotannins on marine herbivores in tropical and temperate oceans. J Phycol 34:195–205
Team RStudio (2022) RStudio: integrated development environment for R. RStudio. PBC, Boston
Tukai R, Maher WA, McNaught IJ, Ellwood MJ, Coleman M (2002) Occurrence and chemical form of arsenic in marine macroalgae from the east coast of Australia. Mar Freshw Res 53:971–980
Vilg JV, Nylund GM, Werner T, Qvirist L, Mayers JJ, Pavia H, Undeland I, Albers E (2015) Seasonal and spatial variation in biochemical composition of *Saccharina latissima* during a potential harvesting season for Western Sweden. Bot Mar 58:435–447
Wernberg T, Coleman MA, Babcock RC, Bell SY, Bolton JJ, Connell SD, Hurd CL, Johnson CR, Marzinelli EM, Shears NT, Steinberg PD, Thomsen MS, Vanderklift MA, Verges A, Wright JT (2019) Biology and ecology of the globally significant kelp *Ecklonia radiata*. Oceanogr Mar Biol 57:265–324
WHO (2011) Safety evaluation of certain food additives and contaminants. World Health Organization, Geneva
Wijffels SE, Beggs H, Griffin C, Middleton JF, Cahill M, King E, Jones E, Feng M, Benthuysen JA, Steinberg CR, Sutton P (2018) A fine spatial-scale sea surface temperature atlas of the Australian regional seas (SSTAARS): Seasonal variability and trends around Australasia and New Zealand revisited. J Mar Syst 187:156–196
Zhang Q, Zhang J, Shen J, Silva A, Dennis DA, Barrow CJ (2006) A simple 96-well microplate method for estimation of total polyphenol content in seaweeds. J Appl Phycol 18:445–450